UAB

Universitat Autònoma de Barcelona

IDENTIFICATION OF TIME- AND SEX-DEPENDENT PATHWAYS INVOLVED IN RENAL ISCHEMIA-REPERFUSION INJURY IN A PORCINE MODEL. LINK TO RENAL CANCER.

Stéphane Nemours

IDENTIFICATION OF TIME- AND SEX-DEPENDENT PATHWAYS INVOLVED IN RENAL ISCHEMIA-REPERFUSION INJURY IN A PORCINE MODEL. LINK TO RENAL CANCER.

Thesis submitted by
Stéphane Nemours

For the degree of Doctor of Biochemistry, Molecular Biology and Biomedicine

Director and Tutor
Anna Meseguer Navarro

PhD Student
Stéphane Nemours

Department of Biochemistry and Molecular Biology
Universitat Autònoma de Barcelona

Barcelona, June 2020

OUTLINES

À

Dieudonne et Ronel,

pour tout...

"I tell my students, 'When you get these jobs that you have been so brilliantly trained for, just remember that your real job is that if you are free, you need to free somebody else. If you have some power, then your job is to empower somebody else. This is not just a grab-bag candy game."

— Toni Morrison

"Our crown has already been bought and paid for. All we have to do is wear it"

— James Baldwin

AKNOWLEDGEMENTS

AKNOWLEDGEMENTS

ABBREVIATIONS

ABBREVIATIONS

ACE2: angiotensin-converting enzyme 2

ACE: angiotensin-converting enzyme

ACTC1: actin alpha cardiac muscle 1

ADCYAP1R1: ADCYAP Receptor Type I

AKI: acute kidney injury

AKT: Protein kinase B

APC: Adenomatous Polyposis Coli

APOD: Apolipoprotein D

AR: androgen receptor

ASPN: Asporin

ASS1: Argininosuccinate Synthase 1

ATF3: AMP-dependent transcription factor 3

ATP1B1: ATPase Na+/K+ Transporting Subunit Beta 1

ATP: Adenosine triphosphate

B4GAT1: Beta-1,4-Glucuronyltransferase 1

BAX: BCL2 Associated X, Apoptosis Regulator

BCL2/3: B-Cell CLL/Lymphoma 2/3

BID: BH3 Interacting Domain Death Agonist

BMP2: Bone Morphogenetic Protein 2

BTG2: BTG Anti-Proliferation Factor 2

BUN: blood urea nitrogen

C4A/C4B: Complement C4A/C4B

C6: Complement C6

CADH1: Cadherin 1

CADH2: Cadherin 2

cAMP: Cyclic adenosine monophosphate

CASP3: caspase 3

CCL2: C-C motif chemokine ligand 2

CCL4: C-C Motif Chemokine Ligand 4

CCL5: C-C motif chemokine ligand 5

CCL8: C-C Motif Chemokine Ligand 8

CCL: C-C motif chemokine ligand

CCR2: C-C Motif Chemokine Receptor 2

ccRCC: clear cell renal cell carcinoma

CD4: cluster of differentiation 4

CD8: cluster of differentiation 8

CD14: cluster of differentiation 14

CD20: B-lymphocyte antigen CD20

CD25: Interleukin 2 Receptor Subunit Alpha

CD68: Macrophage Antigen CD68

CD74: Cluster of differentiation 74

CD80: Cluster of differentiation 80

CD83: Cluster of Differentiation 83

CD109: Cluster of Differentiation 109

CD274: Programmed Cell Death 1 Ligand 1

CDC20: Cell Division Cycle 20

CEBPA: CCAAT Enhancer Binding Protein Alpha

CENPF: Centromere Protein F

CES1: Carboxylesterase 1

CKAP2: Cytoskeleton Associated Protein 2

CKD: chronic kidney disease

CLCNKB: Chloride Voltage-Gated Channel Kb

CMPK2: Cytidine/Uridine Monophosphate Kinase 2

CNA2: Keratan Sulfate Proteoglycan Keratocan

CNTFR: Ciliary Neurotrophic Factor Receptor

COL1A1: collagen type I alpha 1 chain

COL3A1: Collagen Type III Alpha 1 Chain

CREB1: CAMP Responsive Element Binding Protein 1

CX3CL1: C-X3-C Motif Chemokine Ligand 1)

CXCL1: C-X-C motif chemokine ligand 1

CXCL2: C-X-C motif chemokine ligand 2

CXCL8: C-X-C motif chemokine ligand 8

CXCL10/ IP-10: C-X-C Motif Chemokine Ligand 10

CXCL11: C-X-C Motif Chemokine Ligand 11

CXCL: C-X-C motif chemokine

CYC: Cytochrome c

ABBREVIATIONS

CYP2D6: Cytochrome P450 2D6

CYP24A1: Cytochrome P450 Family 24 Subfamily A Member 1

CYP450: Cytochromes P450

DAMP: Damage-associated molecular patterns

DEG: differentially expressed genes

DHRS7: dehydrogenase/reductase 7

DHT: Dihydrotestosterone

DNA: Deoxyribonucleic acid

DNAJB1: DnaJ Homolog Subfamily B Member 1

DUSP1: Dual Specificity Phosphatase 1

E2F1: E2F Transcription Factor 1

EDTA: Ethylenediaminetetraacetic acid

EGFR: epidermal growth factor recepto

EGR1: Early Growth Response 1

ELISA: Enzyme Linked Immunosorbent Assay

EMT: epithelial–mesenchymal transition

eNOS: Endothelial NOS

EPHB3: EPH Receptor B3

ER: Estrogen receptors

ERBB2: Erb-B2 Receptor Tyrosine Kinase 2

ERBB3: Erb-B2 Receptor Tyrosine Kinase 3

EREG: Epiregulin

ERK1/2: extracellular signal-regulated kinase 1/2

ESM1: Endothelial Cell Specific Molecule 1

ESRD: end-stage renal disease

EST: 17β-estradiol

EZRI: ezrin

F9: Coagulation Factor IX

FABP5: fatty acid-binding protein 5

FAM198B: Golgi Associated Kinase 1B

FBG: Fibrinogen Beta Chain

FBS: Fetal bovine serum

FDR: false-discovery rate

FGF9: Fibroblast Growth Factor 9

FGG: Fibrinogen Gamma Chain

FOS: Proto-Oncogene C-Fos

Foxp3: Forkhead Box P3

GBP2/3: Guanylate Binding Protein 2/3

GCM1: Glial Cells Missing Transcription Factor 1

GCR: glucocorticoid receptor

GFR: glomerular filtration rate

GPCR: G-protein–coupled receptors

GPRC6A: G Protein-Coupled Receptor Class C Group 6 Member A

GSEA: Gene Set Enrichment Analysis

HEK293: human embryonic kidney 293 cells

HIF1A: hypoxia-inducible factor 1 alpha

HIF2A: hypoxia-inducible factor 2 alpha

HIFB: hypoxia-inducible factor beta

HIST1H2AD: H2A Clustered Histone 7

HIST1H2AI: H2A Clustered Histone 13

HK-2: human kidney 2

HMMR: Hyaluronan Mediated Motility Receptor

HRG: Histidine Rich Glycoprotein

HSP7C: Heat shock cognate

ICC: immunocytochemistry

ICU: intensive care unit

IFIT1: Interferon Induced Protein with Tetratricopeptide Repeats 1

IFIT3: Interferon Induced Protein with Tetratricopeptide Repeats 3

IFN: Interferon

Ig: Immunoglobulin

IGFR: Insulin-like growth factor receptor

IHC: Immunohistochemistry ()

IL1: interleukin 1

IL1A/B: Interleukin 1 Alpha/Beta

IL2: Interleukin 2

IL2RA: Interleukin 2 Receptor Subunit Alpha

IL6: Interleukin 6

IL8: Interleukin 8

IL10: Interleukin 10

IL11: Interleukin 11

IL12B: Interleukin 12B

IL22: Interleukin 22

IL23: Interleukin 23

IL23A : Interleukin 23 Subunit Alpha

ILCs: 2 innate lymphoid cells

INFy: Interferon gamma

IRF1: Interferon Regulatory Factor 1

IRI: ischemia/reperfusion injury

ITB1: integrin beta-1

JUN: Jun Proto-Oncogene

KAP: kidney androgen regulated protein ()

KCP: Kielin Cysteine Rich BMP Regulator

KIAA0101: PCNA-associated factor

KIF20A: Kinesin Family Member 20A

KIM-1: Kidney Injury Molecule-1

KLHL1: Kelch Like Family Member 1

LDL: Low-density lipoprotein

LEAP2: Liver Enriched Antimicrobial Peptide 2

LOC100512372: organic solute transporter alfa

LRRC66: Leucine Rich Repeat Containing 66

LUM: Lumican

MAPK: mitogen-activated protein kinase

MASP: Mannan Binding Lectin Serine Peptidase 1

MC: mesangial cell

MCP-1: monocyte chemoattractant protein-1

MIP-2: Macrophage Inflammatory Protein 2-Alpha

mMDSCs: monocytic myeloid-derived suppressor cells

MMP7: Matrix Metallopeptidase 7

mRNA: Messenger RNA

MS4A7: Membrane Spanning 4-Domains A7

MTOR: Mechanistic Target of Rapamycin Kinase

MX1: MX Dynamin Like GTPase 1

MyD88: Myeloid Differentiation Primary Response Gene (88)

NF-kB: Nuclear Factor Kappa B

NFKB1: Nuclear Factor Kappa B Subunit 1

NK: Natural killer

NR1I2: Nuclear Receptor Subfamily 1 Group I Member 2

OAT: Ornithine Aminotransferase

PBRM-1: polybromo-1

PBS-(T): Phosphate-Buffered Saline-(Tween)

PDGFB: Platelet Derived Growth Factor Subunit B

PEBP4: Phosphatidylethanolamine Binding Protein 4

PECA1: Platelet endothelial cell adhesion molecule

PGH2: Prostaglandin G/H synthase 2

PI3K/ PIK3AP1: Phosphoinositide 3-kinases

PLEK: Pleckstrin

PLG: Plasminogen

PPARG: Peroxisome Proliferator Activated Receptor Gamma

pRCC: Papillary renal cell carcinoma

PT: proximal tubule

PTEC: proximal tubule epithelial cells

PTN1: PTEN PI-3 phosphatase

PVALB: Parvalbumin

RCC: renal cell carcinoma

RENI: Renin

RGS2: Regulator of G Protein Signaling 2

RHG35: Rho GTPase-activating protein 35

RHOA/J: transforming protein RhoA/J

RNA: Ribonucleic acid

RND1: Rho Family GTPase 1

ROS: reactive oxygen species

RPTEC: Renal Proximal Tubule Epithelial Cells

RSAD2/ IRG6: Radical S-Adenosyl Methionine Domain Containing 2

scRNA-seq: Single-cell RNA sequencing

SELE: Selectin E

SFRP2: Secreted Frizzled Related Protein 2

ABBREVIATIONS

SHBG: Sex Hormone Binding Globulin

SLC2A1: Solute Carrier Family 2 Member 1

SLC4A1: Solute Carrier Family 4 Member 1

SLC5A1: Solute Carrier Family 5 Member 1

SLC5A10: Solute Carrier Family 5 Member 10

SLC6A19: Solute Carrier Family 6 Member 19

SLC27A6: Solute Carrier Family 27 Member 6

SLC38A3: Solute Carrier Family 38 Member 3

SLC51A: Solute Carrier Family 51 Subunit Alpha

SMAD2/3: SMAD Family Member 2/3

SRC: SRC Proto-Oncogene, Non-Receptor Tyrosine Kinase

SREBP: Sterol Regulatory Element Binding Transcription Factor

STAT1: Signal Transducer and Activator of Transcription 1

STAT3: Signal Transducer and Activator of Transcription 3

STAT5A/B: Signal Transducer and Activator of Transcription 5A/B

STS: Steroid Sulfatase

TENA/TNC: tenascin

TGF: Transforming Growth Factor

Th1/2: T helper 1/2

TLR4: Toll Like Receptor 4

TLR5: Toll Like Receptor 5

TLR: Toll Like Receptor

TMEM252: Transmembrane Protein 252

TNF/A: tumor necrosis factor/alpha

TNFAIP3: TNF Alpha Induced Protein 3

TOP2A: DNA Topoisomerase II Alpha

Tregs: Regulatory T cells

TRIF: Toll Like Receptor Adaptor Molecule 1

TRPV5: Transient Receptor Potential Cation Channel Subfamily V Member 5

TSC1/2: TSC Complex Subunit 1

UGT2B11: UDP Glucuronosyltransferase Family 2 Member B11

VCAM1: Vascular Cell Adhesion Molecule 1

VDR: Vitamin D Receptor

VEGF: Vascular Endothelial Growth Factor

VHL: Von Hippel–Lindau

Wnt7b: Wnt Family Member 7B

ZBP1: Z-DNA Binding Protein 1

ZFP36: ZFP36 Ring Finger Protein

SUMMARY

SUMMARY

Kidney diseases arise from congenital defects, acute kidney injury (AKI) or chronic kidney disease (CKD), among other causes. Renal ischemia/reperfusion injury (IRI), which is faced in many clinical situations, is a major cause of AKI leading to injury and death of proximal tubule epithelial cells (PTEC). The severity of AKI and the capacity to regenerate after injury are important determinants of patient morbidity and mortality in the hospital setting. Men are more prone to acute and chronic kidney disease and to progress to end-stage renal disease (ESRD) than women and it is currently accepted that androgens, and not the absence of estrogens, are responsible for that. It is accepted that regeneration by surviving PTEC is the predominant mechanism of repair/regeneration after ischemic tubular injury in the adult mammalian kidney. PTEC are also the site where the clear cell renal cell carcinoma (ccRCC) originates in humans. ccRCC also exhibits sex differences, with males having almost twice the incidence of females globally. This led to the hypothesis that regeneration after kidney injury and ccRCC development might share similar gene expression repertoires. Androgens are very relevant in kidney development, which suggests that regeneration and cancer in proximal tubule cells might recapitulate, in part, androgen-dependent programs in kidney developmental. In this project, we aimed to find targets that participate in renal regeneration and in renal cancer processes. Moreover, we were interested to study the sex hormone regulation of these pathways. Thorough analyses of transcriptomic data from a porcine model of AKI was performed. We determined genes that expressed a sexual dimorphism throughout IRI and we validated theses targets in human samples. Furthermore, we determined the gene sets involved in IRI and characterize them in a time and sex manner. We found that gene sets related to regeneration processes were more active in females than in males. Also, the immune response at injury was higher in males than in females. Afterwards, we linked regeneration processes with ccRCC by the overlap between AKI and ccRCC transcriptome analyses. Besides, we found major differences between the mouse and the pig kidney transcriptomes upon renal injury. An *in vitro* model of renal IRI was established and allowed to partially validate the *in vivo* findings. Among others, we observed that during renal IRI, STAT3 is regulated by phosphorylation of different residues. This study constitutes an extensive characterization of the sex differences that exist during renal IRI. It offers a template for further characterization of sex differences in kidney diseases at the molecular level.

1.INTRODUCTION

1. INTRODUCTION

1.A. THE KIDNEY

1.A.I. Anatomy and Functions

The kidneys are two bean-shaped organs found in vertebrates. They are located on the left and right in the retroperitoneal space. They receive blood through the renal artery. The blood exits into the renal veins[1]. Each kidney is attached to a ureter, a tube that carries excreted urine to the bladder. The outer portion of the kidney is called the renal cortex, which sits directly beneath the kidney's loose connective tissue/fibrous capsule. [1] Deep to the cortex lies the renal medulla, which is divided into 10-20 renal pyramids in humans (Figure 1) [2]. The kidneys are complex organs that have numerous biological roles. In fact, they participate in the control of the volume of various body fluid compartments, fluid osmolality, acid-base balance, various electrolyte concentrations and the removal of toxins[3]. Because the kidneys are poised to sense plasma concentrations of compounds such as sodium, potassium, hydrogen ion, oxygen, and glucose, they are important regulators of blood pressure, glucose metabolism and erythropoiesis[3].
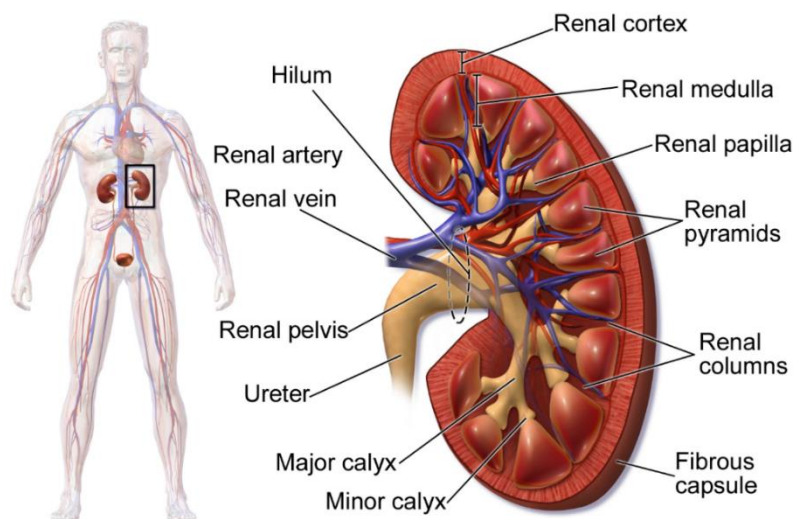
Figure 1. Schematic of kidney anatomy. The kidneys lie in the retroperitoneal space behind the abdomen, and act to filter blood to create urine. (Adapted from Blausen.com staff, *Medical gallery of Blausen Medical*, 2014)[2].

1.A.II. Nephron

The basic functional unit of the kidney is the nephron. There are more than a million nephrons within the cortex and the medulla of each normal adult human kidney. They regulate water and solute within the cortex and medulla of each kidney. The different segments of the nephrons (Figure 2) contribute to blood filtration, reabsorption and secretion of fluid and molecules.

The glomerulus and renal tubules are important components of the nephron. The functional complexity of these structures appears to be associated with different cell types. Along with the glomerular endothelial cells, podocytes synthesize the glomerular basement membrane, which is the final filtration barrier, representing an important seal that prevents the loss of proteins into the urine[4]. The proximal tubule (PT) plays an important role in regulating systemic acid-base balance by controlling Na^+-H^+ and HCO_3^- transport, while the distal convoluted tubule is more involved in electrolyte transport[5–7].
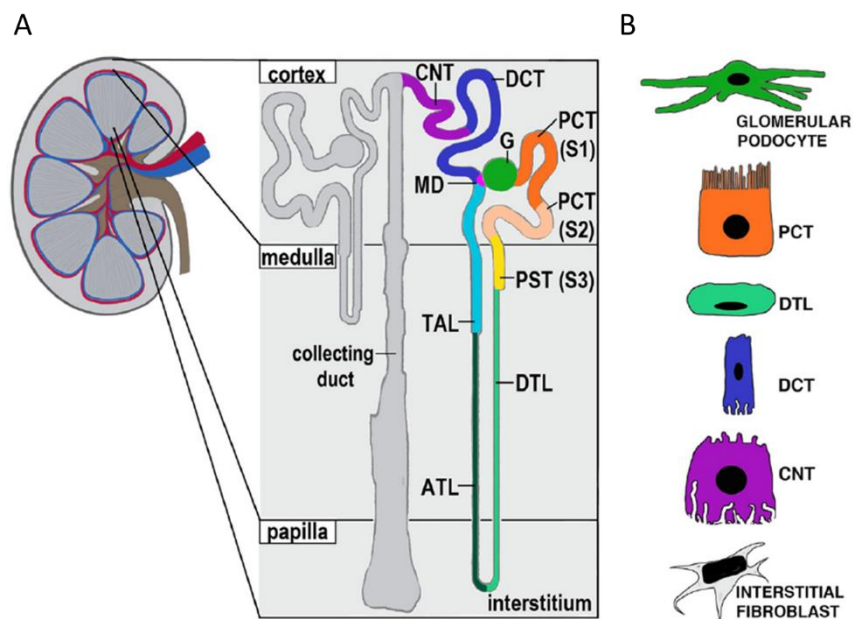
Figure 2. Schematic of a nephron and its heterogenous cell types. A) The kidney is comprised of a cortex, medulla, and papilla regions. Nephrons are segmented epithelial subunits of the kidney. Nephron segments are color-coded to depict the regionalized structure and show varying lengths of intermediate segments throughout the medulla and papilla region, where tracks of the collecting duct system are also found. B) Examples of differentiated nephron cell types, which display unique morphological features. Abbreviations are as follows: ATL, ascending thin limb; G, glomerulus; CNT, connecting tubule; DCT, distal convoluted tubule; DTL, descending thin limb; MD, macula densa; PCT, proximal convoluted tubule; PST, proximal straight tubule; TAL, thick ascending limb. (Adapted by Li *et al.*, *Clin Transl Med*, 2013)[8].

1.A.III. Cellular diversity of kidney tissue

The recent development of next-generation sequencing, high-throughput single-cell analysis and the Human Cell Atlas, have made possible single-cell RNA sequencing (scRNA-seq) of the kidney[9–11]. Not long ago, it was also reported that some renal diseases may be cell type-specific. For example, chronic kidney disease (CKD) is associated with PT cells[12]. In a recent study, Liao et al. obtained a single-cell suspension of the human kidney and performed scRNA-seq analysis[13]. They found a single-cell transcriptome dataset of 23,366 high-quality human kidney cells from three donors, including 20,308 PT cells. (Figure 3) PT cells. were classified into three different clusters according to their markers: proximal convoluted tubule, proximal straight tubule and PT cells of no accurate classification (Figure 3)[13]. Considering the important role of PT cells in renal disease, their results may validate previously reported susceptibility genes for kidney disease.
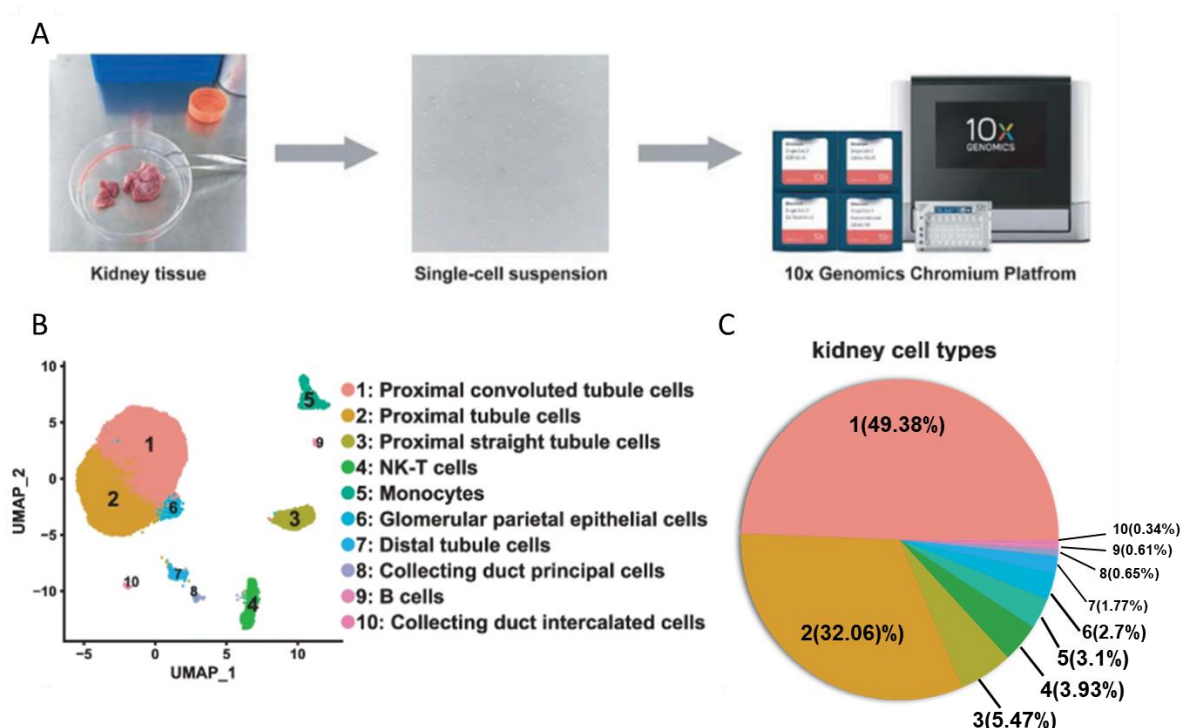
Figure 3. scRNA-seq reveals the cell populations of the human kidney. A) Overview of the scRNA-seq process using human kidney tissue samples. B) Uniform manifold approximation and projection (UMAP) plot showing the unbiased classification of renal cells. C) Pie chart showed the proportion of each kidney cell type. Besides the ones reported in this study, many more cell types are found in renal tissue such as endothelial cells, podocytes, etc. (Adapted from Liao et al., *Sci Data*, 2020)[13].

1.B.   ACUTE KIDNEY INJURY (AKI)

Kidney diseases arise from congenital defects as well as acquired conditions that result from AKI or chronic kidney disease (CKD)[14–18]. AKI is a common clinical event that disrupts renal homeostasis. It is characterized by an abrupt (within 48 hours) reduction in kidney function which can be measured by increases in serum creatinine[15]. CKD is typified by the progressive loss of kidney function over time due to fibrosis and the erosion of healthy tissue[18]. Whether or not patients have preexisting chronic kidney disease (CKD), those who have had AKI have a high risk of developing progressive CKD and ESRD over time[19–21].

1.B.I.   Etiology

AKI can be caused by many factors. Theses factors can be divided into three categories: prerenal, intrinsic renal and postrenal.

In prerenal cases, underlying kidney function may be normal, but decreased renal perfusion associated with intravascular volume depletion (e.g., from vomiting or diarrhea) or decreased arterial pressure (e.g., from heart failure or sepsis) results in a reduced glomerular filtration rate. Autoregulatory mechanisms often can compensate for some degree of reduced renal perfusion to maintain the glomerular filtration rate [22].

Intrinsic renal injury causes are also important sources of AKI and can be categorized by the component of the kidney that is primarily affected (tubular, glomerular, interstitial, or vascular). Acute tubular necrosis is the most common type of intrinsic AKI in hospitalized patients. The cause is usually ischemic (from prolonged hypotension) or nephrotoxic. In contrast to a prerenal etiology, acute kidney injury caused by acute tubular necrosis does not improve with adequate repletion of intravascular volume and blood flow to the kidneys. Both ischemic and nephrotoxic acute tubular necrosis can resolve over time[22].

1.B.II. Epidemiology

1.B.II.1   *Epidemiology of AKI*

The incidence of AKI in hospitalized patients has generally been reported to be in the 2%–7% range, with an incidence of 5% to greater than 10% in the ICU (intensive care unit) population, often in the context of multiorgan disease and sepsis, and is steadily increasing overall[23,24]. The incidence of AKI has grown steadily in many demographic groups, and the yearly community incidence of AKI was estimated to be 550 per 100,000 individuals in 2003, higher than the yearly incidence of stroke[25,26]. Despite advances in preventive strategies and support measures, AKI continues to be associated with high morbidity and mortality, particularly in those admitted to the ICU, where in-hospital mortality rates may exceed 50%[15].

1.B.II.2   *Epidemiology of CKD*

The progression of established CKD is variable and depends on several risk factors or markers. Nonmodifiable factors include genetics, race, age, and sex. For instance, there is much evidence that the rate of progression of CKD is faster among patients who are elderly, male, or African-American[27–29]. The worldwide rise in the number of patients with CKD is reflected in the increasing number of people with ESRD treated by renal replacement therapy (dialysis or transplantation)[30]. In the United States, the total cost of the ESRD program was approximately $49.3 billion, in 2011. These trends correlate with the global rise in the aged population and the increasing prevalence of conditions that cause renal complications, namely cardiovascular disease, hypertension and diabetes[31].

1.C.   RENAL ISCHEMIA REPERFUSION INJURY

1.C.I. Definition

Ischemia-reperfusion is a pathological condition due to an initial restriction of blood supply to an organ followed by the subsequent restoration of perfusion and concomitant reoxygenation[32]. Besides infection and toxic drugs, renal IRI is a major

cause of AKI, which is faced, in many clinical situations such as kidney transplantation, partial nephrectomy, renal artery angioplasty, aortic aneurysm surgery, and elective urological operations. In these conditions, IRI initiates a complex and interrelated sequence of events, resulting in injury and the eventual death of renal cells (Figure 4)[33].
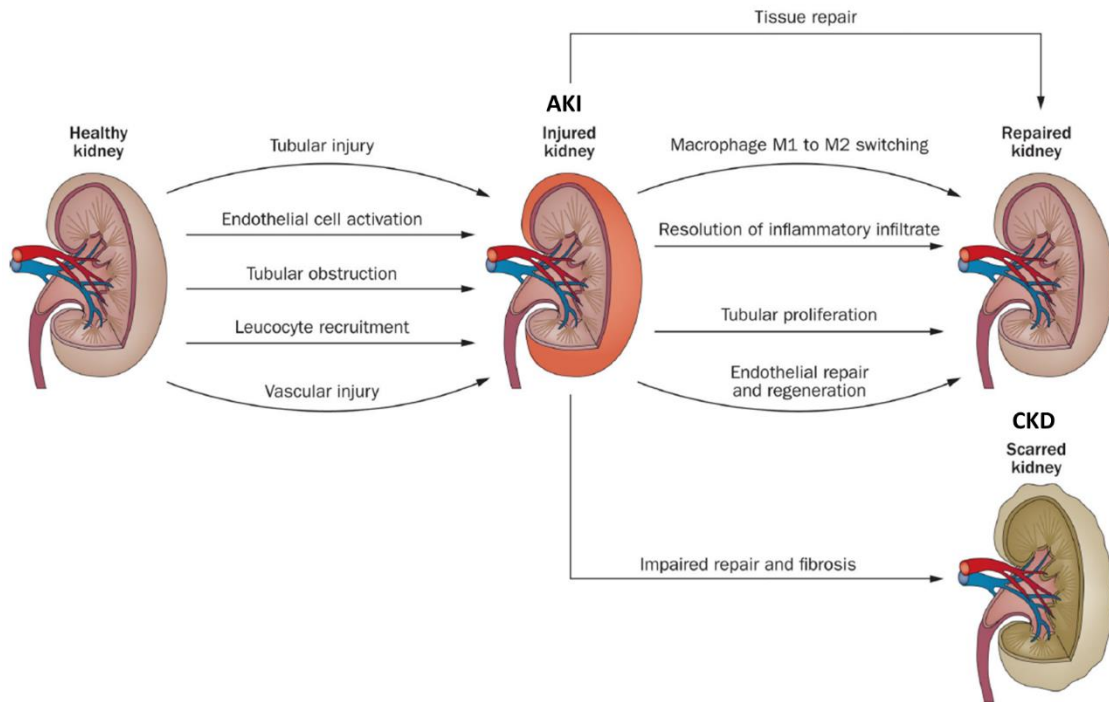
Figure 4. A summary of some of the mechanisms involved in initial tissue injury and subsequent repair of the kidney after AKI. Maladaptive and incomplete repair leads to the development of fibrosis and, ultimately, CDK. (Adapted by Ferenbach and Bonventre, *Nat Rev Nephrol*, 2015)[33].

1.C.II. Histopathology

The PT cells compartment is particularly susceptible to ischemic and/or toxic insults that result in acute renal failure[34]. The subsequent mechanisms for AKI still are controversial. Besides a reduction in glomerular filtration rate, tubular obstruction likely represents a major factor. Briefly, after AKI, cellular debris and protein casts obstruct individual nephrons transiently (Figure 5). Tubular obstruction may last long enough to drive the affected nephron into reversible or irreversible degeneration. In addition, complex interactions with cells of the immune system and release of inflammatory mediators likely play a role during AKI.
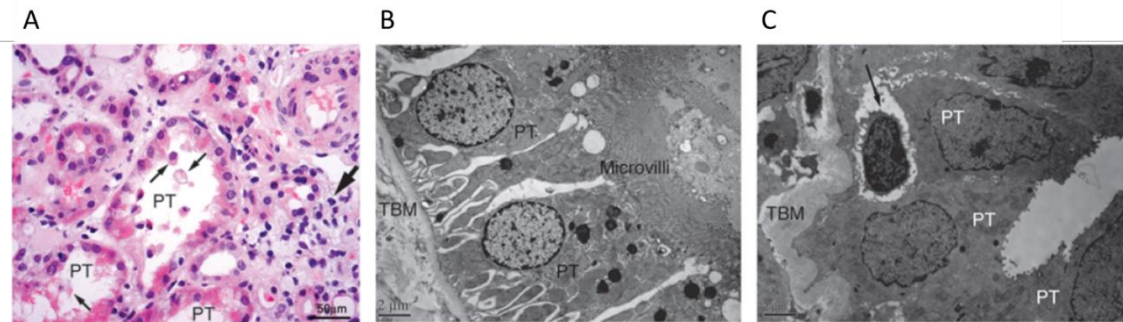
Figure 5. Pathology after ischemia in humans. A) Outer medulla in human ischemic AKI. The proximal tubules (PT) lose brush border, and cells are released into the lumen (thin arrows). Inflammatory cells are seen in the interstitial compartment (thick arrow). Light microscopy: original magnification, ×400; scale bar: 50 µm. B) Electron microscopy sections through normal human proximal tubules. C) In ischemic AKI, lymphocytes are seen infiltrating into the tubule wall (arrow). Scale bars: 2 µm (B–C). TBM, tubular basement membrane. (Adapted by Bonventre and Yang, *J Clin Invest.* 2011)[15].

1.C.III. Tubular cell injury

Ineffective kidney perfusion causes a depletion in intracellular ATP, which is required for essential processes. This reduction leads to cell injury and, if severe enough, cell death by necrosis or apoptosis (Figure 6)[35]. All segments of the nephron can be affected during an ischemic insult, but the most commonly injured epithelial cell is the PT cell. These cells are susceptible to injury for several reasons. As a matter of fact, this cell type has a high metabolic rate required for mediating ion transport and a limited capacity to undergo anaerobic glycolysis. Also, owing to the unique blood flow in the outer stripe of the S3 segment of the nephron, there is marked microvascular hypoperfusion and congestion in this region after injury, which persists and mediates continued ischemia even when cortical blood flow might have returned to near-normal levels[35]. Endothelial cell injury and dysfunction are primarily responsible for this phenomenon, known as the extension phase of AKI (Figure 6)[36].
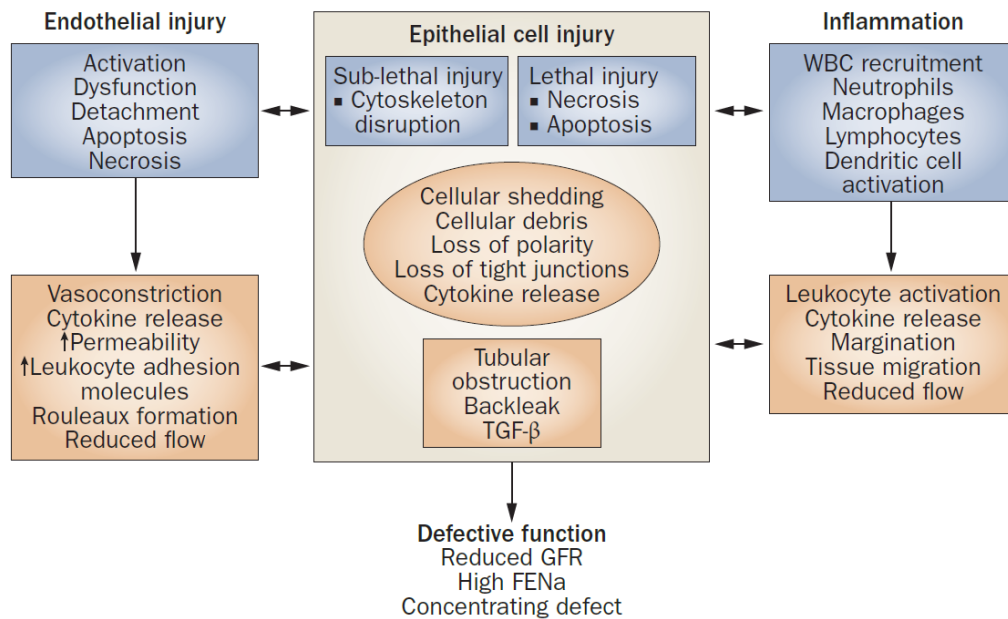
Figure 6. Pathogenesis of ischemic AKI. The major pathways of GFR impairment in ischemic acute tubular injury are caused by ATP depletion in vascular and tubular cells. Numerous interactions exist between endothelial cells, WBCs,and epithelial cells in the pathophysiology of ischemic AKI. These interactions are bidirectional between the cells involved, and result in specific functional and structural alterations. Inflammatory mediators released from proximal tubular cells influence endothelial cell processes (e.g. increase vasoconstriction and expression of cell adhesion molecules) that in turn influence the interactions between WBCs and endothelial cells, leading to reduced microvascular flow and continued hypoxia within the local environment. Abbreviations: AKI, acute kidney injury; TGF-β, transforming growth factor β; WBC, white blood cell. (Adapted by Sharfuddin and Molitori, *Nat. Rev. Nephrol*, 2011)[35].

A hallmark of ischemic injury is loss of the apical brush border of proximal tubular cells. Disruption of microvilli and their detachment from the apical cell surface leads to formation of membrane-bound 'blebs' early following ischemia that are released into the tubular lumen (Figure 5 & 6)[35]. Detachment and loss of tubular cells exposes areas of denuded basement membrane, resulting in focal areas of proximal tubular dilatation, as well as formation of distal tubule casts[37]. The sloughed tubular cells, brush border vesicle remnants, and cellular debris in combination with uromodulin form these granular casts, which have the potential to obstruct the tubule lumen, leading to no GFR in that functional unit[38]. Necrotic cell death is rare and restricted to the highly susceptible outer medullary regions, whereas features of apoptosis are commonly seen in both proximal and distal tubular cells[39].

The actin cytoskeleton has an integral role in maintaining cell structure and function, polarity, endocytosis, signal transduction, motility, movement of organelles, exocytosis, cell division, migration, barrier function of the junctional complexes, and cell–

matrix adhesion[40]. Maintaining the integrity of the cytoskeleton is especially important for proximal tubular cells in which amplification of the apical membrane by microvilli is essential for normal cell function. Depletion of cellular ATP leads to rapid disruption of apical F-actin by depolymerization mediated in part by cofilin, and redistribution of the cytoskeletal F-actin core. This disruption causes instability of the surface membrane and formation of membrane-bound extracellular vesicles or blebs that are either exfoliated into the tubular lumen or internalized to potentially be recycled[41–45].

The disruption of the actin cytoskeleton also leads to the loss of tight junctions and adherens junctions. These junctional complexes actively participate in numerous functions, such as paracellular transport, cell polarity, and cell morphology. Early ischemic injury results in opening of tight junctions, leading to increased paracellular permeability and backleak of the glomerular filtrate into the interstitium[35].

1.D. PRINCIPAL PHYSIOLOGICAL PROCESSES ASSOCIATED TO RENAL IRI

1.D.I. Cell death and apoptosis

The early phase of most kidney disorders is characterized by injury-associated cell death, a process that is often mediated by intracellular production of reactive oxygen species (ROS)[46]. Progenitor and stem cells have a higher resistance to oxidative stress-induced cell death than differentiated cells and this resistance is an important component of the regenerative capacity of tissues[47]. During the later phases of injury, cytokines drive parenchymal cell injury via specific outside–in signalling pathways that lead to programmed forms of cell death, including caspase-1 and caspase-11-mediated pyroptosis, caspase-8-mediated extrinsic apoptosis and receptor-interacting serine/threonine protein kinase 1-mediated necroptosis[48]. It is well established that several forms of necrosis are regulated processes and different molecular pathways of regulated necrosis have been described. The main difference between apoptosis and necrosis is that apoptosis is not inflammatory because the integrity of the plasma membrane is maintained; while in necrosis plasma membrane integrity is lost leading to the release of molecules that trigger inflammation and immunogenic responses[49].

1.D.II. Inflammation

Inflammation is vital for host defense against invasive pathogens. In response to an infection, a cascade of signals leads to the recruitment of inflammatory cells, particularly innate immune cells such as neutrophils and macrophages[50].These cells, in turn, phagocytose infectious agents and produce additional cytokines and chemokines that lead to the activation of lymphocytes and adaptive immune responses. Similar to the eradication of pathogens, the inflammatory response is also crucial for tissue and wound repair[51]. Inflammation as a result of trauma, ischemia–reperfusion injury or chemically induced injury typically occurs in the absence of any microorganisms and has therefore been termed 'sterile inflammation' (Figure 7). Similar to microbially induced inflammation, sterile inflammation is marked by the recruitment of neutrophils and macrophages and the production of proinflammatory cytokines and chemokines, notably tumor necrosis factor (TNF) and interleukin1 (IL1). Although inflammation is important in tissue repair and eradication of harmful pathogens, unresolved, chronic inflammation that occurs when the offending agent is not removed or contained can be detrimental to the host. The production of reactive oxygen species (ROS), proteases and growth factors by neutrophils and macrophages results in tissue destruction, as well as fibroblast proliferation, aberrant collagen accumulation and fibrosis. In IRI, as seen with myocardial infarction and stroke, the restoration of blood flow causes further tissue destruction as a result of neutrophilic infiltration, enhanced production of ROS and inflammatory responses to necrotic cells[52]. Despite the growing list of sterile immune stimuli, the mechanisms by which these stimuli trigger an inflammatory response are still not fully understood.
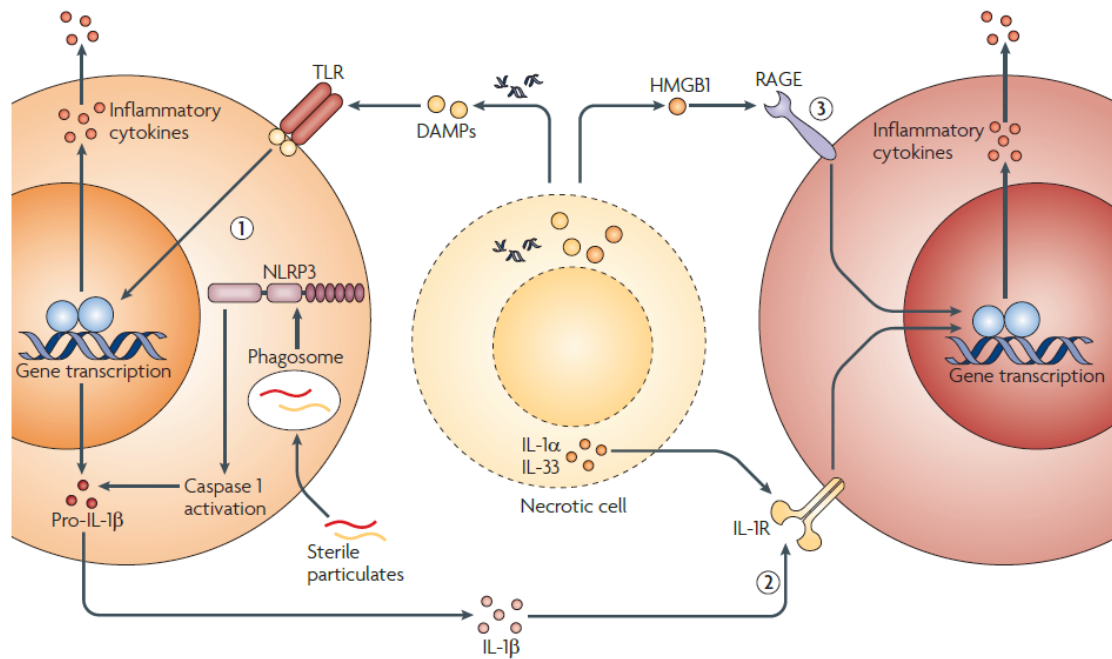
Figure 7. Mechanisms for inducing sterile inflammation. Sterile stimuli that include damage-associated molecular patterns (DAMPs), sterile particulates and intracellular cytokines released from necrotic cells can activate the host immune system to induce sterile inflammation through at least three pathways that are not mutually exclusive. DAMPs and sterile particulates can active host pathogen recognition receptors (PRRs), such as the Toll-like receptors (TLRs) and the nucleotide-binding oligomerization domain (NOD)-like receptor NLRP3 (NOD-, LRR- and pyrin domain-containing 3), which are also used by the host to sense microorganisms. Activation of these receptors results in the upregulation of cytokines and chemokines, such as interleukin-1β (IL-1β), which are released to recruit and activate additional inflammatory cells (1). Intracellular cytokines such as IL-1α and IL-33 that are released by damaged, necrotic cells activate signalling pathways downstream of PRRs (2). Endogenous DAMPs signal directly through host receptors that are not typically considered to be PRRs or to be involved in microbial detection (3). HMGB1, high-mobility group box 1; IL-1R, IL-1 receptor; RAGE, receptor for advanced glycation end-products. (Adapted by Chen and Nunez, *Nat Rev Immunol*, 2010)[50].

1.D.II.1   *Chemokines in renal injury*

Chemokines are a group of chemotactic cytokines that bind to G-protein–coupled receptors (GPCR) and act as potent attractants for leukocytes in acute and chronic inflammation. Chemokines and their corresponding receptors are expressed in different cell types (Figure 8)[53,54]. In kidneys, endothelial cells, podocytes, mesangial cells (MCs), tubular epithelial cells, and interstitial fibroblasts can also produce inflammatory chemokines upon stimulation[55,56].

In the normal kidney, production of inflammatory chemokines is low, but is significantly increased under pathophysiological circumstances such as ischemia, toxin exposure, or acute inflammation[56]. Proinflammatory cytokines, such as TNF and IL-1, and reactive oxygen species are major mediators responsible for chemokine expression [53,56] through the NF-kB pathway[57], including connective tissue growth factor-stimulated NF-B[58]. Inflammatory chemokines are also induced by other mediators, including cyclic adenosine monophosphate, growth factors such as PDGFB, basic fibroblast growth factors, pathogen associated molecules such as lipopolysaccharides, Ig aggregates, LDL, IFN-, and vasoactive substances like angiotensin II, or under diabetic conditions. Activation of TGF/Smad2,3 signaling during renal inflammation also produces a chemotactic effect on macrophages by inducing monocyte chemoattractant protein-1 CCL2 expression[53,59–61].

Rapid accumulation of neutrophils and monocyte/macrophages in injured kidney is an essential feature of the innate immune response induced by IRI[62]. Several chemokine families show a strong relationship to AKI, including the CXCL subfamily CXCL8, CXCL1 and CXCL2 that act primarily on neutrophils (Figure 8), the CCL subfamily), the CX3CL subfamily that have specific effects on monocytes and monocyte-derived lineages, and CCL5 that operate more broadly to attract cells monocytes and lymphocytes (Figure 8)[63].
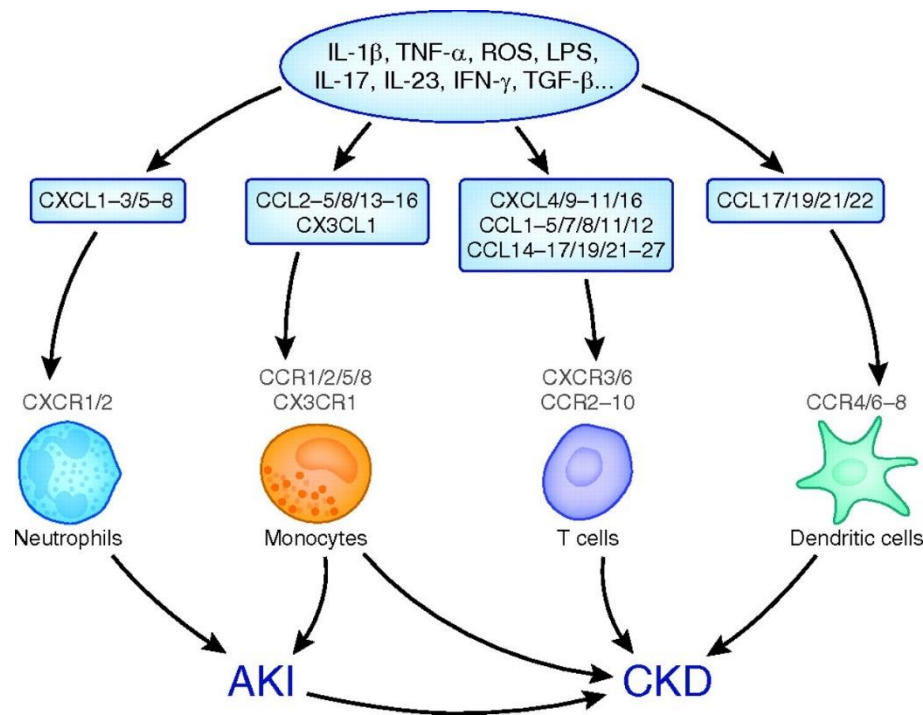
Figure 8. Interaction of chemokines and receptors on leukocyte subsets during acute and chronic kidney injury. Kidney diseases are characterized by the accumulation of various leukocyte subsets that are controlled by chemokines through their corresponding receptors expressed by the different subsets. Although infiltration of neutrophils and monocytes mediate acute kidney injury, activation of T cells, macrophages, and dendritic cells promote progression of chronic kidney disease. (Adapted by Chung, JASN 2011)[64].

1.D.III. Resolution of inflammation

The resolution of inflammation is an active process that reduces the production of proinflammatory and cell-death-inducing mediators[65]. Removal of the injurious trigger is one of the most important mechanisms that drives the resolution of inflammation and enables tissue regeneration[66].

Upon first activation, most immune cells upregulate immunoregulatory proteins. This is a process that limits immunopathology and promotes the secretion of anti-inflammatory cytokines[67]. This immunoregulatory mechanism is observed in infiltrating macrophages, which first acquire a proinflammatory phenotype (M1) in response to DAMP-rich environments, a process driven by TLRs and TNF receptors[68]. Subsequently, M1 macrophages upregulate proteins that counter-regulate proinflammatory signalling pathways[69,70]. This process deactivates these proinflammatory cells and induces a phenotype switch towards alternatively activated M2 macrophages. M2 macrophages

secrete anti-inflammatory and proregenerative mediators, such as IL-10 and TGF-β[68,71].These cytokines alter expression of numerous genes, resulting in downregulation of proinflammatory mediators and induction of growth factors that promote tissue regeneration and repair[65].

1.D.IV. Regeneration

Regeneration enables injured tissues to re-establish homeostasis; hence, the regeneration process involves factors that promote homeostasis. Homeostatic chemokines and their atypical chemokine receptors coordinate important aspects of homeostasis and wound healing, such as stem cell homing, vasculogenesis and epithelial and mesenchymal repair[72].

The mononuclear phagocyte system is involved in all phases of tissue injury including regeneration[73]. Several mononuclear phagocyte-derived cytokines not only have immunosuppressive effects, but also enhance the repair process. The best known of these cytokines is TGF-β, which has immunosuppressive effects and enhances the repair process in some tissues, but drives Smad7-mediated podocyte loss and renal scarring via activation of mesangial cells and/or fibroblasts in the kidney[74–76]. Similarly, post-ischemic tubules secrete DAMPs that activate TLR4 on renal dendritic cells, which is followed by secretion of IL22 that promotes tubule recovery (Figure 9)[77]. M2 macrophages in healing kidneys also secrete Wnt ligands (such as Wnt7b) that accelerate tubule recovery by activating Wnt signalling pathways[78]. In this way, the resident and infiltrating cells of the immune system actively support the regeneration process.

Lymphocytes, including CD4 T cells, natural killer T cells, natural killer cells and B-1 cells, contribute to tissue injury and inflammation in AKI[79–83]. For example, B-1 cells migrate to the post-ischemic kidney and differentiate into plasma cells. As this process limits tubule regeneration, B-cell depletion improves AKI recovery[82]. However, lymphocyte infiltrates do not always indicate tissue inflammation and injury. Several lymphocyte subsets with anti-inflammatory properties that promote kidney healing and repair have been described[84]. The best characterized of these are CD4$^+$,CD25$^+$ and Regulatory T cells (Tregs), which actively promote the regeneration process by suppressing innate immunity in the injured kidney[85,86].

The mechanisms of tubule regeneration are not yet fully understood. However, studies have shown that tubule recovery is, therefore, likely only possible when several intratubular cells with a substantial regenerative capacity survive the injury. Certain subpopulations of tubular epithelial cells have higher stress resistance than others because they cycle less often and express antiapoptotic genes similar to quiescent stem cell populations[87–90]. These potential progenitor cells called scattered tubular cells (STC), which express tubular and stem cell markers (e.g. CD24+/CD133+, vimentin, Kidney Injury Molecule-1 (KIM-1)), are scattered along the proximal and distal tubule in humans and rodents[90–95].
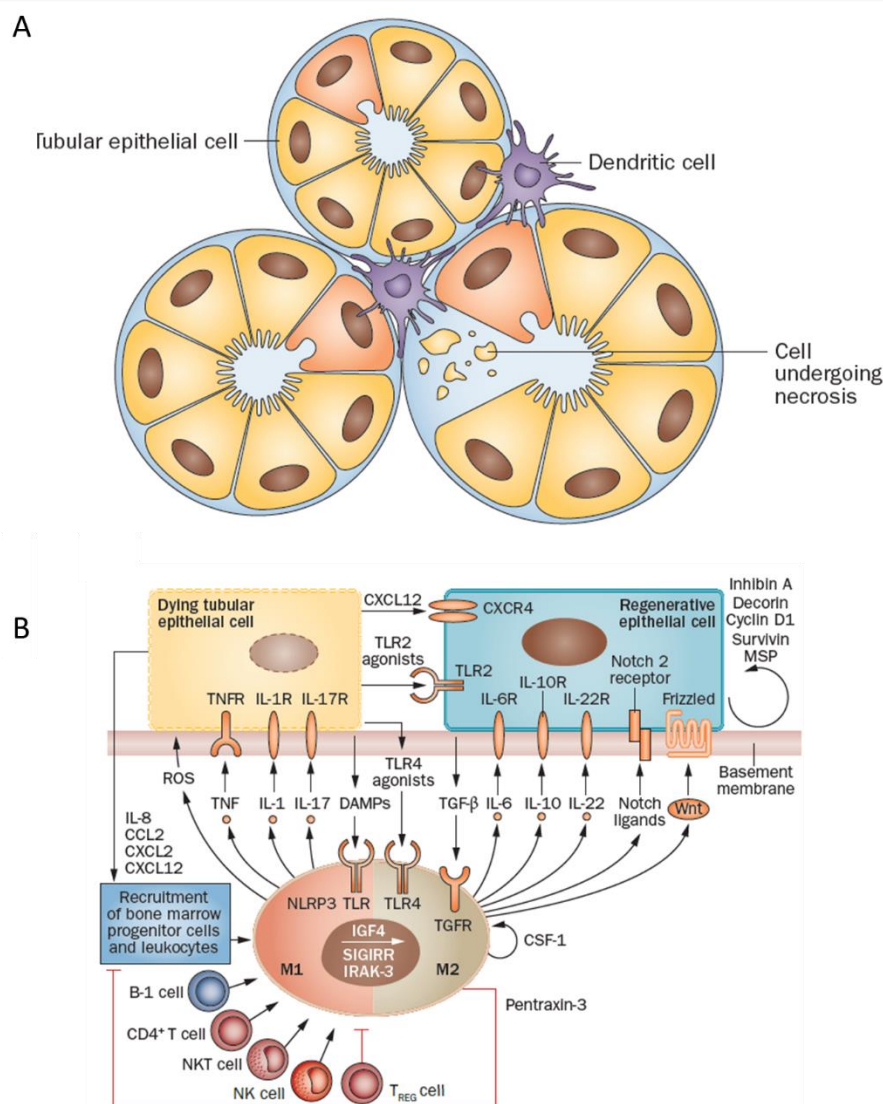
Figure 9. Intrarenal immune cells modulate tubule regeneration. A) Damaged tubule with infiltrating dendritic cells. B) In the early phase of acute tubular necrosis, the injurious trigger induces necrosis and apoptosis via induction of oxidative stress. Dying tubular epithelial cells release DAMPs, which activate proinflammatory M1 macrophages. These macrophages secrete ROS and proinflammatory cytokines that stimulate necroptosis of tubular epithelial cells. The

dying cells release chemokines, which recruit progenitor cells and leukocytes to the site of injury, and CXCL12 and TLR2 agonists, which activate the regenerative capacity of surviving tubular epithelial cells. Infiltrating CD4+ T cells, NKT cells, NK cells and B-1 cells contribute to tissue injury and inflammation, whereas TREG cells suppress innate immunity and promote regeneration. M1 macrophages can undergo a phenotypic switch to anti-inflammatory, proregenerative M2 macrophages. Autocrine effects of CSF1 induce local expansion of M2 macrophages. TLR4 agonists released by dying cells stimulate M2 macrophages to secrete mitogenic cytokines that accelerate tubule re-epithelialization. Notch ligands released by M2 macrophages and autocrine effects of other factors enhance tubular epithelial cell proliferation. E3 ubiquitin-protein ligase Mdm2 and mammalian target of rapamycin signalling also promote proliferation of tubular epithelial cells with regenerative potential. (Adapted by Anders, *Nat Rev Nephrol*, 2014).

1.E.   Sex differences in biomedical research

Very recently, the scientific community has acknowledge the importance of including the sex as a biological variable not only in experimental but also in clinical studies[96]. Several factors such as the susceptibility to develop a disease, the severity and the progression of the disease actively depend on sex[97]. Sex is now a variable that is started to be included in research studies in a more systematic way.

In Europe, the Horizon 2020 (Research and Innovation program) has put effort to consider the sex and/or gender in the design and realization of research projects. Case studies developed in the Gendered Innovations project demonstrate that integrating sex and gender analysis into research sparks creativity by offering new perspectives, posing new questions, and opening new areas to research.

1.E.I.   Sex hormones biosynthesis

The primary male sex hormone is testosterone. Testosterone is a steroid hormone from the androgen group. Testosterone, is synthesized from cholesterol (Figure 10) precursor in the Leydig cells in the testes and secreted into the circulation, where it tends to bind to plasma proteins[98]. Testosterone is primarily secreted in the testes of males and the ovaries of females although small amounts are secreted by the adrenal glands. Only a small percentage (< 1%) of circulating testosterone exists as unbound or free testosterone. The majority, approximately 60%, is bound to sex hormone binding globulin (SHBG) with high affinity, while the remainder is loosely bound to albumin. Both the albumin-bound and free fractions may be biologically active, while SHBG effectively inhibits testosterone action[99,100]. Measurement of the free or unbound fraction of serum

testosterone has been proposed as a means of estimating the physiologically bioactive hormone[101].

The primary female sex hormone is 17β-estradiol (EST) (Figure 10) Estrogen is produced mainly by the ovary, placenta, and in smaller amounts by the adrenal cortex and the male testes. Estradiol is secreted into the blood stream where 98% of it circulates bound to SHBG. To a lesser extent it is bound to other serum proteins such as albumin. Only a tiny fraction circulates as free hormone or in the conjugated form[102]. EST can be synthetized either by testosterone oxidation catalyzed by aromatase cytochrome P- 450, or by aromatization of androstenedione to estrone, another estrogen, which is further reduced to EST through 17β-Hydroxysteroid Dehydrogenase activity[103,104].
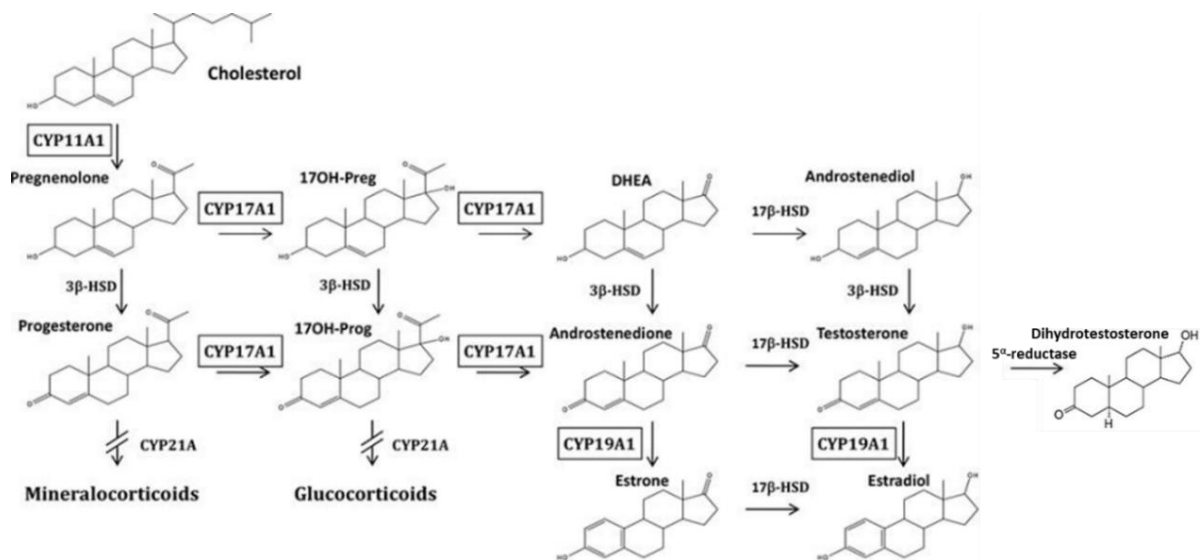
Figure. 10. Sex hormone biosynthesis pathway in vertebrates. (Adapted by Goldstone et al., *Mol Phylogenet Evol.,* 2016)[105].

1.E.II. Sex hormone signaling

Sex hormones primary interact with their specific nuclear receptors to form a nuclear co-activator or co-repressor complexes, which leads to subsequent transcriptional activation or suppression of specific target genes. This process is termed genomic signaling. In turn, non-genomic actions of sex hormones are initiated at binding sites on the plasma membrane, in cytoplasm or organelles and do not primarily require formation of intranuclear receptor protein-hormone complexes[106].

1.E.II.1   Estrogen signaling

Genomic actions of estrogens are mediated by their binding to nuclear estrogen receptors (ER) in target cells, which are activated and act as transcription factors to regulate the expression of target genes, Estrogen activity regulate molecular processes such as cell growth, cell differentiation and homeostasis[107]. Non-genomic "rapid effects" also occur in subpopulations of ERα and ERβ that are in the plasma membrane. Their activation induces a variety of intracellular signaling cascades[108,109]. It is known that non-genomic actions of estrogens involve rapid changes in cAMP, activation of epidermal and insulin-like growth factor receptors (EGFR and IGFR), recruitment and activation of MAPK/ERK signaling cascade, and induction of PI3K/AKT signaling to activate eNOS[108,110–112].

1.E.II.2   Androgens signaling

Genomic effects of testosterone are facilitated by its conversion to DHT through 5α-reductase activity and binding to the androgen receptor (AR), which translocate to the nucleus and acts as a transcription factor. The AR-mediated transcriptional activation is central to the development and proliferation process to maintain physiological homeostasis[113]. Moreover, in a non-genomic signaling, androgens can stimulate rapid ERK phosphorylation and activation after interacting with the G- coupled receptor GPRC6A on the cell membrane[114,115]. Also, androgen activation of membrane localized AR leads to rapid transactivation of EGFR and, as a consequence, activation of MAPK/ERK and AKT pathways[116,117] (Figure 11).

Both androgens and estrogens have shown to trigger genomic and non-genomic events within the renal cortex and in renal tubular cells in culture[118,119].
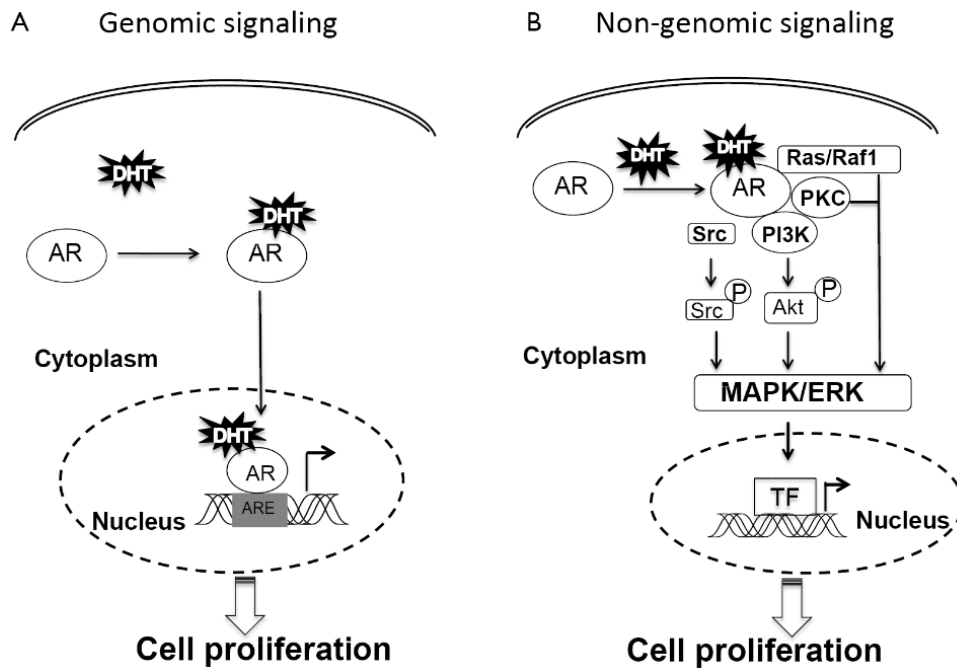
Figure 11. Genomic and non-genomic AR signaling in prostate cancer cells. A) Genomic AR signaling. After binding with the activated form of androgen, 5α-dihydrotestosterone (DHT), AR undergoes a conformational change and translocates to nucleus. In the nucleus, AR binds to the androgen response elements (AREs) on promoter/enhancer regions, recruits coregulators, and forms the transcriptional machinery for AR-regulated gene expression; B) Non-genomic signaling. Activated AR in the cytoplasm can interact with several signaling molecules including the phosphatidyl-inositol 3-kinase (PI3K)/Akt, Src, Ras-Raf-1, and protein kinase C (PKC), which in turn converge on mitogenactivated protein kinase (MAPK)/extracellular signal-regulated kinase (ERK) activation, leading to cell proliferation. (Adapted by Liao *et a*l., *Transl Androl Urol*, 2013).

1.E.III.   Sexual dimorphism of immune responses

The sexual dimorphism of the immune functions is a crucial element that little focus has been put on so far in the field of immunotherapy[120]. Differences observed affect both innate and adaptive immune responses, leading to a considerable functional diversity between females and males[121]. Sex variations include the number and activity of cells as well as intracellular and extracellular signals orchestrating the two branches of immunity (Figure 12).

In general, women exhibit higher CD4+ T cell counts than men[122]. In the innate context, females own APCs that perform antigen presentation more vigorously, have neutrophils and macrophages endowed with higher phagocytic activity, and show a higher frequency of both progenitors and mature group 2 innate lymphoid cells (ILCs), key regulators of type-2 inflammatory responses[123]. On the contrary, males exhibit enhanced numbers of NK cells[121]. In the adaptive context, females exhibit higher CD4+

T cell counts associated with an increased CD4$^+$/CD8$^+$ T-cell ratio, along with Th2 prevalence, and greater proliferation and cytotoxicity of T cells. In contrast, males have higher CD8$^+$ and Treg cell counts associated with Th1 dominance, lower B cell numbers and basal immunoglobulin levels along with weaker antibody responses[124]. Both hormonal and genetic differences concur in the sexual dimorphism of the immune system. The EST-ER axis is a key regulator of innate immune populations. E2 reduces mobility and inflammatory activity of neutrophils, and female mMDSCs seem to be more suppressive than the male counterpart[125,126].

♂ Innate immunity
- ↑ NK counts
- ↑ neutrophils mobility and inflammatory activity

♀ Innate immunity
- ↑ DC antigen presentation
- ↑ DC production of IFNγ
- ↑ macrophages phagocytic activity
- ↑ neutrophils phagocytic activity
- ↑ MDSCs suppressive function
- ↑ frequency of ILCs

♂ Adaptive immunity
- ↑ CD8+ T cell counts
- ↑ IL-17 production by CD4+ T cells
- ↑ Treg cell counts
- ↑ Th1 cell functions
- ↓ B cell counts
- ↓ basal immunoglobulin levels
- ↓ antibody responses

♀ Adaptive immunity
- ↑ CD4+ T cell counts
- ↑ activated and proliferating CD4+ T cells
- ↑ IFNγ production by CD4+ T cells
- ↑ activated and proliferating CD8+ T cells
- ↑ CD8+ T cell cytotoxic activity
- ↑ CD4+/CD8+ T cell ratio
- ↑ Th2 cell functions

Figure 12. Sexual dimorphism of the immune responses. Immune components of both innate and adaptive immunity are differently regulated in females and males. Apparently, females display higher capability of mounting type-2 versus type-1 immune responses, whereas males seem to prefer type-1 immune responses, of which many traits are still unclear. As a matter of fact, the difference of the strength of type-1 immunity between sexes is smaller than that of type 2, preserving the onset of female inflammatory cell-mediated immune responses. (Adapted by Capone et al, *Front. Immunol.*, 2018)[127].

1.E.IV. Sexual dimorphism in renal diseases

Several lines of evidence indicate that there are sex differences in the incidence and severity of cardiovascular and renal disease. Men are more prone to acute and chronic kidney disease and to progresses to ERSD than women, when all-cause

incidence rates are considered[128]. Clinically, an increased mortality rate has been documented among males with acute renal failure. Studies looking at outcomes in AKI patients have shown that men have twice the mortality of women and have found that sex is an independent predictor of mortality in AKI[129–131]. Consistent with the clinical studies in AKI, animal studies have also shown females to be protected against renal IRI[132–134]. Experimental evidence suggests that testosterone increases renal vascular resistance and the extent of renal damage in response to renal IRI[135]. Differences in the severity of kidney injury have been observed between male and female mice in response to tunicamycin, an ER stress agent. Protein markers of ER stress and apoptosis were higher in tunicamycin-treated male mice and testosterone-treated females indicating that kidneys of males are much more susceptible to ER stress-induced acute kidney injury than those of females[136]. Though association of these pathways with gender differences in renal IRI has been found, further research is needed to prove their mechanistic involvement in the sex differences noted.

1.E.V. Sexual dimorphism in kidney transcriptome

Most mammals exhibit obvious phenotypic differences between the male and female sexes, and many of the hormonal, chemical, and anatomical differences between males and females have been well investigated. It is expected that the hormonal and chemical differences between males and females should ultimately result in differential gene expression, which in turn should control mammalian behavior and physiology.

To gain a better understanding of the molecular differences between mammalian sexes, years ago, Rinn *et al.*, performed DNA microarrays to identify differences in the adult male and female kidney transcriptomes. A total of 27 genes were found to have sex-specific expression (Figure 13)[137]. These genes primarily belong to three categories: drug and steroid metabolism, osmotic regulation, and uncharacterized. Together, these results indicated an abundance of genes differentially expressed by sex in the kidney.
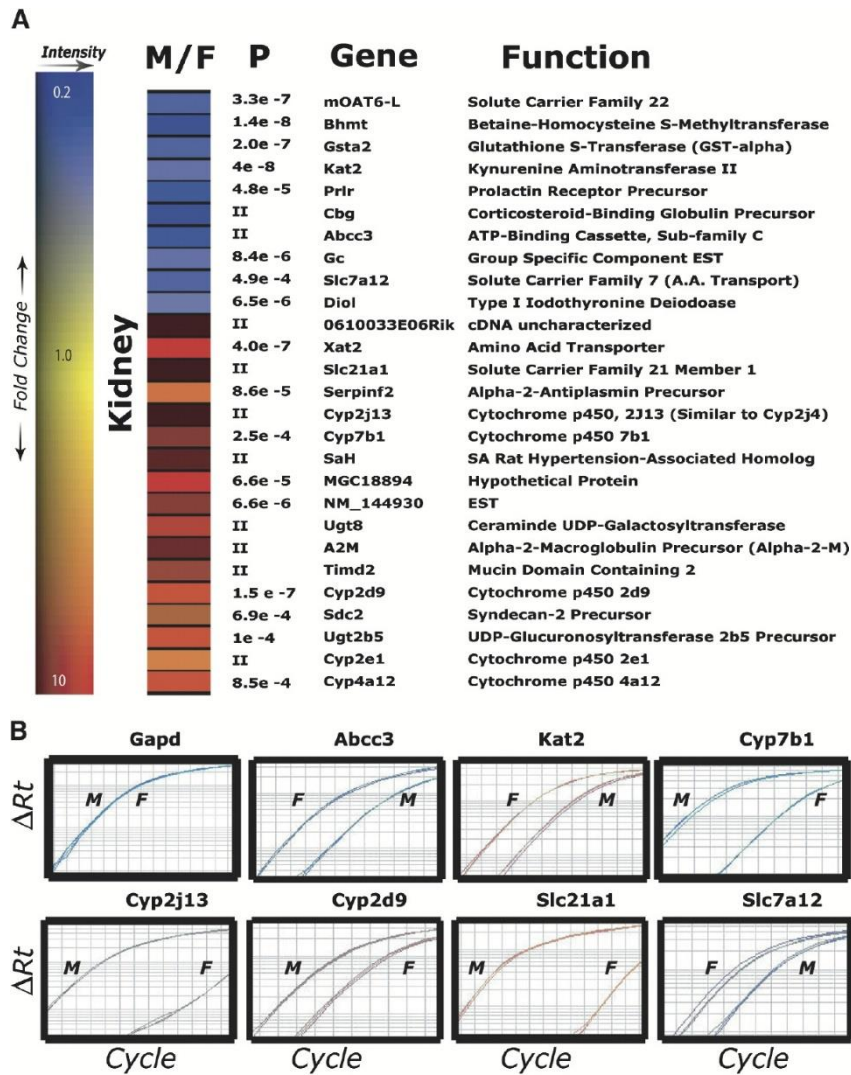
Figure 13. Extensive Sex-Specific Expression in the Kidney. A) Twenty-seven genes were differentially expressed by sex in the kidney. One-quarter, seven, of these genes are drug and steroid metabolism genes. The rest are mainly comprised of osmo-regulation genes or genes with yet unresolved cellular roles. Shades of blue represent the degree to which expression in the male is lower than the female median expression level (female-specific expression). Shades of red indicate the degree to which expression in the male is above the female median expression level (male-specific expression). The brightness of the color represents the amount of expression. p values of differential expression between sexes are also listed. B) The expression of seven genes in the kidney using quantitative real-time PCR was independently verified. Each reaction was performed in triplicate. ΔRT represents the amount of pooled cDNA amplified in the reaction per cycle. 100% of the randomly selected genes demonstrated the same sex-specific expression pattern observed in the microarray data.(Adapted by Rinn et al., *Dev Cell.*, 2004)[137].

1.F.   ANIMAL MODELS OF RENAL IRI

In vitro models, including renal cell cultures, isolated renal tubules, and isolated perfused kidneys, are valuable for the research of the pathophysiological mechanisms of ischemic AKI. Nevertheless, *in vivo* whole animal models are indispensable, because of the limitation of the *in vitro* models to mimic the complexity of human body[138]. Since the 1960s, various animal models of ischemic AKI have been developed and tested, and currently, two kinds of warm renal IRI models are mainly used: bilateral renal IRI[134,139,148–157,140,158–167,141,168–177,142,178–185,143–147] and unilateral renal IRI[186,187,196–202,188–195]. Depending on whether the contralateral kidney is removed, the unilateral model can be further divided into two subtypes: unilateral IRI with or without contralateral nephrectomy (Figure 14). The bilateral ischemic AKI model is commonly used, because it is considered more relevant to human pathological conditions where blood supply is normally affected in both kidneys[86,132,147,162,184,201,203–205].

Bilateral IRI

Unilateral IRI

- controlateral nephrectomy

+ controlateral nephrectomy
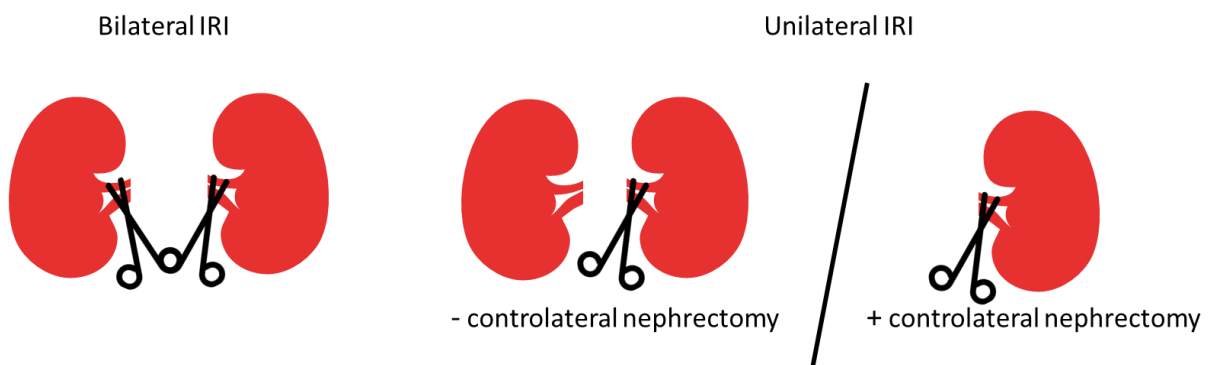
Figure 14. Different type of warm model of ischemia reperfusion injury. Two kinds of warm renal ischemia-reperfusion (IR) models are mainly used: bilateral and unilateral renal ischemia reperfusion. The unilateral model can be further divided into two subtypes: unilateral IR with or without contralateral nephrectomy.

1.F.I.   Rodent models

Mice have a lot of advantages as a model for kidney disease since they can reproduce injury that causes human disease (e.g. ureteric obstruction) and reproduce the consequences of renal injury (e.g. renal ischemia, reduction in renal mass). Moreover, rodent models have the advantages of the reduction in housing costs associated with their relative small size .and can provide with genetically modified

models (Tg and KO)[206]. In recent years, the mouse model of bilateral renal ischemic AKI has been optimized[207].

1.F.II. Porcine models

Large animal models are necessary to develop safe preclinical protocols directly transferable to human. Indeed, preclinical studies using pig or non human primate play an important role in the evaluation of new medical devices and pharmacological therapy efficacy before their use in clinical studies[208]. Pigs are like humans in respect of size, metabolism and renal anatomy. Analyses over 100 physiological variables in pigs in basal conditions, concluded that most porcine values are similar to humans and that some biochemical parameters, such as creatinine and blood urea nitrogen (BUN) are identical between pigs and humans[209]. Mini pigs, research breed of *Sus scrofa domesticus* are very popular for urological studies. They reach sexual maturity at around 4-5 months old corresponding to a body weight of 30 kg. Weight and size of the kidney at this age is similar to the kidney of a 70 kg human[210]. At the genomic level, the pig and human genomes have an extensive homology at the nucleotide level since swine are 3x more similar to humans than mice are to humans. Moreover, the pig genome is ~7% smaller than the human, while the mouse genome is 14% smaller[211,212].

In the context of a previous master thesis, our laboratory has established an *in vivo* renal IRI porcine model (Luis Castro Sader). Male and female mini pigs were subjected to 30 minutes of IRI, followed by 7 days of reperfusion (Figure 15A). The analysis of kidney tissues at different state of the experiment (before ischemia, 5 minutes following ischemia and 7 days after ischemia) revealed that upon renal IRI, male had more tubular damages than the females. Also, the infiltration of immune cells was more important in female tissues at basal state and following IRI (Figure 15B-C). These characteristics correlate with the sexual dimorphism observed in the human immune response[127]. Since the porcine phenotype greatly correspond to the human one, the study of pathological mechanisms involved in the injury and regeneration processes of pig tissues might help to better characterized the human sex differences in AKI.

Figure 15. Assessment of biochemical parameter and histological examination following porcine renal ischemia-reperfusion injury. A) Experimental design of renal unilateral IRI following contralateral nephrectomy. Ischemia was induced for 30 minutes and let to recover 5 minutes and 7 days. B) Blood urea nitrogen and creatinine blood levels reached a peak 24h after ischemia. The levels then drop as days of recovery passed. C) The levels of tubular injury and interstitial infiltration were scored by an expert pathologist and D) the animal were classified by group and sex. Male showed higher level of tubular damage, whereas females showed higher levels of interstitial infiltrates at basal situation and at recovery. (PR: pre-ischemia; PS: post-ischemia; WL: one week later) (master thesis Luis Castro Sader)

1.G. Renal cell carcinoma

1.G.I. Definition

Renal cancer is a disease in which kidney cells become malignant and grow out of control, forming a tumor. Almost all kidney cancers first appear in the lining of tubules in the kidney. This type of kidney cancer is called renal cell carcinoma (RCC). RCC is a heterogeneous group of cancers arising from renal tubular epithelial cells that encompasses 85% of all primary renal neoplasms[213,214]. The most common subtypes of RCC are ccRCC, papillary RCC (pRCC), and chromophobe RCC[213]. The remaining 15% of tumors of the kidney consist of transitional cell carcinoma (8%), nephroblastoma or

Wilms' tumor (5–6%), collecting duct tumors (<1%), renal sarcomas (<1%), and renal medullary carcinomas (<1%)[215].

1.G.II.   Epidemiology of RCC

Renal cell cancer is the third most prevalent urological cancer claiming more than 100,000 lives per year worldwide. The incidence of RCC varies widely in different parts of the world, and the highest incidences are in North America and the Czech Republic[214]. In the US, there are 64,000 new cases of RCC and 14,000 RCC-related deaths each year[216]. Age, ethnicity, and sex also play a role in this disease. RCC is more common in males above the age of 60 (median age for RCC is 65)[217]. Within the USA, Caucasians, African-Americans, Hispanics, and Native Americans have a higher incidence of RCC as compared with Asian-Americans or Pacific Islanders[218,219].

The clinical outcome of RCC patients is highly variable. Due to the lack of symptoms approximately one-third RCC patients have already an advanced disease at the time of diagnosis[220]. Furthermore, 25–30% of RCC patients treated for local disease develop metastasis. Radical or partial nephrectomy remain the only effective method of cure for localized disease[221]. The outcome of RCC patients with metastatic disease is poor with a 5 year survival rate of less than 5%. Treatment options have been limited due to the resistance to chemotherapy and radiation. Recently, the treatment of metastatic RCC has been revolutionized by the development of targeted therapies, in particular by tyrosine kinase inhibitors (sunitinib, sorafenib, pazopanib, axitinib), antiangiogenic agents such as bevacizumab, and mTOR inhibitors, which have been shown to increase the progression-free survival of RCC patients[222].

1.G.III. Etiology of RCC

Multiple risk factors for RCC along with their pathophysiologic mechanisms have been described. These include both genetic and acquired risk factors. The two most common genes involved in the pathogenesis of RCC are the Von Hippel–Lindau (VHL) gene and the protein polybromo-1 (PBRM-1) gene. The most common acquired risk factors for RCC are smoking, hypertension, obesity, chronic analgesic use, and diabetes[223].

1.G.IV. VHL and HIF-1α regulation

The product of the VHL gene is a protein called pVHL, which acts as a tumor suppressor protein. The VHL protein forms complexes with several other proteins in the cell, including elongin B, elongin C, and cellulin 2, to help in the proteasomal degradation of several intracellular proteins. One of the major functions of the VHL gene product is to regulate the levels of several intracellular proteins, including hypoxia-inducible factor 1 alpha and 2 alpha (HIF1A and HIF2A)[224,225]. These intracellular proteins, when bound with each other, serve as transcription factors by binding to the DNA, resulting in upregulation of messenger RNA (mRNA) that codes for several growth factors, including VEGF, PDGFB and TGF. These growth factors play a vital role in the development of highly vascular tumors (such as ccRCC) associated with VHL gene alterations.

Under normal oxygen tension, HIF1A and HIF2A are hydroxylated on proline residues and bind the pVHL, resulting in polyubiquitination of HIFA, which targets it for proteasomal degradation (Figure 16)[226,227]. Under conditions of hypoxia or in the absence of pVHL, hydroxylation of HIF1A and HIF2A does not occur and HIFA accumulates in the cell and dimerizes with hypoxia-inducible factor beta (HIFB). The HIFA–HIFB complex then migrates to the nucleus and acts as a transcription factor, resulting in increased mRNA levels coding for VEGF, PDGFB, TGF, erythropoietin, and extracellular matrix proteins[225,228]. This further suggests the regulatory role of HIF1A in promoting tumor progression, likely through hypoxia-induced VEGF expression pathways.
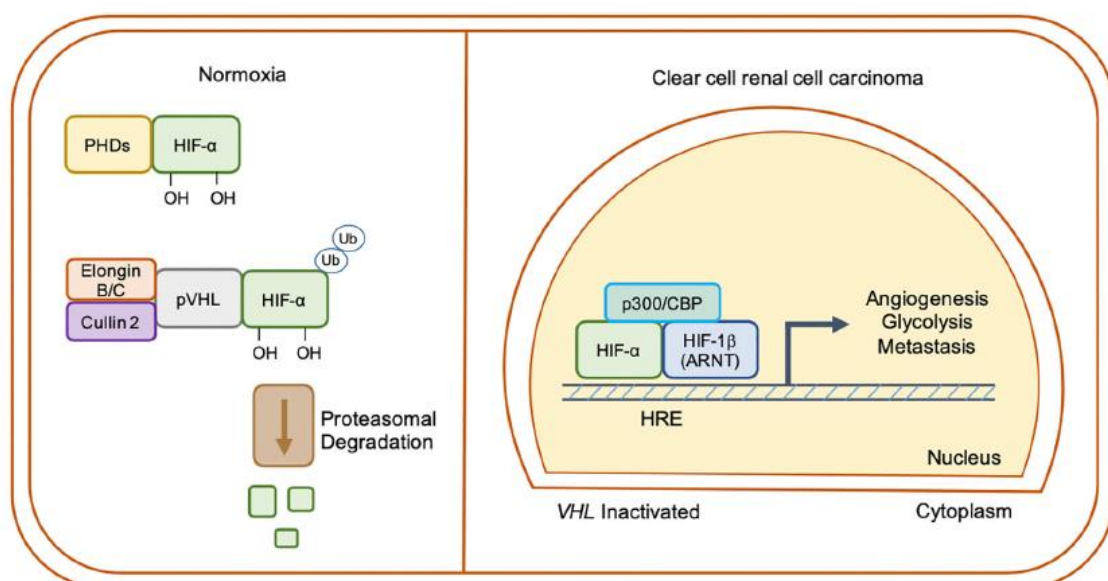
Figure 16. Regulation of hypoxia-inducible factor (HIF) signaling by the von Hippel-Lindau (VHL) tumor suppressor in normal and tumoral cells. Under oxygen-replete conditions, HIF-α subunits are hydroxylated by prolyl hydroxylases (PHDs) and then ubiquitinated by an E3-ubiquitin ligase complex containing pVHL, tagging them for proteasomal degradation. In hypoxia, or when VHL is inactivated (such as in ccRCC), HIF-α subunits escape degradation, translocate to the nucleus, and |heterodimerize with HIF-1β (ARNT). HIFs generally promote a transcriptional program favoring increased angiogenesis, glycolysis, and metastatic capabilities of ccRCC tumors. HRE = hypoxia response element. (Adapted by Sanchez *et al.*, *Biochim Biophys Acta Rev Cancer*, 2018)[215].

1.G.V. Kidney injury molecule-1

KIM-1 is a transmembrane tubular protein that is undetectable in normal kidneys. It is markedly induced in renal injury including AKI[229]. The ectodomain of KIM-1 can be shed and found in the urine and serum and many studies indicate that urinary KIM-1 is a sensitive and specific marker of kidney injury as well as a predictor of prognosis, since it has been implicated not only in the process of kidney injury but also in healing. In situ hybridization and immunohistochemistry revealed that KIM-1 was expressed in dedifferentiated and regenerative proximal tubular epithelial cells in damaged regions after toxic or ischemic injury, playing a role in the regeneration process of tubular epithelial cells, through which it can help reconstitute a continuous epithelial layer[230]. Expression of KIM-1 is also associated with tubulointerstitial inflammation and fibrosis. KIM-1 expressing PTEC play the role as the residential phagocytes, contribute to the removal of apoptotic cells and facilitate the regeneration of injured tubules. However, the precise mechanism of KIM-1 and its shedded ectodomain on restoration of tubular integrity after injury is not fully understood[231].

Human KIM-1 exhibits homology to a monkey gene, the hepatitis virus cell receptor 1, which was identified as a receptor for hepatitis A virus (HAVRC). It's worth mentioning that our group identified for the first time HAVRC/KIM-1 overexpression in ccRCC and described the role of this protein in dedifferentiation events correlating with scattering- and proliferating-related processes[232]. Clinical and functional correlations between HAVCR/KIM-1 expression, ectodomain shedding and ccRCC patient outcome indicated that unexpected, constitutive expression of HAVCR/KIM-1 in normal kidney counterparts of ccRCC tumors represents a susceptibility trait for ccRCC tumor development and that enhanced HAVCR/KIM-1 ectodomain shedding promotes an invasive phenotype *in vitro* and more aggressive tumors in vivo[233].

To examine the biologic function of KIM-1 effects in ccRCC, microarray assays on 769-P ccRCC–derived cells, with upregulated or silenced KIM-1 levels, were conducted and relevant KIM-1 targets were further analyzed in patients with ccRCC. It was found that KIM-1 induces the IL-6/STAT-3/HIF-1A axis in different ccRCC-derived cell lines, which depends on KIM-1 shedding[234]. We also observed that STAT3[Ser727] levels represent an independent prognostic factor to identify ccRCC patients with good or poor prognosis, among individuals classified under the same pathologic and clinical criteria. Accordingly, we conclude that constitutive expression of KIM-1 in normal parenchyma of ccRCC patients and further up-regulation in tumors might represent a novel mechanism to activate tumor growth and angiogenesis through activation of IL6/gp130/STAT3/HIF-1A pathway. STAT3[Ser727] has emerged as an independent prognostic factor for ccRCC patient follow-up[234]. It was postulated that the mechanisms triggered by KIM-1 in renal cancer might recapitulate those undergoing in proximal tubule injury and regeneration upon HAVCR/KIM-1 expression.

Moreover, TPMS technology, based on systems biology, who generates computer models able to reproduce a biological process and thus identify key proteins has been employed for the analysis of the transcriptomic data from KIM-1+ and KIM-1- ccRCC cell lines with the aim of identifying key proteins related to ccRCC and linked to KIM-1. The models created were analyzed through two strategies to identify key proteins related to KIM-1-associated pathways in ccRCC. One strategy employed was the model reversion: this strategy finds proteins whose modulation would turn the behavior of a model (in this case the models created using KIM-1 transcriptomic experiments) into the behaviour of another model (in this case Anaxomics default model without extra information) in respect of a process (ccRCC). The other strategy was the sinks and sources. This strategy allows the identification of the proteins from a set (differential proteins from the transcriptomic experiments) most affected by or that most affect another set of proteins (ccRCC).

Eighty-six proteins have been identified as key proteins associated with KIM-1 pathways involved in ccRCC after assessing the transcriptomic dada through the model reversion strategy (Figure 17) and sinks and sources strategy (Table I). It was found that the main branch linking the key proteins of KIM-1 modulation to ccRCC would be mediated through STAT3 and HIF1A and its downstream effectors, affecting cell proliferation, angiogenesis, apoptosis evasion and metastasis induction. Additional branches include RAS, MAPK and PI3K signaling, MTOR, TSC1, TSC2, PPARG, etc. They also include proteins involved in the metabolic reprogramming.

MODEL REVERSION

KIM-1 over-expression | | | KIM-1 silencing |

CBP	EPHB1	CDC73	CBP	NTRK1
LAT	EPHB2	BIRC5	LAT	TSC1
FOS	EFNB2	IL6	FOS	DDIT4
CDN1A	ITB8	ACE2	CDN1A	CFLAR
BEX3	RAF1	TGFB1	BEX3	TNR6
ERBB3	ITB2	IL1R1	ERBB3	RRAGD
HDAC1	ITAM	IL1R2	HDAC1	HS90B
PPARG	JAK2	THB	PPARG	VGFR1
AAPK1	RASK	NRP1	AAPK1	1433B
TIMP2	RASN	OXYR	NNMT	MMP2
IGF1R	CD19	FINC	NOV	CREB1
GCR	KLF5		APC	FOX
CD209	ILF3		FOXO3	ATF2
DNMT1	NR1I2		IRF1	KS6B2
PARP1	VDR		MTA1	NF1
			NFAC2	SMAD4
			STA5B	SUZ12
			TWST1	TGFB1

Proteins overlapping between KMI-1 over-expression and silencing

CBP
LAT
FOS
CDN1A
BEX3
ERBB3
HDAC1
PPARG
AAPK1

Figure 17. Key proteins identified in the KIM-1 over-expression and KIM-1 silencing reversion model. In the KIM-1 overexpression reversion, 41 proteins have been identified. In the KIM-1 silencing reversion, 36 proteins have been identified. Nine proteins overlap between the KIM-1 overexpression reversion and the KIM-1 silencing reversion. (Doctoral thesis Thais Cuadros)

Table I. Summary of key proteins identified through sources and sink model of KIM-1 over-expression and silencing data.

KIM-1 expression	Sources	Sinks
Over-expressed	**HIF1A**	**STAT3**
	STAT3	KITLG
	IRS1	PRKAG2
	HBEGF	**PPP2R2C**
	MDM2	TLR4
	H4	IRS2
Silenced		PPP2R3A
		IGF1R
	FGFR3	**VEGFA**
	HIF1A	GCR
	VEGFA	**FGFR3**
	PPP2R2C	**HIF1A**
		SOCS3
		SCF

* Proteins in bold, are both sources (affect ccRCC) and sinks (are affected by ccRCC). (Doctoral thesis Thais Cuadros)

2. RATIONALE

2. RATIONALE

Men are at higher risk of suffering AKI and for progression to CKD then women. The prevalence of renal cancer is also more elevated in men. Currently, it is accepted that the presence of androgens and not the absence of estrogens predisposes men to develop renal diseases and cancers (ccRCC). The sex differences that exist and greatly influence the physiology of diseases have recently received increasing attention from basic and clinical scientists as well from the European Union that has prioritized sex/gender research in the *Horizon 2020* program.

PT cells in the kidney are a prominent target in injury/regeneration processes and are also the cells from which ccRCC arises. PT cells and sex hormones play an important role in the inflammatory and immune regulatory responses that occur in AKI and cancer. We hypothesize that the molecular mechanisms that promote renal regeneration following injury and the ones that promote renal cancer are shared (Figure 18). We think that most pathways and targets involved are identic in both processes. For instance, KIM-1 is a good example of a target that plays a key role in both processes. A better comprehension of either process could help understanding better the regulation of both processes.
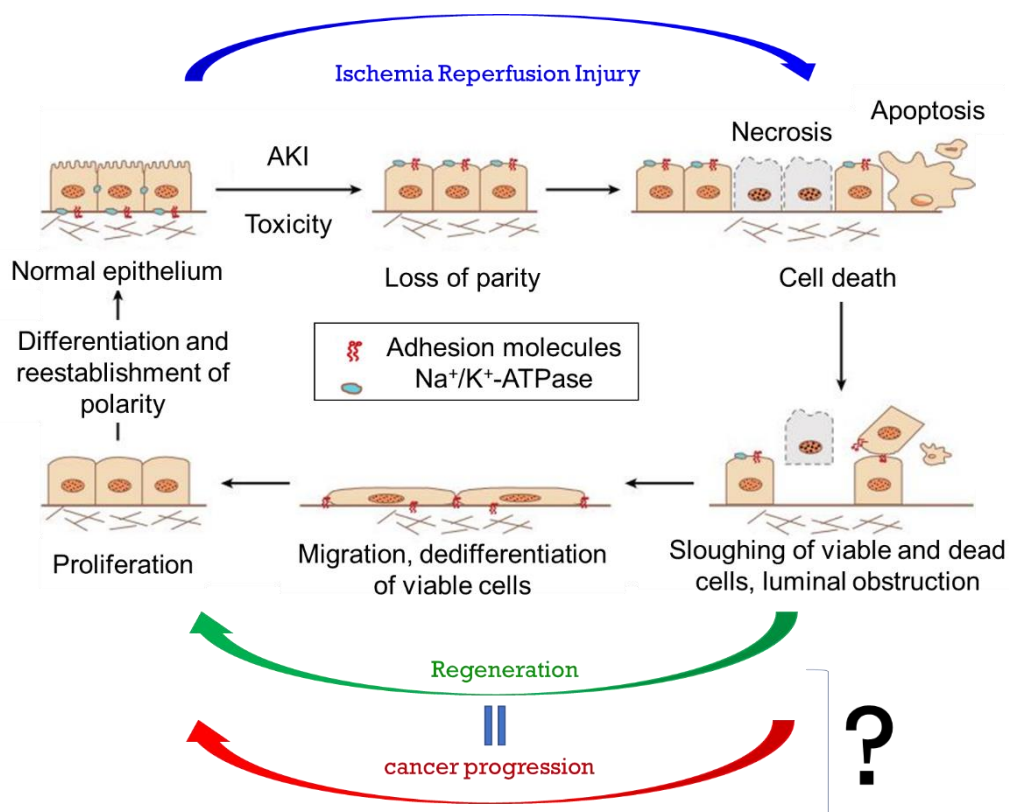
Figure 18. Schematic representation of cellular mechanisms of AKI and regeneration and the possible link with cancer. (Adapted from Vaidya et al., *Annu Rev Pharmacol Toxicol*, 2009)[235].

Therefore, this project aims to find targets other than KIM-1, participating in renal regeneration and in renal cancer processes. Moreover, we are also interested to see how these pathways are regulated by sex hormones. We plan to achieve this goal by a thorough analysis of transcriptomic of AKI and renal cancer data.

3. OBJECTIVES

3. OBJECTIVES

This doctoral thesis has the following objectives:

1. **To establish an *in vivo* renal IRI model that can be translatable to human.**

   1.1.   We perform a thorough analysis of kidney microarray data of mini pigs that underwent renal IRI, including characterization of selected targets.

   1.2.   We evaluate the molecular mechanisms up-regulated in porcine renal IRI in a time and sex sensitive way.

2. **To establish an accessible *in vivo* renal IRI model that can also mimic human pathology.**

   2.1.   We produce an *in vivo* mice model of renal IRI.

   2.2.   We compare mouse and porcine renal transcriptomic and protein expression following renal IRI.

3. **To validate pig renal IRI targets in human samples.**

   3.1.   We validate the expression pattern of selected targets found in the pig model in human ischemic and non-ischemic samples.

4. **To perform system biology analysis of renal IRI porcine microarray data.**

   4.1.   We perform system biology analysis of renal IRI porcine microarray data.

   4.2.   We establish *in vitro* models of IRI in PT cultured cells in order to validate selected target expression and the impact of sex hormones on the regulation of selected targets.

5. **To compare system biology analyses of renal IRI porcine microarray data and a cancer-derived cell line +/- KIM-1 kidney microarray data.**

4. MATERIALS AND METHODS

4.   MATERIALS AND METHODS

4.A.   *IN VIVO* IRI PORCINE STUDIES

Sections 4.A.I. and 4.A.II. were conducted in the context of Luis Castro Sader doctoral thesis.

4.A.I. RNA extraction

4.A.I.1   *Animals*

Different kidney biopsies of animals that underwent renal IRI treatment were obtained from a previous master thesis conducted in our laboratory. The biopsies originated from farm pigs, hybrids between Large White and Landrace. Five females, 5 males and one castrated male of 4 months old, free of specific pathogens, between 30–40 kg of weight were formerly obtained. This age was chosen due to the sexual maturity of the animal, allowing hormones effects. Multiple biopsies were obtained from the same animals at different time points (PR: pre-ischemia; PS: post-ischemia; WL: one week later). All animal care and procedures were performed in accordance with the requirements of the European laws on the protection of animals used for scientific and experimental purposes (86/609 EEC) and had the approval by the Experimental Ethics Committee of the Institut de Recerca Vall d'Hebron (34/08 EAEC).

4.A.I.2   *RNA extraction from kidney biopsies*

There are several methods to isolate RNA, however, the most common is acid guanidinium thiocyanate-phenol-chloroform extraction. In this study, this method was employed to extract total RNA from kidney tissues. RNA was extracted from different biopsies from the pig surgeries (PR, PS, WL) (Figure 15). The extractions were performed starting from 50 mg of each biopsy with the NZYol Kit following manufacturer instructions (NZYTech genes & enzymes).

4.A.I.3   RNA samples quality control

RNA integrity was assessed by Agilent 2100 Bioanalyzer (Agilent, Palo Alto, Ca). This system is an established automated electrophoresis tool for the sample quality control of biomolecules. This instrument provides highly precise analytical evaluation of various samples types in many workflows. In this study, only samples with similar RNA integrity number (RIN) were accepted for microarray analysis.

4.A.II. Microarray assays

4.A.II.1   Experimental design

The main goal of the study is to find differentially expressed genes (DEG) associated with ischemic tissues at different time-points, considering the sex of the individuals.

The experimental conditions to be considered in this analysis are:

3. Sex of the subject:

    -Male pigs (M)

    -Female pigs (F)

4. Time point of sample extraction (Time):

    -Pre-ischemia tissue (PR)

    -Post-ischemia tissue (PS)

    -A week after ischemia (WL)

In order to achieve the main goal of this study, specific objectives were organized, in the following groups of comparisons:

MATERIALS AND METHODS

1. <u>Time comparison</u>: (differences between each time-point accounting by sex:

 a) Between post-ischemic time point and basal time point (M.PS vs M.PR= M.PS - M.PR)/ (F.PS vs F.PR= F.PS - F.PR)

 b) Between recovery time point and post-ischemic time point (M.WL vs M.PS= M.WL - M.PS)/ (F.WL vs F.PS= F.WL - F.PS)

c) Between recovery time point and basal time point (M.WL vs M.PR= M.WL - M.PR)/(F.WL vs F.PR= F.WL - F.PR)

2. <u>Sex comparison</u> (differences between males and females at each time-point):

 a) with pre-ischemia tissues (M.PR vs F.PR = M.PR - F.PR)

 b) with post-ischemia tissues (M.PS vs F.PS = M.PS - F.PS)

 c) with one week later tissues (M.WL vs F.W =LM.WL - F.WL)

      The microarray study is based on 30 samples. A castrated male was included in the QC but not in the subsequent microarray analysis. The table II shows the allocation of each sample to each experimental condition in the sex-centered (unpaired data) analysis and the time-centered (paired data) analysis, respectively. The complete list of biopsies and their characteristics are listed in table III.

Table II. Experimental design of porcine renal IRI microarray assays

Time point of tissue	Sex		Total
	Female	Male	
Pre-ischemia (PR)	5	5	10
Post-ischemia (PS)	5	5	10
A week later after Ischemia (WL)	5	5	10
Total	15	15	30

Table III. List of p samples used for microarray analysis and their characteristics.

Individual	Sex	Time	Group
2	F	PR	F.PR
6	F	PR	F.PR
20	F	PR	F.PR
30	F	PR	F.PR
34	F	PR	F.PR
10	M	PR	M.PR
16	M	PR	M.PR
17	M	PR	M.PR
29	M	PR	M.PR
31	M	PR	M.PR
2	F	PS	F.PS
6	F	PS	F.PS
20	F	PS	F.PS
30	F	PS	F.PS
34	F	PS	F.PS
10	M	PS	M.PS
16	M	PS	M.PS
17	M	PS	M.PS
29	M	PS	M.PS
31	M	PS	M.PS
2	F	WL	F.WL
6	F	WL	F.WL
20	F	WL	F.WL
30	F	WL	F.WL
34	F	WL	F.WL
10	M	WL	M.WL
16	M	WL	M.WL
17	M	WL	M.WL
29	M	WL	M.WL
31	M	WL	M.WL

*PR(pre-ischemia); PS(post-ischemia); WL (one week later);F (female); M(male)

4.A.II.2   *Microarray experiment*

Microarray hybridization were carried out at Hight Technology Unit (UAT) at the Vall d'Hebron Research Institute, Barcelona (VHIR) (Spain). Gene Titan Affymetrix microarray platform and the Genechip Porcine Gene 2.1 ST 16-Array plate were used for this experiment. This array analyzes gene expression patterns on a whole-genome scale on a single array with probes covering many exons on the target genome, and thus

permitting expression summarization at the exon level or gene level. Starting material was 200 ng of total RNA of each sample. Briefly, sense ssDNA suitable for labelling was generated from total RNA with the GeneChip WT Plus Reagent Kit from Affymetrix (Affymetrix, Santa Clara, CA) according to the manufacturer's instructions. Sense ssDNA was fragmented, labelled and hybridized to the arrays with the GeneChip WT Terminal Labeling and Hybridization Kit from the same manufacturer.

4.A.II.3   Microarray data analysis

Bioinformatic analysis was performed at the Statistics and Bioinformatics Unit (UEB) of VHIR (Barcelona, Spain). Robust Multi-array Average (RMA) algorithm[236] was used for pre-processing microarray data. Background adjustment, normalization and summarization of raw core probe expression values were defined so that the exon level values were averaged to yield one expression value per gene. The analysis was done considering the experimental factors (time points and sex) and taking into account the pairing between samples in most of the comparisons performed. Data were subjected to non-specific filtering to remove low signal and low variability genes. Conservative thresholds were used to reduce possible false negative results. This yield a list of 3435 genes to be analyzed. Selection of differentially expressed genes was based on a linear model analysis with empirical Bayes modification for the variance estimates[237]. This method is similar to using a 't-test' with an improved estimate of the variance. To account for multiple testing, P-values were adjusted to obtain stronger control over the false discovery rate (FDR), as described by the Benjamini and Hochberg method[238]. Genes with adjusted P-value below 0.05 and absolute value of log2 fold change over 1 were called differentially expressed.

4.A.III. RT-qPCR

Microarray assays were validated by quantitative reverse transcription PCR (RT-qPCR) method. RT-qPCR is the method of choice for quantification of gene expression and the gold standard for validating results obtained from array analyses. In this method, RNA is first transcribed into cDNA by retro-transcription phase (RT). Then, the resulting cDNA is used as a template for the qPCR reaction in which a sequence of interest is amplified and quantified in each cycle.

Perform reverse transcription (RT)

Prepare the reverse transcription reaction mix
▼
Aliquot reverse transcription reaction mix and RNA to reaction plate or tube
▼
Run RT reaction
▼

Perform real-time PCR amplification (qPCR)

Prepare the PCR reaction mix
▼
Prepare the PCR reaction plate
▼
Run the PCR reaction plate
▼

Analyze the data
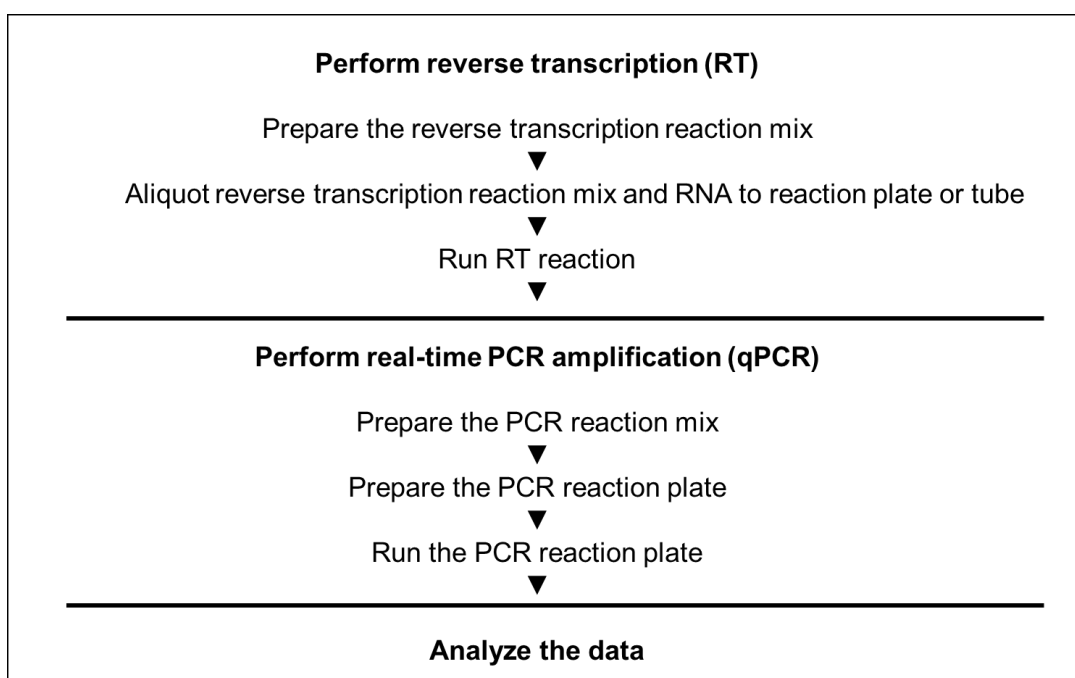
Figure 19. Workflow of RT-qPCR experiments.

Up to 2 ug of total RNA were retro-transcribed using the High Capacity RNA-to-cDNA Master Mix (Applied Biosystems #4387406) following the manufacturer's instructions (Figure 19). To perform quantitative gene expression analyses, we used the TaqMan® Gene Expression Master Mix (Applied Biosystems) kit, following the manufacturer's instructions. qPCR was performed in a 7900HT Fast Real-Time PCR system (Applied Biosystems, Inc.) The specific TaqMan probes we used are listed in table IV. Triplicate PCR amplifications were performed for each sample.

Table IV. List of TaqMan probes used for RT-qPCR experiment in the validation of porcine microarray assays.

gene	TaqMan probe reference
cxcl10	Ss03391845_g1
cd274	Ss03391947_m1
rsad2	Ss03381589_u1
fabp5	Ss03392150_m1
ifit3	Ss04248506_s1
actb	Ss03376160_u1

To analyze the results, the internal control (beta actin, #Ss03376160_u1) was used to normalize samples. Then, a direct comparison of relative abundance across samples was made. The result was expressed as the ratio of gene signal relative to the internal control signal.

4.A.IV.   Ingenuity Pathway Analysis (IPA) studies

PA is a web-based bioinformatics application that allows researchers to upload data analysis results from high-throughput experiments such as microarray and next generation sequencing for functional analysis, integration, and further understanding. It allows the interactive building of networks to represent biological systems. Among its multiple applications, in our study, IPA was used to detect and overlap the most significant genes across the different time and sex comparisons. Each microarray data file was uploaded on the software and an analysis was ran. A distinct data filtering criterion was set: a log fold change cut-off of ± 0.5. Following each analysis, a report that contains the top 10 genes-up and down regulated was obtained. The top genes were then reported in tables and Venn diagrams.

4.A.V.   Gene Set Enrichment Analysis (GSEA) studies

Bioinformatic analyses often result in long lists of genes that require an impractically large amount of manual literature searching to interpret. A standard approach to addressing this problem is pathway enrichment analysis, which summarizes the large gene list as a smaller list of more easily interpretable pathways. Pathways are statistically tested for over-representation in the experimental gene list relative to what is expected by chance, using several common statistical tests that consider the number of genes detected in the experiment, their relative ranking and the number of genes annotated to a pathway of interest. (GSEA) is a computational method that determines whether an *a priori* defined set of genes shows statistically significant, concordant differences between two biological states (e.g. phenotypes).

In order to reveal the different pathways behind the sex and time comparisons following renal IRI, we followed a protocol inspired by a recent published protocol[239].This protocol comprises three major steps: 1) definition of a gene list from omics data, 2) determination of statistically enriched pathways, and 3) visualization and interpretation of the results. The different steps are summarized in figure 20.
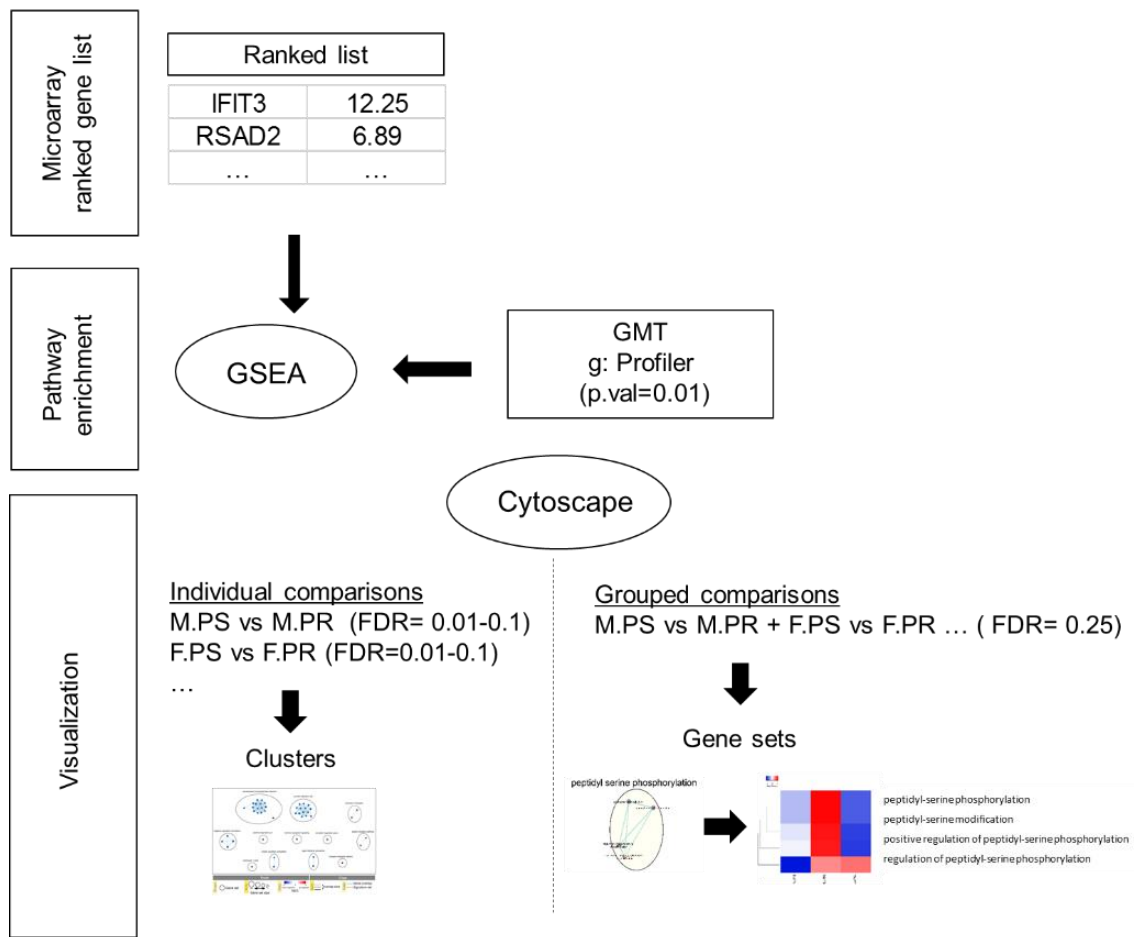
Figure 20. Protocol overview of GSEA analysis. Gene lists derived from diverse omics data undergo pathway enrichment analysis, using GSEA, to identify pathways that are enriched in the experiment. Pathway enrichment analysis results are visualized and interpreted in Cytoscape using its EnrichmentMap, AutoAnnotate, WordCloud and clusterMaker2 applications.

4.A.V.1 Definition of a gene list of interest using omics data

There are two major ways to define a gene list from omics data: list or ranked list. A gene list of interest is a list of genes derived from an omics experiment that is input to pathway enrichment analysis. A ranked gene list can be constructed with many omics data (e.g., that from RNA-seq for gene expression). Genes can be ranked according to some score (e.g., level of differential expression) to provide more information for pathway enrichment analysis. Certain omics data naturally produce a gene list and is suitable for direct input into pathway enrichment analysis using g: Profiler. Other omics data naturally produce ranked lists. For example, a list of genes can be ranked by differential gene expression score or sensitivity in a genome-wide clustered regularly interspaced short palindromic repeats (CRISPR) screen. The GSEA approach is designed to analyze

67

ranked lists of all available genes and do not require a threshold. A whole-genome ranked list is suitable for input into pathway enrichment analysis using GSEA. A partial (non-whole-genome) ranked gene list should be analyzed using g: Profiler. In our study, we defined a ranked gene list with the t-statistic. In statistics, the t-statistic is the ratio of the departure of the estimated value of a parameter from its hypothesized value to its standard error.

4.A.V.2 Pathway enrichment analysis of a ranked gene list using GSEA

Pathway enrichment analysis of a ranked gene list was implemented in the GSEA software[240]. GSEA searches for pathways whose genes are enriched at the top or bottom of the ranked gene list, more so than expected by chance alone. For instance, if the topmost differentially expressed genes are involved in the cell cycle, this suggests that the cell cycle pathway is regulated in the experiment. By contrast, the cell cycle pathway is probably not significantly regulated if the cell cycle genes appear randomly scattered through the whole ranked list[239]. To calculate an enrichment score (ES) for a pathway, GSEA progressively examines genes from the top to the bottom of the ranked list, increasing the ES if a gene is part of the pathway and decreasing the score otherwise. These running sum values are weighted, so that enrichment in the very top- (and bottom) ranking genes is amplified, whereas enrichment in genes with more moderate ranks are not amplified. The ES score is calculated as the maximum value of the running sum and normalized relative to pathway size, resulting in a normalized enrichment score (NES) that reflects the enrichment of the pathway in the list. Positive and negative NES values represent enrichment at the top and bottom of the list, respectively. Finally, a permutation-based P value is computed and corrected for multiple testing to produce a permutation based false-discovery rate (FDR) Q value that ranges from 0 (highly significant) to 1 (not significant). In our study, we used 200 permutations.

Basically, the GSEA approach compared the genes and their rank with gene sets comprised in a Gene Matrix Transposed (GMT) file. By default, the GSEA desktop software searches the MSigDB gene set database, which includes pathways, published gene signatures, microRNA target genes and other gene set types. The user can also provide a custom database as a text-based GMT file in which each line defines a pathway, with its name, identifier and a list of genes it contains. Gene identifiers in the GMT file must match those in the input gene list. For our study, the pathway gene set definition (GMT) files loaded on the software were created with the archived instance of

g:Profiler (Ensembl 93, Ensembl Genomes 40 (rev 1760, build date 2018-10-02) with a p-value cut-off: 0.01 for the microarray files.

4.A.V.3 *Visualization and interpretation of pathway enrichment analysis results*

Pathway information is inherently redundant, as genes often participate in multiple pathways, and databases may organize pathways hierarchically by including general and specific pathways with many shared genes (e.g., 'cell cycle' and 'M-phase of cell cycle'). Consequently, pathway enrichment analysis often highlights several versions of the same pathway. Collapsing redundant pathways into a single biological theme simplifies interpretation. We recommend addressing such redundancy with visualization methods such as EnrichmentMap[241], ClueGO[242] and others[243–245].

The resulting enrichment results were visualized with the Enrichment Map plugin for the Cytoscape network visualization and analysis software. We loaded GSEA individual dataset using a FDR threshold between 0.01 and 0.1. A multi-dataset enrichment map comprising all comparisons was created with a FDR of 0.25. The 3.7.1 Cytoscape version[246] was used with the following apps: EnrichmentMap[239,241], clusterMaker2[247], WordCloud[248], NetworkAnalyzer[249] and AutoAnnotate[250]. Pathways are shown as circles (nodes) that are connected with lines (edges) if the pathways share many genes. Nodes are colored by ES, blue and red meaning down and up-regulated pathways, respectively. Edges are sized on the basis of the number of genes shared by the connected pathways. Network layout and clustering algorithms automatically group similar pathways into major biological themes. The EnrichmentMap software takes as input a text file containing pathway enrichment analysis results and another text file containing the pathway gene sets used in the original enrichment analysis. Gene sets were also visualized by heatmaps using online Heatmapper tool[251].

4.A.VI. Systems Biology studies of porcine microarray

4.A.VI.1 *Anaxomics method-TPMS technology*

Anaxomics is a bioinformatics company molecularly modelling human physiology through systems biology and artificial intelligence. Anaxomics' solutions and services are all supported by a proprietary technology that exploits the latest advances in systems biology to accelerate biomedical research, drug discovery and development:

the Therapeutic Performance Mapping System (TPMS). TPMS creates mathematical models that integrate all available biological, pharmacological and medical knowledge to simulate human physiology in silico. In this manner, Anaxomics can test and evaluate the physiological effects of pharmacological compounds or biological processes at the molecular level, thereby bridging the molecular and the clinical worlds.

4.A.VI.2 Molecular characterization of renal IRI and regeneration and hormonal sex differences

The objective of this project was the identification of key proteins of renal IRI and regeneration, as well as hormonal sex differences on regards to the regulation of proteins involved in renal IRI and regeneration. We also wanted to compare the obtained results with key proteins in ccRCC (KIM-1 dependent). The main clinical and biological processes associated with renal damage after ischemia/ reperfusion and regeneration processes, have been characterized at a molecular level according to Anaxomics internal protocols. The motives characterized at molecular level and considered during the project are summarized in Table V.

Table V.   Motive identified during the molecular characterization of IRI and regeneration ahead of mathematical model construction

Motive name
Autophagy
Cell death
Dedifferentiation of renal epithelial cells
Endothelial-mesenchymal transition
Immune response
Microvascular dysfunction
Oxidative Stress
Regeneration of renal epithelial cells
Hormonal sex differences

4.A.VI.3   *Compilation and processing of transcriptomic data.*

DEG from porcine microarray was used as information to restrict the models (male/female mathematical models). Three transcriptomic time points were used: before the injury (PR), post-injury (PS) and one week after injury (WL). PR and PS experiments were compared with WL (Figure 21). The criteria for considering differentially expressed genes was an adjusted p-value < 0.05. The number of DEG and the number of genes that are translatable to protein is reported in Table VI.
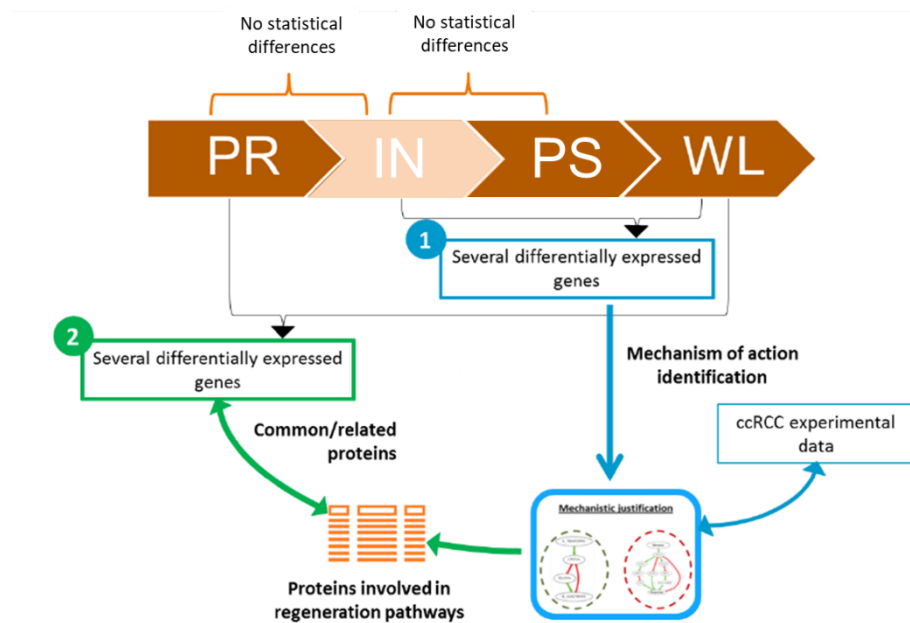
Figure 21. Scheme of workflow execution for compilation and processing of male and female pig transcriptomic data for model restrictions.

Table VI. Summary of the DEG and differential expressed proteins identified per comparison.

	Differentially expressed genes	Differentially expressed genes translatable to proteins
Male WL vs PS	716	565
Female WL vs PS	231	187
Male WL vs PR	864	691
Female WL vs PR	341	277

4.A.VI.4 Generation of mathematical models

In this project, sampling methods have been employed to achieve the objectives. To develop this strategy, the mathematical model is challenged with a stimulus and a response. Then, Anaxomics traces the most probable path (in biological and mathematical terms) that leads from the stimulus to the response through the biological network. In other words, it identifies the most probable mechanism of action (MoA) that achieves a physiological response when the system is stimulated.

Two models have been constructed:

-Male renal IRI and regeneration model.

-Female renal IRI and regeneration model.

Anaxomics analyses the transcriptomics data sample by sample in order to identify those proteins related to kidney I/R injury and regeneration. Two strategies have been employed to identify key proteins associated with kidney I/R injury and regeneration from the transcriptomic data: model reversion and protein sources.

4.A.VI.5 Model reversion

This strategy finds proteins whose modulation would turn the behavior of a model (in this case the model created using male transcriptomic experiments) into the behavior of another model (in this case the model created using female transcriptomic experiments) respect of a process (renal IRI and regeneration) (Figure 22). This strategy allows the identification of proteins not directly detected as differentially expressed but related to them and to the pathology of interest as interesting key proteins.
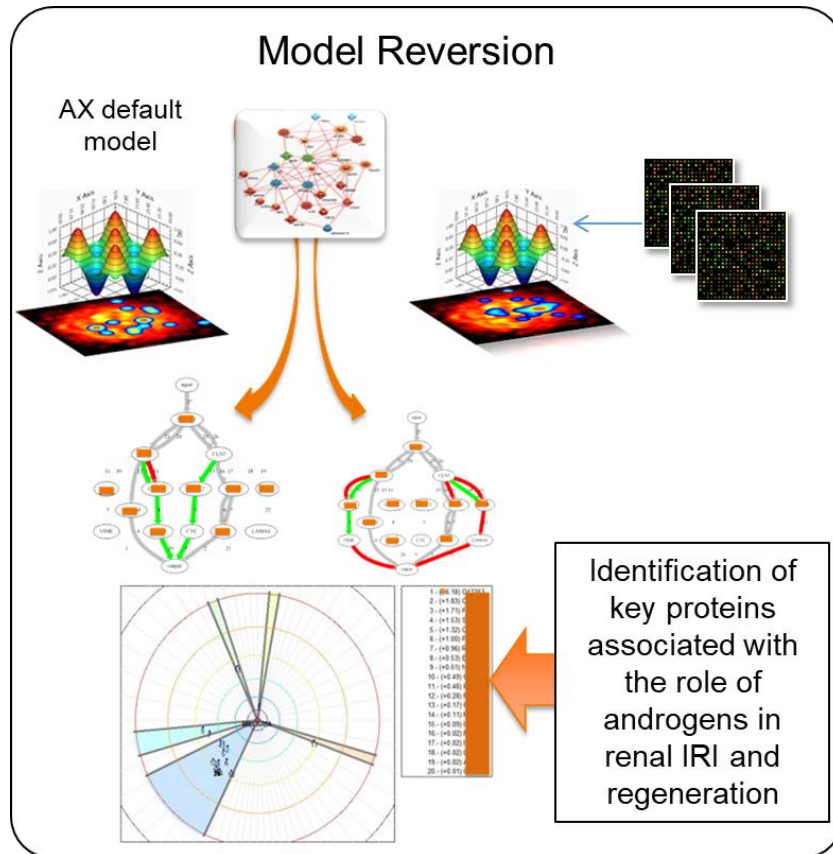
Figure 22. Schematic representation of the model reversion strategy.

4.A.VI.6   Protein sink and sources

For this strategy, the renal IRI and regeneration model is used to identify which of the differential proteins of each of the comparisons are more probable to mediate renal IRI and regeneration (Figure 23).

The analysis of the male data consisted on the identification of the differentially expressed proteins mainly promoting renal damage and hindering regeneration.

The analysis of the female data consisted on the identification of the differentially expressed proteins mainly hindering renal damage and promoting regeneration.
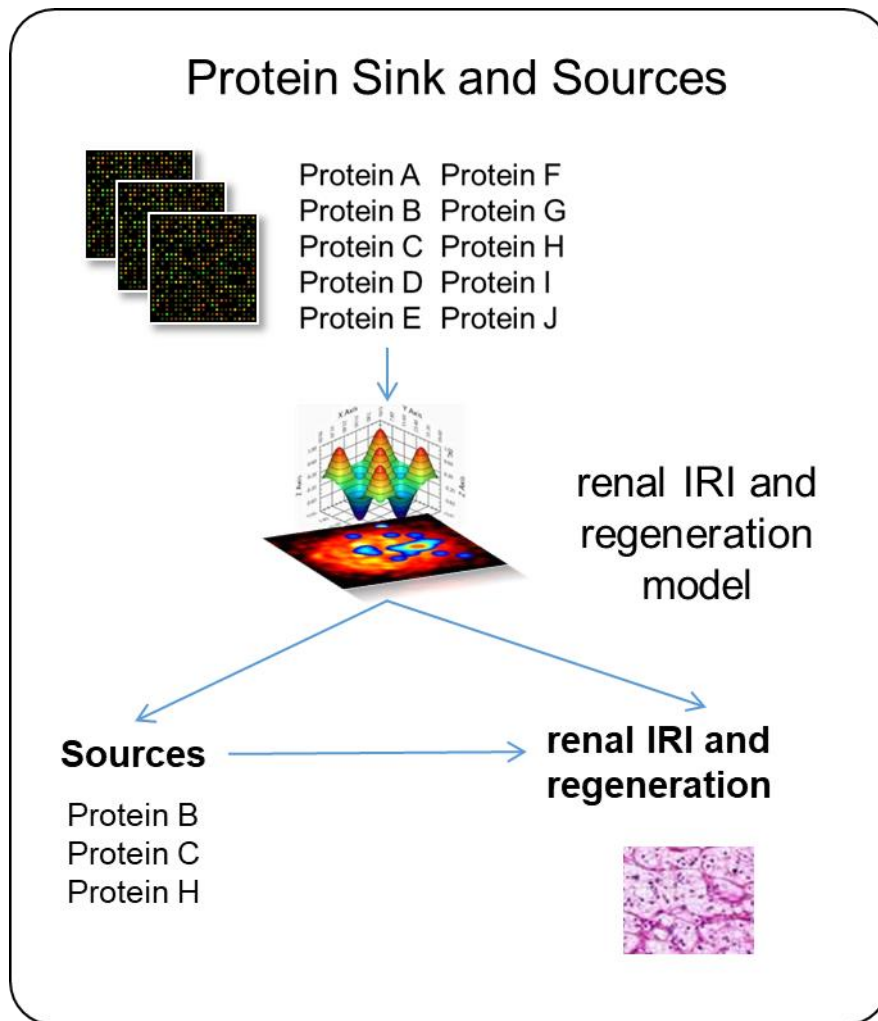
Figure 23. Schematic representation of the protein sinks and sources strategy.

4.A.VII. Protein expression level

Enzyme Linked Immunosorbent Assay (ELISA) assay is a method widely utilized for quantitation and identification of protein, peptides, hormones, and antibodies. In ELISA assay formation, an antigen and antibody are complexed together, where the antigen is immobilized or attached to a solid surface and the antibody is associated with the enzyme. The detection phase of the ELISA assay is accomplished by incubating the enzyme with a substrate and then evaluating the conjugated enzyme reaction. During

detection, antibody-antigen contact, or reaction is an essential element. Several type of ELISA assays exist (Figure 24).
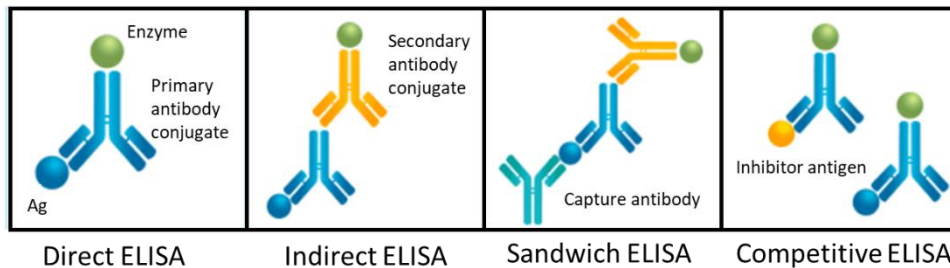
Figure 24. Scheme of different type of the ELISA used in this study.

In this section of the study, selected target protein level in porcine sera were measured by ELISA assays (TableVII). Protein levels were assessed at different time point. (PR, PS and WL) according to the manufacturer protocol.

Table VII. List of targets analyzed in porcine sera by ELISA

Target protein	reference
CXCL10	#ELP-IP10 (Tebu-bio)
FABP5	#E-EL-H1086 (Elabscience)

4.B.   *IN VIVO* RENAL IRI MOUSE MODEL

4.B.I. Surgical experiments

4.B.I.1   Animals

In this part of the study, an in vivo model of renal IRI was established using C57BL/6 mice. Females and males from 8 to 12 weeks old, free of specific pathogens, were obtained by Charles River Laboratories. This age range was chosen because animals have reached sexual maturity and it was possible to observe the hormonal effects on injury/regeneration in gene expression. All animal care and procedures were performed in accordance with the requirements of the European laws on the protection

of animals used for scientific and experimental purposes (86/609 EEC) and has the approval by the Experimental Ethics Committee of the Vall d'Hebron Institute of Research (76/16 EAEC).

4.B.I.2   *Experimental design*

Three to 7 days before surgery, a blood sample was collected from the retro-orbital vein. The samples were kept at room temperature RT for 30-40 minutes for coagulation and then centrifuged. The sera were kept at -80°C.

On the day of experiment, mice underwent bi-lateral IRI for 23 minutes, followed by 5 minute of reperfusion (REP) and/or 72 hours of recovery (REC) (Figure 25). Two Sham group were included for the REP and REC group. Both kidneys and a blood sample were collected at each the time point. Kidney collected were separated and were either snap-frozen or put in a plastic cassette and fixed in 10% formalin. The blood samples were processed as described before. The number of animals used in the experiment is shown in table VIII.
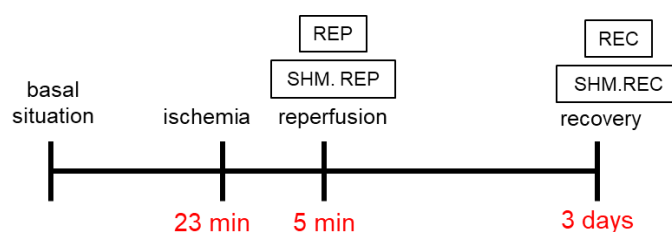
Figure 25. Experimental design of mouse model of renal IRI. Bi-lateral renal IRI was induced for 23 minutes. Samples were collected for analyses 5 minutes and 3 days following the injury. Each group has a SHAM control group.

Table VIII. Experimental design of mice used for renal IRI experiment.

Time-point of Ischemic Tissue	Sex		Total
	Female	**Male**	
Post-ischemic (REP)	6	6	12
3 days after Ischemia (REC)	6	6	12
Sham post-ischemic SHM.ISC)	3	3	6
Sham 3 days after ischemia (SHM.REP)	4	4	8
TOTAL	19	19	38

4.B.II. Biochemical parameter analysis

Assessment of renal injury was done by the analysis and of the sera samples collected before, during and following injury. Throughout the experiment, both sera samples collected for animal were compared. Determination of creatinine and BUN levels was performed by using the automated analyzer for clinical chemistry SPOTCHEM EZ SP-4430. SPOTCHEM EZ performs biochemical measurements easily with the dry method and solid phase reagent. The Kidney-2 kit (#33930, Menarini) kit was used. The instructions of the manufacturer were followed. In the course of a pilot study, biochemical parameters were also measured at the Biochemistry Unit at the Vall d'Hebron hospital.

4.B.III. RT-qPCR

RNA from mice kidney biopsies was isolated and their integrity was assessed. RT-qPCR experiments were executed at the same conditions described earlier in order to compare mRNA levels of selected target genes with the levels of porcine kidney that underwent renal IRI.

Table IX. List of TaqMan probes used for RT-qPCR experiment in mouse tissues

Gene	probe reference
cxcl10	Mm00445235_m1
cd274	Mm00452054_m1
rsad2	Mm00491265_m1
fabp5	Mm00783731_s1
ifit3	Mm01704846_s1
actb	Mm02619580_g1

4.C. HUMAN VALIDATION OF RENAL IRI SELECTED GENETARGETS

Selected target identified in *in vivo* porcine and mice renal IRI studies were validated in human samples.

4.C.I. Gene expression levels

4.C.I.1 Cases selection

In this part of our study, ischemic biopsies of human kidney were analyzed. The normal part of ccRCC patients that underwent total nephrectomy was used. Patients were derived from a cohort of patients hospitalized at the Vall d'Hebron hospital (1997-2001) and were selected by sex and age criteria. Patients were selected based on their age and sex. The list selected patients can be found in table XXXVI (Annexes).

4.C.I.2 RT-qPCR

RNA extraction from the normal ischemic part of the kidney of selected patients was conducted and RNA integrity was assessed, at the same conditions previously described and. RT-qPCR experiments were executed at the same conditions described earlier. The list of target genes characterized are reported in table X. The time point is comparable at the PS time point in the porcine model of renal IRI since the total nephrectomy process last about 30 minutes.

Table X. List of TaqMan probes used for RT-qPCR experiment in human tissues

Gene	Taqman probe reference
cxcl10	Hs00171042_m1
fabp5	Hs02339439_g1
cd274	Hs00204257_m1
rsad2	Hs00369813_m1
ifit3	Hs01922752_s1
actb	Hs01060665_g1

4.C.II. Sera protein levels

4.C.II.1 Case selection

Sera samples from men and women ccRCC patient were analyzed. The samples were collected before the nephrectomy. Patients were derived from two different cohorts of patients hospitalized at the Vall d'Hebron hospital (2008-2011 and 2013-2015).

Patients were selected based on their age and sex. The list of patients selected for human ELISA experiments can be found in table XXXVII (Annexes).

4.C.II.2   ELISA

Sex hormone and protein levels of selected targets were measured by ELISA assays in sera human samples. The experiments were conducted following the manufacturer's instruction of each kit. The list of targets analyzed is reported in table XI.

Table XI. List of hormones and targets analyzed in human sera by ELISA.

hormone /target protein	reference
testosterone	#ab178663; abcam
estrogen	#ab108640; abcam
CXCL10	#ab173194; abcam
FABP5	#ELH-FABP5-1; bionova
PD-L1	#ab214565; abcam
RSAD2	#MBS9923380-96; bionova
CXCL11	#ab187392; abcam

4.D.   IN VITRO RENAL IRI MODEL

4.D.I. Cell culture

4.D.I.1.   Cell lines

Different cell lines were used for the cell experiments:

HK-2 (ATCC® CRL-2190™): human kidney 2 (HK-2) is an immortalized proximal tubule epithelial cell line from normal adult human (male) kidney. The cells were immortalized by transduction with human papilloma virus 16 (HPV-16) E6/E7 genes. HK-2 cells retain functional characteristics of proximal tubular epithelium such as Na^+ dependent / phlorizin sensitive sugar transport and adenylate cyclase responsiveness to parathyroid, but not to antidiuretic hormone. The cells are capable of gluconeogenesis

as evidenced by their ability to make and store glycogen. HK-2 cells are anchorage dependent. HK-2 cells can reproduce experimental results obtained with freshly isolated PTCs.

RPTEC/TERT1 (ATCC® CRL-4031™): RPTEC/TERT1 is an immortalized renal proximal tubular epithelial cell line from normal adult human (male) kidney**.** It has been immortalized using the human telomerase reverse transcriptase (hTERT) subunit only and does not exhibit chromosomal abnormalities. These cells show the characteristic morphology and functional properties of normal proximal tubular epithelial cells.

769-P (ATCC® CRL-1933): 769-P cells originate from a primary clear cell adenocarcinoma of a 63-years-old Caucasian female. 769-P cells have a globular morphology with diffuse borders, have a high nucleus to cytoplasm ratio and exhibit both microvilli and desmosomes. 769-P cell line have many characteristics of ccRCC and are the most commonly used in RCC focused research. They have mutated *vhl* or defective VHL expression, and produce high levels of VEGF which is characteristic of ccRCC.

HEK293T/17 (ATCC® CRL-11268): HEK293T/17 cells are a clone derived from *human embryonic kidney 293 cells* (HEK293). HEK293T cells are very easy to handle and culture because of their high rate growth and they are commonly used in molecular biology and biotechnology industries for protein expression and production of recombinant retroviruses.

4.D.I.2.   Culture conditions

All cells lines were cultured in Dulbecco's Modified Eagle Medium (DMEM) enriched with decomposed bovine fetal serum (incubated at 60 ° C for 30 minutes) and hormones and growth factors (**Table XII & Table XIII**). The lines were maintained and expanded at 37 ° C in a saturated atmosphere of humidity and 5% CO2. The standard practices and sterility conditions required for working with cell cultures have always been followed.

Table XII. Composition of the cell culture medium for RPTEC, HK-2, HEK-293T cells.

Product	[Concentrationl]	References
DMEM	-	Life Technologies #31331-093
HEPES buffer 1M	20 mM	Life Technologies #15630-080
Apo-Transferrin	5 µg/ml	Sigma Aldrich #T1428, 100 mg
Human Insulin solution	5 µg/ml	Sigma Aldrich #I9278, 5 ml
Dexamethasone	50 nM	Sigma Aldrich #D8893
3,3′,5-Triiodo-L-thyronine sodium salt (T3)	3 nM	Sigma Aldrich #T5516, 1 mg
EGF	10 ng/ml	Sigma Aldrich #E4127
Selenium	60 nM	Sigma Aldrich #S9133
FBS	2 % (v/v)	Biological Industries #04-007-1A
Antibiotic/Antimycotic	1% (v/v)	Life Technologies #15240-062 100 ml

Table XIII. Composition of the cell culture medium for 769-P cells.

Product	[Concentrationl]	Reference
Gibco™ DMEM, high glucose, HEPES	-	Gibco™ #42430082
sodium pyruvate	1% (v/v)	Gibco™ #11360039
FBS	10 % (v/v)	Biological Industries #04-007-1A
Antibiotic/Antimicotic	1%(v/v)	Life Technologies #15240-062 100ml
Plasmocin	0,2% (v/v)	Invivogen #ant-mpp

Some experiments required, the absence of hormones. In that case, FBS of the medium was replace by FBS charcoal treated (10 % (v/v)). The FBS charcoal treated was prepared as followed:

<u>FBS charcoal-stripped:</u>

- In a 500 mL FBS bottle add 5 gr. of charcoal (Sigma aldrich, C6197 20 gr.)
- Shake by inversion and aliquot in 50 ml tube.
- Shake overnight at 4°C or inside a cold chamber
- Centrifuge 15 minutes at 3000 rpm
- Filter in 50 mL tube
- Store at -20°C

4.D.I.3   Maintenance and trypsinization

The cell lines require a change of medium every 2-3 days and are usually trypsinized every 3-4 days, at 85-100% confluence, following the later procedure:

Reagents:
- Trypsin-EDTA (Gibco™ #25300062).
- PBS 1X (137 mM NaCl, 2.7 mM KCl, 10 mM Na2HPO4, and 1.8 mM KH_2PO_4) sterile.
- Culture medium (Table XVI & Table XVII).

<u>Trypsinization:</u>

- Warm the reagents at 37 ° C.
- Aspirate the medium with a sterile pasteur pipette and wash the cells with 1x sterile PBS.
- 3.Aspirate PBS 1x and add trypsin (1-2 ml per 75 cm^2 surface).
- 4 Incubate 1-3 minutes at 37°C (until the cells have detached from the surface).
- 5. De-activate trypsin by adding 3 times the volume of medium.and mechanically disaggregated the cells with up and down pipette movements.
- 6.Centrifuge the cells at 1200 rpm for 5 minutes at room temperature.
- 7. Aspirate the supernatant and resuspend the cell pellet in the desired volume of fresh medium depending on passage or subsequent steps.

4.D.I.4.   *Cell counting and seeding*

In order to seed the desired number of cells for the experiments the cells were counted and seeded using the following protocol:

Reagents:

- Trypan Blue (Sigma Aldrich, T-8154).
- PBS 1X
- Neubauer chamber and optical microscope.

Cell counting and seeding:

- From a cell suspension trypsinized, prepare a 1: 5 dilution in Trypan blue.
- Fill the Neubauer chamber with 10 µl of the dilution and count the viable cells (not stained) in the different fields.
- Perform the following calculation: number of viable cells / ml = Number of cells average x dilution factor (5) x 10^4
- Determine the required volume of cell suspension to sow the desired cell density.
- Prepare dilutions of cells and seed in plates.
- Incubate at 37 ºC (5% CO2) until performing each experiment.

4.D.II.   Hormone stimulation experiment

Renal cell lines were stimulated with hormone with DHT and EST. The AR rapid non genomic activation was assessed by MAPK activation. First, the cells were seeded and grown for 48h (Table XVI). Then, the cells were deprived from steroid hormones by complete removal of FBS from the medium for 18h. Then, 10nm of DHT or and EST were added to the cells for 15 minutes. (Figure 26) Following stimulation, the cells were harvested for western blot analyses.
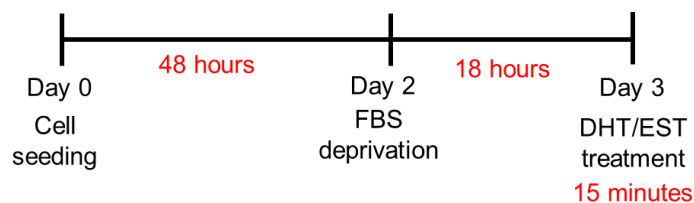
Figure 26. Experimental design of hormone stimulation experiment in renal cells.

Table XVI. Cell seeding conditions for hormone stimulation experiment

cell line	cells/wells	plate
RPTEC	50	6 wells
HK-2	50	6 wells

4.D.III. Androgen receptor transduction in renal cells

Renal cells are known to have AR. The activation of the AR in the kidney is known to regulate genes and molecular processes in the kidney. In this experiment, the AR was transduced by a lentiviral vector in RPTEC cells. The goal was to simulate an *in vivo* model where the impact of androgen could easily be measured at the molecular level.

4.D.III.1 *DNA isolation*

The pLENTI6.3/AR-GC-E2325 (85128, Addgene)[252] vector that contains the androgen receptor (Figure 27) and the pLenti-CMV-Blast-empty (17486, Addgene)[253]. vector that serve as a backbone (Figure 28) were obtained in a bacterial strain. We first proceed to isolation and purification of the plasmid DNA contained in bacteria. Two different column-based kits were used depending on the size of bacterial culture. The Illustra™ plasmid Prep Mini Spin Kit (GE Healthcare #28-9042-70) was used to perform Minipreps from bacterial pre-culture (5 ml), and the NucleoBond® PC100–Plasmid DNA Purification Kit (Macherey-Nagel #740573) was used to perform Midipreps from bacterial culture (100 ml). In both cases, protocols were carried out according to the manufacturer' instructions. Isolated plasmid DNA was then stored at -20°C for downstream applications.
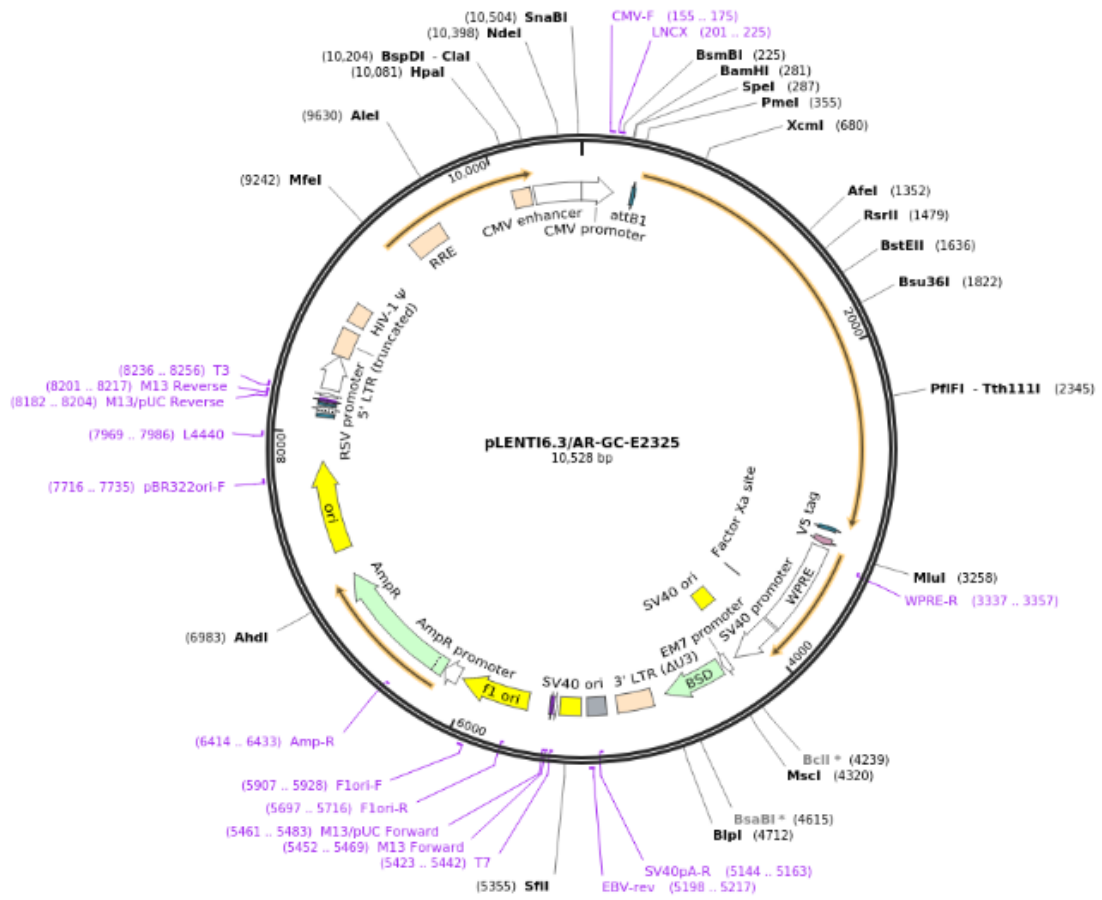
Figure 27. Full sequence of pLENTI6.3/AR-GC-E2325 vector containing the sequence of the androgen receptor.
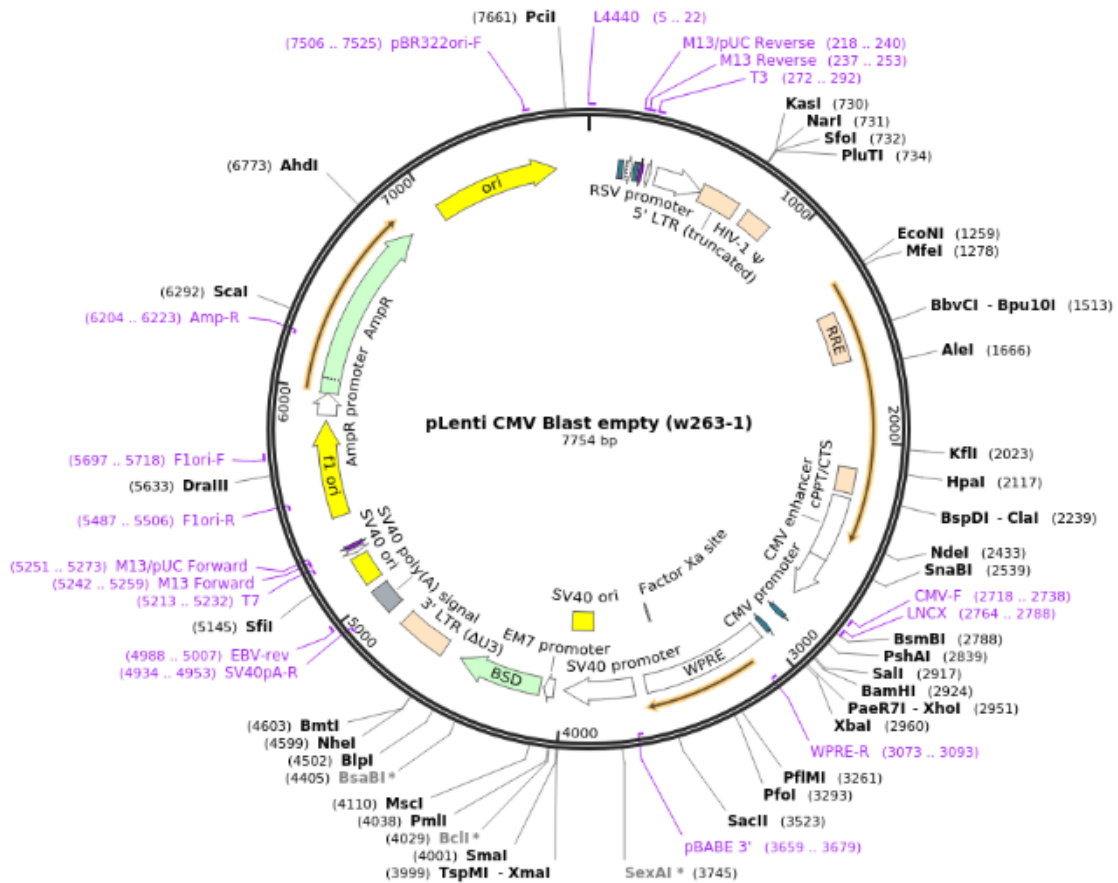
Figure 28. Full sequence of pLenti-CMV-Blast-empty vector that is used as a backbone to the pLENTI6.3/AR-GC-E2325 vector.

4.D.III.2 Nucleic acids quantification

Following plasmid DNA isolation, the concentration and purity of nucleic acids were determined with the Nanodrop™ 2000 (Thermo Scientific™ #ND-2000), following the manufacturer's instructions. The purity of nucleic acids was determined by the 260 nm/280 nm absorbance ratio. A ratio of ~1.8 is generally accepted as "pure" DNA and ~2.0 for "pure" RNA. Lower ratio to these values indicates the presence of proteins, phenol or other contaminants. Following quantification, acid nucleic acids were separated and visualized on agarose-gel electrophoresis.

4.D.III.3   *Sequencing*

Before performing lentiviral transduction, the plasmid DNAs sequence were confirmed by sequencing. Sequencing was carried out by the Macrogen Sequencing Service (Madrid, Spain). For each sequencing reaction, 5 ul of plasmid DNA [100 ng/µl] diluted in MQ H2O, and 5 µl of previously designed primers (5 pmol/µ) were sent to Macrogen facilities. Both the pLENTI6.3/AR-GC-E2325 and the pLenti-CMV-Blast-empty vectors were sequenced with CMV-F primer. After obtaining the results, sequences were aligned and analyzed.

4.D.III.4   *Lentiviral transduction*

Lentiviral transduction is an efficient method to insert genes or other types of molecules into mammalian cells unifying the ease and speed of transient transfection with the robust expression of stable cell lines. In general terms, transduction is the process by which foreign DNA (contained in a virus or viral vector) can be stably introduced into a host cell's genome.

Lentiviral plasmids used included pLENTI6.3/AR-GC-E2325 (transfer), pLenti-CMV-Blast-empty (transfer), VSVG (envelope), pRSV-Rev (Rev-packaging) and PKGPIR (Gag/Pol-packaging). Lentiviral particles were generated through the combine expression of virion packaging elements in cells used as producer of virus. The 1:1:2:4 (envelope:Rev-packaging:Gag/Pol-packaging:transfer) proportion was used. In this study, HEK293T cells were used as a lentivirus producer cell line because they are easily transfectable and express high levels of proteins. The lentiviral particles produced will act as a vehicle for the DNA of interest, in our case In our case, we wanted to introduced the AR and/or his backbone in RPTEC cells to study its effect. These particles, once produced by HEK293T cells, are released into the culture medium and are used to infect our target cells (Figure 29).

Procedure:

- The day before transfection, HEK293T cells are seeded at 80-90% confluence in T-25 flasks.

- 6 µg of DNA (containing the four plasmids: vector, gag-pol, envelope and transfer in 1:1:2:4 ratios are combined with 30µl of the polyethyleneimine transfection reagent in 600 µL of NaCl (150 mM).

- The suspension is incubated for 20 minutes at room temperature and added dropwise to the HEK293T cells.

- The transfected cells are incubated at 37°C in the culture incubator.

- The supernatants of the transfected cells are collected, and 5 ml of fresh medium are added (this process must be repeated at 48- and 72-hours post-transfection).

- Supernatants obtained from transfected cells are passed through 0.22µm filters (Millipore #SLGS033SS) and supplemented with 10% FBS, 8µg/µl polybrene (Sigma Aldrich #TR-1003) and 1% non-essential amino acids (Biological Industries #01-340-1B).

- The cells to be infected (RPTEC) are seeded, the day before infection, at a density of 3 x10^5 cells in a T-25 bottle in an average volume of 5ml.

- The medium containing the viruses is applied to the cells to be infected (this process is repeated 2 times with the medium extracted from HEK293T cells 48- and 72-hours post-transfection).

- After this time, the medium is removed from the infected cells and add fresh medium.

- Transformants are selected for 5 days by addition of Blasticidin [Ibian technologies] at 6µg/ml to the culture medium.

Day 1	-seeding of HEK293T -infetion of HEK293T (O/N)
Day 2	-change of media -incubation of HEK293T at 33°C
Day 3	-seeding of RPTEC cells -1st viral infection
Day 4	-2nd viral infection
Day 5	-removal of viral media
Day 6-12	-selection of transduced-cells by antibiotic
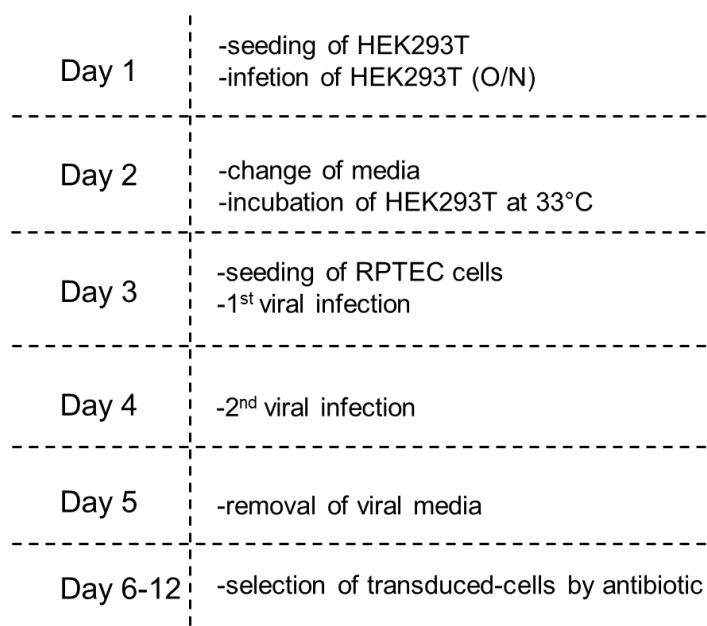
Figure29. Scheme of workflow for lentiviral transduction of renal cells.

4.D.III.5   Hormone stimulation experiment

Renal cell lines were stimulated with DHT. Once again, The AR rapid non genomic activation was assessed by MAPK activation. First, the cells were seeded and grown for 48h (Table XV). Then, the cells were deprived from steroid hormones by complete removal of FBS from the medium for 18h. Then, 100nm of DHT were added to the cells for 15 minutes (Figure 26). Following stimulation, the cells were harvested for western blot analyses.

Table XV. Cell seeding conditions for hormone stimulation experiment of transduced cells

cell line	cells/wells	plate
RPTEC	100,000	6 wells
RPTEC-CMV	100,000	6 wells
RPTEC-AR	100,000	6 wells

4.D.III.6 *Immunocytochemistry (ICC)*

The immunocytochemistry (ICC) is a technique used to anatomically visualize the localization of a specific protein within whole cells. The detection of proteins is usually done by fluorescence under the confocal microscope using fluorophore-conjugate antibodies.

In our case, we wanted to observe the localization of the AR protein expression and the effectiveness of the transduction. A conventional protocol of ICC was followed.

Table XVI. List of antibodies used in ICC experiments

Antibody	Dilution	Reference
occludin	1:100	#71-1500, Invitrogen
hoechst	1:2000	#H1399, thermofischer
AR	1:100	#ab9474, abcam
α-Mouse Alexa Fluor 488	1:500	# A11029, thermofischer
α-Rabbit Alexa Fluor 568	1:500	# A11011, thermofischer

4.D.IV. IRI model in a renal cell system

4.D.IV.1 *Experimental design*

An *in vitro* model of ischemia-reperfusion injury was established in RPTEC and 769-P cell lines. Cells were trypsinized and seeded in 60mm dishes at different concentration (Table XVII) Cells were grown for 3 days, until confluence.

Table XVII. Cell seeding conditions for *in vitro* renal IRI model.

cell line	cells/wells	plate
RPTEC	300,000	60 mm
769-P	500,000	60 mm

Before the induction of IRI, one group of cells were deprived from steroid hormones for 48h by charcoal stripped FBS treatment, as previously described.

Ahead of the treatment, a subsequent group of cells were deprived from steroid hormones at the same conditions mentioned before. Then, the cells were stimulated with 100 nM DHT to the media for 24h, before induction of ischemia (Figure 30). Stimulation was kept for this long in order to detect the presence or not of genomic signaling, which takes more time.
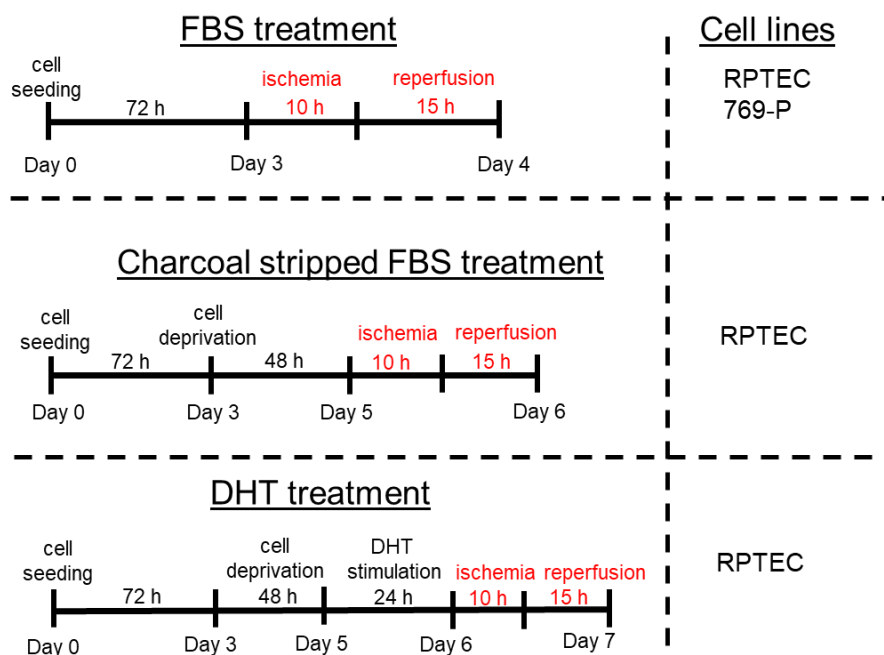
Figure 30. Experimental design of in vitro renal IRI experiments. The day of the experiment, the culture medium of the cells was replaced by a medium (Table XII) without glucose or plain DMEM medium. The cells were incubated in a Withley H35 hypoxystation. The chamber atmosphere was replaced by flushing the chamber with a 0,1% O_2, 5% CO_2 mixture. Hypoxia was maintained for 10 hours. To induce reperfusion, the mediums of all dished were replaced by initial culture medium and the cells were incubated under normoxic conditions for 15h. At the conclusion of reperfusion, the cells were harvested for subsequent analysis.

4.D.IV.2   *Cell viability assay*

The Cell Proliferation Kit II (XTT) is a colorimetric assay for the nonradioactive quantification of cellular proliferation, viability, and cytotoxicity. Colorimetric assays analyze the number of viable cells by the cleavage of tetrazolium salts added to the culture medium. Cell viability of cells was measured at the completion of 10h of ischemia

and after 15 hours of reperfusion with the XTT assay (#11465015001, Roche). Following the treatment, 50 µl of XTT mix, prepared with a 1:50 dilution of labeling reagent and electron-coupling reagent (provided in the kit) were added to the cells and their respective control. Cells were then incubated for 45 minutes at 37°C with 5% CO_2 in the dark. Following incubation, the absorbance was read at 490 nm and 630 nm as the reference wavelength. The results were calculated subtracting the absorbance at 630 nm to 490 nm. Three independent experiments were carried out in triplicate.

4.D.IV.3   Protein extraction

At the end of ischemia and ischemia-reperfusion treatments, the cells were isolated the following way. Treated cells were lysed with SET buffer(10 mM Tris-HCL pH 7,4; 1mM EDTA pH 8; 150 mM NaCl; 1% SDS) and supplemented with protease inhibitor cocktail (PIC) (Sigma Aldrich #S8820) (1:200), Na3Vo4 (Sigma Aldrich #S6508) (1:200) and NaF (Sigma Aldrich #S7920) (1:1000). Briefly, the cells were homogenized, collected in a tube and sonicated.

4.D.IV.4   Protein quantification

The bicinchoninic acid (BCA) assay is a colorimetric method that determines protein concentration by a color change in proportion to a known protein concentration (albumin standard). In our study, the Pierce™ BCA protein assay (Thermo Scientific™ #23225) was carried out following the manufacturer's instructions. Upon quantification protein aliquots were diluted in Laemmli buffer (300 mM Tris-HCl pH 6.8, 50% SDS, 25% glycerol, 10% β-mercaptoethanol, and 0.05% bromophenol blue)(Sigma Aldrich #B5525) and stored at -20°C

44.D.IV.5.   Western blot analysis

Western blot is an extensively used analytical technique to detect a specific single protein within a complex mixture of proteins. This technique also allows a semi-quantitative estimation of proteins derived from the size and intensity of their corresponding band on the blot membrane.

In our case, western blot analyses were performed as follows. First, protein samples (10-20ug) were separated by polyacrylamide (Panreac #A1672)(table XVII) in a vertical electrophoresis system filled with running buffer (25 mM Tris-HCl, 200 mM glycine (Sigma Aldrich #G8898) 0.1% SDS) (table VII). Then proteins were transferred

on PVDF membranes with a transfer buffer (25 mM Tris-HCl, 200 mM glycine, 0.1% SDS, and 20% methanol). Subsequently, membranes were blocked in Tris-buffered/0.1% Tween-20 containing 5% bovine serum albumin (BSA) or 5% NFDM. Next, membranes were incubated with their respective primary antibodies overnight. Later, membranes were incubated with an HRP-conjugated secondary antibody. For protein detection, membranes were soaked with the Immobilon Forte HRP substrate (Merck™ #WBLUF0100). The Odyssey® Fc Imaging System (Li-cor®) system was used for revealing. Membranes were exposed during 5 min for chemiluminescent protein-detection, and 30 seconds in the 600 channel to visualize the molecular weight marker (Figure 31).
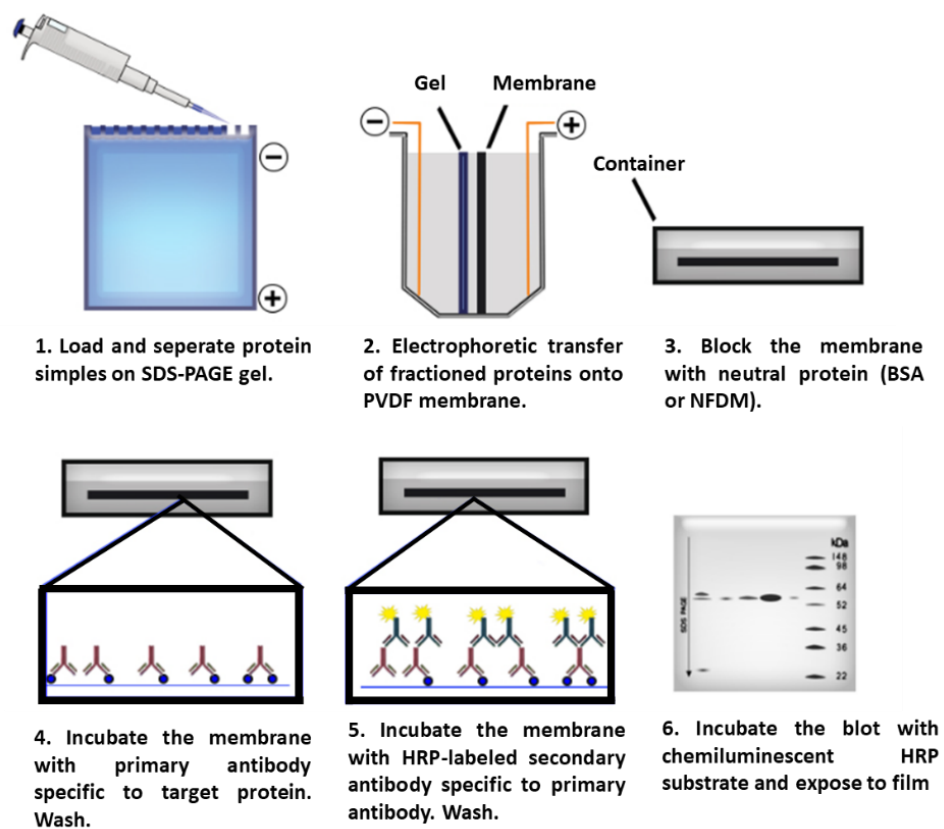
Figure 31. Overview of the western blotting procedure.

Table XVIII. List of components and volumes necessary to prepare western blot gels

	separating gel				stacking gel
	7,5%	10%	12%	15%	
30% acril/0,8% bis-	3.75 ml	5,0 ml	6.0 ml	7.00 ml	0,78 ml
4X Tris-HCl/SDS pH 8.8	3.75 ml	3.75 ml	3.75 ml	3.75 ml	1,50 ml
MQ H2O	7.50 ml	6.25 ml	5.25 ml	3.75 ml	3,66 ml
10% APS	100 µl	100 µl	100 µl	100 µl	60 ul
TEMED	10 µl	10 µl	10 µl	10 µl	12 ul

5. RESULTS

5. RESULTS

5.A   TRANSCRIPTOMIC SEX DIFFERENCES THROUGHOUT RENAL IRI IN PORCINE MODEL

In a previous study in our laboratory, renal IRI was induced in male and female mini pigs. In this current study, the kidney biopsies collected at different time points were recovered for further analyses. RNA was extracted from theses biopsies and microarray-based gene expression analyses were performed. We aimed to better correlate the molecular and the physiological sex differences observed in humans by in depth analysis of the transcriptome of male and female pig kidneys during IRI and regeneration, in a time- and sex-dependent manner.

5.A.I.   Hierarchical clustering of genes

Heat-maps allowed the visualization of common patterns of regulation between different experimental conditions according to the time and sex comparisons (Figure 32). Altogether, for the time comparison, for both sexes, the following pattern is observed: genes that are up-regulated at PR and PS, become down-regulated at WL. The opposite pattern is also identified in both sexes. As for the sex comparison, the global gene expression differences observed at PR and PS between males and females disappeared during the recovery phase (WL), males exhibiting a global female-like phenotype during recovery.
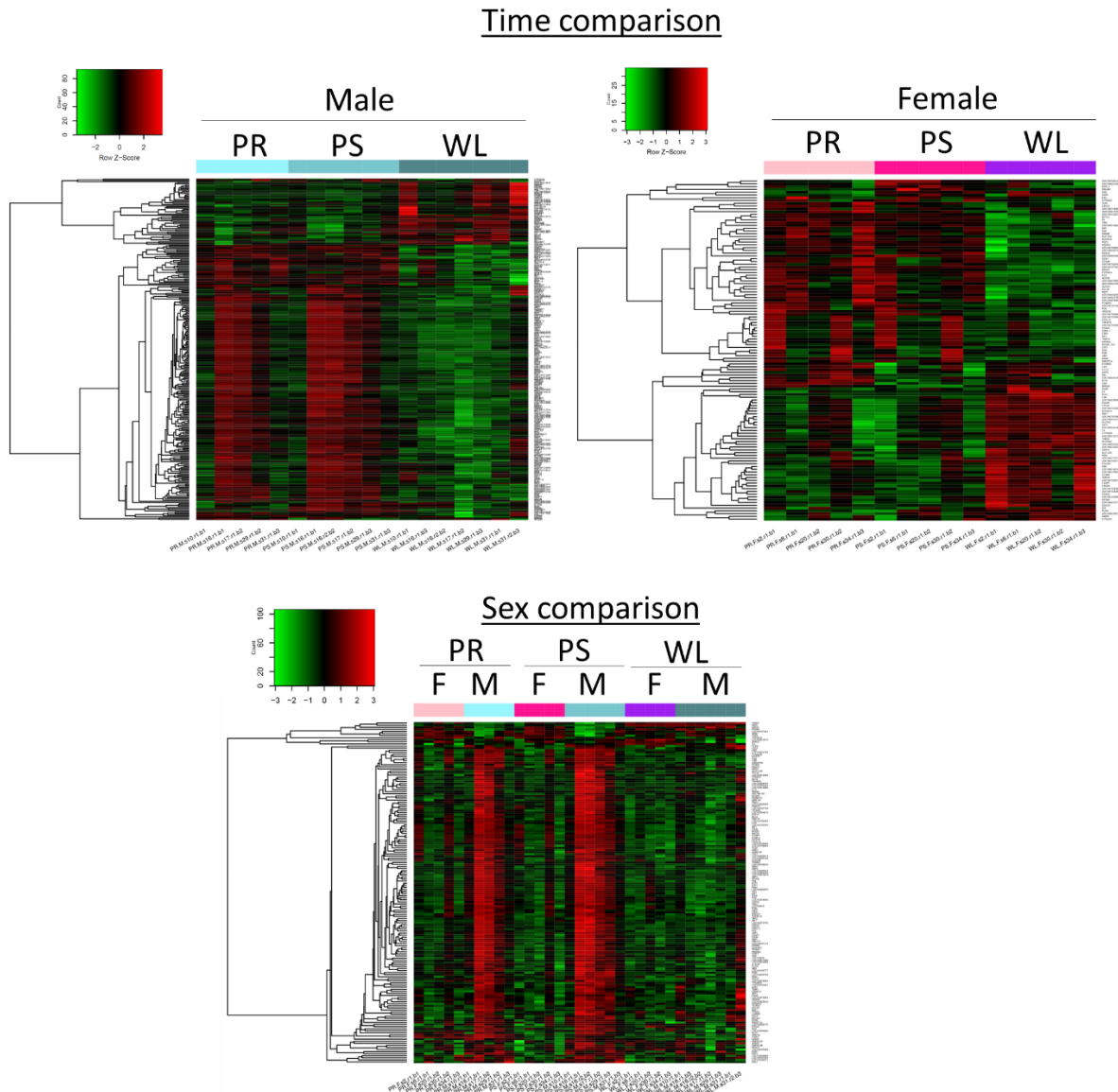
Figure 32. Hierarchical clustering of microarray assays based of kidney porcine throughout renal IRI in a time and sex manner. Gene expression for males and females are compared at different time points. Similar pattern of expression are observed in the time comparison. However, a sexual dimorphism is identified at PR and PS. At WL, both sexes have similar pattern of expression. Gene represented in the heatmaps had adj.P.Val < 0.25 and |log FC| >=1. (F:female; M: male; PR:pre-ischemia; PS: post-ischemia; WL: one week later).

5.A.II. Number of regulated genes throughout renal IRI processes

The next step we took was to quantify and compare the DEG in both sexes. Genes having an adjusted p-value ≤0.25 were considered. Regarding the PS vs PR time comparison, we observed expression changes on a total of 45 genes in females (14 up- and 31 down-regulated) and 8 genes in males (6 up- and 2 down-regulated) (Figure 33 upper part).

The number of genes that changed their expression in WL respect to PS were 1,089 in females (670 up- and 419 down-regulated) and 1,686 in males (674 up- and 1,012 down-regulated) (Figure 33 middle part).

Finally, for the WL vs PR comparison, 1,027 genes were differentially expressed in females (425 up and 602 down-regulated) and 1,754 (793 up- and 961 down-regulated) (Figure33 lower part). These observations showed that more genes are regulated in males during IRI processes.
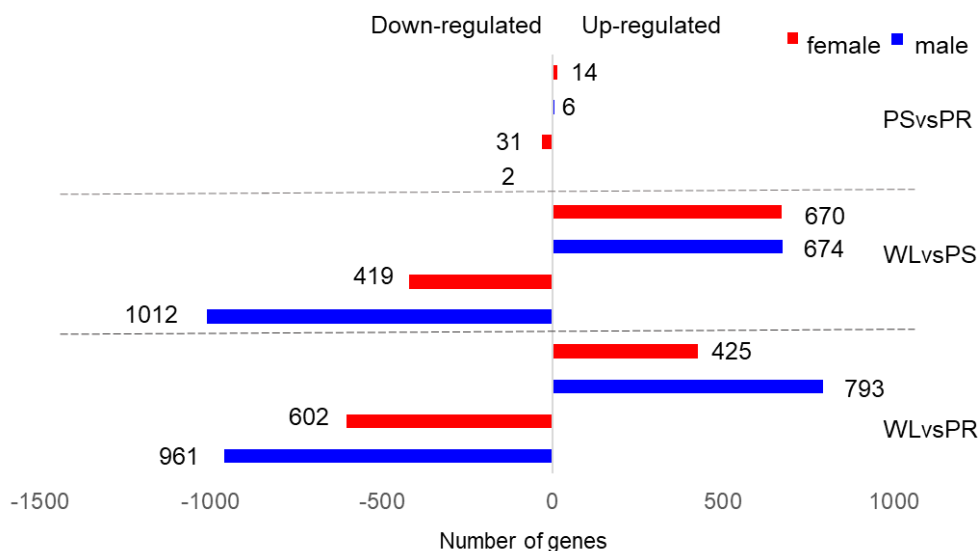
Figure 33. Number of genes differentially expressed throughout renal IRI in porcine kidney males and females at different time point. Primarily, more genes are regulated in males than in females in the renal IRI processes The PS vs PR comparison is the one that shows less difference in the gene regulation. Genes having an adjusted p-value ≤0.25 were considered. (PR:pre-ischemia; PS: post-ischemia; WL: one week later).

With respect to the sex comparison, the number of genes changing their expression at each time point in males and females showed 100 genes differentially expressed in males vs females in basal situation (PR) (72 up- and 28-down-regulated); 858 genes differentially expressed in males vs females at 5 min reperfusion after injury (PS) (582-up and 276 down-regulated) and only 2 genes down-regulated in males vs females at one-week after reperfusion. These results showed that the most DEG between the sexes are observed during injury. One week after injury, all the sex differences observed in the basal situation and at injury are lost (Figure34).
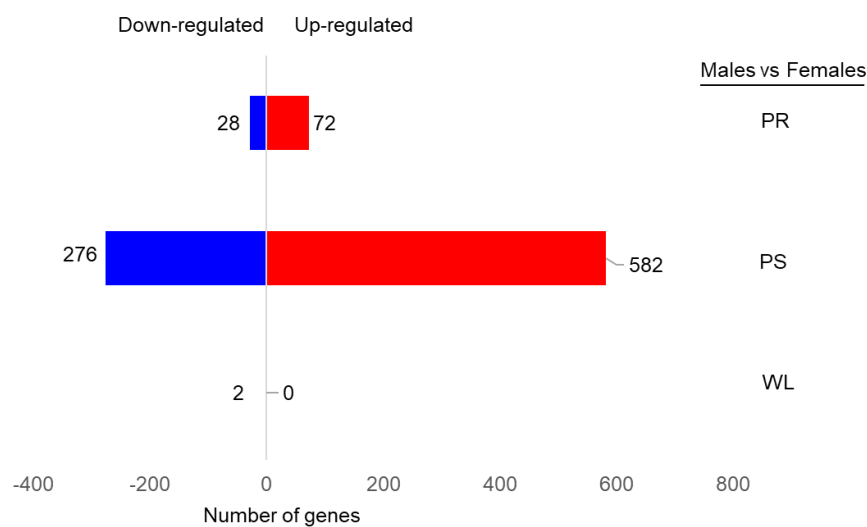
Figure. 34. Number of genes differentially expressed throughout renal IRI in porcine kidney between males and females at the same time point. Most genes'expression was altered during PS and only two genes were differentially regulated between males and females at WL Genes having an adjusted p-value ≤0.25 were considered. (PR:pre-ischemia; PS: post-ischemia; WL: one week later).

5.A.III.   Most DEG throughout renal IRI processes

Once the number of significant DEG was assessed, we filtered these genes to obtain the most up and down regulated in each comparison. To do so, a fold change (|FC |≥ 1) was added to the adjusted p-value ≤0.25, for the gene selection. Venn diagrams in Figure 35 allow visualization of number of genes shared in different experimental conditions for the time and sex comparisons.

For the time comparison in males, 174 genes are conserved in the WL vs PR and WL vs PS comparisons; 52 are exclusive of WL vs PS and 50 only found in the WL vs PR comparison. From the eight genes that are different between PS and PR, only two are exclusive of this comparison. Similar patterns but lower numbers of genes for each comparison were exhibited by females, indicating that the injury and recovery processes in the kidney have a lower overall gene expression impact in females than males.

As for the sex comparison,51 of the 53 DEG between sexes at PR remain different for both sexes after injury, males changing the expression of another 109 genes in this phase. All the changes found at PR and PS for males and females disappear at one-week post-reperfusion and that only two genes (LOC 100512372: organic solute transporter alfa and DHRS7) appeared differentially expressed between males and females at recovery.
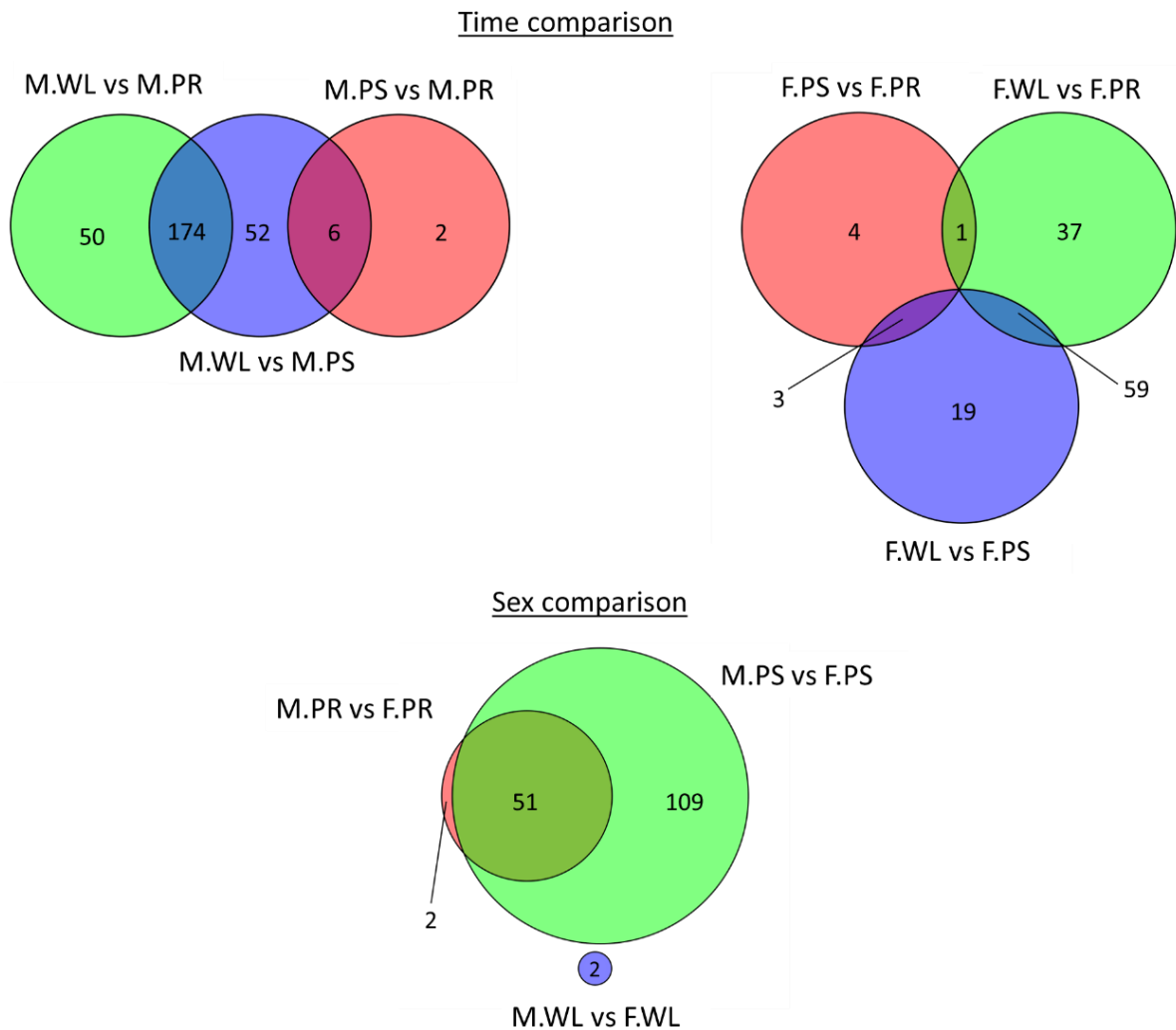
Figure 35. Venn diagram of time and sex comparisons between males and females throughout renal IRI. Up-regulated and down-regulated genes were analyzed together. Genes at the intersection correspond to common genes, while genes at the outer sets correspond to

specific genes of each comparison. adj. p-value ≤0.25 and log |FC |≥ 1. (M: Male; F: Female; PR: pre-ischemia; PS: post-ischemia; WL: one week later).

5.A.IV.   Validation of microarray assays by RT-qPCR

To continue, we validated the microarray assays. Randomly chosen genes changing expression in a time and sex-dependent manner, including ifit3, fabp5, cxcl10, rsad2 (irg6) and cd274 (Table XIX), were analyzed by RT-qPCR using specific TaqMan probes.

Table XIX. Gene expression level of selected microarray targets (time and sex comparisons)

Genes	Males vs Females			Males		Females	
	PR	PS	WL	WL vs PR	WL vs PS	WL vs PR	WL vs PS
ifit3	2,71	3,26	-	-3,34	-3,3	-	-
fabp5	-	-1,01	-	2,1	1,94	0,94	1,14
cxcl10	2,59	3,11	-	-3,87	-3,84	-1,91	-1,51
rsad2	0,92	3,24	-	-3,01	-3,08	-	-
cd274	2,31	2,89	-	-2,44	-2,6	-	-

*Values reported had a log |FC |≥ 1and an adj. p-value ≤0.25 (PR: pre-ischemia; PS: post-ischemia; WL: one week later)

The results obtained are in agreement with the microarray assay results (Figure 36). For each gene validated, we assessed the pattern of expression in a time and sex manner. For the time comparison in males, rsad2, cxcl10, ifit3 and cd274 genes are down regulated at recovery (WL) compared with PR and PS, whereas no differences are observed in females. In the sex comparison for these genes, males mRNA levels are higher than the females at PR and PS, but become similar at WL. We observe a different pattern of expression for fabp5 gene. For the time comparison, for both sexes, the gene is up-regulated at WL, compared to PR and PS. However, for the sex comparison, when we compare each time point, the levels are significantly higher in females than in males at PS. We determined that rsad2, cxcl10, ifit3 and cd274 expression correspond to the hierarchical clustering of microarray assays (Figure 32).
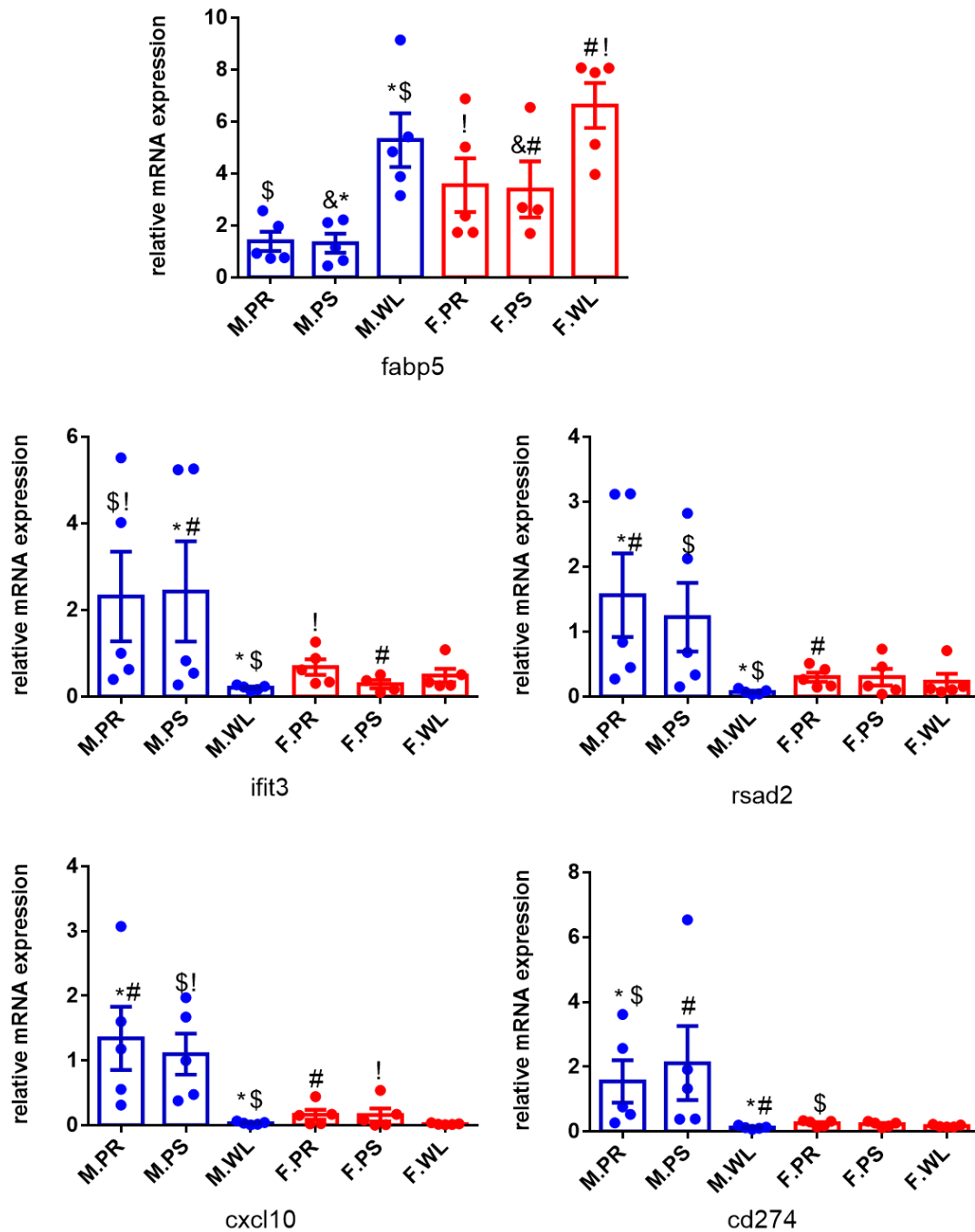
Figure 36. Validation of porcine renal IRI microarray assays by RT-qPCR experiments. The mRNA levels of selected target genes that displays a different regulation throughout IRI processes were measured (fabp5,ifit3, rsad2, cxcl10, cd274). For the time comparison, the different time points (PR, PS, WL) were compared with each other for each sex. For the sex comparison, a selected time point in male was compared to the equivalent time point in female. A positive validation was obtained for each gene. Comparisons that are significant different have at least a p-value ≤0.05. (M: Male; F: Female; PR: pre-ischemia; PS: post-ischemia; WL: one week later)

5.A.V.   Validation of selected DEG in pig sera samples

In previous experiments, we have found an important sexual dimorphism at the transcriptomic level. Next, we wanted to determine if the sex differences found at the mRNA level were conserved at the protein level, since the protein level is the one which determine the activity of the targets.

We have encountered many difficulties to find antibody that were specific to porcine tissues. Following different trials with different antibody, we were able to determine RSAD2 and IFIT3 protein expression in kidney biopsies by western blot. No significant differences of protein expression were observed when we compared the samples between the different time points (PR, PS, WL) or when we compared male and female samples at a selected time point. No correlation could be made between the mRNA and protein levels.

Since no difference in the time and sex comparison was found in kidney tissues, we decided to investigate if a sexual dimorphism could be observed for our selected target that are soluble in the sera.FABP5 and CXCL10 sera protein levels were measured at different time points (PR, PS, WL) in both sexes (Figure 37). For FABP5, no significant differences are detected in the time and/or sex comparison. However, for CXCL10, at the sex comparison M.PS vs F.PS, the sex differences observed at the mRNA level are conserved for the sera protein level. Some correlation between the mRNA and sera protein levels could be made. Nonetheless, the validation of more targets is necessary to determine targets that display sex difference at the protein level.
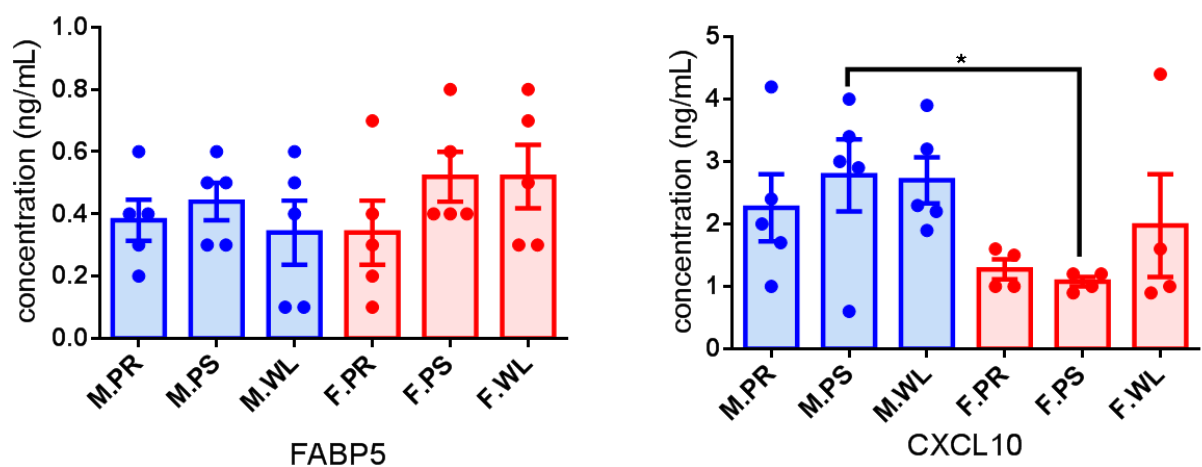
Figure 37. Porcine sera protein levels of selected target of renal IRI. ELISA assays were conducted to measure sera protein level of FABP5 and CXCL10. CXCL10 levels showed a sex difference at PS, while no significant changes were observed for FABP5. (M: Male; F: Female; PR: pre-ischemia; PS: post-ischemia; WL: one week later) (*: P-value ≤ 0.05)

5.A.VI.   Determination of top regulated genes by IPA

Following the validation of the microarray assays by RT-qPCR experiments, we extended our analysis of the microarray data by using bioinformatic tools. The Ingenuity Pathway Analysis (Qiagen, Redwood, CA) software, generated a dossier for each time (F.PS vs F.PR, FWL vs F.PS, F.WL vs F.PR, M.PS vs M.PR, M.WL vs M.PS ; M.WL vs M.PR) and sex (M.PR vs F.PR, M.PS vs F.PS, M.WL vs F.WL) comparison. The most top 10 up- and top 10 down-regulated genes from each time and sex comparisons was obtained.

For the time comparison, among the top 10 genes found up-regulated in both sexes after injury (PS vs PR), DNAJB1, RGS2, EGR1, JUN, FOS and ZFP36 were common for males and females, while DUSP1, LEAP2, BTG2 and CD109 were specific for males and ATF3, TRPV5, KCP and CXCL8 for females (Table XX & XXI). None of the top 10 down-regulated genes by injury were shared by males and females. During recovery (WL vs PS), SLC6A19 and CENPF were up-regulated while CXCL10 and UBD were down-regulated in both sexes. FABP5, CKAP2, TOP2A and CNA2 were up-regulated in males, and C4A/C4B, CYP24A1, CD109, HIST1H2AD and E2F1 in females. Down-regulated genes in the recovery phase included: FBG, FG, IFIT3, CXCL11, IFIT1, RSDA2 and MX1 in males and F9, HRG, STS, SLC5A10 and ACTC1 in females. All these genes remained expressed in the same manner one-week after injury respect to basal pre-injury situation (WL vs PR) for both males and females. Specific up-regulated genes during the recovery phase (WL vs PS) include SFRP2 and COL3A1 for males, KIAA0101 and SLC38A3 for females and HIST1H2AI for both sexes. Among those down-regulated we found RND1 in males and SELE, TMEM252 and CD83 in females. Up-regulated genes in the top10 list that were differentially expressed at one-week post-reperfusion vs the basal situation (WL vs PR) include C6, CDC20, EPHB3, KIF20A for males and CYP2D6 and HMMR for females. CMPK2 for males and PLG, SLC5A1 and OAT for females were down-regulated in this comparison. It is not certain the differences between PR vs WL would remain at longer recovery times or if the male pattern of expression would be restored to its pre-injury basal situation with time.

Table XX List of IPA top up-and down-regulated genes for the time comparison in females and Venn diagram representation.

Female

PSvsPR	Exp Log Ratio	WLvsPR	Exp Log Ratio	WLvsPS	Exp Log Ratio
FOS	1,696	SLC6A19	2,082	SLC6A19	2,218
ATF3	1,046	C4A/C4B	1,957	C4A/C4B	1,925
TRPV5	1,01	CYP24A1	1,956	CYP24A1	1,832
DNAJB1	1,009	CD109	1,792	CENPF	1,797
RGS2	0,996	FOS	1,672	CD109	1,667
EGR1	0,991	HIST1H2AD	1,568	KIAA0101	1,635
JUN	0,98	CYP2D6	1,538	HIST1H2AH	1,561
ZFP36	0,968	E2F1	1,535	HIST1H2AD	1,524
CXCL8	0,834	HMMR	1,531	SLC38A3	1,503
KCP	0,829	CENPF	1,528	E2F1	1,458
SFRP2	-1,103	F9	-2,223	F9	-1,999
GNLY	-1,092	HRG	-2,211	STS	-1,912
CCL21	-1,088	STS	-2,163	SELE	-1,737
CPE	-1,033	SLC5A10	-1,937	HRG	-1,714
KCNAB2	-1,028	CXCL10	-1,911	TMEM252	-1,565
KLF5	-1,02	PLG	-1,802	SLC5A10	-1,563
EREG	-0,996	ACTC1	-1,795	CD83	-1,543
NCAM1	-0,952	UBD	-1,767	UBD	-1,533
LOX	-0,942	SLC5A1	-1,683	CXCL10	-1,507
ASPN	-0,892	OAT	-1,677	ACTC1	-1,469

F.PSvsF.PR: **ATF3, DNAJB1, EGR1, ZFP36, KCP**, GNLY, CPE, KLF5, NCAM1, ASPN, SFRP2, CCL21, KCNAB2, EREG, LOX

F.WLvsF.PR: **CYP2D6, HMMR**, SLC5A1, PLG, OAT

FOS

SLC6A19, C4A/C4B, CYP24A1, CD109, F9, HRG, STS / **HIST1H2AD, E2F1, CENPF**, SLC5A10, CXCL10, ACTC1, UBD

KIAA0101, HIST1H2AH, SLC38A3, SELE, TMEM252, CD83

F.WLvsFPS

* Bolded genes are up-regulated and highlighted genes are down-regulated. (PR: pre-ischemia; PS: post-ischemia; WL: one week later).

Table XXI List of IPA top up-and down-regulated genes for the time comparison in males and Venn diagram representation.

Male

PSvsPR	Exp Log Ratio	WLvsPR	Exp Log Ratio	WLvsPS	Exp Log Ratio
FOS	2,449	SLC6A19	2,239	FABP5	1,942
DNAJB1	1,362	FABP5	2,102	ASS1	1,858
JUN	1,255	CKAP2	1,978	CENPF	1,795
EGR1	1,18	TOP2A	1,846	TOP2A	1,707
DUSP1	1,178	CENPF	1,751	CCNA2	1,694
RGS2	1,147	C6	1,686	SLC6A19	1,652
LEAP2	1,037	CDC20	1,669	CKAP2	1,634
BTG2	1,027	CCNA2	1,58	SFRP2	1,591
ZFP36	0,95	EPHB3	1,46	COL3A1	1,534
CD109	0,901	KIF20A	1,455	HIST1H2AI	1,426
ASS1	-0,841	FGB	-4,248	FGG	-4,236
TNF	-0,809	FGG	-4,146	FGB	-4,081
GNLY	-0,732	CXCL10	-3,867	CXCL10	-3,836
MASP2	-0,672	IFIT3	-3,344	CXCL11	-3,341
FMOD	-0,615	CXCL11	-3,234	IFIT3	-3,297
NR1H3	-0,615	IFIT1	-3,085	UBD	-3,186
MS4A6A	-0,594	RSAD2	-3,007	RSAD2	-3,08
NKG7	-0,58	CMPK2	-2,829	IFIT1	-2,992
UCP2	-0,576	UBD	-2,819	RND1	-2,935
STS	-0,575	MX1	-2,809	MX1	-2,677

M.PSvsM.PR: **FOS, JUN, DUSP1, LEAP2, ZFP36**, DNAJB1, EGR1, RGS2, BTG2, CD109, TNF, MASP2, NR1H3, NKG7, GNLY, FMOD, MS4A6A, UCP2, STS

M.WLvsM.PR: **C6, CDC20, EPHB3**, **KIF20A**, CMPK2

ASS1

SLC6A19, FABP5, CKAP2, FGB, FGG, CXCL10, IFIT3, UBD / **TOP2A, CENPF, CCNA2**, CXCL11, IFIT1, RSAD2, MX1

SFRP2, COL3A1, HIST1H2AI, RND1

M.WLvsMPS

* Bolded genes are up-regulated and highlighted genes are down-regulated. (PR: pre-ischemia; PS: post-ischemia; WL: one week later).

The sex comparison, results (Table XXII) show the top 10 up-regulated genes in males respect to females in basal conditions (PR) include: MX1, IFIT1, MASP, CXCL11, FGG, IFIT3, CXCL10, RSAD2, GBP3 and CD74. These genes are related with innate immune responses, cytokine signaling, complement activation, antigen presentation, NOD-like receptor signaling pathway and wound repair. Most down-regulated genes in males include PVALB, SFRP2, B4GAT1, KLHL1, ASPN, LUM, GPRC6A, FGF9, EPHB3 and FABP5, which are related with calcium binding, extracellular matrix structure, collagen binding, cell growth, morphogenesis and lipoprotein metabolism.

The 10 top up-regulated genes in males compared to females after one-week reperfusion (WL), include: CCL4, IL1B, CCL8, PLEK, CD80, TNF, EREG, ESM1, IL1A and MMP7. These genes encode for potent pro-inflammatory cytokines, chemokines, co-stimulatory signals for T cell activation, apoptosis, tissue remodeling and wound healing related proteins. Down-regulated genes in males vs females at WL include SLC27A6, UGT2B11, SLC51A, PEBP4, CLCNKB, SLC2A1, DHRS7, CES1, CNTFR and CYP2D6, encoding for proteins involved in drug metabolism, synthesis of cholesterol, steroids and other lipids, transport of conjugated steroids, lipid metabolism, PPAR signaling, glucose transport and voltage-gated chloride channels. It is apparent that at one week after reperfusion, males seem to be more actively involved in inflammatory processes and tissue remodeling and less active in metabolic and transport processes than females, which might compromise the resolution of the injury, promoting sterile inflammation and pro-fibrotic processes.

Table XXII. List of IPA top up-and down-regulated genes for the time sex and Venn diagram representation.

Male vs Female

PR	Exp Log Ratio	PS	Exp Log Ratio	WL	Exp Log Ratio
CXCL11	3,482	**CXCL11**	3,825	**CCL4**	1,479
FGG	2,749	**FGG**	3,76	**IL1B**	1,321
IFIT3	2,714	**IFIT3**	3,262	**CCL8**	1,087
CXCL10	2,59	**RSAD2**	3,239	**PLEK**	1,072
RSAD2	2,541	**CXCL10**	3,107	**CD80**	1,055
MX1	2,431	**FGB**	2,933	**TNF**	1,043
GBP3	2,388	**GBP3**	2,924	**EREG**	1,028
MASP	2,387	**CD274**	2,892	**ESM1**	1,014
CD274	2,308	**CXCL9**	2,884	**IL1A**	1,012
IFIT1	2,289	**UBD**	2,78	**MMP7**	0,987
SFRP2	-1,544	FGF9	-1,613	SLC27A6	-1,353
FGF9	-1,265	GRB7	-1,461	UGT2B11	-1,353
EPHB3	-1,197	ASS1*	-1,458	SLC51A	-1,272
FABP5	-1,081	EPHB3	-1,117	PEBP4	-1,256
PVALB	-1,048	TP53INP1	-1,036	CLCNKB	-1,234
B4GAT1	-1,002	FABP5	-1,015	SLC22A1	-1,19
KLHL14	-0,979	CYP2B6	-0,997	DHRS7	-1,039
ASPN	-0,978	CD34	-0,987	CES1	-1,011
LUM	-0,949	COLCA2	-0,987	CNTFR	-1,01
GPRC6A	-0,946	IGSF5	-0,982	CYP2D6	-0,967

Venn diagram (Male vs Female):

M.PRvsF.PR — M.PSvsF.PS — M.WLvsF.WL

- M.PRvsF.PR only: **MX1 IFIT1** PVALB KLHL1 LUM / **MASP** SFRP2 B4GAT1 ASPN GPRC6A
- Intersection (PR ∩ PS): **CXCL11 FGG IFIT3 CXCL10** FGF9 / **RSAD2 GBP3 CD274** EPHB3 FABP5
- M.PSvsF.PS only: **FGB UBD** ASS1 CYP2B6 COLCA2 / **CXCL9** GRB7 TP53INP1 CD34 IGSF5
- M.WLvsF.WL only: **CCL4 PLEK EREG MMP7** SLC51A SLC22A1 CNTFR / **IL1B CD80 ESM1** SLC27A6 PEBP4 DHRS7 CYP2D6 / **CCL8 TNF IL1A** UGT2B11 CLCNKB CES1

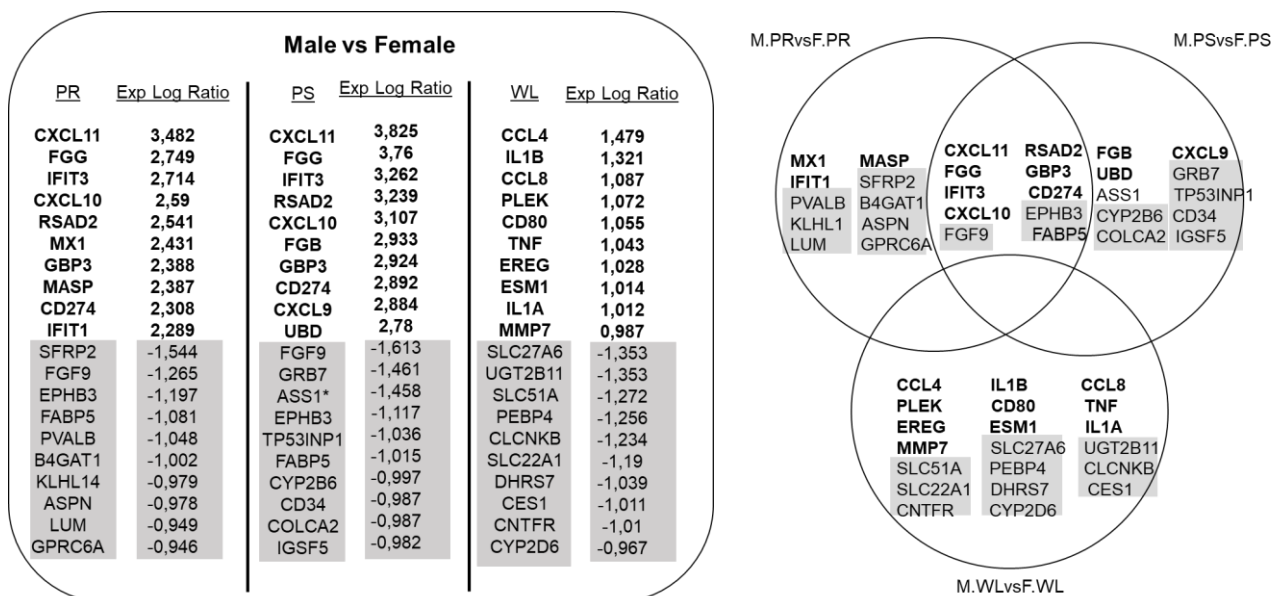* Bolded genes are up-regulated and highlighted genes are down-regulated. (PR: pre-ischemia; PS: post-ischemia; WL: one week later)

Representative heatmaps of these genes in sex- (MPR vs FPR) and time- (MPR vs MWL) comparisons were generated (Figures 38). The heatmaps generated also include the microarray results of a single castrated male (MC). This sample, which was not included in the enrichment pathway analyses, shows that the castrated male exhibits a similar expression pattern than females in basal conditions (PR) and that the expression changes observed between PR and WL in males do not occur in castrated males (MC). These results indicate that the presence of androgens in males rather than presence of estrogens in females strongly contribute to the sexual dimorphic pattern of expression before and after injury.
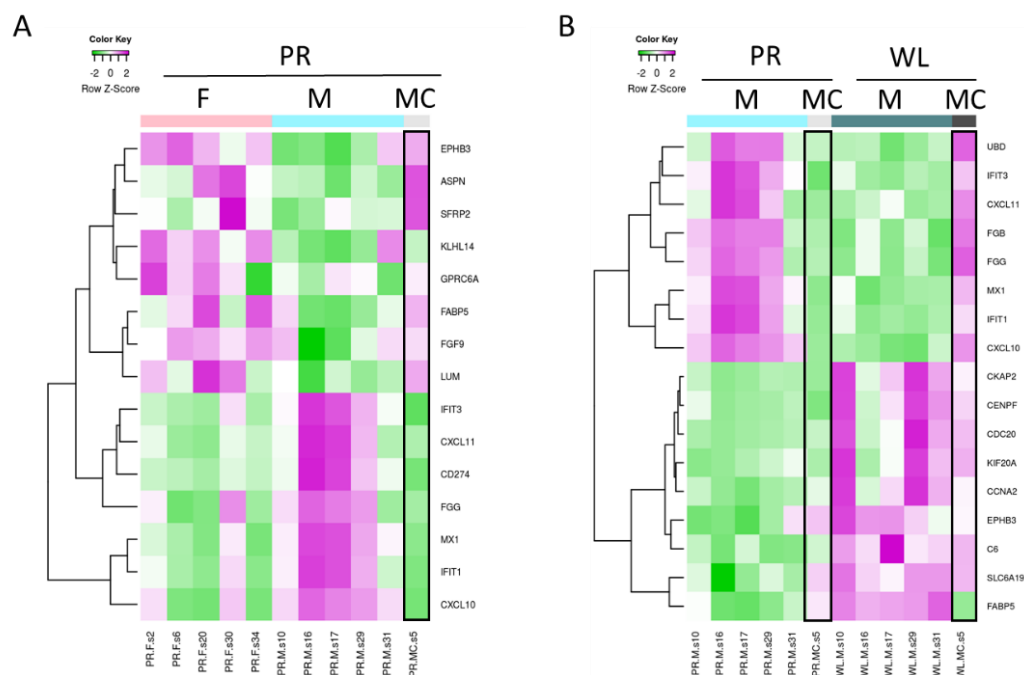
Figure 38. IPA heatmap gene expression representation of top regulated genes. Hierarchical clustering of top up and down regulated genes in A) a sex- (MPR vs FPR) and B) time- (MPR vs MWL) comparisons. A castrated male was added to the male and female group. (F: female; M: male; MC: castrated male; PR: pre-ischemia; WL: one week later).

5.A.VII.   Pathway enrichment analyses

The -omic data obtained in this study has produced lists of genes differentially expressed in female and male pig kidney transcriptomes in basal conditions, injury and recovery. We have made several comparisons, including: i) longitudinal comparisons of same individuals of the same sex and ii) sex-specific comparisons at the same time points. To gain mechanistic insight into the time- and sex-related differences that govern injury and recovery processes in pig kidneys, we aimed to identify biological pathways enriched more than would be expected by chance in a given gene list. Pathway enrichment analyses, visualization and interpretation of results was performed by using freely available and updated software, including g:Profiler, Gene Set Enrichment Analysis (GSEA) and Cytoscape, following a protocol that has been recently described[239].

Results shown in Figure 39A represent an example of individual sex comparisons depicting the GSEA enrichment map of males vs females at one-week post reperfusion (FDR:0,25). The map allows visualization of clusters containing nodes in which red and blue represent up- or down-regulated gene sets for each node. The clusters take their

name from the most common containing names of the nodes within the cluster (See Figure 39B for complete list of nodes in a given cluster). For this particular sex comparison (MWL vs FWL), up-represented clusters include biosynthesis, regulation and production of cytokines and interleukins, immune somatic recombinant, microtubule cytoskeleton organization, actin organization, which is in agreement with the top 10 up-regulated genes in IPA, encoding for potent pro-inflammatory cytokines, chemokines, co-stimulatory signals for T cell activation, apoptosis, tissue remodeling and wound healing related proteins, for this comparison (Table XXII) Similarly, down-represented clusters contain nodes related with metabolism of fatty acids and steroid hormones, nucleotide biosynthetic processes, amino acid catabolism, response to xenobiotic stimulus, etc. (Figure 39B) which, again, are in accordance with down-regulated top genes selected by IPA (Table XXII). All the individual comparisons are included in the annex section (Figure 60-68) in high resolution. The use of microarray ranked gene lists, GSEA pathway enrichment analyses and Cytoscape visualization have provided deeper insight and more integrative understanding of the processes under study than those given by gene list collections.

A
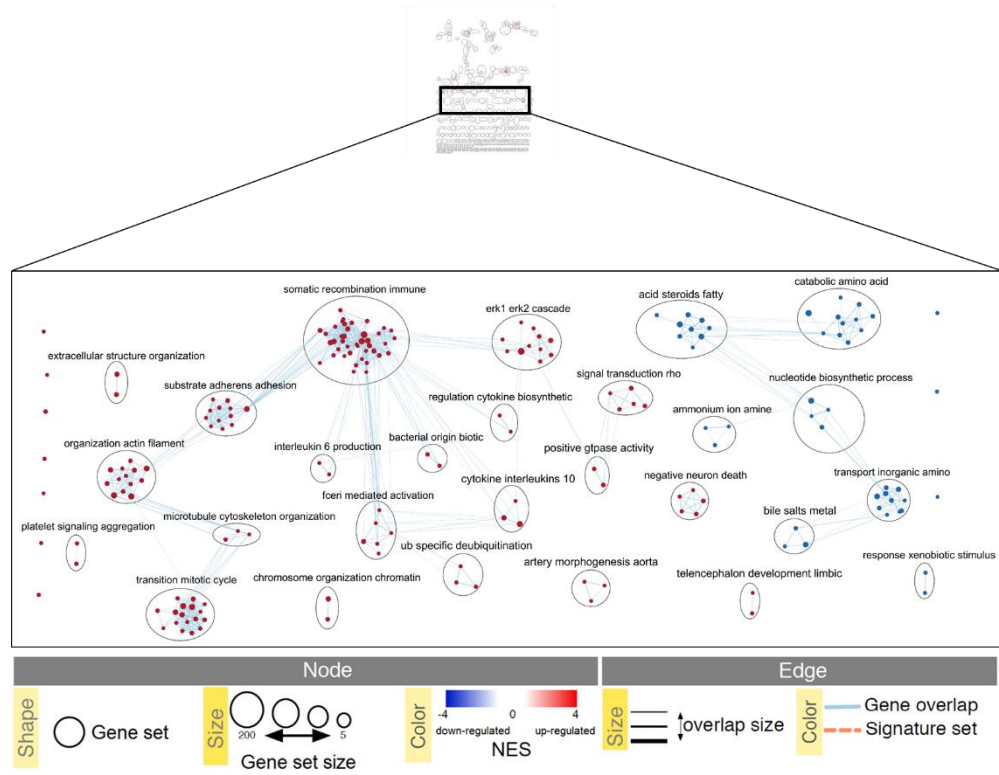
B
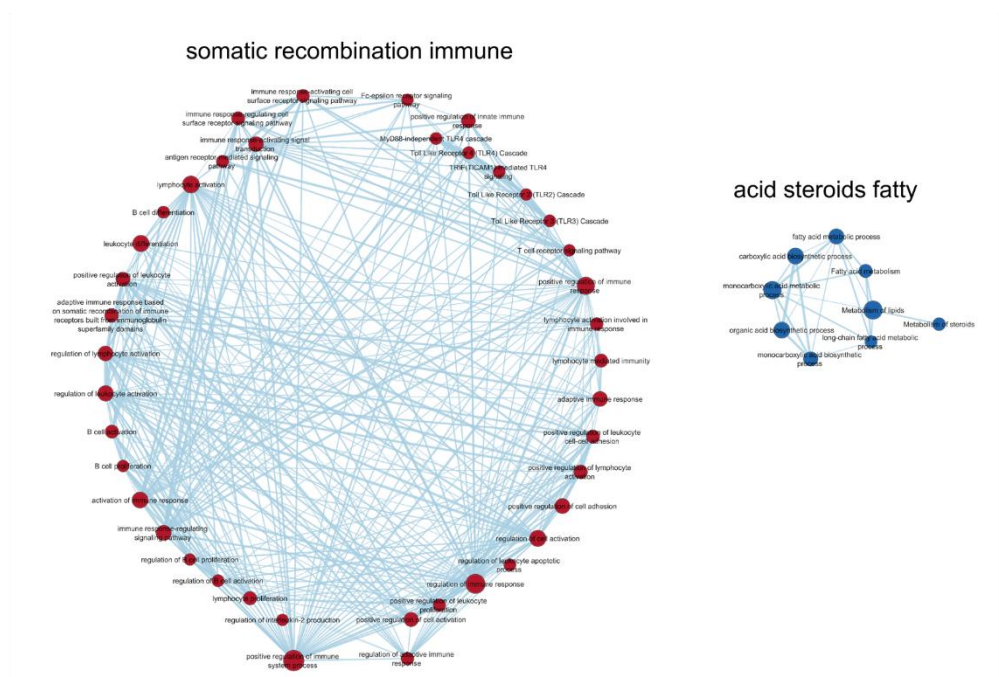
Figure 39. Enrichment map of over-represented genes in individual sex comparisons M.WL vs F.WL following GSEA analyses. A) Representation of different clusters (nodes) regulated in the comparison. B) Representation of different gene sets that form a given node, where red and blue nodes represent up- or down-regulated gene sets, respectively. (FDR:0,01-0,1).

Besides individual comparison analyses, we also did a grouped comparisons visualization of the enrichment analyses. A single enrichment map that comprise the 6 time comparisons (F.PS vs F.PR; FWL vs F.PS; F.WL vs F.PR; M.PS vs M.PR; M.WL vs M.PS ; M.WL vs M.PR) and the 3 sex comparisons (M.PR vs F.PR, M.PS vs F.PS, M.WL vs F.WL) was created. From this enrichment map, we chose nine clusters to analyze in depth. These clusters are: Immune cell regulation, Morphogenesis development migration, Ion transport transmembrane, Apoptotic intrinsic extrinsic, Oxygen levels hypoxia, Alcohol biosynthetic process, Steroid hormone response, Regulation hormone secretion and Phagocytosis endocytosis invagination. These clusters were selected based on the high number of gene sets they contained, which suggest their importance. They were also selected based on the relevance they have with the current study.

5.A.VIII.   Gene sets regulation pattern in time comparison (GSEA)

The various gene sets of a selected cluster were represented in heatmaps. They allowed the visualization of common patterns of gene sets regulation between different experimental conditions and revealed five prominent patterns for time comparison (from 1 to 5), that are schematically represented in Figure 40A. The red and blue color refer to gene sets that are over- or under-represented in the heat-maps. A summary of pattern combinations for gene sets that are up-regulated is shown in Figure 40B. As an example, if we look at gene sets included in *Immune cell regulation* for instance, we observe that there is one cluster of each kind out of the 5 possible patterns for the time comparison. Across the 9 selected clusters, genes set that share the same pattern of expression were manually summarized and reported in tables XXIII- XXVII. Our analysis only focused on the time points where the gene sets are active (up-regulated).

Pattern 1 represents pathways that are over-represented during the recovery process (WL vs PS) in females and in the injury process (PSvsPR) in males. Theses pathways include gene sets such as: regulation of alpha-beta T cell activation, positive regulation of leukocyte migration, Ca^{2+} regulation, concentration and transport, steroid metabolic process and regulation of endocytosis, among others (Table XXIII).

Pattern 2 represents pathways that are only over-represented during the recovery process (WL vs PS) in females but that are not up-regulated in males. These gene sets include: humoral immune response, positive regulation of adaptive immune response,

negative regulation of epithelial cell proliferation, positive regulation of endocytosis, etc. (Table XXIV).

Pattern 3 includes gene sets containing pathways that are only over-represented in males during injury. This gene sets include: toll-Like receptors Cascades, MyD88 cascade TLR4 TRIF, positive regulation of endothelial cell migration, EMT and negative regulation of extrinsic apoptotic signaling pathway, cellular response to hormone, positive regulation of hormone secretion, cytokine secretion, among others (Table XXV).

Pattern 4 includes pathways over-represented during the recovery process (WLvsPS) and at one-week post-reperfusion (WL vs PR) in females and that are over-represented only during injury in males. Some of the gene sets included: neutrophil activation, myeloid cell activation, regulation of lipid biosynthetic process, cholesterol biosynthetic process, response to estradiol (Table XXVI).

Pattern 5 includes pathways are over-represented only during injury in both sexes. Some of the gene sets include DNA damage response, negative regulation of ERK1 and ERK2 cascade, negative regulation of MAP kinase activity, positive regulation of secretion of hormone metabolism processes (Table XXVII).
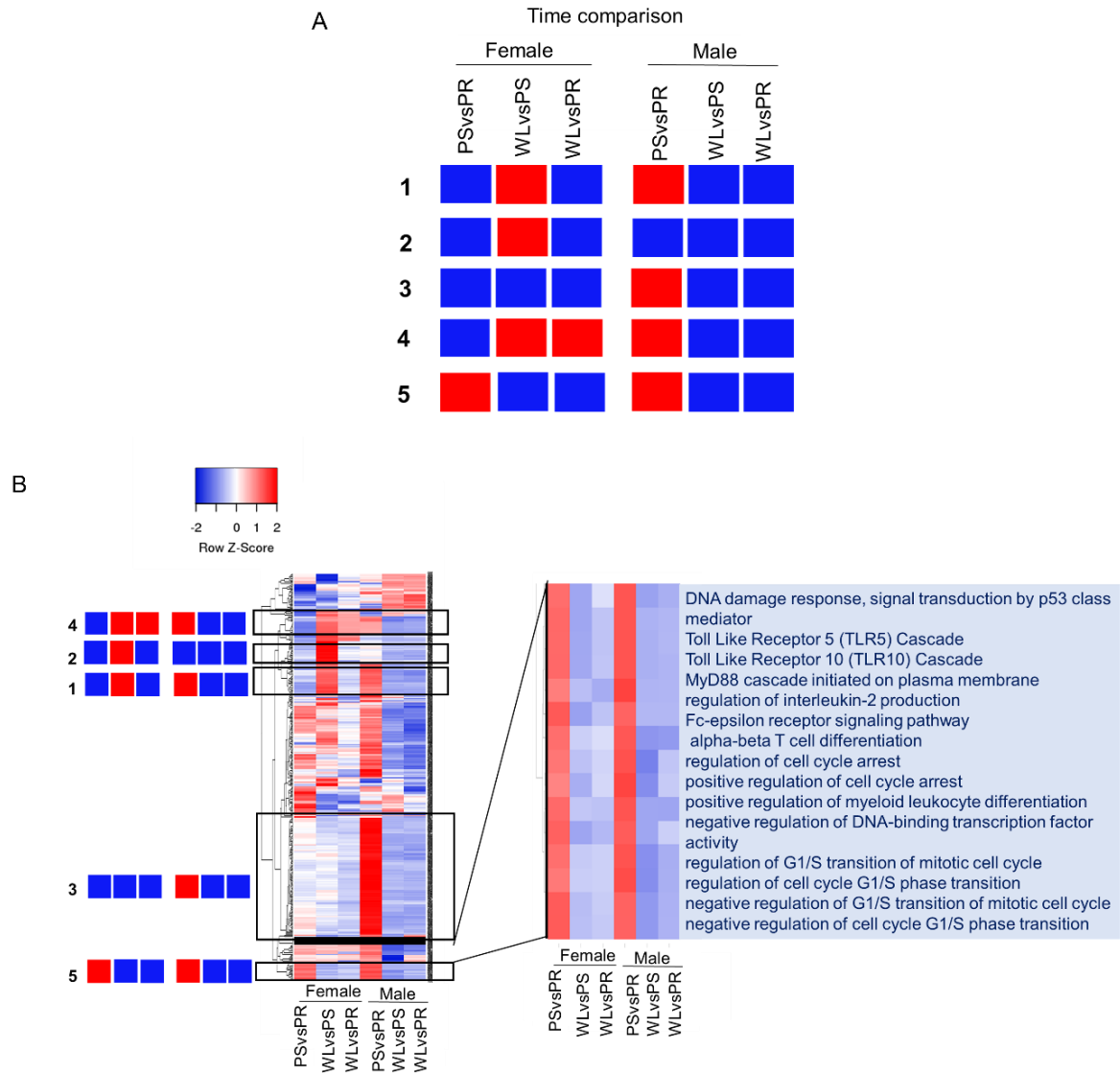
Figure 40. Patterns of gene sets regulation in male and female kidneys throughout renal IRI in the time comparison. A) five prominent patterns for time comparison. were determined B) on heatmaps representation. Heatmaps were created with the normalized enrichment score (NES) values given by GSEA analysis. The red and blue color refer to gene sets that are over- or under-represented in the heat-maps. (PR: pre-ischemia; PS: post-ischemia; WL: one week later).

Table XXIII. Summary of clusters and gene sets included in the pattern 1 for the renal IRI time comparison following GSEA.

		Female			Male		
		PSvsPR	WLvsPS	WLvsPR	PSvsPR	WLvsPS	WLvsPR
	Pattern 1	🟦	🟥	🟦	🟥	🟦	🟦
I-Immune cell regulation	myeloid cell differentiation						
	negative regulation of cell cycle						
	regulation of alpha-beta T cell activation						
	positive regulation of T cell activation and differentiation						
	positive regulation of cell-cell adhesion						
II-Morphogenesis development migration	positive regulation of mononuclear cell migration						
	regulation of leukocyte migration						
	positive regulation of leukocyte chemotaxis						
III-Ion transport transmembrane	Ca^{2+} regulation, concentration and transport						
	negative regulation of phosphate metabolic process						
VI-Alcohol biosynthetic process	regulation of cholesterol metabolic process						
	alcohol biosynthetic process						
	steroid biosynthetic process						
	steroid metabolic process						
	lipid metabolism						
VII-Steroid hormone response	response to organonitrogen compound						
IX-Phagocytosis endocytosis invagination	phagocytosis, engulfment						
	regulation of endocytosis						
	regulation of vesicle-mediated transport						
	endocytosis						

*Gene sets up and down-regulated are represented by red and blue squares, respectively. (PR: pre-ischemia; PS: post-ischemia; WL: one week later).

Table XXIV. Summary of clusters and gene sets included in the pattern 2 for the renal IRI time comparison following GSEA.

		Female			Male		
		PSvsPR	WLvsPS	WLvsPR	PSvsPR	WLvsPS	WLvsPR
Pattern 2		🟦	🟥	🟦	🟦	🟦	🟦
I-Immune cell regulation	inflammatory response						
	increase TNF production						
	necrotic cell death						
	humoral immune response						
	positive regulation of adaptive immune response						
II-Morphogenesis development migration	negative regulation of blood vessel morphogenesis						
	negative regulation of angiogenesis						
	negative regulation of epithelial cell proliferation						
IX-Phagocytosis endocytosis invagination	positive regulation of endocytosis						
	membrane invagination						
	receptor metabolic process						

*Gene sets up and down-regulated are represented by red and blue squares, respectively. (PR: pre-ischemia; PS: post-ischemia; WL: one week later).

Table XXV. Summary of clusters and gene sets included in the pattern 3 for the renal IRI time comparison following GSEA.

	Female			Male		
	PSvsPR	WLvsPS	WLvsPR	PSvsPR	WLvsPS	WLvsPR
Pattern 3	🟦	🟦	🟦	🟥	🟦	🟦

I-Immune cell regulation	T cell proliferation and activation
	regulation of leukocyte cell-cell adhesion
	regulation of mononuclear cell proliferation
	toll-Like receptors cascades
	MyD88 cascade TLR4 TRIF
II-Morphogenesis development migration	biomineral tissue development
	positive regulation of endothelial cell migration
	regulation of smooth muscle cell migration
	bone mineralization
	retina development
	regulation of cell motility
	EMT
III-Ion transport transmembrane	regulation of ion transmembrane transporter activity
	phosphorylation
	fatty acid transport
IV-Apoptotic intrinsic extrinsic	negative regulation of extrinsic apoptotic signaling pathway
V-Oxygen levels hypoxia	response to decreased oxygen levels
	cellular response to hypoxia
VII-Steroid hormone response	cellular response to lipid
	cellular response to insulin
	cellular response to hormone
VIII-Regulation hormone secretion	positive regulation of hormone secretion
	protein transport
	protein localization
	cytokine secretion

*Gene sets up and down-regulated are represented by red and blue squares, respectively. (PR: pre-ischemia; PS: post-ischemia; WL: one week later).

Table XXVI. Summary of clusters and gene sets included in the pattern 4 for the renal IRI time comparison following GSEA.

		Female			Male		
		PSvsPR	WLvsPS	WLvsPR	PSvsPR	WLvsPS	WLvsPR
Pattern 4		🟦	🟥	🟥	🟥	🟦	🟦
I-Immune cell regulation	neutrophil degranulation						
	neutrophil activation						
	neutrophil mediated immunity						
	granulocyte activation						
	myeloid cell activation						
	leukocyte degranulation						
	humoral immune response mediated by circulating immunoglobulin						
III-Ion transport transmembrane	negative regulation of ion transmembrane transport						
	negative regulation of cation transmembrane transport						
VI-Alcohol biosynthetic process	metabolism of steroids						
	organic acid biosynthetic process						
	regulation of lipid biosynthetic process						
	cholesterol biosynthetic process						
VII-Steroid hormone response	response to organophosphorus						
	response to organic cyclic compound						
	response to estradiol						

*Gene sets up and down-regulated are represented by red and blue squares, respectively. (PR: pre-ischemia; PS: post-ischemia; WL: one week later).
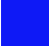
Table XXVII. Summary of clusters and gene sets included in the pattern 5 for the renal IRI time comparison following GSEA.

| | | Female | | | Male | | |
		PSvsPR	WLvsPS	WLvsPR	PSvsPR	WLvsPS	WLvsPR
	Pattern 5	🟥	🟦	🟦	🟥	🟦	🟦
I-Immune cell regulation	α-β T cell activation						
	DNA damage response						
	TLR5/TLR10						
	MyD88 cascade						
	IL-2						
	regulation of cell cycle arrest						
III-Ion transport transmembrane	negative regulation of ERK1 and ERK2 cascade						
	negative regulation of MAP kinase activity						
VIII-Regulation hormone secretion	positive regulation of secretion of hormone metabolism processes						
	hormone secretion						
	protein transport						
	protein localization						
	cytokine secretion						

*Gene sets up and down-regulated are represented by red and blue squares, respectively. (PR: pre-ischemia; PS: post-ischemia; WL: one week later).

5.A.IX.   Gene sets regulation pattern in sex comparison (GSEA)

Heatmaps were also created for the sex comparison and revealed four prominent patterns for sex comparison (from A to E), that are schematically represented in Figure 41A. For instance, for the gene sets included in immune cell regulation, we observe that there are two A and three B patterns for the sex comparison (Figure 41B). The same way with the time comparison, across the 9 selected clusters, gene sets that share the same pattern of expression were summarized in tables. Here also, our analysis only focused on the time points where the gene sets were active.

Pattern A represents gene sets that are up-regulated in males in respect to females at the same time points PR and PS but are down-regulated at WL This gene sets include: T cell differentiation and activation in immune response, INFy production, NF-kB signaling, Cellular response to chemokine, Ca^{2+} transport, intrinsic apoptotic signaling pathway, steroid biosynthetic process, lipid biosynthesis and metabolism, cellular response to hormone stimulus, among others. The high number of gene sets included in this pattern is in agreement with the general gene expression profile shown in the sex comparison in Figure 32. The remarkable weight of the immune system category indicates the relevance of this system in the sex-related differences underlying kidney injury and regeneration (Table XXVIII).

The second pattern (Pattern B) includes pathways which are less represented in males than in females in PR and PS but over-represented in males after one week reperfusion (Figure 41A) .Some gene sets include DNA damage checkpoint, humoral immune response, B cell proliferation and activation, blood vessel morphogenesis, endothelial cell migration and proliferation, kidney development, phagocytosis, etc. (Table XXIX).

The third pattern found (Pattern C) includes pathways under-represented in males only at PR. Some of the gene sets include positive regulation of epithelial cell proliferation, positive regulation of Wnt signaling pathway, receptor-mediated endocytosis (Table XXX).

Pattern D includes over-represented patterns in males only at PS. Some of the gene set include potassium ion transport, amino acid transport, steroid metabolic process, cellular response to organonitrogen compound (Table XXXI).
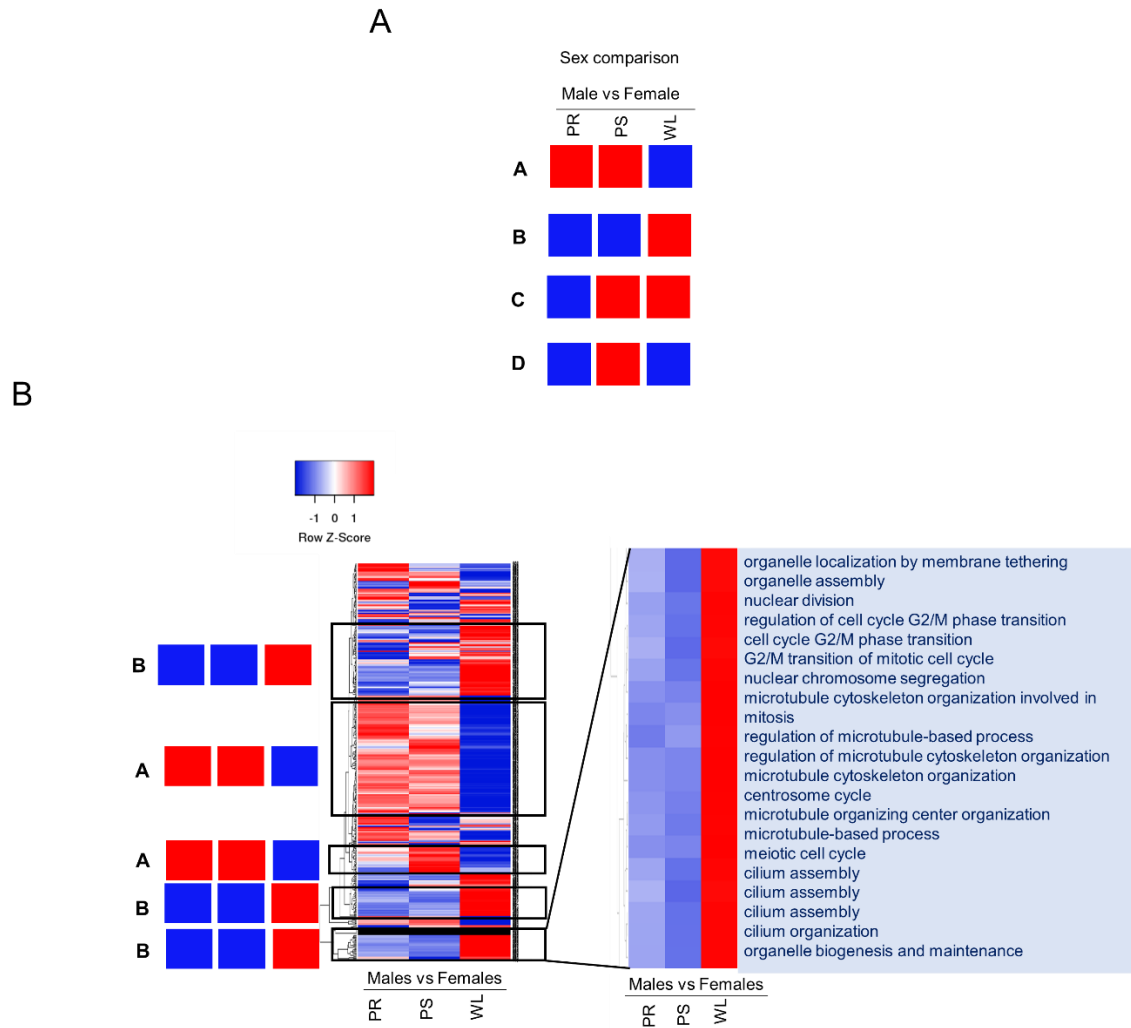
Figure 41. Patterns of gene sets regulation in male and female kidneys throughout renal IRI in the sex comparison. A) Four prominent patterns for sex comparison. were determined B) on heatmaps representation. Heatmaps were created with the NES values given by GSEA analysis. The red and blue color refer to gene sets that are over- or under-represented in the heat-maps. (PR: pre-ischemia; PS: post-ischemia; WL: one week later).

Table XXVIII. Summary of clusters and gene sets included in the pattern A for the renal IRI sex comparison following GSEA.

	Male vs Female PR PS WL
Pattern A	🟥 🟥 🟦

I-Immune cell regulation	leucocyte cell-cell adhesion
	T cell diferentiation and activation in immune response
	TNF production
	INFy production
	NF-kB signaling
	toll-like receptor signaling pathway (TLR3/TLR4)
	complement cascade
II-Morphogenesis development migration	positive regulation of leucocyte chemotaxis and migration
	Cellular response to chemokine
	Positive regulation of mononuclear cell migration
III-Ion transport transmembrane	cytosolic Ca^{2+}
	Ca^{2+} transport
	positive regulation of cytosolic calcium ion concentration
IV-Apoptotic intrinsic extrinsic	intrinsic apoptotic signaling pathway
	intrinsic apoptotic signaling pathway by p53 class mediator
	regulation of signal transcription by p53
VI-Alcohol biosynthetic process	steroid biosynthetic process
	regulation of cholesterol biosynthesis by SREBP (SREBF)
	metabolism of steroids
	lipid biosynthesis and metabolism
	inositol phosphate metabolic process
	cellular ketone metabolic process
VII-Steroid hormone response	cellular response to hormone stimulus
	peptide
	estradiol
	cellular response to insulin stimulus (insulin receptor signaling pathway)
VIII-Regulation hormone secretion	regulation of peptide, protein, hormone secretion and transport by cell

*Gene sets up and down-regulated are represented by red and blue squares, respectively. (PR: pre-ischemia; PS: post-ischemia; WL: one week later).

Table XXIX. Summary of clusters and gene sets included in the pattern B for the renal IRI sex comparison following GSEA.

	Male vs Female		
Pattern B	PR (blue)	PS (blue)	WL (red)
I-Immune cell regulation	IL6-6/IL-2		
	TLR 5/10		
	DNA damage checkpoint		
	cell cycle checkpoint		
	mast cell activation		
	humoral immune response		
	mitotic DNA integrity checkpoint		
	negative regulation of G1/S transition		
	B cell proliferation and activation		
	TLR1, TLR2 cascade, TLR6		
	cell-substrate adherens		
	cell-matrix adhesion		
II-Morphogenesis development migration	angiogenesis		
	blood vessel morphogenesis		
	endothelial cell migration and proliferation		
	canonical Wnt signaling pathway /non-canonical Wnt signaling pathway		
	kidney development		
	mesonephric epithelium development and tubular development		
	morphogenesis of a polarized epithelium		
IX-Phagocytosis endocytosis invagination	positive regulation of endocytosis		
	phagocytosis		
	receptor metabolic process		
	regulation of vesicle-mediated transport		

*Gene sets up and down-regulated are represented by red and blue squares, respectively. (PR: pre-ischemia; PS: post-ischemia; WL: one week later).

Table XXX. Summary of clusters and gene sets included in the pattern C for the renal IRI sex comparison following GSEA.

| | Male vs Female | | |
	PR	PS	WL
Pattern C	(blue)	(red)	(red)
II-Morphogenesis development migration	positive regulation of epithelial cell proliferation		
	eye morphogenesis		
	positive regulation of endothelial cell proliferation		
	positive regulation of Wnt signaling pathway		
IX-Phagocytosis endocytosis invagination	internalization		
	engulfment		
	import into cell		
	receptor-mediated endocytosis		

*Gene sets up and down-regulated are represented by red and blue squares, respectively. (PR: pre-ischemia; PS: post-ischemia; WL: one week later).

Table XXXI. Summary of clusters and gene sets included in the pattern D for the renal IRI sex comparison following GSEA.

	Male vs Female
	PR PS WL
Pattern D	

III-Ion transport transmembrane	inorganic cation transport and homeostasis
	potassium ion transport
	striated muscle contraction
	amino acid transport
IV-Apoptotic intrinsic extrinsic	negative regulation of intrinsic apoptotic signaling pathway
V-Oxygen levels hypoxia	cellular response to hypoxia
VI-Alcohol biosynthetic process	cholesterol metabolic process
	steroid metabolic process
	regulation of fatty acid metabolic process
VII-Steroid hormone response	cellular response to organonitrogen compound

*Gene sets up and down-regulated are represented by red and blue squares, respectively. (PR: pre-ischemia; PS: post-ischemia; WL: one week later).

125

5.B. SEX DIFFERENCES IN MOUSE MODEL OF RENAL IRI

5.B.I. Kidney function following IRI

Beside establishing a porcine model of renal IRI model, one goal of this study was to also establish a mouse model. In comparison to the pig model, the mouse is a more practical model to use. Indeed, it is easier to manipulate and work with rodents than corpulent animals. The elevated total cost associated to research with swine is also a factor that can lead to the use of a lower-cost model. Therefore, we tried to construct a model of renal IRI comparable to the pig model, but more accessible.

First, we conducted a pilot study with 8 weeks old C57BL6/J mice. Previously, for the pig model, we had determined that at 7 days following renal IRI, creatinine and BUN levels are back to basal level The intention of the pilot study was to determine the time required to observe a similar pattern of the biochemical parameter in the mice model, in order to compare both animal models at equivalent time points. Male mice were submitted to 23 minutes of bi-lateral renal IRI followed by different time of recovery. As expected, the peak of injury which is determined by increased levels of creatinine and BUN was observed 24 hours following injury (Figure 42). We determined that 72 hours were necessary for a return of the biochemical parameters to pre-injury levels.
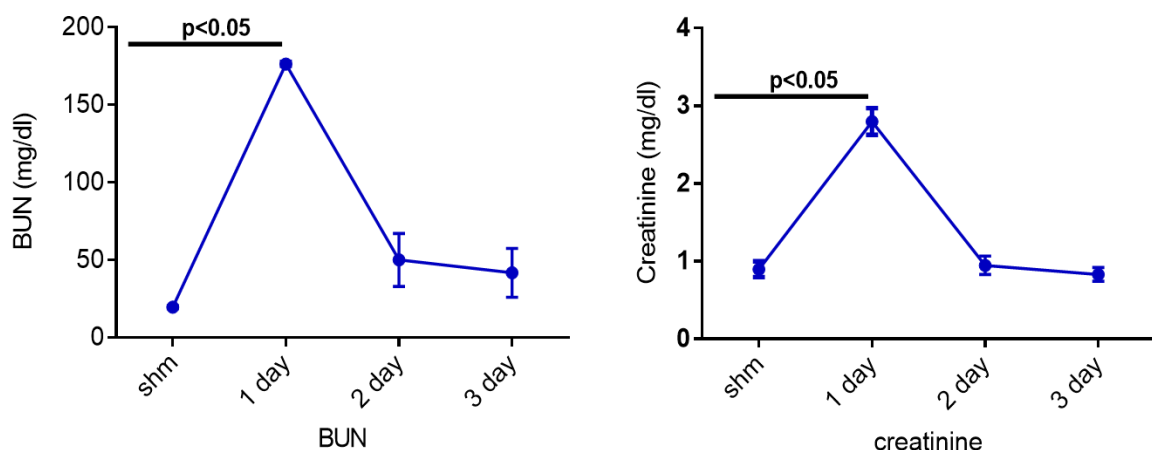
Figure 42. Renal function following renal IRI in male mice. AKI was induced by bilateral renal ischemia for 23 min in male mice. Recovery was allowed for up to 3 days. Blood samples were collected in sham group (shm) and at 1, 2 and 3 days in injured mice. The BUN and creatinine levels were measured at these different time points. A peak of injury is observed 24 hours following injury. Three days after AKI, biochemical parameters are equivalent to the basal situation. Biochemical parameters were measured by the Biochemistry Unit of the Vall d'Hebron hospital. p value<0.05 (BUN, blood urea nitrogen)

Following our pilot study, we conducted the renal IRI experiments. Male and female mice sexually mature where subjected to 23 minutes of bi-lateral renal IRI, followed by 3 days of recovery. Kidney biopsies were obtained before ischemia (PR), five minutes following injury (PS) and 3 days following IRI (REC).

5.B.II. Comparison of mouse and pig models of renal IRI

Next, we compared the mouse with the pig model of renal IRI at the gene expression level. First, we looked at the mRNA levels in mice kidney tissues. Five selected genes that were identified as being regulated by renal IRI and that showed a sexual dimorphism in the pig model (rsad2, ifit3, fabp5, cxcl10, cd274) were selected to be compared in mice tissues. We wanted to evaluate if a correlation existed between both species. RNA extractions from kidney biopsies were done and RT-qPCR experiment were conducted (Figure 43).

5.B.II.1. *Gene expression of selected target in mice kidneys*

First, we proceeded to a time and sex comparison for the mice gene expression, as it was done for the pigs. In the time comparisons (SHM vs PS, PS vs REC, SHM vs REC) for males, a different regulation was observed for rsad2, cd274 and ifit3. Whereas, no significant difference in the expression was found for cxcl10 and fabp5. For the females, different patterns of expression were observed for all 5 genes except for rsad2 who showed a significant difference in the mRNA level throughout the process.

As for the sex comparison (M.SHM vs F.SHM, M.PS vs F.PS, M.REC vs F.REC), sex differences were observed for cd274, fabp5 and ifit3 only. Overall, mice showed a sexual dimorphism in the selected targets genes expression. However, the clear pattern that was observed in pig gene expression was not identified here.
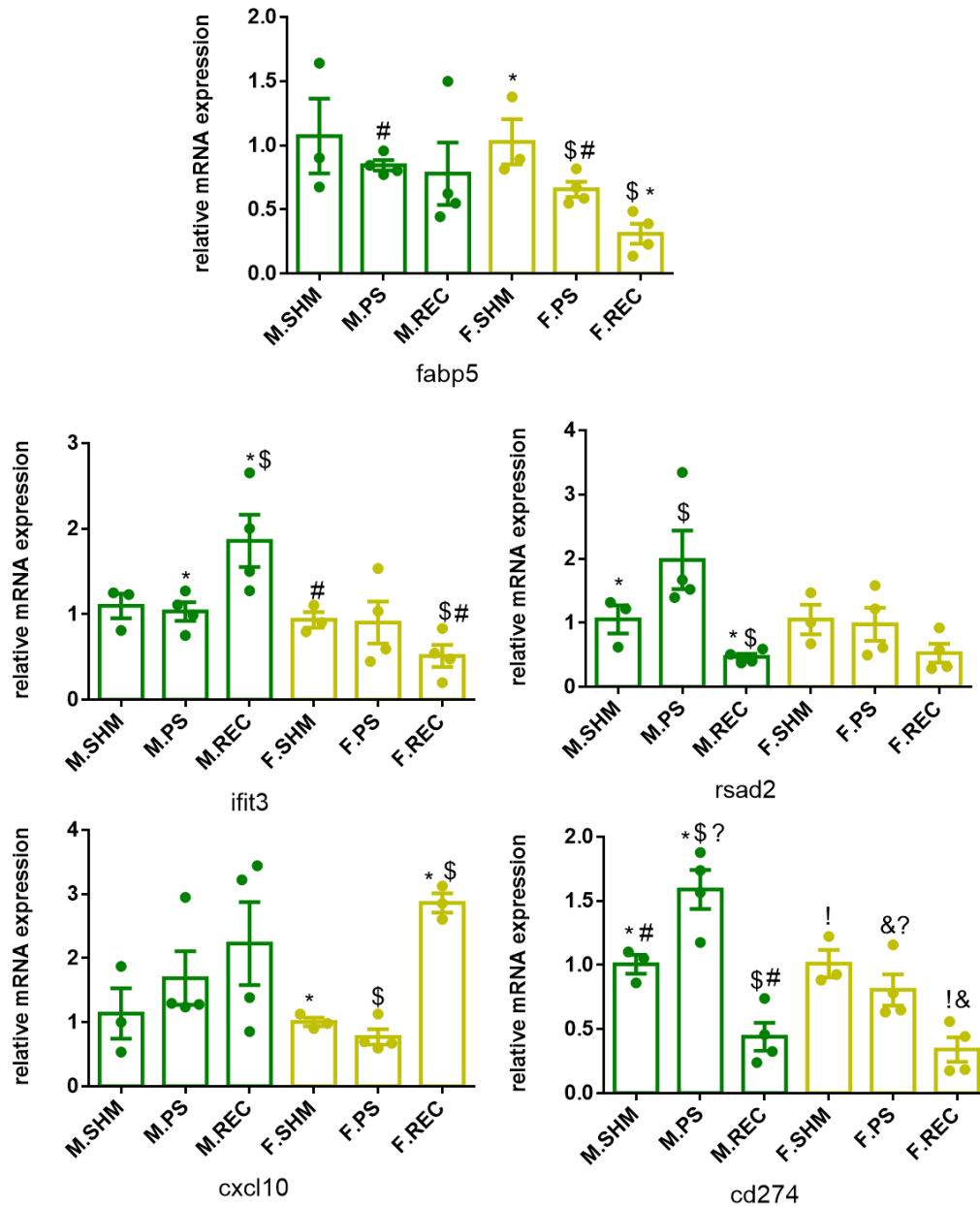
Figure 43. Evaluation of mRNA levels of selected targets in male and female mice kidneys by RT-qPCR experiments. RT-qPCR experiments were conducted with RNA from different kidney biopsies. The gene expression for rsad2, cxcl10, cd274, fabp5 and ifit3 was evaluated post-surgery (PS), 72 hours following surgery (REC) and also in their control group (SHM). (M: male; F: female).

5.B.II.2. Comparison of expression pattern of selected targets in pigs and mice kidney

Next, we compared the targets selected in pig and mouse kidney tissues. We compared the pattern of expression of mouse and pig males throughout renal IRI (Figure 44). No correlation was found between both species. Similar analysis with female mice and pigs revealed similar results. While intraspecies sexual dimorphism is observed, no correlation exists between the pattern of expression of common regulated genes between species.
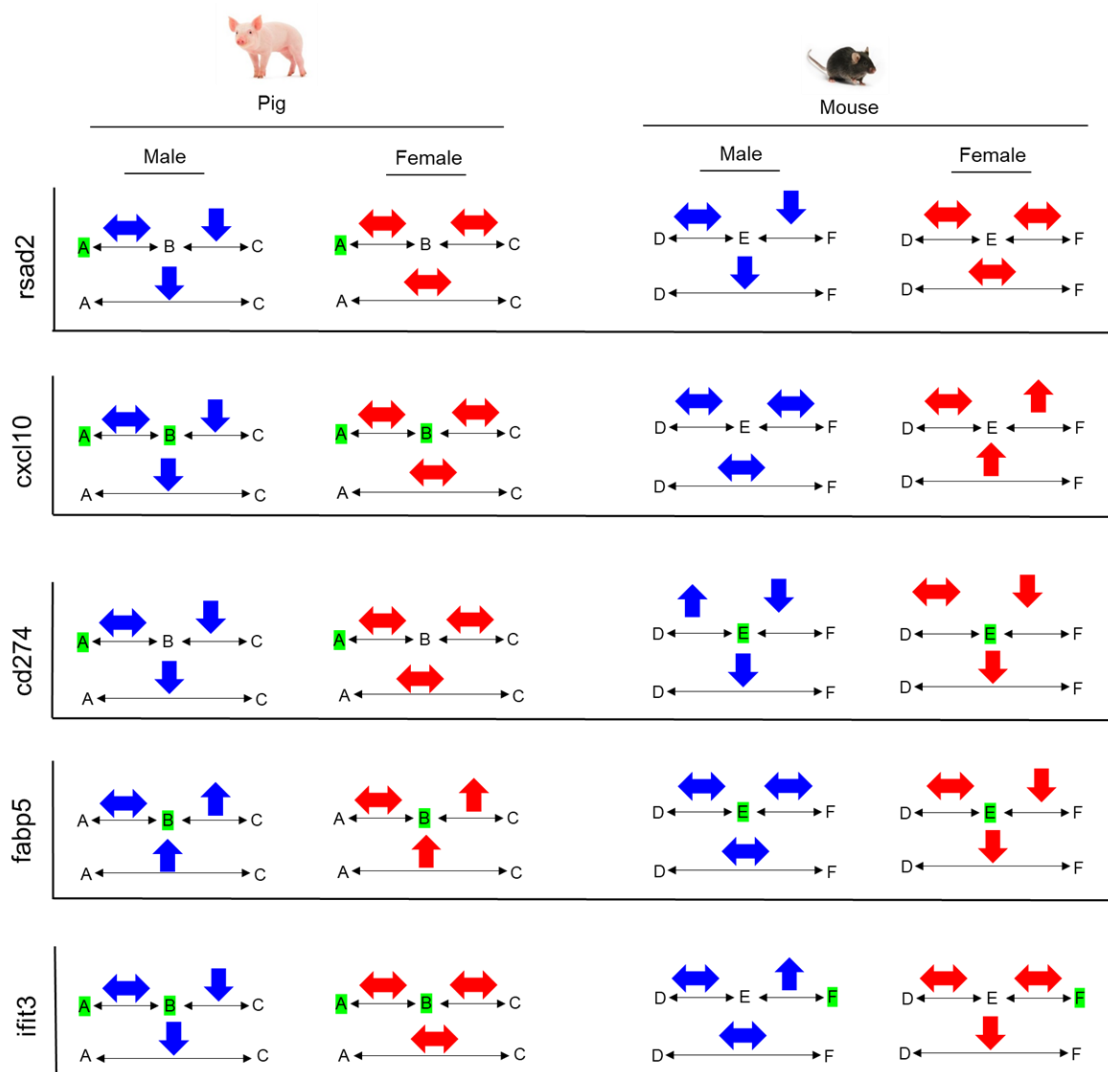
Figure 44. Comparison of selected target genes 'expression pattern throughout renal IRI by sex and specie. The pattern of expression between time points (A-E) was assesses for male and female mice and pigs for rsad2, cxcl10, cd274, fabp5 and ifit3. An ⇧ arrow indicate an up-regulation, whereas a ⇩ indicate a down-regulation. A ⇔ arrow indicate no significant change in the expression. Highlighted time points in green indicate the presence of a sex difference in the

interspecies at the selected time point. (A: PR=pre-ischemia; B: PS=post-ischemia; C: WL=one week later; D: SHM=sham; E:PS=post-ichemia; F:REC=3 days recovery)

The initial pilot study helped us to determine the time duration necessary to have a recovery in mice equivalent to the pigs. The very poor correlation we observed between species have raised the question whether the biochemical parameters (creatinine, BUN) in this new mouse cohort were still equivalent to the pig one. We then decided to validate the biochemical parameters of this new cohort.

During the renal IRI experiment in mice, two sera samples were collected for each animal. One sample was collected 3 to 7 days before the surgery (PR) and another one was collected 3 days following IRI (REC). The kidney functionality of theses samples was assessed by measuring BUN and creatinine levels. We compared the biochemical parameters in a time and sex manner as it was done in the porcine model. For the time comparison, for both sexes, creatinine and BUN levels are increased in a significant manner at REC compared to PR (Figure 45). For the sex comparison, for both proteins, no significant sex differences were observed at PR. However, at recovery (REC), males showed higher levels of BUN and creatinine levels than females (Figure 47).

These results revealed that unlike in the pilot study, renal function is not recovered in males (or females) 3 days following injury. Furthermore, females had a better recovery of renal function than the males. The comparison of gene expression pattern in pigs and mice at time points where the renal function is different might in part explain the absence of correlation between both species.

Figure 45. Effect of sex on renal function following renal IRI in mice. AKI was induced by bilateral renal ischemia for 23 min in males (M) and females (F). Recovery was allowed for 3
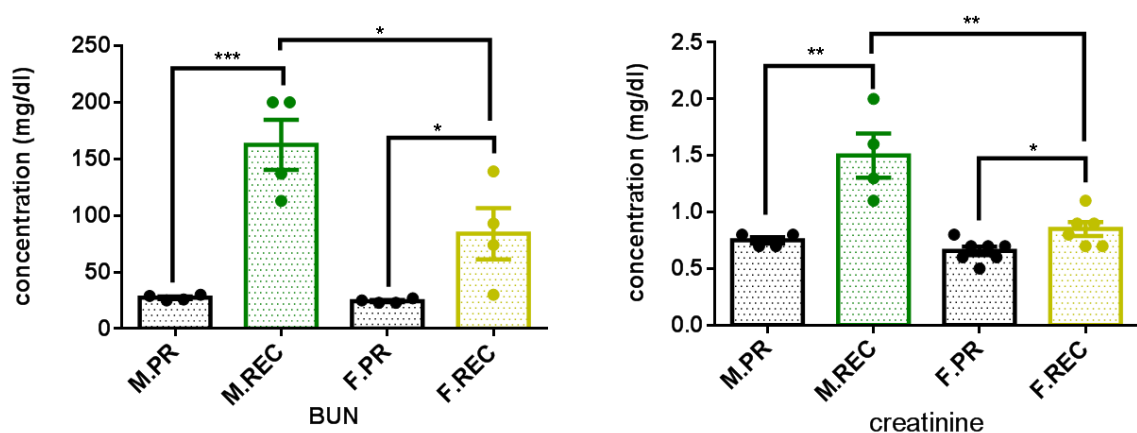
days. Blood samples were collected 3-7 days before the surgery (PR), and 3 days following IRI (REC). The BUN and creatinine levels were measured at PR and REC. (BUN, blood urea nitrogen) *: P-value ≤ 0.05, **: P-value ≤ 0.01; ***: P-value ≤ 0.001.

5.B.II.3.   *Comparison of pigs and mice transcriptome throughout renal IRI*

Having contradictory results for the biochemical parameter levels 3 days following renal IRI in mice, we decided to compare our results with similar published studies. We found a study, where a renal IRI model, very similar to our model. In their case Liu *et al.*, developed a bilateral renal IRI model in male mice, where they monitored the kidney gene expression 2 hours, 4 hours, 1 day, 2 days, 3 days, 1 week, 2 weeks, 4 weeks, 6 months, and 12 months following injury[254].

They found that 3 days following renal IRI, the creatinine levels are elevated and present significant difference compared to basal situation level. This is exactly what we observed in our second experiment. This tendency was also described elsewhere[135]. According to our results and their results, we concluded that in the mouse model, 7 days following injury is the time point that corresponds to the recovery time point (WL) in the pig model. We therefore shift our focus to the gene expression 7 days following injury.

With different renal biopsies, Liu *et al.*, performed RNAseq analyses. They found thousands of genes whose expression was altered by IRI at different moment in time. These genes were grouped and clustered into seven modules. Briefly, the GO analysis revealed that 7 days following IRI, there is a persistence in the up-regulation of genes regulating cell death, proliferation, cell adhesion, inflammation, adaptive immune responses and downregulation of genes related to tubular function in kidneys of male mice[254]. Furthermore, with only a single renal injury, these mice would go on to developed chronic kidney injury.

Next, we compared our pig transcriptomic data with their public available mice data. We compared list of genes differentially regulated between basal situation and 7 days following IRI in male mice with the genes differentially expressed in male pigs at the same time points (MWL vs M.PR).

By comparing both species omics data, we only found 30 common genes whose expression were altered in mice and pig (Table XXXII From these 30 genes, the expression pattern (up- or down-regulation) of only 8 genes was shared between both species (COL1A1, COL3A1, FAM198B, C6, ACE, GCM1, HRG and LRRC66). From

these genes, 50% of them are related to tubular function. Moreover, the 22 other genes differentially regulated in both male species were involved in inflammatory, immune response process, etc. These genes were up-regulated in male mice whereas they were down regulated in male pigs. The difference in the regulation of common genes could suggest a specie-specific outcome following renal IRI. In fact, Liu *et al.* reported that with only a single renal injury, these mice developed chronic kidney injury.

Table XXXII.   List of common regulated genes between pig and mouse males upon renal IRI (basal situation vs one week later comparison).

Gene	Expression 7 days after IRI vs basal situation	
	Mice	Pigs
TNFAIP3	↑	↓
ADCYAP1R1	↑	↓
APOD	↑	↓
BCL3	↑	↓
BMP2	↑	↓
CD14	↑	↓
COL1A1	↑	↑
COL3A1	↑	↑
CSF1	↑	↓
CXCL10	↑	↓
FAM198B	↑	↑
RHOJ	↑	↓
TNC	↑	↓
C6	↑	↑
CASP1	↑	↓
CXCL9	↑	↓
GBP2	↑	↓
MS4A7	↑	↓
MX1	↑	↓
PIK3AP1	↑	↓
PLEK	↑	↓
UBD	↑	↓
VCAM1	↑	↓
ZBP1	↑	↓
ACE	↓	↓
ASS1	↓	↑
GCM1	↓	↓
HRG	↓	↓

LRRC66	↓	↓
SLC4A1	↓	↑

*List of genes differentially expressed in both mice and pig in the comparison of basal state vs one week later comparison, and whether they are up (↑) or down (↓) regulated. Genes with similar pattern in both species are highlighted in green.

5.C. VALIDATION OF PORCINE MODEL OF RENAL IRI IN HUMAN SAMPLES

Following the comparison of the mice and pig models of renal IRI, we decided to study the possible correlation between pig and human tissues by comparing the gene and protein expression pattern at equivalent time points.

5.C.I. mRNA levels of human post-ischemic tissue

Selected genes that were identified as being regulated by renal IRI and that showed a sexual dimorphism in the pig model were selected to be studied in human ischemic biopsies. Kidney biopsies of normal tissue were obtained from renal cancer patients that underwent nephrectomy. These post-ischemic tissues (PS) were collected following the surgery and correspond to the post-surgery (PS) in the pig tissue model. mRNA levels at that time point in men and women allowed us to perform a sex comparison (Figure 46).

As for the sex comparison, we observed a difference in the human mRNA levels for rsad2 and cd274 genes. The genes fabp5, ifit3 and cxcl10 showed no significant level of expression between men and women. We also found that the two genes that showed a sex difference in human showed the exact same pattern of expression in pig tissues. Overall, partial correlation was found between the mRNA levels of both species.
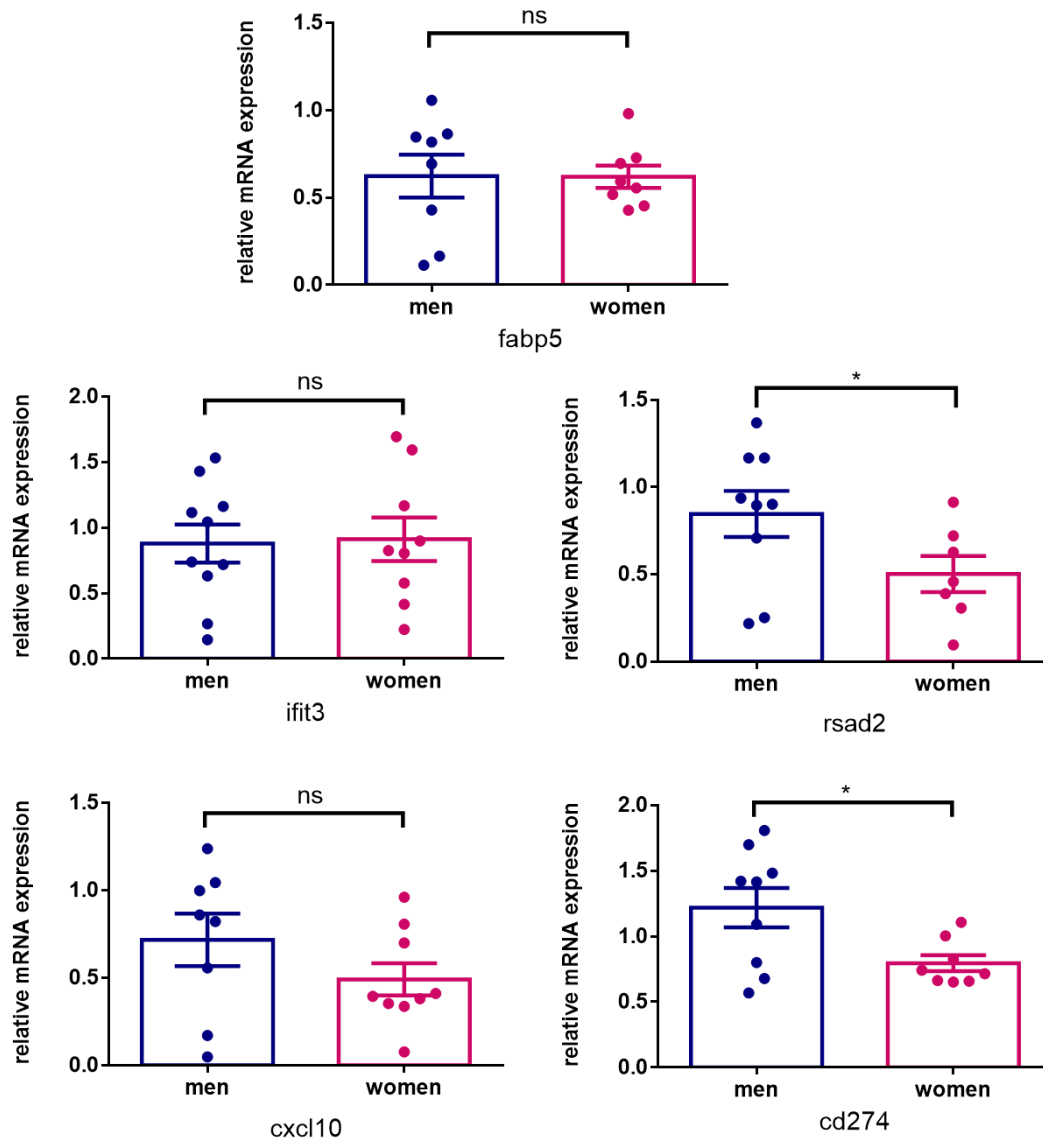
Figure 46. Evaluation of mRNA levels of selected targets in human ischemic kidney biopsies by RT-qPCR experiments. RT-qPCR experiments were conducted with RNA from normal kidney tissues. The gene expression for rsad2, cxcl10, cd274, fabp5 and ifit3 was evaluated post-surgery (PS) in men and women. *: P-value ≤ 0.05, ns: not significant.

5.C.II. Sera protein level of human at basal situation

Following the assessment of the mRNA levels of the five randomly selected target in pigs in human renal tissue, we determined the sera protein levels in human samples. Sera protein levels of selected targets were measured in patients before nephrectomy (PR) by ELISA. This time point corresponds to the PR time point in the pig model of injury.

First, sexual hormones levels were evaluated in men and women, to confirm hormone activity. As expected, men showed greater levels of testosterone and women had greater levels of estrogen (Figure 47). Then, the sera protein levels of selected targets where measured. FABP5, CXCL10 and PD-L1(cd274) showed not only a sexual dimorphism, but their pattern of regulation correlate with the pig. These results showed the overall great correlation that exist between pig and human in the regulation of renal genes.
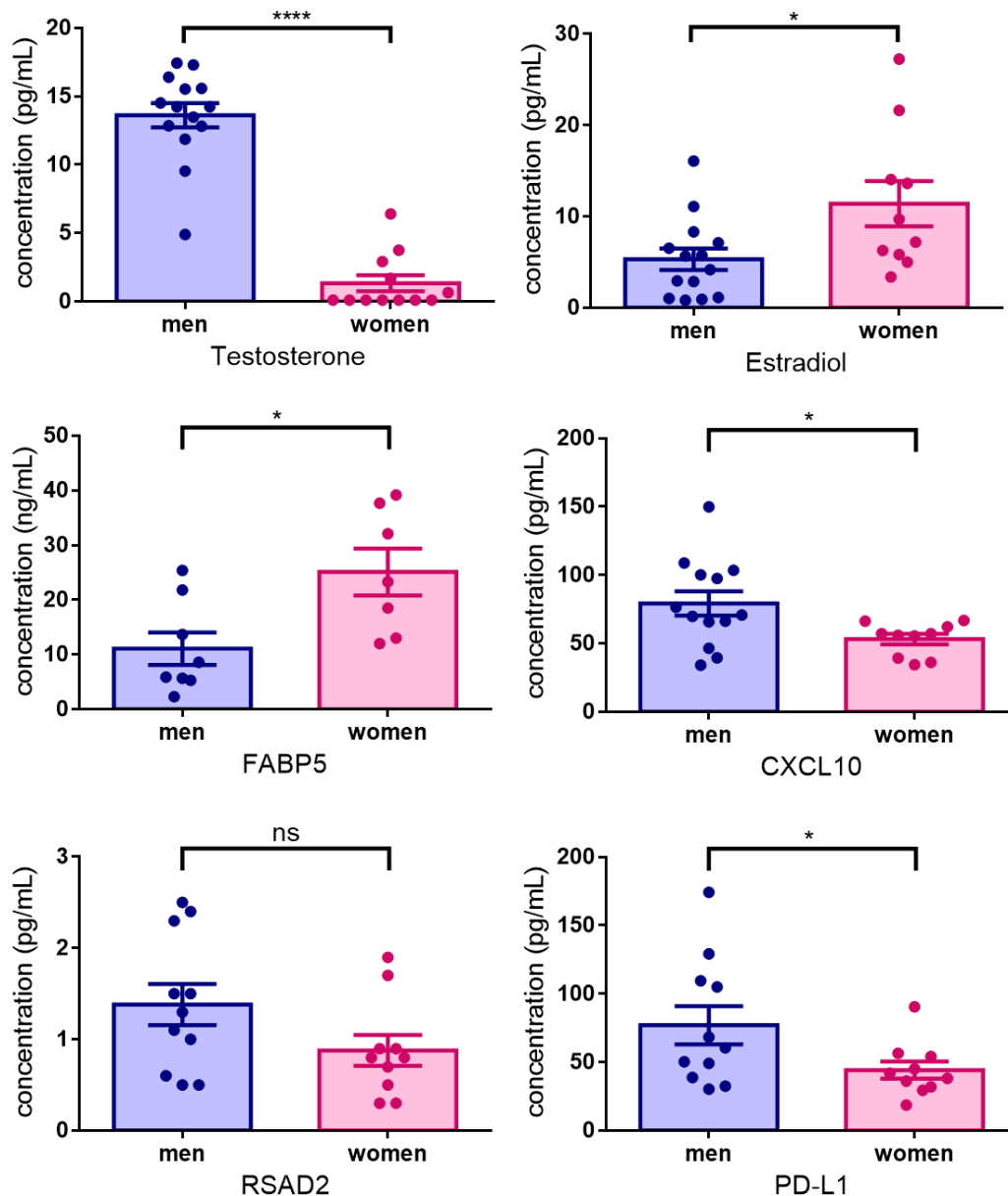
Figure 47. human sera protein level of selected targets at basal situation. ELISA were performed to determine the sera protein level of sex hormones (testosterone, estradiol) and selected targets (FABP5, CXCL10, RSAD2, PD-L1) in men and women samples. *: P-value ≤ 0.05; ***: P-value ≤ 0.001, ns: not significant.

5.D. SYSTEM BIOLOGY ANALYSIS OF RENAL IRI PORCINE MICROARRAY DATA

One of our goal in this project was to perform system biology analysis of renal IRI porcine microarray data. To further our analysis, Anaxomics' TPMS technology was used. The project focused on the identification of key proteins and pathways associated with the role of androgens in renal IRI and regeneration. Mathematical models were created and were analyzed through two different strategies to identify key proteins related to androgen-associated pathways in IRI/regeneration. The model reversion strategy found proteins whose modulation would turn the behavior of a model into the behavior of another model. In this case, we identify the proteins that differentiate the male IRI/regeneration model from the female IRI/regeneration model. Whereas the sources strategy allowed the identification of the proteins from a set (differential proteins from the pig microarray) that most affect another set of proteins (IRI/regeneration).

The reversion model strategy has identified 47 key proteins. Whereas the sources strategy has identified 5 key proteins (Figure 48). The male source proteins promote renal damage and impair regeneration, while the female sources proteins reduce renal damage and promote regeneration. One protein (CEBPA) was identified through both the reversion model and sources strategy.

Figure 48. Summary of renal IRI key proteins identified through model reversion and sources strategies in Anaxomics analysis. The reversion model strategy identified 47 proteins,

whereas 5 proteins were identified through the source strategy. Protein highlighted in blue are differentially expressed within the porcine microarray data.

5.D.I.   Model reversion key proteins

A total of 47 were identified as key proteins related to androgens IRI injury and regeneration (Table XXXIII). From the 47 proteins identified as androgen associated proteins through model reversion, 9 proteins are differentially expressed in the male WL vs PS comparison (pig microarray), and 3 are differentially expressed in the female WL vs PS comparison. Moreover, all 47 proteins have a direct interaction with at least one protein differentially expressed in the male WL vs PS comparison.

When considering the differential expression data from WL vs PR comparison, 12 proteins are differentially expressed for the males, and 6 are differentially expressed proteins for the female. All 47 proteins have a direct interaction with at least one protein differentially expressed in WL vs PR comparison (in male and female).

Table XXXIII. Key proteins identified through model reversion

Protein	Microarray WL vs PS		Distance 1 Microarray WL vs PS		Microarray WL vs PR		Distance 1 Microarray WL vs PR		ccRCC	
Name	M	F	M	F	M	F	M	F	Key protein	D1
ACE	↓	↓	✓	✓	↓	↓	✓	✓	-	✓
CASP1	↓	-	✓	✓	↓	-	✓	✓	-	✓
IRF7	↓	-	✓	✓	↓	-	✓	✓	-	✓
CXL10	↓	-	✓	✓	↓	↓	✓	✓	-	✓
PPIF	↓	-	✓	✓	-	-	✓	✓	-	✓
IRF1	↓	-	✓	✓	↓	-	✓	✓	✓	✓
REL	↓	-	✓	✓	↓	-	✓	✓	-	✓
CEBPB	↓	-	✓	✓	↓	-	✓	✓	-	✓
E2AK2	↓	-	✓	✓	↓	-	✓	✓	-	✓
CEBPA	-	↑	✓	✓	↑	-	✓	✓	-	✓
BCL2	-	↓	✓	✓	↓	↓	✓	✓	-	✓
TWST2	-	-	✓	-	-	-	✓	✓	-	✓
TLR5	-	-	✓	-	-	-	✓	✓	-	✓
MITF	-	-	✓	-	-	-	✓	✓	-	✓
AHR	-	-	✓	✓	-	-	✓	✓	-	✓

YBOX1	-	-	✓	✓	-	-	✓	✓	-	✓
CD28	-	-	✓	✓	-	-	✓	✓	-	✓
SP3	-	-	✓	✓	-	-	✓	✓	-	✓
GBG2	-	-	✓	✓	-	-	✓	✓	-	✓
TLR4	-	-	✓	✓	↓	↓	✓	✓	✓	✓
PO2F1	-	-	✓	✓	-	-	✓	✓	-	✓
APEX1	-	-	✓	✓	-	-	✓	✓	-	✓
NEP	-	-	✓	✓	-	-	✓	✓	-	✓
ING4	-	-	✓	✓	-	-	✓	✓	-	✓
BID	-	-	✓	✓	-	-	✓	✓	-	✓
NR1I2	-	-	✓	✓	-	-	✓	✓	✓	✓
GRP75	-	-	✓	✓	-	-	✓	✓	-	✓
BRCA1	-	-	✓	✓	-	-	✓	✓	-	✓
BAX	-	-	✓	✓	-	-	✓	✓	-	✓
JUNB	-	-	✓	✓	-	-	✓	✓	-	✓
B2CL1	-	-	✓	✓	-	-	✓	✓		✓
PPARG	-	-	✓	✓	-	-	✓	✓	✓	✓
GCR	-	-	✓	✓	-	-	✓	✓	✓	✓
VDR	-	-	✓	✓	-	-	✓	✓	✓	✓
RENI	-	-	✓	✓	-	-	✓	✓	-	✓
ACE2	-	-	✓	✓	↓	↓	✓	✓	✓	✓
STA5B	-	-	✓	✓	-	-	✓	✓	✓	✓
IKKA	-	-	✓	✓	-	-	✓	✓	-	✓
IL8*	-	-	✓	✓	-	-	✓	✓	-	✓
CREB1	-	-	✓	✓	-	-	✓	✓	✓	✓
CCL2	-	-	✓	✓	-	-	✓	✓	-	✓
SPI1	-	-	✓	✓	-	-	✓	✓	-	✓
VDAC1	-	-	✓	✓	-	-	✓	✓	-	✓
PTN11	-	-	✓	✓	-	-	✓	✓	-	✓
CYC	-	-	✓	✓	-	↑	✓	✓	-	✓
KPCG	-	-	✓	✓	-	-	✓	✓	-	✓
HDAC4	-	-	✓	✓	-	-	✓	✓	-	✓

*Arrows in microarray WL vs PS/ WL vs PR columns means that the protein is differentially expressed in the comparison, and whether it is up (↑) or down (↓) regulated. A tick in distance 1 microarray WL vs PS/ WL vs PR columns means that the protein is directly related to at least one differentially expressed in the WL vs PS/ WL vs PR comparisons. ccRCC columns contain information from the analysis of ccRCC data, a tick in key protein means that the protein has been reported as a key protein within the ccRCC data analysis, whereas a tick in D1 Column means that the protein is directly related to at least one key protein from ccRCC data analysis. F: female, M: Male; PR: pre-ischemia; PS: post-ischemia; WL: one week later.

Some of the identified key proteins in this model strategy have already been reported to play a key role in renal I/R injury and regeneration. In fact, BCL2, BAX, CYC, BID, TLR5, TLR4, CXCL10, IL8, CCL2, RENI, ACE, ACE2, STAT5B have been described to play a roles in some of the following processes: cell death, innate and adaptive immune system, oxidative stress, microvascular dysfunction and regeneration of renal epithelial cells.

Moreover, a total of 9 of the identified key proteins related to androgens IRI/regeneration were also reported to play a key role in ccRCC. Moreover, 44 of the key proteins present a direct interaction with at least one key protein of ccRCC (Figure 17).

5.D.II. Sources model key proteins

The sources strategy identified proteins that mostly affect IRI/regeneration (Table XXXVI). The analysis of the male data consisted on the identification of the proteins mainly promoting renal damage and hindering regeneration, whereas the analysis of the female data focused on the identification of the proteins hindering renal damage and promoting regeneration. As a result: STAT1 and STAT5A reduction was identified as protein modulations mostly promoting renal damage and hindering regeneration in males. CEBPA and HSP7C increase and PTN1 reduction were identified as protein modulations mostly hindering renal damage and promoting regeneration in females. The protein CEBPA, identified through this strategy for the female analysis was also identified as a key protein through model reversion.

Table XXXVI. Key proteins identified through protein sources strategy

Protein	Source		Microarray WL vs PS		Distance 1 WL vs PS Microarray		Microarray WL vs PR		Distance 1 WL vs PR Microarray		ccRCC	
Name	M	F	M	F	M	F	M	F	M	F	Key protein	D 1
CEBPA	-	✓	-	↑	✓	✓	↑	-	✓	✓	-	✓
PTN1	-	✓	↓	↓	✓	✓	↓	-	-	-	-	✓
HSP7C	-	✓	-	↑	✓	✓	-	↑	-	-	-	✓
STAT1	✓	-	↓	-	✓	✓	↓	-	-	-	-	✓
STA5A	✓	-	↓	-	✓	✓	↓	-	-	-	-	✓

* A tick in sources males and sources females columns means that the protein has been identified as key protein in each one of the comparisons. Arrows in microarray WL vs PS/ WL vs PR columns means that the protein is differentially expressed in the comparisons, and whether it is

up (↑) or down (↓) regulated. A tick in distance 1 microarray WL vs PS/ WL vs PR   columns means that the protein is directly related to at least one differentially expressed in the comparison. ccRCC? columns contain information from the analysis of ccRCC data: A tick in key protein means that the protein has been reported as a key protein within the ccRCC data analysis, whereas a tick in D1 Column means that the protein is directly related to at least one key protein from ccRCC data analysis. F: female, M: Male; PR: pre-ischemia; PS: post-ischemia; WL: one week later

5.D.III. Mechanistic justification of the role of androgens in IRI

Another goal of this project was to determine the role of androgens in renal IRI. By combining our pig microarray data with Anaxomics' TPMS technology, we determined that androgens affect renal IRI by increasing oxidative stress, dedifferentiation of renal epithelial cells, endothelial to mesenchymal transition, immune response and cell death, and by impairing regeneration of renal epithelial cells, hence enhancing renal damage and disrupting the kidney's regeneration process (Figure 49).
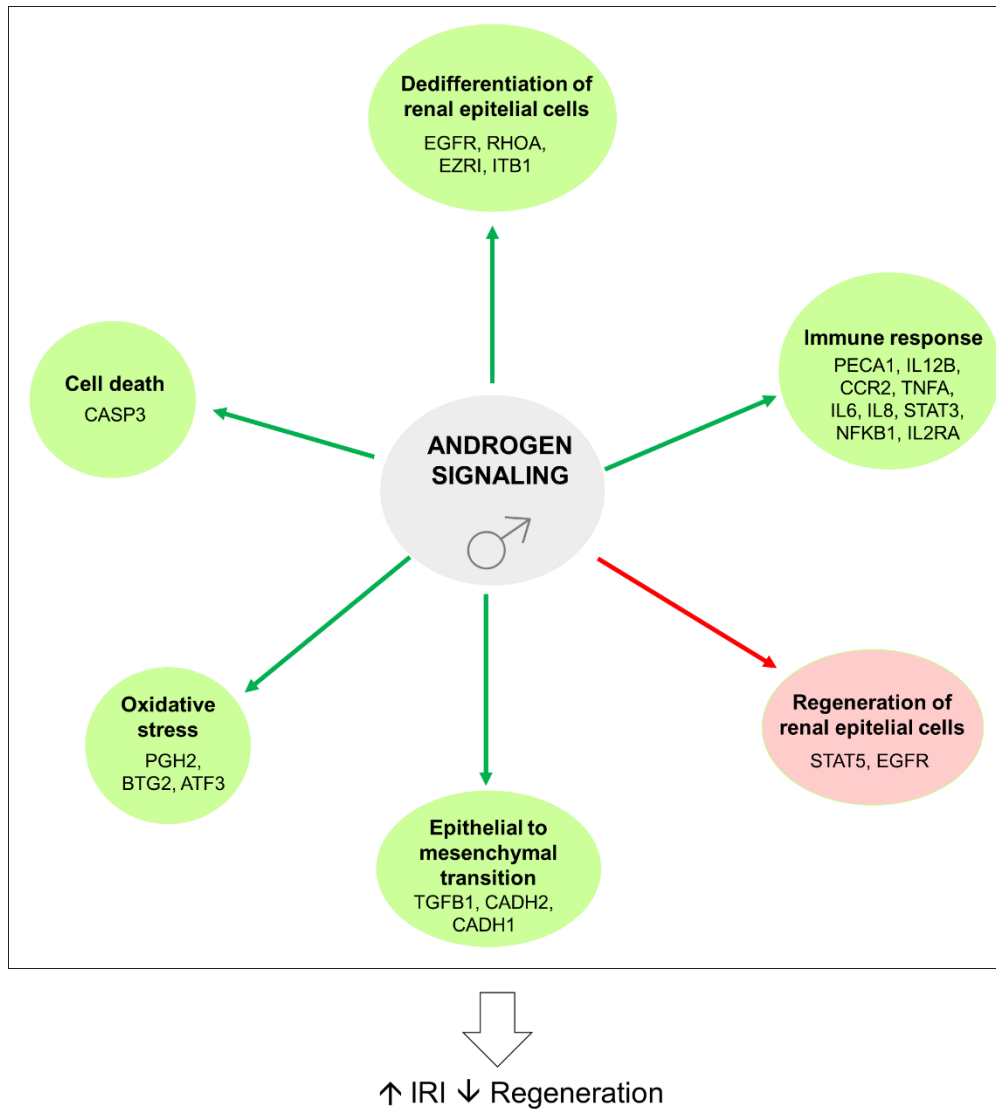
Figure 49. Scheme representing the different roles of androgens in renal IRI/ regeneration.

Androgens signaling affects renal I/R injury and regeneration by enhancing oxidative stress through PGH2 upregulation, and BTG2 and ATF3 down regulation. The increase of dedifferentiation of renal epithelial cells by augmenting EGFR signaling and diminishing RHOA, EZRI and ITB1 availability and activity also occurs in androgen related injury. The endothelial-to-mesenchymal transition by intensifying TGF activity, CADH2 upregulation and CADH1 expression repression is also enhanced in androgen signaling upon injury. The up regulation of the Immune response by increasing PECA1 intracellular signaling and IL12B expression promoting neutrophils transmigration; upregulating CCR2 expression increasing monocytes chemotaxis; enhancing expression of proinflammatory cytokines such as TNF, IL6 and IL8 directly, or through STAT3 and NFKB1 activation; lessening Tregs immune suppression through IL2RA

downregulation are also important factor of androgen regulation in injury. The increase of cell death by inducing CASP3 activation is also affected by sex male hormones signaling. Finally, androgens signaling affects renal I/R injury and regeneration by diminishing the regeneration of renal epithelial cells by impairing STAT5 activation and EGFR signaling.

Key and relevant proteins justifying the role of androgens in renal IRI/ regeneration are represented in a mechanism of action (MoA) (Figure 50). Information from the links of the MoA are reported in Table XXXVIII (Annexes). According to the identified mechanism of action FOS, TENA, PECA1, TNFA, ATF3, SMAD3 and STAT5A expression modulation after IRI injury may be directly associated with androgens signaling.
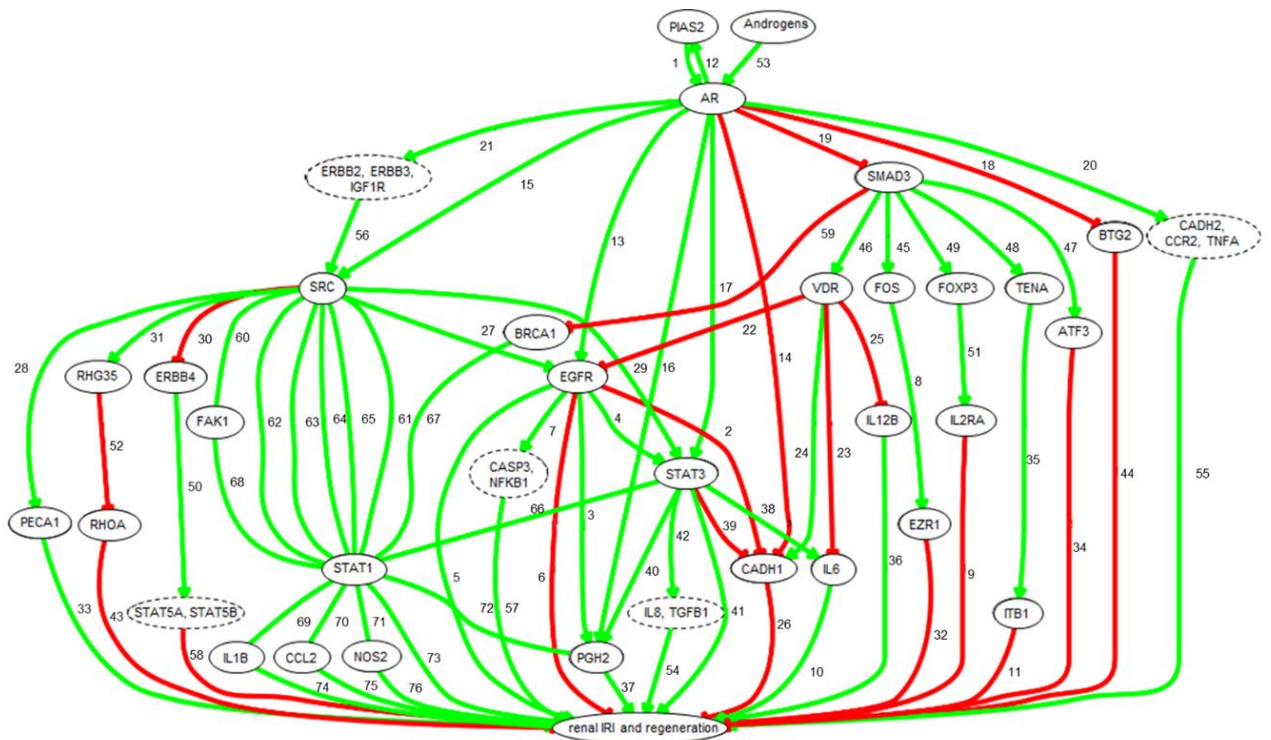
Figure 50. Representation of mechanism of action (MoA) justifying the roles of androgens in renal IRI/ regeneration.

5.D.VI.   Renal cells stimulation with sexual hormones

The *in vivo* model of renal IRI and its analysis has detailed the sexual dimorphism that exist in renal genes and gene sets regulation. The subsequent construction of

mathematical models determined the impact of androgens in promoting injury versus regeneration.

In the next step, we tried to validate some of the theoretical results obtained in the course of this study. First, we established whether renal proximal tubular cells were sensitive to sexual hormone stimulation by evaluating the occurrence of non-genomic signaling of the AR. RPTEC, HK-2 cells were deprived from steroid hormones, than stimulated 10 minutes with either DHT, EST and with EGF and ETOH as positive and negative control, respectively. Following the cells stimulation, the activation of MAPK was evaluated on WB (Figure 51). The stimulation of renal cells with DHT or EST did not activate pERK1/2 phosphorylation in neither cell line, meaning that these cells do not respond to quick stimulation with sexual hormones.
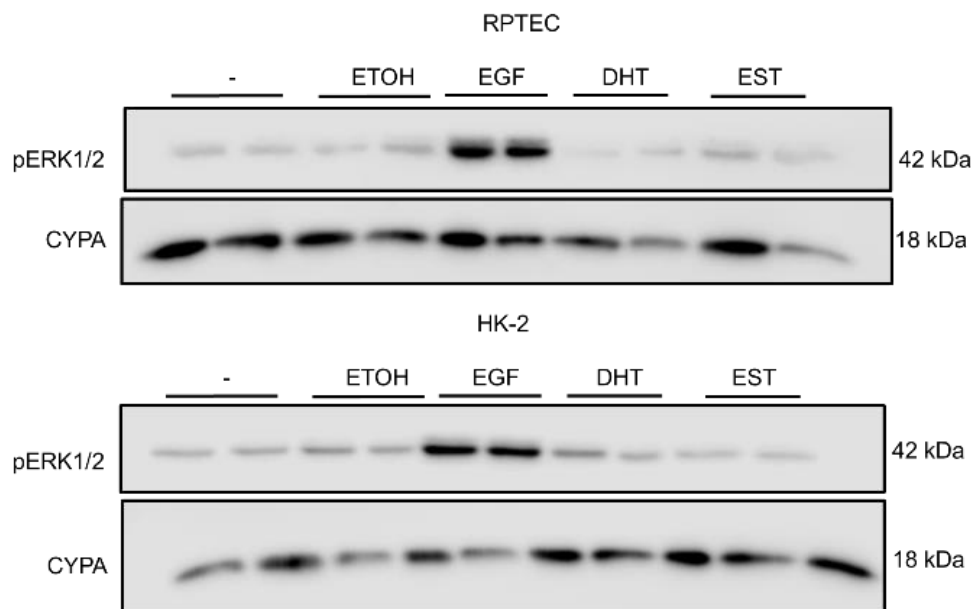
Figure 51. Sex hormone stimulation of renal cells. RPTEC and HK-2 cells were stimulated with DHT and EST for 10 minutes. Their capacity to respond to the sex hormone treatment was determined by the activation of MAPK. Neither cell lines responded to the hormone stimulation treatment. (ETOH: ethanol; EGF: epidermal growth factor; DHT: dihydrotestosterone; EST: estradiol)

5.D.V.   AR transduction in RPTEC cells

Following the lack of response of our cells following hormone stimulation, we determined the mRNA levels of the AR in RPTEC. We found cycle thresholds (CT) over

30, meaning that the expression of the gene is nonexistent. There seems to be a loss of the AR expression from the renal tissue to the cells in culture.

To resolve this issue, we decided to create a stably transduced RPTEC cell line with the AR. The success of the transduction was assessed by measuring the protein levels of the AR in the cells and by the visualization of transduced cells by ICC (Figure 52A-B).

Later, hormone stimulation experiment was conducted to evaluate the sensitivity of RPTEC cells stably transduced with the AR (RPTEC-AR) to hormone stimulation. DHT stimulation of RPTEC-AR cells did not activate the MAPK, suggesting the AR is not functional in these transduced cells (Figure 52C). Overall, we have not been able to have an in vitro model that respond to sex hormones.
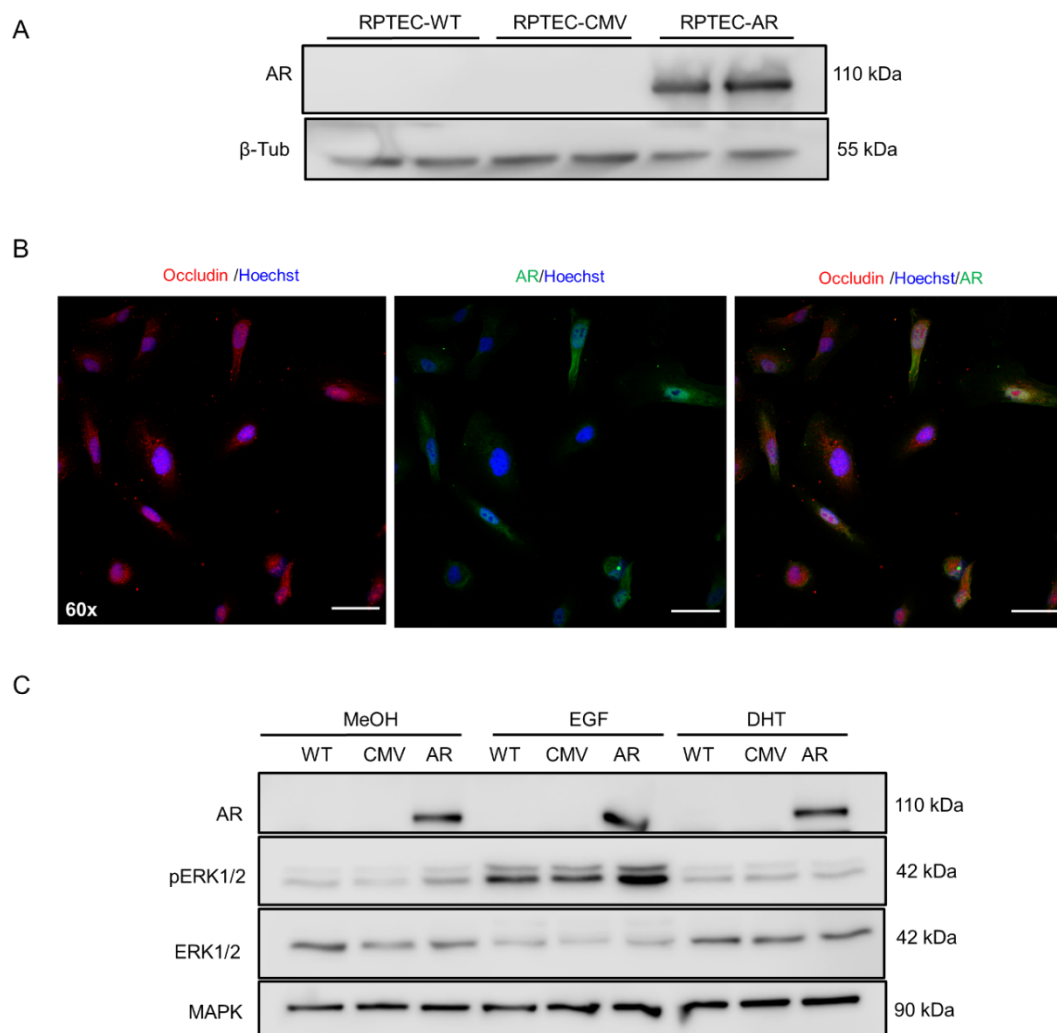
Figure 52. Functionality of the AR transduced in RPTEC. A) The AR protein expression was assessed in RPTEC cells stably transduced with the AR. RPTEC-AR show high level of AR,

whereas cells transduced with an empty plasmid (RPTEC-CMW) show no protein expression, as for the WT. B) Cells transduced were observed by ICC; 31µM. C) DHT stimulation of the AR did not activate MAPK, suggesting that the receptor do not function.

5.D.VI.   IRI model in RPTEC cells

Even though the cells used in *in vitro* experiments did not respond to hormone stimulation, they could still be used to validate the regulation of our selected targets by IRI. An *in vitro* model of IRI was conducted. The treatment consisted of inducing ischemia by removing glucose from the cells media and by incubating the cells in a hypoxia chamber (0,1% O_2, 5% CO_2). Reperfusion was induced by providing glucose and normoxic conditions to the cells for 15 hours. In that experiment, before inducing the treatment, a group of cells was deprived from steroid hormones with charcoal stripped-FBS. In a third group, cells were deprived from steroid hormones at the same conditions and then stimulated with DHT for 24h. Cells were harvested following ischemia and at the end of reperfusion.

An XTT test was performed to determine the percentage of cell viability. No significant changes were observed between the different conditions (Figure 53). However, cell pictures indicate a loss of cells during ischemia and an increase of cell density a reperfusion.

Next, protein expression was measured by WB analyses. First, the expression of HIF1α was measured. HIF1α was used as a marker of hypoxia induction in the hypoxia chamber. HIF1α expression was up-regulated under hypoxic conditions and down-regulated under normoxic conditions, as expected. Then, the expression of key proteins of renal IRI and regeneration determined in previous analyses were measured by WB. STAT3 levels were determined. STAT3 was defined as an important protein in the MoA justifying the role of androgens in renal injury (Figure 50). In our in vitro IRI model, for the first time, we observed that STAT3 was regulated by the phosphorylation of different residues throughout renal IRI. In fact, STAT3^{Ser727} was up-regulated during ischemia and down regulated during reperfusion. To the contrary, STAT3^{Tyr705} was down-regulated during ischemia but up-regulated at reperfusion (Figure 53).

STAT1 who was identified as another important protein, was also validated in our *in vitro* system. We found that STAT1 was also regulated at the level of phosphorylation. While the total STAT1 protein levels remain the same throughout the treatment, STAT1^{Ser727} was up-regulated during ischemia.

In this experiment, we stimulated the RPTEC with DHT for 24 h prior to the IRI treatment (DHT samples), to evaluate if the androgens could trigger a genomic response and if it could be observed in the expression of selected targets of the Moa (Figure 50). No difference of expression was determined between cells stimulated or not with DHT, throughout the experiment. It means that the AR does not have a genomic signaling in our cellular model. However, the cells are responsive to the IRI treatment.
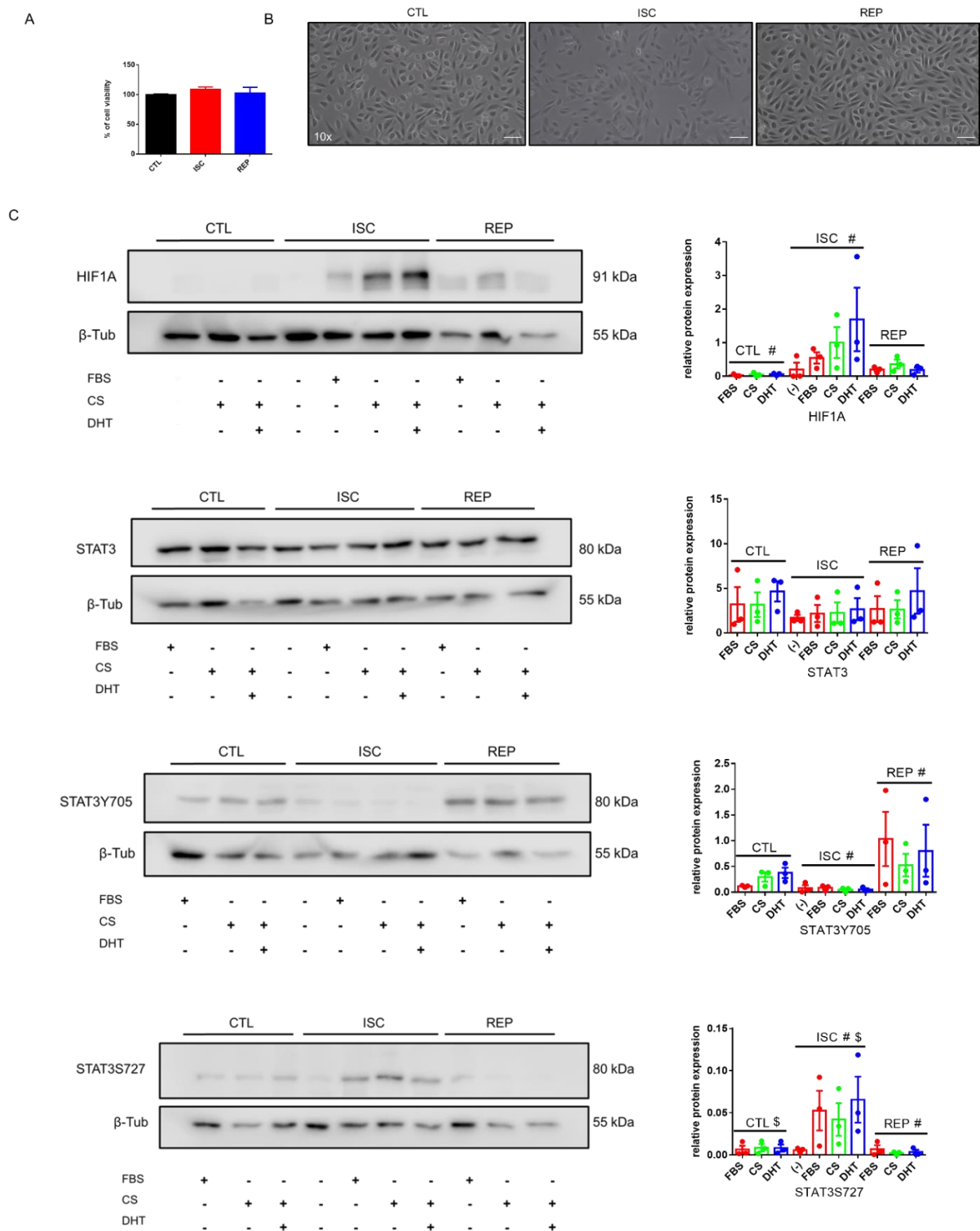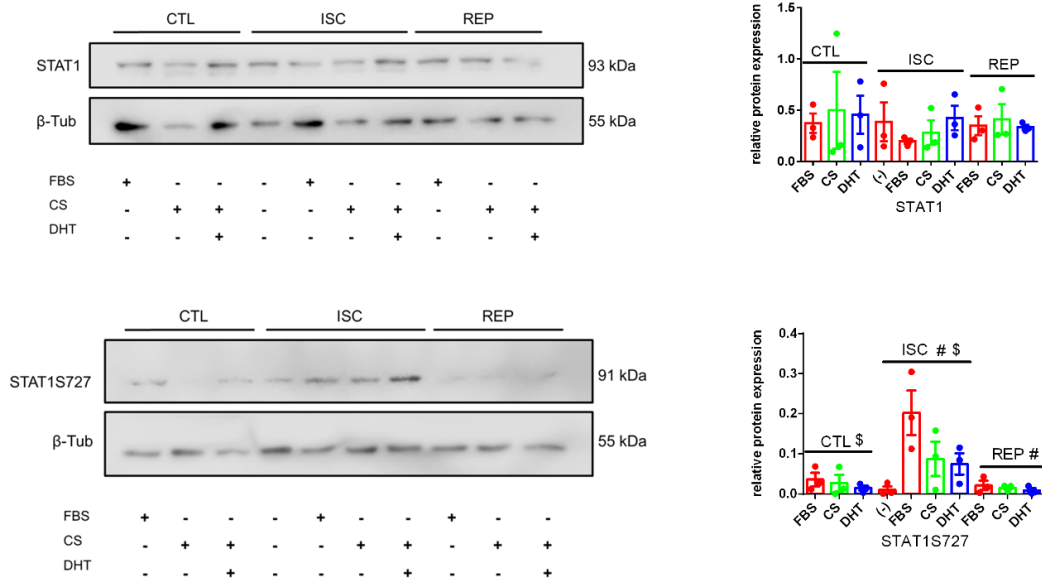
Figure 53. RPTEC protein expression of selected targets following IRI treatment. Three group of cells underwent the IRI treatment. The first group (FBS) contains full FBS. The second group (CS) was deprived from steroid hormones with charcoal stripped-FBS. In a third group (DHT), cells were deprived from steroid hormones at the same conditions as the CS group and then stimulated with DHT for 24h. The cultured conditions were maintained throughout the experiment. Cells underwent 10h of ischemia followed by 15 h of reperfusion. Ischemia consisted of removing the glucose (ISC FBS, ISC CS, ISC DHT) from the cell media or maintaining only plain DMEM no glucose media (ISC-) and the incubation of the cells in a hypoxic chamber (0,1% O_2, 5% CO_2). Reperfusion was induced by providing glucose and oxygen to the cells for each condition (REP FBS, REP CS, REP DHT). A) The percentage of viable cells was not altered in a significant way. B) However, pictures showed a decrease in the cells attached to the dish;49mm. C) STAT3 was regulated at the level of phosphorylation. STAT3^{Ser727} was up-regulated at ischemia, whereas STAT3^{Tyr705} was activated during reperfusion. STAT1 was also regulated at the level of phosphorylation. Throughout the experiment, for each treatment, no significant difference of expression was found between the different groups.

Other targets (IFIT3, CADH1) that were determined to be regulated by androgen IRI have be analyzed in our i*n vitro* model. No differences of expression were observed throughout the ischemic treatment for these targets. Overall, we validated some IRI targets with our RPTEC IRI model. To complete the validation, a model sensible to sex hormone stimulation is necessary. The absence of sex hormone sensitivity might also explain in part the flat pattern of expression in some targets.

5.E. COMPARISON OF SYSTEM BIOLOGY ANALYSES OF RENAL IRI PORCINE AND A RENAL CANCER-DERIVED CELL LINE MICROARRAY DATA.

5.E.I. Key proteins overlap between androgen renal IRI and ccRCC

One of our goal in this project was to find a possible link between renal IRI/ regeneration and cancer, as they may share common pathways. The obtained results for the system biology analysis of renal IRI were compared with key proteins in ccRCC (KIM-1 dependent). ccRCC key proteins, were previously determined in an Anaxomics project led in our laboratory that used microarray data of 769-P cell with and without KIM-1.

A total of 9 proteins were both identified as key proteins related to androgens IRI/regeneration, and to ccRCC (Table XXXV). Most of these proteins (all of them except for NR1I2) have already been described in the literature to play a role in renal IRI/regeneration and/or in ccRCC. This result highlights the existence of a link between renal IRI injury/ regeneration and ccRCC. It also shows the similarities and differences among the target proteins.

Table XXXV. Overlapping key proteins between androgens in IRI/ regeneration and ccRCC.

Protein	WL vs PS		WL vs PR		Sign	
Name	Male	Female	Male	Female	↑IRI ↓regeneration	↑ccRCC
ACE2	-	-	↓	↓	🔻	🔺
CREB1	-	-	-	-	🟧	🔺
GCR	-	-	-	-	🔻	🔻
IRF1	↓	-	↓	-	🔺	🔻
NR1I2	-	-	-	-	🟧	🟧
PPARG	-	-	-	-	🔻	🔻
STAT5B	-	-	-	-	🔺	🔺
TLR4	-	-	↓	↓	🔺	🔺
VDR	-	-	-	-	🔻	🔻

*Arrows in WL vs PS / WL vs PR columns means that the protein is differentially expressed in the comparisons, and whether it is up (↑) or down (↓) regulated. *Sign* column indicates in which state is or may be the protein when promoting IRI or impairing regeneration, and the state in which it

promotes ccRCC according to bibliography; green upwards arrow means activated, red downwards arrow means inhibited and yellow square means unknown role of the protein. (PR: pre-ischemia; PS: post-ischemia; WL: one week later)

5.E.II.   IRI model in 769-P cells

With the help of system biology analyses throughout this project, a link has been established between IRI/regeneration and cancer. Next, we wanted to evaluate in a *in vitro* renal cancer model the expression of STAT3, which has been determined as a key protein in IRI in this project and whose important role in ccRCC has also been studied thoroughly in our laboratory. 769-P cells were submitted to the IRI treatment, as previously described. The percentage of cell viability decreased during ischemia and was recovered during reperfusion. (Figure 54A). The cells were affected by the ischemic treatment. This was visible by the different phenotype of the cells during ischemia and during reperfusion (Figure 54B). STAT3 protein expression level was measured by western blot. We observed that total STAT3 is downregulated during ischemia. At reperfusion, we observed an increase in total STAT3. Contrary to the RPTEC cells, in 769-P, STAT3 was not regulated at the level of phosphorylation upon injury. The level of phosphorylation was not altered during the treatment (Figure 54C). Overall, STAT3 is regulate in both normal and cancer cell lines, but in different ways. Further experiments are necessary to characterize the link between normal and cancerous cells.
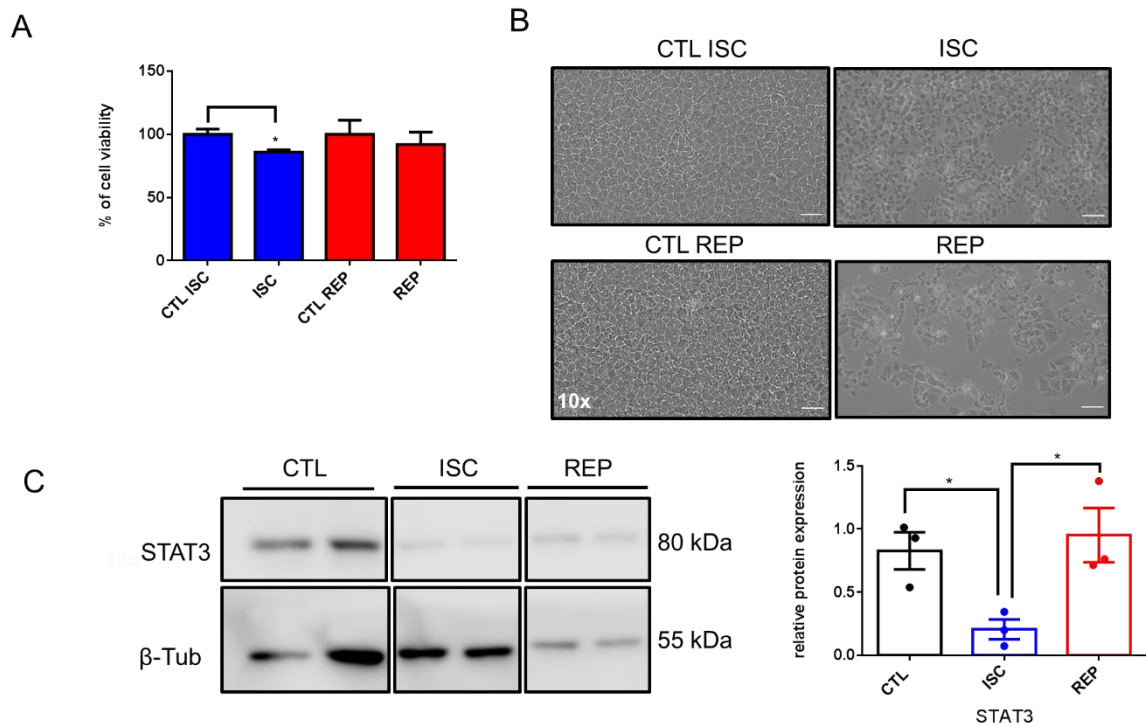
Figure 54. STAT3 protein expression upon IRI in 769-P cells. Cells underwent 10h of ischemia followed by 15 h of reperfusion. Ischemia consisted of removing the glucose from the cell media and the incubation of the cells in a hypoxic chamber (0,1% O_2, 5% CO_2). Reperfusion was induced by providing glucose and oxygen to the cells. A) The percentage of viable cells decreased in cells during ischemia. B). Cell pictures showed a decrease in the cell population during ischemia and an increase at the end of reperfusion; 49 mm. C) Total STAT3 protein expression was downregulated during ischemia. At reperfusion, total STAT3 level was increased.

6. DISCUSSION

6. DISCUSSION

6.A.   TRANSCRIPTOMIC ANALYSES OF *IN VIVO* MODELS OF RENAL IRI

This research project aimed to characterize the sex differences that exist in the context of renal IRI. We wanted to determine important targets and the molecular processes in which they are involved. We also wanted to explore the possible link between regeneration following IRI and renal cancer progression. Our singular approach has brought some insightful results that could be used as a template for future studies.

6.A.I.   Sex differences in number of DEG in different renal model of disease

In this study, microarray assays analyses have revealed the attenuation of a sexual dimorphism that exist before injury, at the recovery state. The sex differences in the kidney transcriptome at basal situation that is observed in mice[137] was also identified in the pig kidneys. Similar to our experimental approach a former study evaluated the sex differences in the transcriptome of male and female mouse and human healthy and disease kidney tissues[255]. For both species a decrease of the number of DEG from basal to diseased state was observed (Figure 55). In the pig transcriptome, following injury we also observed a decrease in the number of DEG between sexes. Overall, we can say that in every specie, regardless of the type of injury or disease, the initial sex differences at the transcriptomic level are reduced following renal damage.
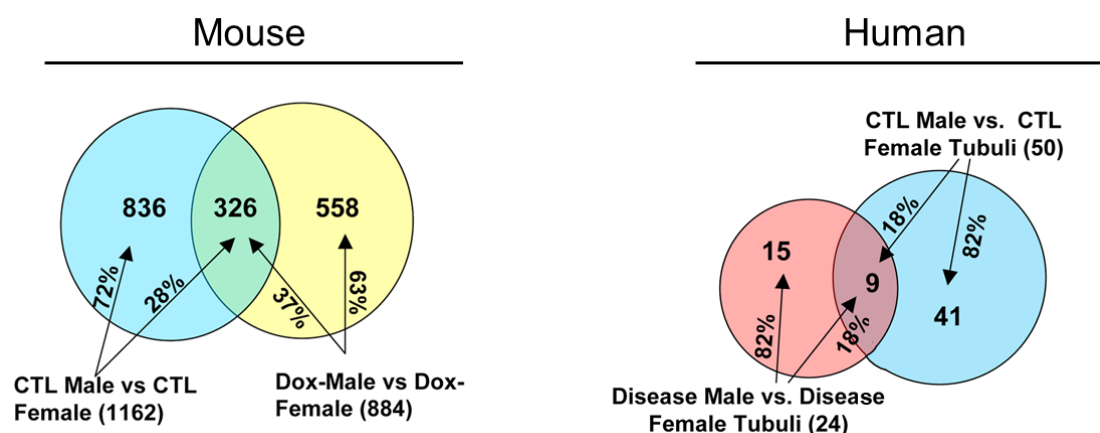
Figure 55. Gene expression differences in doxorubicin injected male and female Balb/c mice and in control and diseased human (tubule) kidney samples. Overlap of sexually dimorphic genes in healthy and diseased condition. (Adapted by Si *et al.*, *PLoS One,* 2009)[255].

However, the overlapping number of DEG between human and mouse kidney transcriptome at basal situation and at disease state, respectively (Figure 56), revealed the poor conservation in regulated genes between both species at a selected time point. This could be explained by their difference in genome size[212]. This study showed that human and murine kidneys show sex- and species-specific gene expression differences in response to injury[255].
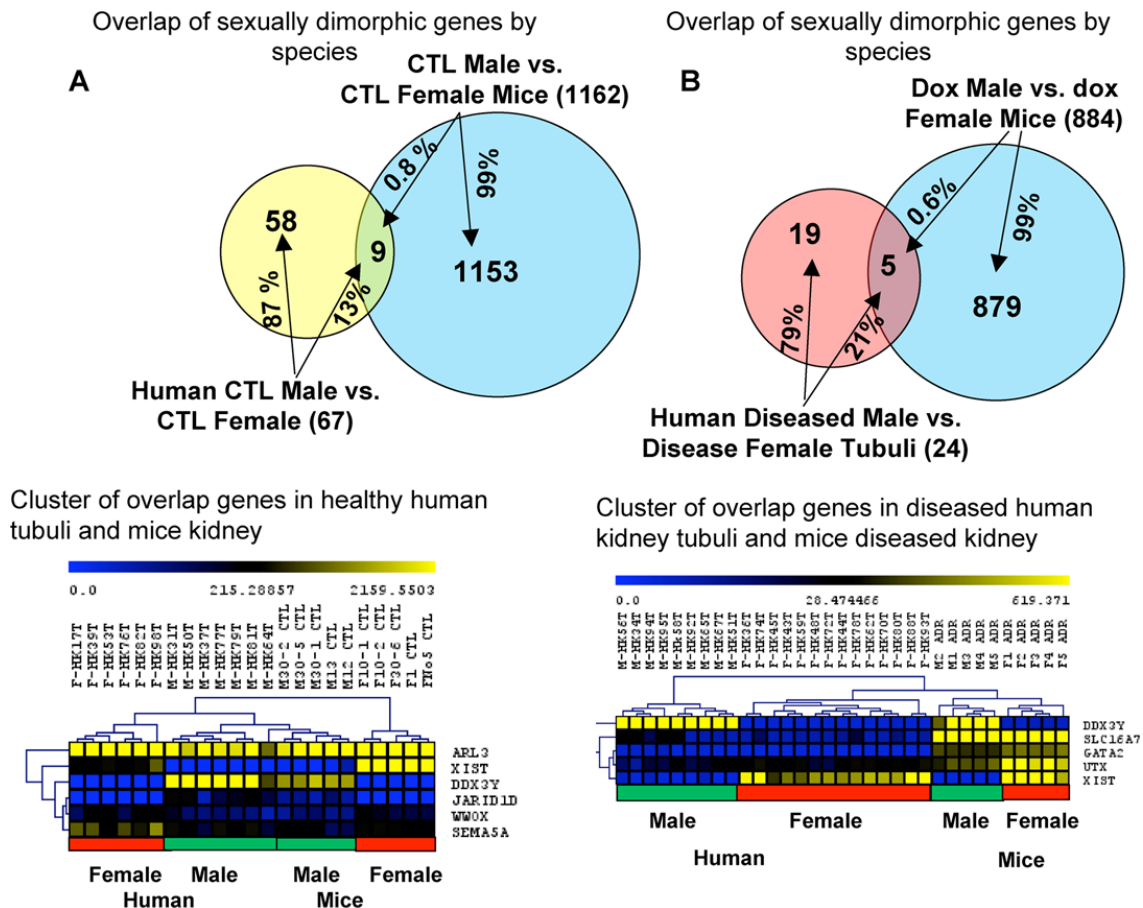
Figure 56. Species specific gene expression differences. (A) Upper panel: overlap of sexually dimorphic genes in kidneys of healthy people and mice; (B) Upper panel: overlap of sexually dimorphic genes of diseased human kidneys and diseased murine kidneys. Lower panel: hierarchical clustering (complete linkage) of the overlapping genes identified between diseased human and murine kidneys. (Adapted by Si *et al.*, *PLoS One,* 2009)[255].

Within our data, we found that one week following renal IRI, male and female pigs shared similar pattern of gene expression. By comparing a few pig and human samples, at comparable time point, we found a general correlation between both species. The

parallels drawn between both species validated the use of the porcine model of renal IRI for subsequent analyses.

The pig model grants us access to multiple biopsies for the same animal. For obvious ethical reasons, it would not be possible to perform our experimental design on AKI patients. Therefore, this animal model gives access to new knowledge that would not be possible to gain otherwise. we have determined that the findings of this project are translatable to humans.

6.A.II. Differential mRNA expression studies

Differential mRNA expression studies implicitly assume that changes in mRNA expression have biological meaning, most likely mediated by corresponding changes in protein levels. Across many studies, genome-wide correlation between expression levels of mRNA and protein have been determined to be generally low[256,257].The disparity is usually attributed to other levels of regulation between transcript and protein product[258]. However, differences in mRNA expression between conditions, is commonly used for biological discovery. Thus, despite the known poor overall correlation between mRNAs and their protein products, there is an implicit assumption that differentially expressed mRNAs impact their respective experimental conditions via differences in proteins.

Most studies of mRNA-protein expression correspondence examine the question from a genome-wide viewpoint. These genome-wide studies calculate a correlation coefficient of mRNA expression versus the corresponding protein expression across a large number of genes (Figure 57A)[259–264]. Only a limited number of studies have investigated correspondence for individual genes across samples or experimental conditions (Figure 57B)[263,264,273–275,265–272]. For this project, the individual gene analysis was chosen because it was better suited to our objectives.
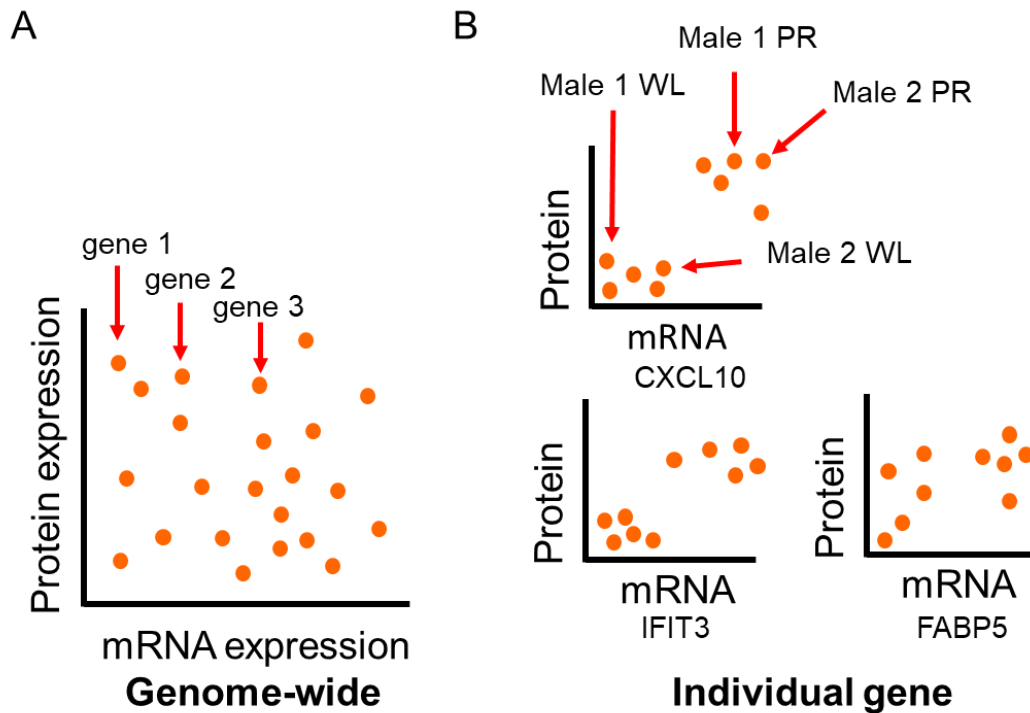
Figure 57. Genome-wide versus individual gene correlation analyses. A) Most studies of mRNA-protein correspondence calculate a single correlation coefficient (or other correspondence metric) representing the correlation between mRNA expression and protein expression across all genes. Individual points upon which the correlation is calculated are a single value or an average of multiple samples/conditions, which do not necessarily have to be the same between mRNA and protein experiments. This correlation represents a general measure of how well mRNA and protein expression corresponds across the entire genome. B) Studies of individual gene correspondence calculate a correlation coefficient (or other correspondence metric) for every gene, representing the correlation between the expression of a mRNA and its protein product across multiple samples or conditions. Individual points upon which the correlation is calculated are a single value or averaged samples for a single condition, which must correspond to the same sample or condition for both mRNA and protein measurements. This correlation represents how well the expression levels of a particular mRNA-protein pair correspond dynamically across the samples or conditions in the experiment. (Adapted by Koussounadis *et a*l, *Sci Rep.* ,2015)[276].

Only recently a research group addressed the question of how consistently differentially expressed mRNAs translate into protein differences. Koussounadis *et a*l. examined mRNAs that are differentially expressed across experimental conditions and their relationships to their protein products in ovarian cancer xenograft models[276].Compared to genes whose mRNA is not differentially expressed within a condition, they found that genes with differentially expressed mRNA have significantly higher correlations between mRNA and protein. This result provides support for the implicit assumption that differential mRNA expression reflects a difference between conditions at the functional level of proteins. They found this significant correspondence despite also finding poor correlations from a genome-wide perspective, as have other studies.

This recent observation confirms the adequacy of our experimental approach of individual gene selection, as we indeed found some interesting mRNA-protein correlation for targets that were differentially regulated in males and females in pig and human.

6.A.III. Variability of biochemical parameters

In the course of the *in vivo* study, we obtained contradictory results by measuring the biochemical parameters in mice. In the pilot study, we observed recovery of renal function 3 days following injury. To the contrary, in the second study, renal recovery was not attained at that point. The measurement of the biochemical parameters for both experiments were conducted at different time and also in different laboratories (Biochemistry unit of Vall d'Hebron hospital/ animal room VHIR). A few years ago, a study investigated the variability in the measurement of creatinine levels. amongst laboratories[277]. In fact, systematic errors associated with the serum creatinine measurement is a problem faced in clinical laboratories[278]. Traditionally, the lack of standardization of most clinical laboratories to a common gold standard has been thought to be responsible for these systematic errors[279]. In Joffe *et al.*'s study, samples from 14 different laboratories were used for measurement of creatinine repetitively over time. They found that there was substantial variability in creatinine assays across laboratories (Figure 58) and over time. Since their analysis was based on a 'split sample' approach, the observed differences in creatinine measurement cannot be due to changes in renal function or other biological causes, but rather were due to assay measurement issues. In our case, we measured different samples in the different studies. However, it is very unlikely that the changes observed are due to renal function. It is most probably due to a technical cause. Measurement variation of creatinine occurs based on machine type and manufacturer, method, and calibration to standards[280,281]. College of American Pathologists surveys have shown that calibration 'bias' in serum creatinine measurements is very common, and in fact it is the analyte most frequently showing a significant calibration bias among routine chemistry panels[279,282]. The results of this interesting study could explain the difference we observed between the measurement of the biochemical parameter in our 2 experiments.
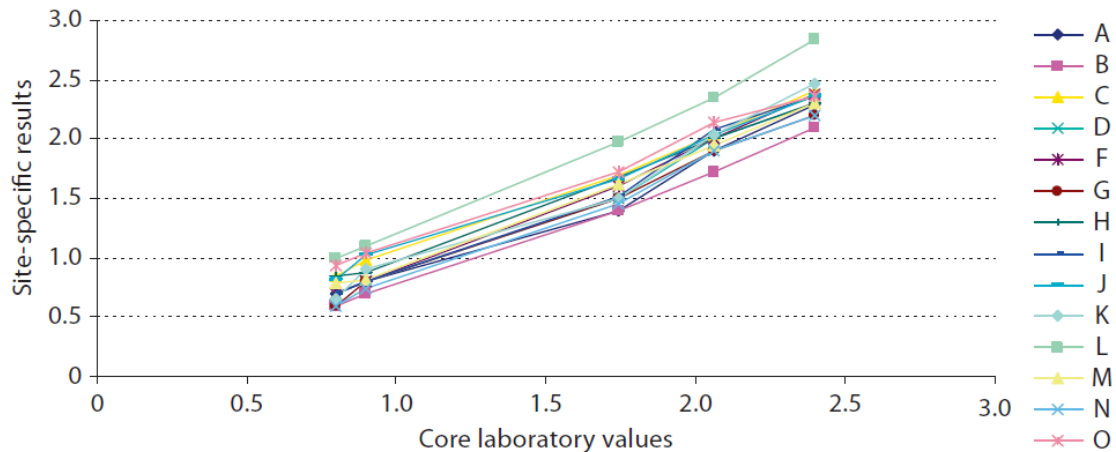
Figure 58. Variation in creatinine by site. Each point represents the measured Cr value of a particular plasma sample at the core laboratory (x-axis) and at each one of the other laboratory sites, A–O (y-axis). Each line connects measurements from the same laboratory. (Adapted by Joffe *et al.*, *Am J Nephrol*,2010)[277].

6.A.IV. Transcriptomic differences between mouse and pig models of renal IRI

In this project, we compared our pig transcriptomic data with public available mice RNAseq data. We found very few genes that were commonly regulated by renal IRI in both specie. Interestingly, the expression pattern most common genes (up- or down-regulation) were of opposite direction. For instance, genes involved in inflammatory, immune response process, etc, were up-regulated in mice, whereas they were down-regulated in pigs. It has been demonstrated that the mice developed maladaptive repair and fibrosis following an ischemic insult[254]. However, the pig transcriptomic data suggest recovery in male kidney tissues. A lengthier transcriptomic and histological analyses would be necessary to determine if a single injury could lead to CKD in pigs. Given the great similarity between human and porcine kidneys and the fact that human kidneys have shown great capacity to recover from AKI, we expect that the porcine kidneys would recover. We can also expect recovery in the porcine model of IRI since we have a clean model of IRI, which means that some risk factors that can lead to CKD such as obesity, hypertension or diabetes mellitus are excluded in our model[283].

Considering this, it seems that the mouse would be a better suited model of IRI, to study maladaptive repair that lead to CKD, whereas the pig is better suited to an IRI model where recovery is expected.

6.A.IV.1   The absence of KAP in human and pig tissues

Our group has been a national and international referent for the study of androgen action in kidney. A lot of focus has been put on the study of the kidney androgen regulated protein (KAP) gene. In mice, the KAP gene is exclusively expressed in epithelial cells of proximal tubules, where it displays a sophisticated segment-specific regulation by androgens in S1 and S2 segments and by estrogens and thyroid hormone in the S3 segment[284–290]. It has a functional androgen response element in its proximal promoter indicating that it is a direct target of androgens[291,292].

KAP transgenic (Tg) mice have exhibited renal defects that include focal segmental glomerulosclerosis, proteinuria, glycosuria, and fibrosis[293]. Moreover, Tg mice exhibit activation of the sympathetic nervous system and the renin-angiotensin system and demonstrate a complex mechanism of positive feed-back, as angiotensin II increases oxidative stress not only peripherally but also in the central nervous system[294]. Because androgens stimulate various key components of the systemic and renal renin-angiotensin system, the endothelin system, the arachidonic acid metabolism by CYP450s cytochrome family members and oxidative stress [209,295–297] which ultimately may exacerbate the progression of renal disease, it was concluded that KAP is very relevant to understand gender-specific differences in arterial blood pressure and that KAP mediates androgen action on those systems.

Moreover, in the human proximal tubule derived HK-2 cell line it was observed that KAP expression significantly prevents production of IL-6 by exogenous TNF alfa, when compared to control cells, demonstrating the direct effect of KAP on inflammation mediated by pro-inflammatory stimulus[298]. Recently, an exhaustive study in collaboration with Dr. Roderic Guigó our laboratory determined that there is no KAP orthologue in humans. Since KAP has profound effects in mouse kidney physiopathology, it raises the question as whether mice are an adequate experimental model for translational kidney research in humans. Results obtained in the current study exemplify strong differences between rodents and pigs/humans in relation to genetic differences affecting renal disease. Therefore, the mouse might not be an adequate model to study renal diseases, especially for sex difference studies.

6.A.V. Sex and time coordination of renal IRI

In this study, we observed that more genes are regulated in males than in females pig kidneys, following renal IRI. Moreover, at recovery, the general pattern of gene expression of the males is reminiscent of the females (Figure 32). Our different results in this study indicate that females manage better the recovery following renal injury than males. Perhaps, following the females' pattern of gene regulation is a strategy for the males to better cope with the regenerations processes. The analysis of the molecular pathways involved in injury processes lead to a better understanding about the sex differences.

Molecular processes involved in renal IRI such as sterile inflammation, apoptosis, EMT and many more have previously been described. However, one the goal of this project was to determine the sex and time regulation of these processes. Our analysis focused on gene sets that were up-regulated, which we assume lead to higher activity of the genes involved.

Out of the 5 regulation patterns that we found in the time comparison (Figure 42), one of them (5th) is conserved between male and females. This pattern is up-regulated in males and females only at the injury phase. This pattern involves gene sets such as DNA damage response, regulation of cell cycle arrest function, negative regulation of MAP kinase activity, cytokine secretion. In general, these gene sets are associate with cellular damage. These processes are not regulated by sex hormones. Therefore, a similar pattern between the sexes is not surprising.

The pattern 1 is interesting because it shows gene sets that are un-regulated in females during recovery and these same gene sets are only up-regulated during the injury phase in males, by contrast. These genes set include among others: myeloid cell differentiation, regulation of leukocyte migration, steroid metabolic process, regulation of endocytosis. Following an injury, theses are all active gene sets that can be associated to recovery from the insult. However, during regeneration, these genes are down-regulated in males. This might explain in part the longer recovery process observed in males at the clinical level.

The pattern 2 represent gene sets that are active in females during recovery but down-regulated in male throughout the whole process. These gene sets include, positive regulation of adaptive immune response, inflammatory response, negative regulation of epithelial cell proliferation, positive regulation of endocytosis. Once again, these are all

processes that have been described to take place following injury to promote regeneration and the regulation is in decline in males compared to females.

The pattern 3 represent gene sets that are only active in males during the injury phase and are inactive in females throughout the injury. This arrangement represents the general pattern that we observed in the porcine microarray, where the initial sexual dimorphism disappeared one week after injury (Figure 32). The pattern 3 include gene sets such as toll-like receptors cascades, MyD88 cascade TLR4 TRIF, EMT, cellular response to hypoxia, etc. MyD88 plays a central role in the innate and adaptive immune response. This protein functions as an essential signal transducer in the IL1 and Toll-like receptor signaling pathways. These pathways regulate that activation of numerous proinflammatory genes. These gene sets suggest a strong immune response at the injury phase for and a sensitivity to hypoxic conditions for males. This result correlate with the known evidences that the injury insult is greater in males than in females.

The 4th pattern is similar to the 1st pattern. It represents gene sets that are up more activate in females at the end of the process, compared to the basal situation and injury phase. For the males, they are up-regulated at the injury phase. These gene sets include myeloid cell activation, negative regulation of ion transmembrane transport, regulation of lipid biosynthetic process, response to estradiol. These genes set highly active in females are involved in regeneration processes and the promotion of homeostasis.

Taking into account how each gene sets behave toward time for each sex, we can say that males show a stronger immune response than females toward IRI. In addition, gene sets that promote regeneration and resolution of inflammation following injury have a more active regulation in females than in males. These finding correspond with the clinical phenotype that male recovery is harder and more often incomplete in comparison to their female counterpart. The female tolerance to renal IRI was demonstrated In a recent study[299]. Female C57BL/6 mice tolerated 28 minutes of warm IRI, with substantial but survivable injury that resulted in significant fibrosis, whereas male subjected to the same 28-minute period of warm ischemia all developed renal failure and required sacrifice by 48 hours. It was determined that 15 minutes of warm renal IRI in male mice yielded injury equivalent to that induced by 28 minutes of warm IRI in female mice in terms of the BUN rise and time to recovery[299].

Previous studies have determined some of the molecular mechanisms of sex differences in renal IRI[300]. However, in this project, for the first time, we provide an

exhaustive report on the different molecular mechanism involved in renal IRI by highlighting their time and sex-dependant expression.

The sex comparison at different time point of injury has also demonstrate the important differences that exist in the gene sets regulation upon renal IRI (Figure 43). The pattern A represent genes that are more activate in males before and during the injury phase: These gene sets include: INFγ production, T cell differentiation and activation in immune response, cellular response to chemokine, cellular response to hormone stimulus, etc. These gene sets show a strong immune response upon injury. Even though female renal tissues have more infiltrates than males at basal situation, the immune response upon injury is stronger in males. This arrangement is the one that represent the general pattern that we observed in the porcine microarray (Figure 33).

The pattern B represent gene set that are more activated in males one week following injury, compared to the females. These gene sets include DNA damage checkpoint, humoral immune response, B cell proliferation and activation, endothelial cell migration and proliferation, kidney development, etc. These gene set suggest that male one week following IRI, males are still involved in pro-active regeneration processes, than the females who might have completed these processes.

The pattern C is similar to the pattern B. It represents gene sets that are more activated in males compared to females at injury and also one week following IRI. Theses genes sets include positive regulation of epithelial cell proliferation, positive regulation of Wnt signaling pathway, receptor-mediated endocytosis. This gene set suggested an immediate strong cellular response against the renal damage in males.

The pattern D represent gene sets that are over-represented in males at injury compared to females. Theses gene sets include potassium ion transport, amino acid transport, steroid metabolic process, etc. Given that males seem to be more sensible to and more affected by IRI, it is compatible that gene sets involved in renal function and homeostasis are up-regulated at the time of injury. A recent study corroborates the renal function protection in a female molecular environment[301]. Eight-week-old male C57BL/6 mice who where injected with human endometrial regenerative cells 2 hours prior to renal IRI showed improved renal function compared to untreated mice. In fact, their BUN and creatinine levels were lower[301].The different regulation of renal injury between the sexes might also explained in part the different outcome detected between men and women. In a recent study, it was shown that rat females were protected from the development of CKD following AKI comparing to males. Early antioxidant defense and higher TGF-β,

HIF1α and eNOS were among the renoprotective mechanisms that female demonstrated[302].

In a next step, for a selected gene set, we could superpose the sex and time comparisons to form a crossover. By combining both comparisons, we could obtain information on the behaviour of a gene set in time. In addition, we would also get clue on the actual activity level between the sexes. For instance, at a selected time point, the down regulation of gene set in males, does not exclude overall higher level of activity at this time point compared to females. The tools provided in this project will allow this type of deep analysis.

6.B   SYSTEM BIOLOGY ANALYSIS OF RENAL IRI AND RENAL CANCER

6.B.I.   Mechanism of action justifying the role of androgen in renal IRI

In this study, we wanted to determine how the androgens influence renal IRI. We have determined key androgen-related processes and the important proteins involved in these processes, by combining our microarray date, a literature review and the construction of mathematical models of renal IRI/regeneration.The activation of the AR in males leads to the modulation of several pathways that may ultimately increase renal damage and decrease regeneration by affecting on processes such as oxidative stress, dedifferentiation of renal epithelial cells, endothelial to mesenchymal transition, immune response, cell death and regeneration of renal epithelial cells (Figure 49).

6.B.I.1 Oxidative stress

Organ dysfunction induced by ischemia is paradoxically exacerbated by reperfusion, due to oxidative stress induction[303]. PGH2 has been reported to participate in renal ischemic injury by activating endothelial cells and inducing oxidative stress[304]. Androgens may aggravate oxidative stress by directly upregulating PGH2 expression [305,306], or indirectly through increasing its levels through epidermal growth factor receptor (EGFR) signaling [307,308] or STAT3 signaling [309].

On the other hand, protein BTG2 is a potent mediator of cytoprotection against oxidative stress [310], which may be involved in preventing from IRI oxidative damage. BTG2 expression has been described to be reduced by miR-32, which is expressed in

response to androgens [311]. Thereby, androgens may also promote oxidative damage though BTG2 downregulation.

ATF3 is induced by oxidative stress and renal ischemic injury. It plays a key role in inhibiting oxidative stress induced cell death[312], hence protecting from IRI. Androgens signaling may prevent ATF3 activation through SMAD3 inhibition, as SMAD3 has been reported to activate ATF3 expression[313].

6.B.I.2. Dedifferentiation of renal epithelial cells

IRI induces loss of brush borders and disorganization of the cytoskeleton leading to tubule cell dedifferentiation and dysfunction[314]. Even very short ischemic insults provoke cellular changes in surface membrane polarity and junctional complexes mediated by the actin cytoskeleton[40]. Dedifferentiation of renal epithelial cells relies, in part, on the increased EGFR signaling[315], and on decreased availability and activity of proteins such as RHOA[316], EZRI[316] and ITB1[317].

EGFR expression and signaling is modulated by several proteins. The receptor signaling appears to be critical in dedifferentiation after ischemic or oxidant injury[315].

RHOA inhibition is a consequence of the activation of its negative regulator RHG35[318] by SRC[319]. RHOA inactivation has been reported as a consequence of ischemia, due to ATP depletion, leading to actin cytoskeleton depolarization and redistribution, causing microvillar structure deterioration[316].

EZRI expression has been reported to be increased by FOS[320]. FOS is induced by SMAD3 signaling[321]. Even though AR activation has been reported to not influence on SMAD3 levels or phosphorylation, it has been shown to interfere on SMAD3 DNA binding affecting its transcriptional modulation activity[322,323]. EZRI is an actin-stabilizing protein. ATP depletion associated with ischemia causes the dissociation of the actin-stabilizing proteins, including EZRI, allowing actin depolymerization and microvillar breakdown[316]. Hence, AR activation by androgens can eventually abolish EZRI positive regulation and may further worsen tubular cells structural loss.

The state of ITB1 activation has been reported to be critical for the maintenance of tubule epithelial integrity, and after ischemia integrins have been reported to redistribute to the apical membrane causing cell detachment[316,317]. Pre-ischemic intravenous administration of an antibody anti-activated ITB1 results in preservation of renal histopathology and function, maintenance of cell binding to basal lamina[316]. ITB1

acts as a receptor for TENA) and it is activated upon TENA binding[324]. As EZRI, TENA expression is positively regulated by SMAD3 binding[325]. Accordingly, androgens may exacerbate cell detachment and epithelial integrity loss.

6.B.I.3. Epithelial to mesenchymal transition

Dedifferentiated tubular epithelial cells present characteristics similar to mesenchymal cells rather than epithelial. If these cells are not able to re-differentiate into tubular epithelial cells, the process continues and finally ends with EMT, which results in tissue fibrosis[326,327]. During the EMT, the endothelial cells acquire a mesenchymal phenotype characterized by the loss of specific endothelial markers and by the gain of mesenchymal markers. Proteins involved in this cellular phenotypic and functional change include TGF, CADH2 and CADH1.

TGF has widely been described to be involved in EMT and fibrosis induction in the kidney[328–330]. Androgens modulation of TGF activity is mediated by STAT3, which can be activated by the AR directly[331], or through SRC[332,333]. Once activated, STAT3 promotes TGF expression and regulates TGF DNA-binding affinity and transcription[334].

CADH2 expression is upregulated during EMT[335]. CADH2, has been described to be necessary for the increased motility that entails EMT[336]. Interestingly, active AR has been described to induce CADH2 expression[337].

The EMT of renal tubular epithelial cells is characterized by the loss of CADH1 or E-cadherin[338]. CADH1 is a calcium-dependent cell-cell adhesion molecule with pivotal roles in epithelial cell behavior, tissue formation, and suppression of cell migration[339]. The very same AR has been reported to act as a repressor of CADH1 expression[340].

Moreover, androgens, by the modulation of several other pathways, can also finally decrease CADH1 expression. Activation of EGFR has been shown to be accompanied by a decrease in CADH1 levels[341]. Activation of SRC enhances STAT3 signaling[332,333], and STAT3 induces CADH1 reduced expression[342,343]. VDR has been reported to be able to induce de novo CADH1 expression[344]. Nonetheless, according to the Moa (Figure 50) androgens prevent VDR activation by inhibiting SMAD3[322,323].

Changes in these TGF, CADH2 and CADH1 protein levels and activity eases the endothelial cells to move from their normal organized cell layer and invade the underlying tissue inducing interstitial fibrosis and favoring the development of chronic kidney disease[335].

6.B.I.4. Immune response

As a consequence of IRI inflammation may become excessive and injury and repair become unbalanced with innate immune cells playing a critical role in mediating injury responses[345]. The observed immune response is characterized by the activity of classical cells belonging to the immune system, such as neutrophils, macrophages, dendritic cells, lymphocytes, and also tubular epithelial cells and endothelial cells[346].

PECA1, a member of the immunoglobulin-associated cell adhesion molecule family, is present on neutrophils and endothelial cells and mediates the final common pathway of neutrophil trans endothelial migration[347]. PECA1 expression has been found increased in endothelial cells after IRI[327].PECA1 intracellular signaling can be activated by SRC-dependent phosphorylation[348]. Androgens have been reported to increase SRC[Tyr 416] phosphorylation and activation[349]. Moreover, AR promotes receptor ERBB2 expression[350], and signaling[351]; ERBB3 expression[351]; and IGF1R expression[352]. These three receptors can also activate SRC[332,353–355].

IL12B together with IL23A forms IL23, contributes to neutrophils activation and infiltration[356]. IL12B expression can be downregulated by VDR[357]. In consequence, SMAD3 inhibition by AR[322,323], may promote IL12B expression by preventing VDR activation mediated by SMAD3[358].

Macrophages migration in renal IRI depends on CCR2[356]. As a matter of fact, CCR2-deficient animal models appear to be protected from renal IRI[346].

AR has been reported to enhance monocyte chemotaxis by upregulating CCR2 expression[359].

Proinflammatory cytokines and cytokines such as TNFA and IL6 play a major role in renal dysfunction of IRI[360]. Both cytokines, as well as IL8, have been reported to be highly secreted during IRI[300,335].Androgens have been reported to be involved in proinflammatory cytokines expression. For instance, AR has been shown to locally increase TNFA expression[359]. On the other hand, androgens may promote IL6 and IL8 expression through STAT3 activation[361,362], or by avoiding VDR activation, which can act as an IL6 repressor[363].

STAT3 phosphorylation has been reported to be increased in renal IRI injury, as a consequence of JAK/STAT signaling activation[364]. JAK/STAT signaling has been described to directly mediate many proinflammatory cytokines involved in progression of renal IRI[360]. According to the proposed mechanism of action, androgens may also lead

to STAT3 activation, either directly[365], or indirectly by promoting EGFR signaling[366–369] and/or SRC activation[332,333].

NFKB1 is part of the NF-κB complex. NF-κB activation has been reported to be triggered by TLR activation after IRI. The nuclear translocation of NF-κB subsequently upregulates proinflammatory cytokines and chemokines[370]. Conforming to the suggested mechanism of action (Figure 50), AR-dependent NFKB1 activation relies on EGFR signaling, which has been reported to promote NF-κB dependent transcription[371,372]. Moreover, AR signaling has been shown to enhance EGFR signaling, both by upregulating the transcriptional and translational activities of EGFR and by increasing EGFR phosphorylation[373,350]. The described crosstalk between AR and EGFR signaling may be mediated by SRC, which when phosphorylated presents increased catalytic activity and can phosphorylate and activate EGFR[374,375].

IL2RA activation drives proliferation to sustain Tregs numbers *in vivo.* Inhibition of IL2RA by anti-body targeting has been described to be sufficient to exacerbate renal IRI in animal models[86]. ILR2A expression is upregulated by FOXP3[376], and FOXP3 can be induced by SMAD3[377–379]. Hence, androgens may diminish IL2RA expression by inhibiting SMAD3 DNA-binding activity [322,323].

6.B.I.5. Cell death

IRI has been described to activate different programs of cell death, including apoptosis[335]. Androgen-related cell death induction appears to be associated with CASP3 activation[300]. As previously described, androgens can modulate EGFR activity either directly[350,373], or through the modulation of other proteins including SRC[349,374,375]. Moreover, EGFR levels also depend on VDR, which has been shown to bind and repress EGFR expression[380]. Finally, activated EGFR can induce cell death by activating the caspase-dependent apoptotic pathway[381].

6.B.I.6. Regeneration of renal epithelial cells

After IRI, there is also induction of proteins that play a crucial role in regeneration and repair processes. During the repair phase, the kidney microenvironment mediates the transition of macrophage activation from a proinflammatory to a reparative phenotype. Such phenotype switch is partly due to STAT5 activation[382].

Androgens signaling may impair renal regeneration by preventing STAT5 activation through stimulating SRC signaling. Active SRC has been reported to mediate inhibitory regulation of ERBB4 nuclear signaling[383], which is involved in STAT5 activation[383–386].

There are genetic and pharmacologic evidences that point out an important role of EGFR signaling in the renal functional and morphological recovery. Even though the clear mechanism has not been described yet, deletion of EGFR in renal proximal tubule epithelial cells delays recovery from AKI[154]. Nonetheless, the role of EGFR appears to be complex, as apart from its role in regeneration, it is also involved in the induction of renal epithelial cells dedifferentiation. Accordingly, EGFR signaling effect may vary over time. Therefore, the role of EGFR needs to be further studied.

In order to summarize, the identified mechanism of action indicates that androgens may increase oxidative stress, dedifferentiation of renal epithelial cells, endothelial to mesenchymal transition, immune response and cell death, and impair regeneration of renal epithelial cells, hence enhancing renal damage and disrupting the kidney's regeneration process. Some of the targets identified in these processes, were also found in the pig microarray data (CASP3, BTG2, TGF-β, STAT5A, TNF, IL8, STAT3, NFKB1). Our analysis targeted the presence of androgens as the responsible for the negative impact on the renal kidney regulation upon injury. Although estrogen administration can partially reduce kidney injury associated with renal IRI, in a mouse model, it was reported that, it is the presence of testosterone, more than the absence of estrogen, that plays a critical role in sex differences in susceptibility of the kidney to ischemic injury[387].

6.B.II. Overlap between androgens renal IRI/regeneration and ccRCC

Cells of the kidney rarely divide but following injury the renal tubules possess a remarkable regenerative ability, which is essential for the maintenance of tubular structural integrity and kidney's function[388,389]. Adult stem cells have also been postulated as plausible cell of origin in some cancers. Interestingly, the transcriptional profile of proximal tubule progenitor cells has been described to present significant resemblance to that of pRCC type ; and proximal tubule cells are thought to be the origin for ccRCC[90,390].Accordingly, there is a potential connexion between regeneration and ccRCC as the cells surviving and being activated after IRI may be both involved in tubule repopulation, and in originating oncogenic transformation[90,391].

In the course of our project, nine proteins were both identified as key proteins related to androgens IRI/regeneration and to ccRCC (Table XXXVII).Most of these proteins (all of them except for NR1I2) have already been described in the literature to play a role in renal IRI /regeneration and/or in ccRCC.

ACE2 downregulation has been reported to enhance renal damage by promoting oxidative stress and immune response[392,393]. On the other hand, ACE2 expression has been associated with enhanced migration and invasion of ccRCC cells [394].

In this work, we have determined CREBB1 as a key protein of IRI/regeneration. CREB1 has not been previously reported to be associated with renal IRI/regeneration, but it has been shown that increased phosphorylation of this protein promotes growth and metastatic activity of RCC[395].

GCR has been associated with augmented ATP1B1 cell-cell adhesion function, improving RCC patient's outcome[396]. ATP1B1 is the non-catalytic component of the active enzyme Na/K ATPase, which catalyzes the hydrolysis of ATP coupled with the exchange of Na^+ and K^+ ions across the plasma membrane. The beta subunit regulates, through assembly of alpha/beta heterodimers, the number of sodium pumps transported to the plasma membrane. Hence, it is involved in cell adhesion and establishing epithelial cell polarity[397]. Considering the above described role of GCR signaling, it could reduce IRI and promote regeneration by diminishing loss of tubule cells polarity and a re-distribution of Na/K ATPase from its normal location in the basolateral membrane to the apical membrane[35].

Increased expression of IRF1 promotes cancer cells apoptosis[398]. Taking into account the described role of apoptosis in renal IRI[370], increased levels of IRF1 may worsen cell viability.

PPARG agonists have been shown to inhibit ccRCC cell proliferation[399]. On the other hand, increased PPARG activity could reduce renal IRI due to its anti-inflammatory and anti-oxidant effect[400]. Moreover, it might be involved in accelerating mitochondrial function recovery[401].

STAT5B activity has been associated both with ccRCC and renal IRI/regeneration. Increased levels of STAT5 have been associated with immune system evasion in ccRCC[402]. Moreover, increased STAT5 activity is necessary for macrophage to switch to a reparative phenotype that supports tubular proliferation after ischemic injury[382].

TLR4 activation leads the immune response after IRI[403], hence promoting renal damage. On the other hand, even though a role for TLR4 has not been described in ccRCC, it has been shown to be overexpressed[404].

VDR signaling has been described to play an anti-carcinogenic role by regulating transcription of genes in cell adhesion, growth and immunity[405]. For instance, VDR can promote the expression of CADH1 which is lost during epithelial-to-mesenchymal transition (EMT)[344]; and repress the expression of cytokines such as IL12 and IL6 [357,363]. These processes are also associated with renal IRI, in relation to the observed immune response and dedifferentiation of renal epithelial cells leading to renal dysfunction[314,345]. Accordingly, VDR may play a role in renal IRI.

EMTs are phenotypic plasticity processes that confer migratory and invasive properties to epithelial cells during development, wound-healing, fibrosis and cancer[406–409]. EMTs are driven by SNAIL, ZEB and TWIST transcription factors[410,411] together with microRNAs that balance this regulatory network[412,413]. TGF-β is a potent inducer of developmental and fibrogenic EMTs[409,414,415]. Aberrant TGF-β signaling and EMT are implicated in the pathogenesis of renal fibrosis, alcoholic liver disease, non-alcoholic steatohepatitis, pulmonary fibrosis and cancer[409,416]. TGF-β depends on RAS and MAPK pathway inputs for the induction of EMTs[417–424]. This year, significant progress has been made on the subject. It was confirmed that metastasis is due to reprogramming of tumor cells, which acquire regenerative stem cell properties[425]. The study focused on liver metastases from pancreatic cancer. They showed how these signals coordinately trigger EMTs and integrate them with broader pathophysiological processes. This result goes in the same direction with the hypothesis of thus work that the mechanisms that drive kidney cancer and regeneration after damage are shared.

In summary, some proteins play direct roles in regeneration, and ccRCC progression by influencing on cell reorganization and immune switch to reparative/evasive phenotype (GCR, STAT5B). Some proteins play direct roles in renal IRI and ccRCC progression through processes such as inflammation, cell adhesion and proliferation., having coinciding sings in both conditions (PPARG, VDR and TLR4). While other proteins have opposite signs (ACE2 and IRF1) and affect processes that are not related to the relationship between IRI/regeneration and ccRCC: apoptosis and metastasis. Further analysis will be necessary to characterize the role of CREB1 and NR1I2 in renal IRI/regeneration and ccRCC.

6.B.III.   Renal cells' response to sex hormone stimulation

Androgens and estrogens have shown to trigger genomic and non-genomic events within the renal cortex and in renal tubular cells in culture[118,426–428]. Sex hormones. androgens can also stimulate MAPK/ERK[116] and AKT pathways[117] after interacting with the AR or the G-coupled receptor GPRC6A on the cell membrane[114,115].

We tried to establish an *in vitro* model where we could play with sex hormones. The sensitivity of renal cell lines to hormone stimulation was tested by repeating an experiment that was recently done by a group[428]. Briefly, the cells were serum starved and treated with DHT or EST for 10min. Then, by western blot analysis, ERK phosphorylation was analyzed as control that the cells were responsive of sex hormone treatment. In our cells (RPTEC, HK-2,), we did not observe MAPK activation, like it was reported to be activated in renal primary cultured cells[428]. Following discussion with the authors, they pointed out that the cells did not consistently respond to the hormone stimulation treatment.

In following experiments, we decided to stimulate the cells for a longer time in order to assess the possible occurrence of a genomic response. Unfortunately, we did not observe a difference in the regulation of selected target that are proven to be regulated by sex hormones *in vivo*. Moreover, neither the AR stably transduced in a renal cell line triggered response to sex hormone stimulation. We were not able to play with androgens in our system.

We did not reach our goal to have a cell line sensible to the AR. However, a group managed to do so. The AR was co-transfected in CV-1 cells (monkey normal kidney) with a constitutively active STAT3 mutant, one of our key targets[429]. The transfected cells responded to the hormone stimulation. Among other things, they found that STAT3 stimulates the transcriptional activity of the AR in a hormone-dependent manner. They suggested that STAT3 can enhance the transactivation of AR and that activated STAT3 could have a role in the development or progression of a hypersensitive of the AR. Their results are in accordance with our MoA on the link between STAT3 and the AR (Figure 50) and that androgens play a major role on the regulation of his targets in the resolution of injury.

6.B.VI. Regulation of STAT3 in renal cells upon IRI

Our *in vitro* model of renal IRI has allowed us to partially validate the selected target protein determined by bioinformatic analyses. We were able to determine the regulation of some targets by ischemia-reperfusion injury.

In this work, for the first time, we reported that STAT3 was regulated at the level of phosphorylation in renal IRI. Serine and tyrosine phosphorylation go in different direction during the process of injury regeneration in RPTEC. STAT3 phosphorylation (tyrosine) has previously been shown to be up-regulated in post-ischemic (24h/48h) rat kidney tissue.[364] This result correlates with our current results. However, the information about the phosphorylation of the serine residues is rarely available. Similar to our experiment, other AKI studies have found an up-regulation of STAT3[Tyr705] at regeneration that contribute to cell re-epithelialization[77].

We also evaluated STAT3 regulation renal cancer cells (769-P) under IRI conditions. However, contrary to the normal cells, total STAT3 expression was down-regulated under ischemia treatment. STAT3 regulates the transcription of genes involved in various essential cellular functions like cell survival, proliferation, migration, differentiation, etc[430]. The upstream signals that triggers activation of STAT3 signaling via phosphorylation of conserved tyrosine 705 residue is known to be as canonical pathway of activation (Figure 59). The canonical pathway of STAT3 signaling is known to be responsible for regulating expression of genes involved in various aspects of cancer progression like immune evasion, angiogenesis, proliferation, inhibition of apoptosis etc. For many years, the activation of STAT3 pathway in cancers has been used as a biomarker marker for breast cancer, colon cancer, osteosarcoma and many other cancers for predicting the disease prognosis and overall survival[431].

Recently, many reports that have highlighted existence of an alternative pathway of STAT3 activation that may or may not depend upon the classical canonical STAT3 pathway[432] (Figure 58). The non-canonical pathway of STAT3 signaling has been implicated to STAT3 function independent of classical tyrosine 705 phosphorylation. STAT3 can also be phosphorylated at the serine 727 residue. Many reports have demonstrated the independent role of STAT3[Tyr705] and STAT3[Ser727] in regulating STAT3 function in cancer. It either has a reciprocal inhibitory effect or may have an opposite effect on STAT3[Tyr705] function. In our laboratory, it was demonstrated that STAT3[Ser727] is an independent prognostic factor for ccRCC[433–435].
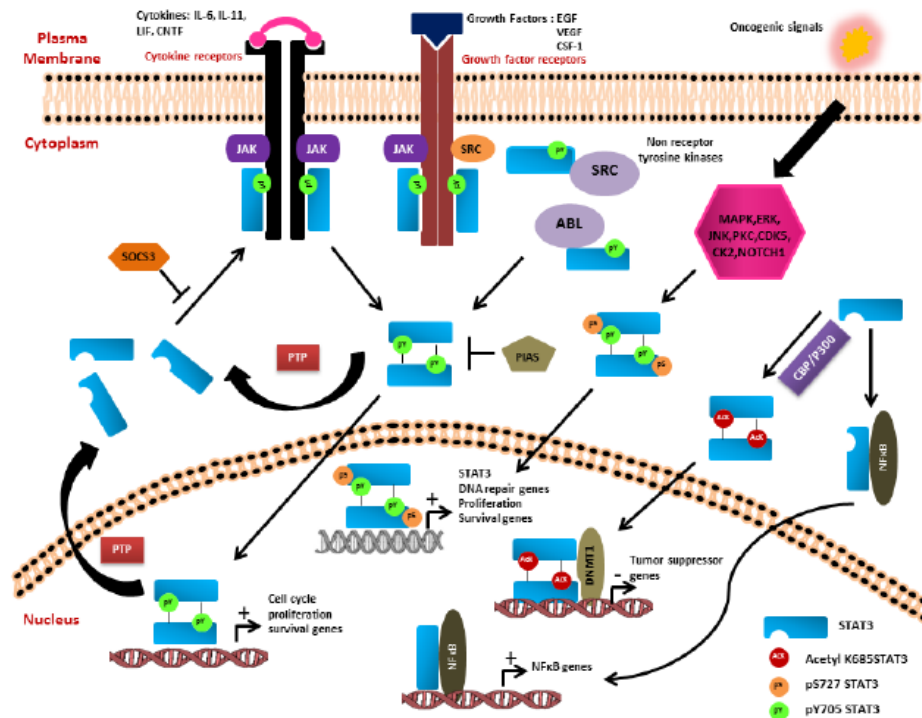
Figure 59. Classical Canonical and Non-Canonical Pathway of STAT3 Activation. The canonical pathway of STAT3 is activated by both receptor tyrosine kinases and non-receptor tyrosine kinases upon stimulus with various growth factors or cytokines. The activated receptors phosphorylate the Y705 residue of Stat3 leading to homodimerization and nuclear translocation of the dimers followed by increase in transcription of cell cycle, proliferation, cell survival genes. The active Stat3 signaling is constantly kept under check via various negative feedback loops like SOCS3, PIAS and PTPs to inhibit the active pathway. The S727 residue of Stat3 is known to be activated in response to various upstream kinases (MAPK, ERK, CDK5, CK2) and some unknown mechanism. pS727 either alone or together with pY705 forms the non-canonical pathway that downstream activates genes involved in cell proliferation, survival, DNA repair, drug resistance and some unknown genes. Apart from phosphorylation of S727 residue, STAT3 also undergoes acetylation at K685 residue that induces Stat3 homodimerization even in the absence of pY075 and pS727. The acetylated Stat3 dimers interact with DNMT1 and methylate the promoter of tumor suppressor genes like CDKN2A, DLEC1, STAT1, TP53, SHP-1 and SOCS3 to inhibit its expression. The non-phospho form of STAT3 is known to interact and form complex with NFκB to downstream activate the transcription of NFκB related genes. (Adapted by Dimri *et al*., *Integr Mol Med*, 2017)[431].

A recent study evaluated the impact of ischemia on gene expression in renal cell carcinoma tissue. They demonstrate that prolonged warm ischemia is associated with significant changes in gene expression profiles for genes like Bax and CA9[436]. This is the same tendency that we observed with our in vitro system STAT3 expression in cancer cells was altered during ischemia treatment.

Despite the different type of regulation of STAT3 in normal and cancer cells, STAT3 has proven to be a key target to study the links between IRI/regeneration and ccRCC in future experiments.

Moreover, even if we were not able to validate it, our results suggested that STAT3 is also a target regulated by the AR activation in renal cells, as it was found to be in prostate cells[331].

In fact, in prostate cells, WNT3A and beta catenin can recruit the AR to the promoter regions of several genes[437]. Additionally, the activation of CDK1, PKA, PI3K/AKT and STAT3 may enhance the AR transcriptional responses[438]. In prostate cells, CDK1 phosphorylates the AR and stabilizes the receptor[439]. The activation of the PI3K/AKT pathway results in the AR phosphorylation and promotion of cell survival[440]. STAT3 can form a heterologous complex with the AR[441]. Therefore, whenever STAT3 is activated, for example as a response to EGF and IL6, then the AR is activated[442].

In this project, we have also worked with prostate cells (LNCaP-AD). While the cells responded to the hormone stimulation treatment, no differences of expression were observed in our key targets (STAT3 and STAT1) under the IRI treatment for either the total protein level or at the phosphorylation level. Therefore, no further experiment was conducted with this cell line.

6.C. LIMITATIONS AND FUTURE PERSPECTIVES

Since the swine model is genetically closer to the human than the rodent model, the results presented in this study bring insightful information about the molecular mechanism processes that regulate men and women kidney function. This study offers a rich template for future studies. The curated information can be helpful to direct the focus on a selected gene or a pathway.

We tried to establish an *in vitro* system that could validate some of the interesting target found throughout the project. Unfortunately, we were not able to build a system that respond to the androgens. As we showed, sex hormones play a crucial role in the regulation of genes and gene sets. Thus, our model did not allow us to fully validate the influence of sex hormones on targets.

In the pursuit of this project, the use of a more robust *in vitro* system would be necessary. For instance, the use of kidney organoids who can better replicate the complexity of an organ could be used for IRI experiments. The system chosen should also be sensible to hormone stimulation.

The *in vivo* analysis has revealed the crucial role of the immune system during renal IRI processes. For that reason, an eventual step would be to perform co-culture

assays of renal cell with blood cells. We would study in more details STAT3 regulation in IRI with the presence of the immune system.

7.CONCLUSIONS

7. CONCLUSIONS

1. Porcine kidney tissues display sex differences at the gene and protein level throughout renal IRI.

2. Gene sets involves in renal IRI processes can be characterized in a time and sex way.

3. The pig is a more adequate animal model to study the role of androgens in kidney diseases than the mouse.

4. Androgens play a key role in the regulation of renal IRI.

5. Key proteins involved in renal IRI/regeneration and renal cancer strongly suggest shared common mechanism between both processes.

6. STAT3 is regulated in both renal IRI/regeneration and renal cancer and is a solid target to further study the shared common mechanism between renal IRI/regeneration and renal cancer

8. BIBLIOGRAPHY

8. BIBLIOGRAPHY

1.   Nyush, A. Boron and Boulpaep Textbook of Medical Physiology 2nd updated edition.pdf.

2.   staff, B. co. & staff, B. co. Medical gallery of Blausen Medical 2014. *WikiJournal Med.* **1**, 10 (2014).

3.   HALL, J. E. *GUYTON AND HALL TEXTBOOK OF MEDICAL PHYSIOLOGY.* (ELSEVIER - HEALTH SCIENCE, 2020).

4.   Brunskill, E. W., Georgas, K., Rumballe, B., Little, M. H. & Potter, S. S. Defining the Molecular Character of the Developing and Adult Kidney Podocyte. *PLoS One* **6**, e24640 (2011).

5.   Aronson, P. S. Mechanisms of active H+ secretion in the proximal tubule. *Am. J. Physiol. - Ren. Fluid Electrolyte Physiol.* **14**, (1983).

6.   Guo, Y. M. *et al.* Na+/HCO3-cotransporter NBCn2 mediates HCO3- reclamation in the apical membrane of renal proximal tubules. *J. Am. Soc. Nephrol.* **28**, 2409–2419 (2017).

7.   Stephanou, A. Role of STAT-1 and STAT-3 in ischaemia / reperfusion injury. **8**, 519–525 (2004).

8.   Li, Y. & Wingert, R. A. Regenerative medicine for the kidney: stem cell prospects & challenges. *Clin. Transl. Med.* **2**, 11 (2013).

9.   Macosko, E. Z. *et al.* Highly parallel genome-wide expression profiling of individual cells using nanoliter droplets. *Cell* **161**, 1202–1214 (2015).

10.   Regev, A., Teichmann, S. A. & Lander, E. S. The Human Cell Atlas. doi:10.7554/eLife.27041.001.

11.   Young, M. D. *et al.* Single-cell transcriptomes from human kidneys reveal the cellular identity of renal tumors. *Science (80-.).* **361**, 594–599 (2018).

12.   Qiu, C. *et al.* Renal compartment–specific genetic variation analyses identify new pathways in chronic kidney disease. *Nat. Med.* **24**, 1721–1731 (2018).

13.   Liao, J. *et al.* Single-cell RNA sequencing of human kidney. *Sci. Data* **7**, 1–9 (2020).

14.   Schedl, A. Renal abnormalities and their developmental origin. *Nature Reviews Genetics* vol. 8 791–802 (2007).

15.   Bonventre, J. V. & Yang, L. Cellular pathophysiology of ischemic acute kidney injury. *Journal of Clinical Investigation* vol. 121 4210–4221 (2011).

16.   Murugan, R. & Kellum, J. A. Acute kidney injury: What's the prognosis? *Nature Reviews Nephrology* vol. 7 209–217 (2011).

17.   Venkatachalam, M. A. *et al.* Acute kidney injury: A springboard for progression in chronic kidney disease. *American Journal of Physiology - Renal Physiology* vol. 298 F1078-94 (2010).

18.   El Nahas, A. M. & Bello, A. K. Chronic kidney disease: The global challenge. in *Lancet* vol. 365 331–340 (2005).

19.   Hsu, C. Y. *et al.* Nonrecovery of kidney function and death after acute on chronic renal failure. *Clin. J. Am. Soc. Nephrol.* **4**, 891–898 (2009).

20.   Ishani, A. *et al.* Acute kidney injury increases risk of ESRD among elderly. *J. Am. Soc. Nephrol.* **20**, 223–228 (2009).

21.   Coca, S. G., Yusuf, B., Shlipak, M. G., Garg, A. X. & Parikh, C. R. Long-term Risk of Mortality and Other Adverse Outcomes After Acute Kidney Injury: A Systematic Review and Meta-analysis. *Am. J. Kidney Dis.* **53**, 961–973 (2009).

22.   Rahman, M., Shad, F. & Smith, M. C. Acute kidney injury: A guide to diagnosis and management. *Am. Fam. Physician* **86**, 631–639 (2012).

23.   Lameire, N., Van Biesen, W. & Vanholder, R. The changing epidemiology of acute renal failure. *Nature Clinical Practice Nephrology* vol. 2 364–377 (2006).

24.   Waikar, S. S., Liu, K. D. & Chertow, G. M. Diagnosis, epidemiology and outcomes of acute kidney injury. *Clinical Journal of the American Society of Nephrology* vol. 3 844–861 (2008).

25.   Hsu, C. Y. *et al.* Community-based incidence of acute renal failure. *Kidney Int.* **72**, 208–212 (2007).

26.   Goldstein, L. B. *et al.* Guidelines for the primary prevention of stroke: A Guideline for Healthcare Professionals from the American Heart Association/American Stroke Association. *Stroke* **42**, 517–584 (2011).

27.   Jungers, P. *et al.* Age and gender-related incidence of chronic renal failure in a French urban area: a prospective epidemiologic study. *Nephrol. Dial. Transplant* **11**, 1542–6 (1996).

28.   T, H. *et al.* Factors affecting progression in advanced chronic renal failure. *Clin. Nephrol.* **39**, 312–320 (1993).

29.   Hsu, C.-Y., Lin, F., Vittinghoff, E. & Shlipak, M. G. Racial differences in the progression from chronic renal insufficiency to end-stage renal disease in the United States. *J. Am. Soc. Nephrol.* **14**, 2902–7 (2003).

30.   Lysaght, M. J. Maintenance dialysis population dynamics: Current trends and long-term implications. *J. Am. Soc. Nephrol.* **13**, (2001).

31.   Weiner, D. E. Public health consequences of chronic kidney disease. *Clinical Pharmacology and Therapeutics* vol. 86 566–569 (2009).

32.   Eltzschig, H. K. & Eckle, T. Ischemia and reperfusion-from mechanism to translation. *Nature Medicine* vol. 17 1391–1401 (2011).

33.   Ferenbach, D. A. & Bonventre, J. V. Mechanisms of maladaptive repair after AKI leading to accelerated kidney ageing and CKD. *Nat. Rev. Nephrol.* **11**, 264–276 (2015).

34.   Parekh, N., Esslinger, H. U. & Steinhausen, M. Glomerular filtration and tubular reabsorption during anuria in postischemic acute renal failure. *Kidney Int.* **25**, 33–41 (1984).

35.   Sharfuddin, A. A. & Molitoris, B. A. Pathophysiology of ischemic acute kidney injury. *Nat. Rev. Nephrol.* **7**, 189–200 (2011).

36.   Molitoris, B. A. & Sutton, T. A. Endothelial injury and dysfunction: Role in the extension phase of acute renal failure. in *Kidney International* vol. 66 496–499 (Blackwell Publishing Inc., 2004).

37.   Solez, K., Morel-Maroger, L. & Sraer, J. D. The morphology of 'acute tubular necrosis' in man: analysis of 57 renal biopsies and a comparison with the glycerol model. *Medicine (Baltimore).* **58**, 362–76 (1979).

38.   Failure, L. R.-A. R. & 2001, undefined. The morphologic basis of acute renal failure. *WB Saunders, Philadelphia*.

39.   Saikumar, P. & Venkatachalam, M. A. Role of Apoptosis in Hypoxic/Ischemic Damage in the Kidney. *Semin. Nephrol.* **23**, 511–521 (2003).

40.   Molitoris, B. A. *et al.* Actin cytoskeleton in ischemic acute renal failure. *Kidney Int.* **66**, 871–883 (2004).

41.   Ashworth, S. L., Sandoval, R. M., Tanner, G. A. & Molitoris, B. A. Two-photon microscopy: Visualization of kidney dynamics. *Kidney International* vol. 72 416–421

(2007).

42. Molitoris, B. A., Dahl, R. & Hosford, M. Cellular ATP depletion induces disruption of the spectrin cytoskeletal network. *Am. J. Physiol. - Ren. Fluid Electrolyte Physiol.* **271**, (1996).

43. Ashworth, S. L., Sandoval, R. M., Hosford, M., Hamburg, J. R. & Molitoris, B. A. Ischemic injury induces ADF relocalization to the apical domain of rat proximal tubule cells. *Am. J. Physiol. - Ren. Physiol.* **280**, (2001).

44. Ashworth, S. L. *et al.* ADF/cofilin mediates actin cytoskeletal alterations in LLC-PK cells during ATP depletion. *Am. J. Physiol. - Ren. Physiol.* **284**, F852-62 (2003).

45. Atkinson, S. J., Hosford, M. A. & Molitoris, B. A. Mechanism of Actin Polymerization in Cellular ATP Depletion. *J. Biol. Chem.* **279**, 5194–5199 (2004).

46. Sedeek, M., Nasrallah, R., Touyz, R. M. & Hébert, R. L. NADPH oxidases, reactive oxygen species, and the kidney: Friend and foe. *Journal of the American Society of Nephrology* vol. 24 1512–1518 (2013).

47. Tothova, Z. *et al.* FoxOs Are Critical Mediators of Hematopoietic Stem Cell Resistance to Physiologic Oxidative Stress. *Cell* **128**, 325–339 (2007).

48. Linkermann, A., De Zen, F., Weinberg, J., Kunzendorf, U. & Krautwald, S. Programmed necrosis in acute kidney injury. *Nephrol. Dial. Transplant* **27**, 3412–9 (2012).

49. Martin-Sanchez, D. *et al.* Targeting of regulated necrosis in kidney disease. *Nefrologia* **38**, 125–135 (2018).

50. Chen, G. Y. & Nuñez, G. Sterile inflammation: Sensing and reacting to damage. *Nat. Rev. Immunol.* **10**, 826–837 (2010).

51. Martin, P. & Leibovich, S. J. Inflammatory cells during wound repair: The good, the bad and the ugly. *Trends in Cell Biology* vol. 15 599–607 (2005).

52. Kumar Mbbs, V. *et al. I II III Robbins and Cotran PATHOLOGIC BASIS OF DISEASE Seventh Edition.* http://www.elsevier.com (2005).

53. Galliera, E., Corsi, M., Bonecchi, R., Locati, M. & Mantovani, A. Chemokines as Pharmacological Targets. *Mini-Reviews Med. Chem.* **8**, 638–646 (2008).

54. Lukacs-Kornek, V., Engel, D., Tacke, F. & Kurts, C. The role of chemokines and their receptors in dendritic cell biology. *Frontiers in Bioscience* vol. 13 2238–2252 (2008).

55. Segerer, S. & Nelson, P. J. Chemokines in renal diseases. *ScientificWorldJournal.* **5**, 835–844 (2005).

56. Segerer, S., Nelson, P. J. & Schlöndorff, D. Chemokines, chemokine receptors, and renal disease: From basic science to pathophysiologic and therapeutic studies. *Journal of the American Society of Nephrology* vol. 11 152–176 (2000).

57. Sanz AB, Sanchez-Niño MD, Ramos AM, Moreno JA, Santamaria B, Ruiz-Ortega M, Egido J, O. A. NF-kB in renal inflammation. *J Am Soc Nephrol.* **21**, 1254–1262 (2010).

58. Sánchez-López, E. *et al.* CTGF promotes inflammatory cell infiltration of the renal interstitium by activating NF-κB. *J. Am. Soc. Nephrol.* **20**, 1513–1526 (2009).

59. Tang, S. C. W., Leung, J. C. K., Chan, L. Y. Y., Tsang, A. W. L. & Lai, K. N. Activation of tubular epithelial cells in diabetic nephropathy and the role of the peroxisome proliferator-activated receptor-γ agonist. *J. Am. Soc. Nephrol.* **17**, 1633–1643 (2006).

60. Chung, A. C. K. *et al.* Disruption of the Smad7 gene promotes renal fibrosis and inflammation in unilateral ureteral obstruction (UUO) in mice. *Nephrol Dial Transpl.* **24**, 1443–1454 (2009).

61. Huang, X. R., Chung, A. C. K., Zhou, L., Wang, X. J. & Lan, H. Y. Latent TGF-β1

protects against crescentic glomerulonephritis. *J. Am. Soc. Nephrol.* **19**, 233–242 (2008).

62.	Furuichi, K., Kaneko, S. & Wada, T. Chemokine/chemokine receptor-mediated inflammation regulates pathologic changes from acute kidney injury to chronic kidney disease. *Clinical and Experimental Nephrology* vol. 13 9–14 (2009).

63.	Holdsworth, S. R. & Tipping, P. G. Leukocytes in glomerular injury. *Seminars in Immunopathology* vol. 29 355–374 (2007).

64.	Chung, A. C. K. & Lan, H. Y. Chemokines in renal injury. *J. Am. Soc. Nephrol.* **22**, 802–809 (2011).

65.	Serhan, C. N. Resolution Phase of Inflammation: Novel Endogenous Anti-Inflammatory and Proresolving Lipid Mediators and Pathways. *Annu. Rev. Immunol.* **25**, 101–137 (2007).

66.	Jensen, J. U. S. *et al.* Kidney failure related to broad-spectrum antibiotics in critically ill patients: Secondary end point results from a 1200 patient randomised trial. *BMJ Open* **2**, e000635 (2012).

67.	Biswas, S. K. & Lopez-Collazo, E. Endotoxin tolerance: new mechanisms, molecules and clinical significance. *Trends in Immunology* vol. 30 475–487 (2009).

68.	Anders, H. J. & Ryu, M. Renal microenvironments and macrophage phenotypes determine progression or resolution of renal inflammation and fibrosis. *Kidney International* vol. 80 915–925 (2011).

69.	Günthner, R., Kumar, V. R. S., Lorenz, G., Anders, H. J. & Lech, M. Pattern-recognition receptor signaling regulator mRNA expression in humans and mice, and in transient inflammation or progressive fibrosis. *Int. J. Mol. Sci.* **14**, 18124–18147 (2013).

70.	Günthner, R. & Anders, H.-J. Interferon-regulatory factors determine macrophage phenotype polarization. *Mediators Inflamm.* **2013**, 731023 (2013).

71.	Sica, A. & Mantovani, A. Macrophage plasticity and polarization: In vivo veritas. *Journal of Clinical Investigation* vol. 122 787–795 (2012).

72.	Nibbs, R. J. B. & Graham, G. J. Immune regulation by atypical chemokine receptors. *Nature Reviews Immunology* vol. 13 815–829 (2013).

73.	Lech, M. & Anders, H. J. Macrophages and fibrosis: How resident and infiltrating mononuclear phagocytes orchestrate all phases of tissue injury and repair. *Biochimica et Biophysica Acta - Molecular Basis of Disease* vol. 1832 989–997 (2013).

74.	Schiffer, M. *et al.* Apoptosis in podocytes induced by TGF-β and Smad7. *J. Clin. Invest.* **108**, 807–816 (2001).

75.	Yang, L., Besschetnova, T. Y., Brooks, C. R., Shah, J. V. & Bonventre, J. V. Epithelial cell cycle arrest in G2/M mediates kidney fibrosis after injury. *Nat. Med.* **16**, 535–543 (2010).

76.	Bottinger, E. P. & Bitzer, M. TGF-beta signaling in renal disease. *J. Am. Soc. Nephrol.* **13**, 2600–2610 (2002).

77.	Kulkarni, O. P. *et al.* Toll-like receptor 4-induced IL-22 accelerates kidney regeneration. *J. Am. Soc. Nephrol.* **25**, 978–989 (2014).

78.	Lin, S. L. *et al.* Macrophage Wnt7b is critical for kidney repair and regeneration. *Proc. Natl. Acad. Sci. U. S. A.* **107**, 4194–4199 (2010).

79.	Burne, M. J. *et al.* Identification of the CD4(+) T cell as a major pathogenic factor in ischemic acute renal failure. *J. Clin. Invest.* **108**, 1283–90 (2001).

80.	Li, L. *et al.* NKT Cell Activation Mediates Neutrophil IFN-γ Production and Renal Ischemia-Reperfusion Injury. *J. Immunol.* **178**, 5899–5911 (2007).

81.   Zhang, Z.-X. *et al.* NK Cells Induce Apoptosis in Tubular Epithelial Cells and Contribute to Renal Ischemia-Reperfusion Injury. *J. Immunol.* **181**, 7489–7498 (2008).

82.   Jang, H. R. *et al.* B cells limit repair after ischemic acute kidney injury. *J. Am. Soc. Nephrol.* **21**, 654–665 (2010).

83.   Linfert, D., Chowdhry, T. & Rabb, H. Lymphocytes and ischemia-reperfusion injury. *Transplant. Rev.* **23**, 1–10 (2009).

84.   Kinsey, G. R., Sharma, R. & Okusa, M. D. Regulatory T cells in AKI. *J. Am. Soc. Nephrol.* **24**, 1720–1726 (2013).

85.   Gandolfo, M. T. *et al.* Foxp3+ regulatory T cells participate in repair of ischemic acute kidney injury. *Kidney Int.* **76**, 717–729 (2009).

86.   Kinsey, G. R. *et al.* Regulatory T cells suppress innate immunity in kidney ischemia-reperfusion injury. *J. Am. Soc. Nephrol.* **20**, 1744–1753 (2009).

87.   Cheung, T. H. & Rando, T. A. Molecular regulation of stem cell quiescence. *Nature Reviews Molecular Cell Biology* vol. 14 329–340 (2013).

88.   Maeshima, A., Yamashita, S. & Nojima, Y. Identification of Renal Progenitor-Like Tubular Cells that Participate in the Regeneration Processes of the Kidney. *J. Am. Soc. Nephrol.* **14**, 3138–3146 (2003).

89.   Gupta, S. *et al.* Isolation and characterization of kidney-derived stem cells. *J. Am. Soc. Nephrol.* **17**, 3028–3040 (2006).

90.   Lindgren, D. *et al.* Isolation and characterization of progenitor-like cells from human renal proximal tubules. *Am. J. Pathol.* **178**, 828–837 (2011).

91.   Sallustio, F. *et al.* TLR2 plays a role in the activation of human resident renal stem/progenitor cells. *FASEB J.* **24**, 514–525 (2010).

92.   Langworthy, M., Zhou, B., De Caestecker, M., Moeckel, G. & Baldwin, H. S. NFATc1 identifies a population of proximal tubule cell progenitors. *J. Am. Soc. Nephrol.* **20**, 311–321 (2009).

93.   Rabelink, T. J. & Little, M. H. Stromal cells in tissue homeostasis: Balancing regeneration and fibrosis. *Nature Reviews Nephrology* vol. 9 747–753 (2013).

94.   Kitamura, S. *et al.* Establishment and characterization of renal progenitor like cells from S3 segment of nephron in rat adult kidney. *FASEB J.* **19**, 1789–1797 (2005).

95.   Angelotti, M. L. *et al.* Characterization of renal progenitors committed toward tubular lineage and their regenerative potential in renal tubular injury. *Stem Cells* **30**, 1714–1725 (2012).

96.   Clayton, J. A. & Collins, F. S. NIH to balance sex in cell and animal studies. *Nature* vol. 509 282–283 (2014).

97.   Becker, J. B. & Koob, G. F. Sex differences in animal models: Focus on addiction. *Pharmacological Reviews* vol. 68 242–263 (2016).

98.   Chen, H., Ge, R. S. & Zirkin, B. R. Leydig cells: From stem cells to aging. *Molecular and Cellular Endocrinology* vol. 306 9–16 (2009).

99.   DUNN, J. F., NISULA, B. C. & RODBARD, D. Transport of Steroid Hormones: Binding of 21 Endogenous Steroids to Both Testosterone-Binding Globulin and Corticosteroid-Binding Globulin in Human Plasma. *J. Clin. Endocrinol. Metab.* **53**, 58–68 (1981).

100.   VERMEULEN, A. Physiology of the Testosterone-Binding Globulin in Man. *Ann. N. Y. Acad. Sci.* **538**, 103–111 (1988).

101.   Vermeulen, A., Verdonck, L. & Kaufman, J. M. A critical evaluation of simple methods for the estimation of free testosterone in serum. *J. Clin. Endocrinol. Metab.* **84**, 3666–3672

(1999).

102. Nelson, L. R. & Bulun, S. E. Estrogen production and action. *J. Am. Acad. Dermatol.* **45**, S116–S124 (2001).

103. Kellis, J. T. & Vickery, L. E. Purification and characterization of human placental aromatase cytochrome P-450. *J. Biol. Chem.* **262**, 4413–20 (1987).

104. Rae, M. T. & Hillier, S. G. Steroid signalling in the ovarian surface epithelium. *Trends in Endocrinology and Metabolism* vol. 16 327–333 (2005).

105. Goldstone, J. V. *et al.* Genetic and structural analyses of cytochrome P450 hydroxylases in sex hormone biosynthesis: Sequential origin and subsequent coevolution. *Mol. Phylogenet. Evol.* **94**, 676–687 (2016).

106. Hammes, S. R. & Davis, P. J. Overlapping nongenomic and genomic actions of thyroid hormone and steroids. *Best Practice and Research: Clinical Endocrinology and Metabolism* vol. 29 581–593 (2015).

107. Meyer, M. R., Haas, E. & Barton, M. Gender differences of cardiovascular disease: New perspectives for estrogen receptor signaling. *Hypertension* vol. 47 1019–1026 (2006).

108. Hammes, S. R. & Levin, E. R. Extranuclear steroid receptors: Nature and actions. *Endocrine Reviews* vol. 28 726–741 (2007).

109. Meyer, M. R., Haas, E., Prossnitz, E. R. & Barton, M. Non-genomic regulation of vascular cell function and growth by estrogen. *Molecular and Cellular Endocrinology* vol. 308 9–16 (2009).

110. Hammes, S. R. & Levin, E. R. Minireview: Recent advances in extranuclear steroid receptor actions. *Endocrinology* vol. 152 4489–4495 (2011).

111. Filardo, E. J., Quinn, J. A., Bland, K. I. & Frackelton, J. Estrogen-induced activation of Erk-1 and Erk-2 requires the G protein-coupled receptor homolog, GPR30, and occurs via trans-activation of the epidermal growth factor receptor through release of HB-EGF. *Mol. Endocrinol.* **14**, 1649–1660 (2000).

112. Ho, K. J. & Liao, J. K. Nonnuclear actions of estrogen. *Arterioscler. Thromb. Vasc. Biol.* **22**, 1952–61 (2002).

113. Shukla, G. C., Plaga, A. R., Shankar, E. & Gupta, S. Androgen receptor-related diseases: What do we know? *Andrology* **4**, 366–381 (2016).

114. Wang, C., Liu, Y. & Cao, J. M. G protein-coupled receptors: Extranuclear mediators for the non-genomic actions of steroids. *International Journal of Molecular Sciences* vol. 15 15412–15425 (2014).

115. Pi, M., Parrill, A. L. & Quarles, L. D. GPRC6A mediates the non-genomic effects of steroids. *J. Biol. Chem.* **285**, 39953–39964 (2010).

116. Sen, A. *et al.* Paxillin regulates androgen- and epidermal growth factor-induced MAPK signaling and cell proliferation in prostate cancer cells. *J. Biol. Chem.* **285**, 28787–28795 (2010).

117. Freeman, M. R. *et al.* Transit of hormonal and EGF receptor-dependent signals through cholesterol-rich membranes. *Steroids* **72**, 210–217 (2007).

118. Verzola, D. *et al.* Androgen-mediated apoptosis of kidney tubule cells: Role of c-Jun amino terminal kinase. *Biochem. Biophys. Res. Commun.* **387**, 531–536 (2009).

119. Reed, D. K. & Arany, I. Sex hormones differentially modulate STAT3-dependent antioxidant responses during oxidative stress in renal proximal tubule cells. *In Vivo* **28**, 1097–100.

120. Mirandola, L. *et al.* Sex-driven differences in immunological responses: Challenges and opportunities for the immunotherapies of the third millennium. *International Reviews of*

Immunology vol. 34 134–142 (2015).

121.   Klein, S. L. & Flanagan, K. L. Sex differences in immune responses. *Nature Reviews Immunology* vol. 16 626–638 (2016).

122.   Maini, M. K. *et al.* Reference ranges and sources of variability of CD4 counts in HIV-seronegative women and men. *Genitourin. Med.* **72**, 27–31 (1996).

123.   Laffont, S. *et al.* Androgen signaling negatively controls group 2 innate lymphoid cells. *J. Exp. Med.* **214**, 1581–1592 (2017).

124.   Pennell, L. M., Galligan, C. L. & Fish, E. N. Sex affects immunity. *Journal of Autoimmunity* vol. 38 J282–J291 (2012).

125.   Zilio, S. & Serafini, P. Neutrophils and Granulocytic MDSC: The Janus God of Cancer Immunotherapy. *Vaccines* **4**, 31 (2016).

126.   Lu, C., Redd, P. S., Lee, J. R., Savage, N. & Liu, K. The expression profiles and regulation of PD-L1 in tumor-induced myeloid-derived suppressor cells. *Oncoimmunology* **5**, e1247135 (2016).

127.   Capone, I., Marchetti, P., Ascierto, P. A., Malorni, W. & Gabriele, L. Sexual Dimorphism Of Immune Responses: A new perspective in cancer immunotherapy. *Front. Immunol.* **9**, 1–8 (2018).

128.   Collins, A. J., Foley, R. N., Gilbertson, D. T. & Chen, S. C. United States Renal Data System public health surveillance of chronic kidney disease and end-stage renal disease. *Kidney Int. Suppl.* **5**, 2–7 (2015).

129.   Mehta, R. L., Pascual, M. T., Gruta, C. G., Zhuang, S. & Chertow, G. M. Refining predictive models in critically ill patients with acute renal failure. *J. Am. Soc. Nephrol.* **13**, 1350–1357 (2002).

130.   Paganini, E. P., Halstenberg, W. K. & Goormastic, M. Risk modeling in acute renal failure requiring dialysis: the introduction of a new model. *Clin. Nephrol.* **46**, 206–11 (1996).

131.   Chertow, G. M. *et al.* Predictors of mortality and the provision of dialysis in patients with acute tubular necrosis. The Auriculin Anaritide Acute Renal Failure Study Group. *J. Am. Soc. Nephrol.* **9**, 692–8 (1998).

132.   Wei, Q., Wang, M. H. & Dong, Z. Differential gender differences in ischemic and nephrotoxic acute renal failure. *Am. J. Nephrol.* **25**, 491–499 (2005).

133.   Müller, V. *et al.* Sexual dimorphism in renal ischemia-reperfusion injury in rats: Possible role of endothelin. *Kidney Int.* **62**, 1364–1371 (2002).

134.   Park, K. M., Kim, J. I., Ahn, Y., Bonventre, A. J. & Bonventre, J. V. Testosterone is responsible for enhanced susceptibility of males to ischemic renal injury. *J. Biol. Chem.* **279**, 52282–52292 (2004).

135.   Kang, K. P. *et al.* Effect of gender differences on the regulation of renal ischemia-reperfusion-induced inflammation in mice. *Mol. Med. Rep.* **9**, 2061–2068 (2014).

136.   Hodeify, R. *et al.* Gender differences control the susceptibility to ER stress-induced acute kidney injury. *Am. J. Physiol. - Ren. Physiol.* **304**, F875-82 (2013).

137.   Rinn, J. L. *et al.* Major molecular differences between mammalian sexes are involved in drug metabolism and renal function. *Dev. Cell* **6**, 791–800 (2004).

138.   Lieberthal, W. & Nigam, S. K. Acute renal failure. II. Experimental models of acute renal failure: Imperfect but indispensable. *American Journal of Physiology - Renal Physiology* vol. 278 (2000).

139.   Nam, J. K., Kim, J. H., Park, S. W. & Chung, M. K. The Association of Phosphodiesterase 5 Inhibitor on Ischemia-Reperfusion Induced Kidney Injury in Rats.

Urol. J. **17**, 91–96 (2020).

140. Yoo, E. J. *et al.* Transcriptional Regulator TonEBP Mediates Oxidative Damages in Ischemic Kidney Injury. *Cells* **8**, 1284 (2019).

141. García-Ortuño, L. E. *et al.* Resilience to acute kidney injury in offspring of maternal protein restriction. *Am. J. Physiol. - Ren. Physiol.* **317**, F1637–F1648 (2019).

142. Mobasheran, P., Rajai, N., Kohansal, P., Dehpour, A. R. & Shafaroodi, H. The effects of acute sumatriptan treatment on renal ischemia/reperfusion injury in rat and the possible involvement of nitric oxide. *Can. J. Physiol. Pharmacol.* **98**, 252–258 (2020).

143. Rossi, M. *et al.* HO-1 mitigates acute kidney injury and subsequent kidney-lung cross-talk. *Free Radic. Res.* **53**, 1035–1043 (2019).

144. Ji, Z., Wang, L., Wang, S. & Liang, G. Dexmedetomidine hydrochloride up-regulates expression of hypoxia inducible factor-1α to alleviate renal ischemiareperfusion injury in diabetic rats. *Nan Fang Yi Ke Da Xue Xue Bao* **39**, 944–949 (2019).

145. Park, W. S. *et al.* Hesperidin Shows Protective Effects on Renal Function in Ischemia-induced Acute Kidney Injury (Sprague-Dawley Rats). *Transplant. Proc.* **51**, 2838–2841 (2019).

146. Çakır, M., Tekin, S., Doğanyiğit, Z., Çakan, P. & Kaymak, E. The protective effect of cannabinoid type 2 receptor activation on renal ischemia–reperfusion injury. *Mol. Cell. Biochem.* **462**, 123–132 (2019).

147. Altmann, C. *et al.* Macrophages mediate lung inflammation in a mouse model of ischemic acute kidney injury. *Am. J. Physiol. - Ren. Physiol.* **302**, (2012).

148. Amura, C. R. *et al.* Complement activation and toll-like receptor-2 signaling contribute to cytokine production after renal ischemia/reperfusion. *Mol. Immunol.* **52**, 249–257 (2012).

149. Arany, I. *et al.* Chronic nicotine exposure exacerbates acute renal ischemic injury. *Am. J. Physiol. - Ren. Physiol.* **301**, (2011).

150. Arfian, N. *et al.* ET-1 deletion from endothelial cells protects the kidney during the extension phase of ischemia/reperfusion injury. *Biochem. Biophys. Res. Commun.* **425**, 443–449 (2012).

151. Balasubramanian, S., Jansen, M., Valerius, M. T., Humphreys, B. D. & Strom, T. B. Orphan nuclear receptor Nur77 promotes acute kidney injury and renal epithelial apoptosis. *J. Am. Soc. Nephrol.* **23**, 674–686 (2012).

152. Basile, D. P. *et al.* Impaired endothelial proliferation and mesenchymal transition contribute to vascular rarefaction following acute kidney injury. *Am. J. Physiol. - Ren. Physiol.* **300**, (2011).

153. Celie, J. W. A. M. *et al.* Tubular epithelial syndecan-1 maintains renal function in murine ischemia/reperfusion and human transplantation. *Kidney Int.* **81**, 651–661 (2012).

154. Chen, J., Chen, J. K. & Harris, R. C. Deletion of the epidermal growth factor receptor in renal proximal tubule epithelial cells delays recovery from acute kidney injury. *Kidney Int.* **82**, 45–52 (2012).

155. El-Achkar, T. M. *et al.* Tamm-horsfall protein-deficient thick ascending limbs promote injury to neighboring S3 segments in an MIP-2-dependent mechanism. *Am. J. Physiol. - Ren. Physiol.* **300**, 999–1007 (2011).

156. Funk, J. A. & Schnellmann, R. G. Persistent disruption of mitochondrial homeostasis after acute kidney injury. *Am. J. Physiol. - Ren. Physiol.* **302**, F853-64 (2012).

157. Hu, M. C. *et al.* Klotho deficiency is an early biomarker of renal ischemia-reperfusion injury and its replacement is protective. *Kidney Int.* **78**, 1240–1251 (2010).

158. Huang, L. *et al.* Overexpression of stanniocalcin-1 inhibits reactive oxygen species and

renal ischemia/reperfusion injury in mice. *Kidney Int.* **82**, 867–877 (2012).

159. Humphreys, B. D. *et al.* Repair of injured proximal tubule does not involve specialized progenitors. *Proc. Natl. Acad. Sci. U. S. A.* **108**, 9226–9231 (2011).

160. Jayakumar, C., Mohamed, R., Ranganathan, P. V. & Ramesh, G. Intracellular kinases mediate increased translation and secretion of netrin-1 from renal tubular epithelial cells. *PLoS One* **6**, e26776 (2011).

161. Jiang, M. *et al.* Autophagy in proximal tubules protects against acute kidney injury. *Elsevier*.

162. Kelly, K. J., Plotkin, Z. & Dagher, P. C. Guanosine supplementation reduces apoptosis and protects renal function in the setting of ischemic injury. *J. Clin. Invest.* **108**, 1291–1298 (2001).

163. Kim, H. J. *et al.* Reverse signaling through the costimulatory ligand CD137L in epithelial cells is essential for natural killer cell-mediated acute tissue inflammation. *Proc. Natl. Acad. Sci. U. S. A.* **109**, E13-22 (2012).

164. Krishnamoorthy, A. *et al.* Fibrinogen β-derived Bβ15-42 peptide protects against kidney ischemia/reperfusion injury. *Blood* **118**, 1934–1942 (2011).

165. Lee, T. *et al.* Articles in PresS. *Am J Physiol Ren. Physiol* **303**, (2012).

166. Li, L. *et al.* IL-17 produced by neutrophils regulates IFN-γ-mediated neutrophil migration in mouse kidney ischemia-reperfusion injury. *J. Clin. Invest.* **120**, 331–342 (2010).

167. Li, S. *et al.* Transgenic expression of proximal tubule peroxisome proliferator-activated receptor-α in mice confers protection during acute kidney injury. *Kidney Int.* **76**, 1049–1062 (2009).

168. Li, X. *et al.* Acute renal venous obstruction is more detrimental to the kidney than arterialocclusion: Implication for murine models of acute kidney injury. *Am. J. Physiol. - Ren. Physiol.* **302**, (2012).

169. Linkermann, A. *et al.* Rip1 (Receptor-interacting protein kinase 1) mediates necroptosis and contributes to renal ischemia/reperfusion injury. *Kidney Int.* **81**, 751–761 (2012).

170. Megyesi, J., Andrade, L., Vieira, J. M., Safirstein, R. L. & Price, P. M. Coordination of the cell cycle is an important determinant of the syndrome of acute renal failure. *Am. J. Physiol. - Ren. Physiol.* **283**, (2002).

171. Nath, K. A., Croatt, A. J., Warner, G. M. & Grande, J. P. Genetic deficiency of Smad3 protects against murine ischemic acute kidney injury. *Am. J. Physiol. - Ren. Physiol.* **301**, (2011).

172. Ongeri, E. M., Anyanwu, O., Reeves, W. B. & Bond, J. S. Villin and actin in the mouse kidney brush-border membrane bind to and are degraded by meprins, an interaction that contributes to injury in ischemia-reperfusion. *Am. J. Physiol. - Ren. Physiol.* **301**, (2011).

173. Park, J. S., Pasupulati, R., Feldkamp, T., Roeser, N. F. & Weinberg, J. M. Cyclophilin d and the mitochondrial permeability transition in kidney proximal tubules after hypoxic and ischemic injury. *Am. J. Physiol. - Ren. Physiol.* **301**, (2011).

174. Park, K. M. *et al.* Exocyst Sec10 protects epithelial barrier integrity and enhances recovery following oxidative stress, by activation of the MAPK pathway. *Am. J. Physiol. - Ren. Physiol.* **298**, (2010).

175. Peng, Q. *et al.* C3a and C5a Promote Renal Ischemia-Reperfusion Injury. *J Am Soc Nephrol* **23**, 1474–1485 (2012).

176. Renner, B., Ferreira, V., Cortes, C., international, R. G.-K. & 2011, undefined. Binding of factor H to tubular epithelial cells limits interstitial complement activation in ischemic injury. *Elsevier*.

177. Schley, G. *et al.* Hypoxia-Inducible Transcription Factors Stabilization in the Thick Ascending Limb Protects against Ischemic Acute Kidney Injury. *J Am Soc Nephrol* **22**, (2004).

178. Singaravelu, K. & Padanilam, B. J. p53 target siva regulates apoptosis in ischemic kidneys. *Am. J. Physiol. - Ren. Physiol.* **300**, 1130–1141 (2011).

179. Song, J. *et al.* Characterization and Fate of Telomerase-expressing Epithelia during Kidney Repair. *J Am Soc Nephrol* **22**, 2256–2265 (2011).

180. White, L. *et al.* Lung endothelial cell apoptosis during ischemic acute kidney injury. *journals.lww.com.*

181. Xu, X. *et al.* Delayed ischemic preconditioning contributes to renal protection by upregulation of miR-21. *Elsevier.*

182. Yasuda, K. *et al.* Functional consequences of inhibiting exocytosis of Weibel-Palade bodies in acute renal ischemia. *Am. J. Physiol. - Ren. Physiol.* **302**, (2012).

183. Yu, W. *et al.* H 2 O 2 activates G protein, α 12 to disrupt the junctional complex and enhance ischemia reperfusion injury. *Natl. Acad Sci.* doi:10.1073/pnas.1116800109.

184. Zager, R. A., Vijayan, A. & Johnson, A. C. M. Proximal tubule haptoglobin gene activation is an integral component of the acute kidney injury 'stress response'. *Am. J. Physiol. - Ren. Physiol.* **303**, (2012).

185. Zhou, D. *et al.* Tubule-specific ablation of endogenous β-catenin aggravates acute kidney injury in mice. *Elsevier.*

186. Grist, J. T., Mariager, C. Ø., Qi, H., Nielsen, P. M. & Laustsen, C. Detection of acute kidney injury with hyperpolarized [13C, 15N]Urea and multiexponential relaxation modeling. *Magn. Reson. Med.* (2019) doi:10.1002/mrm.28134.

187. Taylor, A. *et al.* Multimodal Imaging Techniques Show Differences in Homing Capacity Between Mesenchymal Stromal Cells and Macrophages in Mouse Renal Injury Models. *Mol. Imaging Biol.* (2019) doi:10.1007/s11307-019-01458-8.

188. Menshikh, A. *et al.* Capillary rarefaction is more closely associated with CKD progression after cisplatin, rhabdomyolysis, and ischemia-reperfusion-induced AKI than renal fibrosis. *Am. J. Physiol. Renal Physiol.* **317**, F1383–F1397 (2019).

189. Nensén, O., Hansell, P. & Palm, F. Role of carbonic anhydrase in acute recovery following renal ischemia reperfusion injury. *PLoS One* **14**, (2019).

190. Sedaghat, Z., Fatemikia, H., Tanha, K., Zahiri, M. & Assadi, M. Scintigraphic evaluation of remote pre-conditioning protection against unilateral renal ischemia/reperfusion injury in rats: a longitudinal study. *Int. Urol. Nephrol.* **51**, 2083–2089 (2019).

191. Perry, H. M. *et al.* Perivascular CD73+ cells attenuate inflammation and interstitial fibrosis in the kidney microenvironment. *Am. J. Physiol. Renal Physiol.* **317**, F658–F669 (2019).

192. Chen, Y. *et al.* Determinants of preferential renal accumulation of synthetic polymers in acute kidney injury. *Int. J. Pharm.* **568**, 118555 (2019).

193. Soranno, D. E. *et al.* Matching human unilateral AKI, a reverse translational approach to investigate kidney recovery after ischemia. *J. Am. Soc. Nephrol.* **30**, 990–1005 (2019).

194. Alikhan, M. A. *et al.* Colony-stimulating factor-1 promotes kidney growth and repair via alteration of macrophage responses. *Am. J. Pathol.* **179**, 1243–1256 (2011).

195. Braun, H. *et al.* Cellular senescence limits regenerative capacity and allograft survival. *J. Am. Soc. Nephrol.* **23**, 1467–1473 (2012).

196. Chen, J. *et al.* Early interleukin 6 production by leukocytes during ischemic acute kidney injury is regulated by TLR4. *Kidney Int.* **80**, 504–515 (2011).

197. Ferenbach, D. A. *et al.* Macrophage/monocyte depletion by clodronate, but not diphtheria toxin, improves renal ischemia/reperfusion injury in mice. *Kidney Int.* **82**, 928–933 (2012).

198. Gall, J. M. *et al.* Hexokinase regulates Bax-mediated mitochondrial membrane injury following ischemic stress. *Kidney Int.* **79**, 1207–1216 (2011).

199. J.G., G. *et al.* Identification of a microRNA signature of renal ischemia reperfusion injury. *Proc. Natl. Acad. Sci. U. S. A.* **107**, 14339–14344 (2010).

200. Ko, G. J. *et al.* Transcriptional analysis of infiltrating T cells in kidney ischemia-reperfusion injury reveals a pathophysiological role for CCR5. *Am. J. Physiol. - Ren. Physiol.* **302**, (2012).

201. Lan, R. *et al.* PTEN loss defines a TGF-(β-induced tubule phenotype of failed differentiation and JNK signaling during renal fibrosis. *Am. J. Physiol. - Ren. Physiol.* **302**, (2012).

202. Lee, D. H., Wolstein, J. M., Pudasaini, B. & Plotkin, M. INK4a deletion results in improved kidney regeneration and decreased capillary rarefaction after ischemia-reperfusion injury. *Am. J. Physiol. - Ren. Physiol.* **302**, 183–191 (2012).

203. Brooks, C., Wei, Q., Cho, S. G. & Dong, Z. Regulation of mitochondrial dynamics in acute kidney injury in cell culture and rodent models. *J. Clin. Invest.* **119**, 1275–1285 (2009).

204. Brown, W. C. *et al.* Renin and acute circulatory renal failure in the rabbit. *Circ. Res.* **30**, 114–22 (1972).

205. Duffield, J. S. & Bonventre, J. V. Kidney tubular epithelium is restored without replacement with bone marrow-derived cells during repair after ischemic injury. in *Kidney International* vol. 68 1956–1961 (2005).

206. Becker, G. J. & Hewitson, T. D. Animal models of chronic kidney disease: useful but not perfect. *Nephrol Dial Transpl.* **28**, 2432–2438 (2013).

207. Wei, Q. & Dong, Z. Mouse model of ischemic acute kidney injury: technical notes and tricks. *Am. J. Physiol. Physiol.* **303**, F1487–F1494 (2012).

208. Hauet, T. *et al.* Contribution of large pig for renal ischemia-reperfusion and transplantation studies: The preclinical model. *J. Biomed. Biotechnol.* **2011**, (2011).

209. Hannon, J. P., Bossone, C. A. & Wade, C. E. Normal physiological values for conscious pigs used in biomedical research. *Lab. Anim. Sci.* **40**, 293–298 (1990).

210. Schwalb, D. *et al.* The Minipig as a Practical Endourologic Model. *J. Endourol.* **3**, 85–90 (1989).

211. Schook, L. B. *et al.* Swine Genome Sequencing Consortium (SGSC): A strategic roadmap for sequencing the pig genome. in *Comparative and Functional Genomics* vol. 6 251–255 (2005).

212. Gregory, S. G. *et al.* A physical map of the mouse genome. *Nature* **418**, 743–750 (2002).

213. Hsieh, J. J. *et al.* Renal cell carcinoma. *Nat. Rev. Dis. Prim.* **3**, 17009 (2017).

214. Chow, W. H., Dong, L. M. & Devesa, S. S. Epidemiology and risk factors for kidney cancer. *Nature Reviews Urology* vol. 7 245–257 (2010).

215. Nabi, S., Kessler, E. R., Bernard, B., Flaig, T. W. & Lam, E. T. Renal cell carcinoma: a review of biology and pathophysiology. *F1000Research* **7**, 307 (2018).

216. Siegel, R. L., Miller, K. D. & Jemal, A. Cancer statistics, 2017. *CA. Cancer J. Clin.* **67**, 7–30 (2017).

217. Thompson, R. H. *et al.* Renal Cell Carcinoma in Young and Old Patients-Is There a

Difference? *J. Urol.* **180**, 1262–1266 (2008).

218. Siegel, R., Naishadham, D. & Jemal, A. Cancer statistics, 2012. *CA. Cancer J. Clin.* **62**, 10–29 (2012).

219. Tanoue, L. T. Cancer Statistics, 2011: The Impact of Eliminating Socioeconomic and Racial Disparities on Premature Cancer Deaths. *Yearb. Pulm. Dis.* **2012**, 62–64 (2012).

220. Silverberg, E. & Lubera, J. Cancer Statistics, 1987. *CA. Cancer J. Clin.* **37**, 2–19 (1987).

221. Russo, P. Renal cell carcinoma: Presentation, staging, and surgical treatment. *Seminars in Oncology* vol. 27 160–176 (2000).

222. Motzer, R. J. & Basch, E. Targeted drugs for metastatic renal cell carcinoma. *Lancet* vol. 370 2071–2073 (2007).

223. Motzer, R. J. *et al.* Kidney Cancer, Version 2.2017: Clinical practice guidelines in oncology. *JNCCN Journal of the National Comprehensive Cancer Network* vol. 15 804–834 (2017).

224. Kaelin, W. G. Molecular basis of the VHL hereditary cancer syndrome. *Nature Reviews Cancer* vol. 2 673–682 (2002).

225. Barry, R. E. & Krek, W. The von Hippel-Lindau tumour suppressor: A multi-faceted inhibitor of tumourigenesis. *Trends in Molecular Medicine* vol. 10 466–472 (2004).

226. Kim, W. Y. & Kaelin, W. G. Role of VHL gene mutation in human cancer. *Journal of Clinical Oncology* vol. 22 4991–5004 (2004).

227. Pugh, C. W. & Ratcliffe, P. J. Regulation of angiogenesis by hypoxia: Role of the HIF system. *Nature Medicine* vol. 9 677–684 (2003).

228. Maxwell, P. H., Pugh, C. W. & Ratcliffe, P. J. Activation of the HIF pathway in cancer. *Current Opinion in Genetics and Development* vol. 11 293–299 (2001).

229. Han, W. K., Bailly, V., Abichandani, R., Thadhani, R. & Bonventre, J. V. Kidney Injury Molecule-1 (KIM-1): A novel biomarker for human renal proximal tubule injury. *Kidney Int.* **62**, 237–244 (2002).

230. Bailly, V. *et al.* Shedding of kidney injury molecule-1, a putative adhesion protein involved in renal regeneration. *J. Biol. Chem.* **277**, 39739–39748 (2002).

231. Lim, A. I., Tang, S. C. W., Lai, K. N. & Leung, J. C. K. Kidney injury molecule-1: More than just an injury marker of tubular epithelial cells? *J. Cell. Physiol.* **228**, 917–924 (2013).

232. Vilà, M. R. *et al.* Hepatitis A virus receptor blocks cell differentiation and is overexpressed in clear cell renal cell carcinoma. in *Kidney International* vol. 65 1761–1773 (Blackwell Publishing Inc., 2004).

233. Cuadros, T. *et al.* Hepatitis A virus cellular receptor 1/kidney injury molecule-1 is a susceptibility gene for clear cell renal cell carcinoma and hepatitis A virus cellular receptor/kidney injury molecule-1 ectodomain shedding a predictive biomarker of tumour progression. *Eur. J. Cancer* **49**, 2034–2047 (2013).

234. Cuadros, T. *et al.* Molecular and cellular pathobiology HAVCR/KIM-1 activates the IL-6/STAT-3 pathway in clear cell renal cell carcinoma and determines tumor progression and patient outcome. *Cancer Res.* **74**, 1416–1428 (2014).

235. Vaidya, V. S., Ferguson, M. A. & Bonventre, J. V. Biomarkers of Acute Kidney. *Annu. Rev. Pharmacol. Toxicol.* 1–29 (2009) doi:10.1146/annurev.pharmtox.48.113006.094615.Biomarkers.

236. Irizarry, R. A. *et al.* Exploration, normalization, and summaries of high density oligonucleotide array probe level data. *Biostatistics* **4**, 249–264 (2003).

237. Smyth, G. K. Linear models and empirical bayes methods for assessing differential expression in microarray experiments. *Stat. Appl. Genet. Mol. Biol.* **3**, (2004).

238. Benjamini, Y. & Hochberg, Y. Benjamini-1995.pdf. *Journal of the Royal Statistical Society B* vol. 57 289–300 (1995).

239. Reimand, J. *et al.* Pathway enrichment analysis and visualization of omics data using g:Profiler, GSEA, Cytoscape and EnrichmentMap. *Nat. Protoc.* **14**, 482–517 (2019).

240. Subramanian, A. *et al.* Gene set enrichment analysis: A knowledge-based approach for interpreting genome-wide expression profiles. *Proc. Natl. Acad. Sci. U. S. A.* **102**, 15545–15550 (2005).

241. Merico, D., Isserlin, R., Stueker, O., Emili, A. & Bader, G. D. Enrichment map: A network-based method for gene-set enrichment visualization and interpretation. *PLoS One* **5**, (2010).

242. Bindea, G. *et al.* ClueGO: a Cytoscape plug-in to decipher functionally grouped gene ontology and pathway annotation networks. *Bioinforma. Appl. NOTE* **25**, 1091–1093 (2009).

243. Maere, S., Heymans, K. & Kuiper, M. BiNGO: a Cytoscape plugin to assess overrepresentation of Gene Ontology categories in Biological Networks. *Bioinforma. Appl. NOTE* **21**, 3448–3449 (2005).

244. Eden, E., Navon, R., Steinfeld, I., Lipson, D. & Yakhini, Z. GOrilla: A tool for discovery and visualization of enriched GO terms in ranked gene lists. *BMC Bioinformatics* **10**, (2009).

245. Wang, J., Duncan, D., Shi, Z. & Zhang, B. WEB-based GEne SeT AnaLysis Toolkit (WebGestalt): update 2013. doi:10.1093/nar/gkt439.

246. Shannon, P. *et al.* Cytoscape: A software Environment for integrated models of biomolecular interaction networks. *Genome Res.* **13**, 2498–2504 (2003).

247. Morris, J. H. *et al.* ClusterMaker: A multi-algorithm clustering plugin for Cytoscape. *BMC Bioinformatics* **12**, (2011).

248. Oesper, L., Merico, D., Isserlin, R. & Bader, G. D. WordCloud: A Cytoscape plugin to create a visual semantic summary of networks. *Source Code Biol. Med.* **6**, (2011).

249. Assenov, Y., Ramírez, F., Schelhorn, S.-E., Lengauer, T. & Albrecht, M. Computing topological parameters of biological networks. *Bioinforma. Appl.* **24**, 282–284 (2008).

250. Kucera, M., Isserlin, R., Arkhangorodsky, A. & Bader, G. D. AutoAnnotate: A Cytoscape app for summarizing networks with semantic annotations [version 1; referees: 2 approved]. *F1000Research* **5**, (2016).

251. Babicki, S. *et al.* Heatmapper: web-enabled heat mapping for all. *Nucleic Acids Res.* **44**, 147–153 (2016).

252. Olsen, J. R. *et al.* Context dependent regulatory patterns of the androgen receptor and androgen receptor target genes. *BMC Cancer* **16**, 1–15 (2016).

253. Campeau, E. *et al.* A versatile viral system for expression and depletion of proteins in mammalian cells. *PLoS One* **4**, (2009).

254. Liu, J. *et al.* Molecular characterization of the transition from acute to chronic kidney injury following ischemia/reperfusion. *JCI insight* **2**, 1–18 (2017).

255. Si, H. *et al.* Human and murine kidneys show gender- And species-specific gene expression differences in response to injury. *PLoS One* **4**, 1–12 (2009).

256. De Sousa Abreu, R., Penalva, L. O., Marcotte, E. M. & Vogel, C. Global signatures of protein and mRNA expression levels. *Molecular BioSystems* vol. 5 1512–1526 (2009).

257. Vogel, C. & Marcotte, E. M. Insights into the regulation of protein abundance from proteomic and transcriptomic analyses. *Nat. Rev. Genet.* **13**, 227–232 (2012).

258. Maier, T., Güell, M. & Serrano, L. Correlation of mRNA and protein in complex biological samples. *FEBS Letters* vol. 583 3966–3973 (2009).

259. Kawamoto, S., Matsumoto, Y., Mizuno, K., Okubo, K. & Matsubara, K. Expression profiles of active genes in human and mouse livers. *Gene* **174**, 151–158 (1996).

260. De Godoy, L. M. F. *et al.* Comprehensive mass-spectrometry-based proteome quantification of haploid versus diploid yeast. *Nature* **455**, 1251–1254 (2008).

261. Ly, T. *et al.* A proteomic chronology of gene expression through the cell cycle in human myeloid leukemia cells. *Elife* **2014**, (2014).

262. Greenbaum, D., Colangelo, C., Williams, K. & Gerstein, M. Comparing protein abundance and mRNA expression levels on a genomic scale. *Genome Biology* vol. 4 (2003).

263. Jayapal, K. P. *et al.* Uncovering Genes with Divergent mRNA-Protein Dynamics in Streptomyces coelicolor. *PLoS One* **3**, e2097 (2008).

264. Maier, T. *et al.* Quantification of mRNA and protein and integration with protein turnover in a bacterium. *Mol. Syst. Biol.* **7**, 511 (2011).

265. Ideker, T. *et al.* Integrated genomic and proteomic analyses of a systematically perturbed metabolic network. *Science (80-.).* **292**, 929–934 (2001).

266. Tian, Q. *et al.* Integrated genomic and proteomic analyses of gene expression in mammalian cells. *Mol. Cell. Proteomics* **3**, 960–969 (2004).

267. Fournier, M. L. *et al.* Delayed correlation of mRNA and protein expression in rapamycin-treated cells and a role for Ggc1 in cellular sensitivity to rapamycin. *Mol. Cell. Proteomics* **9**, 271–284 (2010).

268. Chen, G. *et al.* Discordant protein and mRNA expression in lung adenocarcinomas. *Mol. Cell. Proteomics* **1**, 304–313 (2002).

269. Chen, G. *et al.* Proteomic analysis of lung adenocarcinoma: Identification of a highly expressed set of proteins in tumors. *Clin. Cancer Res.* **8**, 2298–2305 (2002).

270. Fessler, M. B., Malcolm, K. C., Duncan, M. W. & Scott Worthen, G. A genomic and proteomic analysis of activation of the human neutrophil by lipopolysaccharide and its mediation by p38 mitogen-activated protein kinase. *J. Biol. Chem.* **277**, 31291–31302 (2002).

271. SM, H. *et al.* Integrating cancer genomics and proteomics in the post-genome era. *Proteomics* **2**, 69–75 (2002).

272. Lichtinghagen, R. *et al.* Different mRNA and protein expression of matrix metalloproteinases 2 and 9 and tissue inhibitor of metalloproteinases 1 in benign and malignant prostate tissue. *Eur. Urol.* **42**, 398–406 (2002).

273. Huber, M. *et al.* Comparison of proteomic and genomic analyses of the human breast cancer cell line T47D and the antiestrogen-resistant derivative T47D-r. *Molecular and Cellular Proteomics* vol. 3 43–55 (2004).

274. Shankavaram, U. T. *et al.* Transcript and protein expression profiles of the NCI-60 cancer cell panel: An integromic microarray study. *Mol. Cancer Ther.* **6**, 820–832 (2007).

275. Pascal, L. E. *et al.* Correlation of mRNA and protein levels: Cell type-specific gene expression of cluster designation antigens in the prostate. *BMC Genomics* **9**, (2008).

276. Koussounadis, A., Langdon, S. P., Um, I. H., Harrison, D. J. & Smith, V. A. Relationship between differentially expressed mRNA and mRNA-protein correlations in a xenograft model system. *Sci. Rep.* **5**, 1–9 (2015).

277. Joffe, M. *et al.* Variability of Creatinine Measurements in Clinical Laboratories: Results from the CRIC Study. *Am. J. Nephrol.* **31**, 426–434 (2010).

278. Hsu, C. Y., Chertow, G. M. & Curhan, G. C. Methodological issues in studying the epidemiology of mild to moderate chronic renal insufficiency. *Kidney Int.* **61**, 1567–1576 (2002).

279. Ross, J. W., Miller, W. G., Myers, G. L. & Praestgaard, J. The accuracy of laboratory measurements in clinical chemistry: a study of 11 routine chemistry analytes in the College of American Pathologists Chemistry Survey with fresh frozen serum, definitive methods, and reference methods. *undefined* (1998).

280. WG, M. *et al.* Creatinine Measurement: State of the Art in Accuracy and Interlaboratory Harmonization. *Arch. Pathol. Lab. Med.* **129**, (2005).

281. Verhave, J. C., Fesler, P., Ribstein, J., Du Cailar, G. & Mimran, A. Estimation of renal function in subjects with normal serum creatinine levels: Influence of age and body mass index. *Am. J. Kidney Dis.* **46**, 233–241 (2005).

282. Coresh, J. *et al.* Calibration and random variation of the serum creatinine assay as critical elements of using equations to estimate glomerular filtration rate. *Am. J. Kidney Dis.* **39**, 920–929 (2002).

283. Kazancioğlu, R. Risk factors for chronic kidney disease: An update. *Kidney Int. Suppl.* **3**, 368–371 (2013).

284. Meseguer, A., Watson, C. S. & Catterall, J. F. Nucleotide sequence of kidney androgen-regulated protein mRNA and its cell-specific expression in Tfm/Y mice. *Mol. Endocrinol.* **3**, 962–7 (1989).

285. Meseguer, A. & Catterall, J. F. Cell-specific expression of kidney androgen-regulated protein messenger RNA is under multihormonal control. *Mol. Endocrinol.* **4**, 1240–8 (1990).

286. Meseguer, A. & Catterall, J. F. Effects of pituitary hormones on the cell-specific expression of the KAP gene. *Mol. Cell. Endocrinol.* **89**, 153–162 (1992).

287. Solé, E., Calvo, R., Obregón, M. J. & Meseguer, A. Thyroid hormone controls the cell-specific expression of the kidney androgen-regulated protein gene in S3 mouse kidney cells. *Endocrinology* **135**, 2120–9 (1994).

288. Solé, E., Calvo, R., Obregón, M. J. & Meseguer, A. Effects of thyroid hormone on the androgenic expression of KAP gene in mouse kidney. *Mol. Cell. Endocrinol.* **119**, 147–159 (1996).

289. Teixido, N., Soler, M., Rivera, N., Bernués, J. & Meseguer, A. CCAAT/enhancer binding protein-mediated role of thyroid hormone in the developmental expression of the kidney androgen-regulated protein gene in proximal convoluted tubules. *Mol. Endocrinol.* **20**, 389–404 (2006).

290. Ouar, Z. *et al.* Pleiotropic effects of dihydrotestosterone in immortalized mouse proximal tubule cells. *Kidney Int.* **53**, 59–66 (1998).

291. Soler, M. *et al.* Hormone-specific regulation of the kidney androgen-regulated gene promoter in cultured mouse renal proximal-tubule cells. *Biochem. J.* **366**, 757–766 (2002).

292. Tornavaca, O. *et al.* Kidney androgen-regulated protein transgenic mice show hypertension and renal alterations mediated by oxidative stress. *Circulation* **119**, 1908–1917 (2009).

293. Grande, M. T. *et al.* Increased oxidative stress, the renin-angiotensin system, and sympathetic overactivation induce hypertension in kidney androgen-regulated protein transgenic mice. *Free Radic. Biol. Med.* **51**, 1831–1841 (2011).

294. Baltatu, O. *et al.* Abolition of hypertension-induced end-organ damage by androgen

receptor blockade in transgenic rats harboring the mouse Ren-2 gene. *J. Am. Soc. Nephrol.* **13**, 2681–2687 (2002).

295. Reckelhoff, J. F., Zhang, H. & Srivastava, K. Gender differences in development of hypertension in spontaneously hypertensive rats: Role of the renin-angiotensin system. in *Hypertension* vol. 35 480–483 (2000).

296. Iliescu, R., Cucchiarelli, V. E., Yanes, L. L., Iles, J. W. & Reckelhoff, J. F. Impact of androgen-induced oxidative stress on hypertension in male SHR. *Am. J. Physiol. - Regul. Integr. Comp. Physiol.* **292**, (2007).

297. Capdevila, J. H. Regulation of ion transport and blood pressure by cytochrome p450 monooxygenases. *Current Opinion in Nephrology and Hypertension* vol. 16 465–470 (2007).

298. De Quixano, B. B. *et al.* Kidney Androgen-Regulated Protein (KAP) Transgenic Mice Are Protected Against High-Fat Diet Induced Metabolic Syndrome. *Sci. Rep.* **7**, 1–13 (2017).

299. Aufhauser, D. D. *et al.* Improved renal ischemia tolerance in females influences kidney transplantation outcomes. *J. Clin. Invest.* **126**, 1968–1977 (2016).

300. Kher, A. *et al.* Cellular and molecular mechanisms of sex differences in renal ischemia-reperfusion injury. *Cardiovasc. Res.* **67**, 594–603 (2005).

301. Sun, P. *et al.* Human endometrial regenerative cells attenuate renal ischemia reperfusion injury in mice. *J Transl Med* **14**, 28 (2016).

302. Lima-Posada, I. *et al.* Gender Differences in the Acute Kidney Injury to Chronic Kidney Disease Transition. *Sci. Rep.* **7**, 1–13 (2017).

303. Choi, E. K. *et al.* Inhibition of Oxidative Stress in Renal Ischemia-Reperfusion Injury. *Anesth. Analg.* **124**, 204–213 (2017).

304. Feitoza, C. Q. *et al.* Inhibition of COX 1 and 2 prior to renal ischemia/reperfusion injury decreases the development of fibrosis. *Mol. Med.* **14**, 724–730 (2008).

305. Chen, C. C. *et al.* Androgen receptor promotes the migration and invasion of upper urinary tract urothelial carcinoma cells through the upregulation of MMP-9 and COX-2. *Oncol. Rep.* **30**, 979–985 (2013).

306. Yazawa, T. *et al.* Androgen/androgen receptor pathway regulates expression of the genes for cyclooxygenase-2 and amphiregulin in periovulatory granulosa cells. *Mol. Cell. Endocrinol.* **369**, 42–51 (2013).

307. Patrignani, P. & Dovizio, M. COX-2 and EGFR: Partners in Crime Split by Aspirin. *EBioMedicine* vol. 2 372–373 (2015).

308. Hu, H. *et al.* Elevated COX-2 Expression Promotes Angiogenesis Through EGFR/p38-MAPK/Sp1-Dependent Signalling in Pancreatic Cancer. *Sci. Rep.* **7**, (2017).

309. Xiong, H. *et al.* A positive feedback loop between STAT3 and cyclooxygenase-2 gene may contribute to Helicobacter pylori-associated human gastric tumorigenesis. *Int. J. Cancer* **134**, 2030–2040 (2014).

310. Karve, T. M. & Rosen, E. M. B-cell translocation gene 2 (BTG2) stimulates cellular antioxidant defenses through the antioxidant transcription factor NFE2L2 in human mammary epithelial cells. *J. Biol. Chem.* **287**, 31503–31514 (2012).

311. Jalava, S. E. *et al.* Androgen-regulated miR-32 targets BTG2 and is overexpressed in castration-resistant prostate cancer. *Oncogene* **31**, 4460–4471 (2012).

312. Yoshida, T. *et al.* ATF3 protects against renal ischemia-reperfusion injury. *J. Am. Soc. Nephrol.* **19**, 217–224 (2008).

313. Kang, Y., Chen, C.-R. & Massagué, J. A self-enabling TGFbeta response coupled to stress signaling: Smad engages stress response factor ATF3 for Id1 repression in

epithelial cells. *Mol. Cell* **11**, 915–26 (2003).

314. Han, S. J., Kim, J. H., Kim, J. I. & Park, K. M. Inhibition of microtubule dynamics impedes repair of kidney ischemia/reperfusion injury and increases fibrosis. *Sci. Rep.* **6**, 1–13 (2016).

315. Chang-Panesso, M. & Humphreys, B. D. Cellular plasticity in kidney injury and repair. *Nature Reviews Nephrology* vol. 13 39–46 (2017).

316. Tavafi, M. Suggestions for attenuation of renal ischemia reperfusion injury based on mechanisms involved in epithelial cells damages. *J. nephropharmacology* **4**, 1–3 (2015).

317. Devarajan, P. Update on mechanisms of ischemic acute kidney injury. *Journal of the American Society of Nephrology* vol. 17 1503–1520 (2006).

318. Ling, L. & Lobie, P. E. RhoA/ROCK activation by growth hormone abrogates p300/histone deacetylase 6 repression of Stat5-mediated transcription. *J. Biol. Chem.* **279**, 32737–32750 (2004).

319. Tripathi, B. K. & Zelenka, P. S. Cdk5-Dependent Regulation of Rho Activity, Cytoskeletal Contraction, and Epithelial Cell Migration via Suppression of Src and p190RhoGAP. *Mol. Cell. Biol.* **29**, 6488–6499 (2009).

320. Gao, S. Y. *et al.* Sp1 and AP-1 regulate expression of the human gene VIL2 in esophageal carcinoma cells. *J. Biol. Chem.* **284**, 7995–8004 (2009).

321. Piek, E. *et al.* Functional Characterization of Transforming Growth Factor β Signaling in Smad2- and Smad3-deficient Fibroblasts. *J. Biol. Chem.* **276**, 19945–19953 (2001).

322. Yu, X. *et al.* Androgen receptor signaling regulates growth of glioblastoma multiforme in men. *Tumor Biol.* **36**, 967–972 (2015).

323. Chipuk, J. E. *et al.* The androgen receptor represses transforming growth factor-β signaling through interaction with Smad3. *J. Biol. Chem.* **277**, 1240–1248 (2002).

324. Katoh, D. *et al.* Binding of αvβ1 and αvβ6 integrins to tenascin-C induces epithelial-mesenchymal transition-like change of breast cancer cells. *Oncogenesis* **2**, e65–e65 (2013).

325. Jinnin, M. *et al.* Tenascin-C upregulation by transforming growth factor-β in human dermal fibroblasts involves Smad3, Sp1, and Ets1. *Oncogene* **23**, 1656–1667 (2004).

326. Jiang, Y. S., Jiang, T., Huang, B., Chen, P. S. & Ouyang, J. Epithelial-mesenchymal transition of renal tubules: Divergent processes of repairing in acute or chronic injury? *Med. Hypotheses* **81**, 73–75 (2013).

327. Curci, C. *et al.* Endothelial-to-mesenchymal transition and renal fibrosis in ischaemia/reperfusion injury are mediated by complement anaphylatoxins and Akt pathway. *Nephrol. Dial. Transplant* **29**, 799–808 (2014).

328. Wang, Q. *et al.* Cooperative interaction of CTGF and TGF-β in animal models of fibrotic disease. *Fibrogenes. Tissue Repair* **4**, 4 (2011).

329. Yeh, Y. C. *et al.* Transforming growth factor-β1 induces Smad3-dependent β1 integrin gene expression in epithelial-to-mesenchymal transition during chronic tubulointerstitial fibrosis. *Am. J. Pathol.* **177**, 1743–1754 (2010).

330. Zeng, R. *et al.* Role of Sema4C in TGF-β1-induced mitogen-activated protein kinase activation and epithelial-mesenchymal transition in renal tubular epithelial cells. *Nephrol. Dial. Transplant* **26**, 1149–56 (2011).

331. Matsuda, T. *et al.* Cross-talk between signal transducer and activator of transcription 3 and androgen receptor signaling in prostate carcinoma cells. *Biochem. Biophys. Res. Commun.* **283**, 179–187 (2001).

332. Hawthorne, V. S. *et al.* ErbB2-mediated Src and signal transducer and activator of

transcription 3 activation leads to transcriptional up-regulation of p21Cip1 and chemoresistance in breast cancer cells. *Mol. Cancer Res.* **7**, 592–600 (2009).

333. Schreiner, S. J., Schiavone, A. P. & Smithgall, T. E. Activation of STAT3 by the Src family kinase Hck requires a functional SH3 domain. *J. Biol. Chem.* **277**, 45680–45687 (2002).

334. Li, C. *et al.* Noncanonical STAT3 Activation Regulates Excess TGF-β1 and Collagen I Expression in Muscle of Stricturing Crohn's Disease. *J. Immunol.* **194**, 3422–3431 (2015).

335. Salvadori, M., Rosso, G. & Bertoni, E. Update on ischemia-reperfusion injury in kidney transplantation: Pathogenesis and treatment. *World J. Transplant.* **5**, 52 (2015).

336. Maeda, M., Johnson, K. R. & Wheelock, M. J. Cadherin switching: Essential for behavioral but not morphological changes during an epithelium-to-mesenchyme transition. *J. Cell Sci.* **118**, 873–887 (2005).

337. Cottard, F. *et al.* Constitutively Active Androgen Receptor Variants Upregulate Expression of Mesenchymal Markers in Prostate Cancer Cells. *PLoS One* **8**, e63466 (2013).

338. Lu, Q. *et al.* Quercetin inhibits the mTORC1/p70S6K signaling-mediated renal tubular epithelial-mesenchymal transition and renal fibrosis in diabetic nephropathy. *Pharmacol. Res.* **99**, 237–247 (2015).

339. Van Roy, F. & Berx, G. The cell-cell adhesion molecule E-cadherin. *Cellular and Molecular Life Sciences* vol. 65 3756–3788 (2008).

340. Liu, Y.-N., Liu, Y., Lee, H.-J., Hsu, Y.-H. & Chen, J.-H. Activated Androgen Receptor Downregulates E-Cadherin Gene Expression and Promotes Tumor Metastasis. *Mol. Cell. Biol.* **28**, 7096–7108 (2008).

341. Liu, X., Su, L. & Liu, X. Loss of CDH1 up-regulates epidermal growth factor receptor via phosphorylation of YBX1 in non-small cell lung cancer cells. *FEBS Lett.* **587**, 3995–4000 (2013).

342. Xiong, H. *et al.* Roles of STAT3 and ZEB1 proteins in E-cadherin down-regulation and human colorectal cancer epithelial-mesenchymal transition. *J. Biol. Chem.* **287**, 5819–5832 (2012).

343. Xiong, H. *et al.* Inhibition of JAK1, 2/STAT3 signaling induces apoptosis, cell cycle arrest, and reduces tumor cell invasion in colorectal cancer cells. *Neoplasia* **10**, 287–297 (2008).

344. Lopes, N. *et al.* 1Alpha,25-dihydroxyvitamin D 3 induces de novo E-cadherin expression in triple-negative breast cancer cells by CDH1-promoter demethylation. in *Anticancer Research* vol. 32 249–257 (2012).

345. Slegtenhorst, B. R., Dor, F. J. M. F., Rodriguez, H., Voskuil, F. J. & Tullius, S. G. Ischemia/Reperfusion Injury and its Consequences on Immunity and Inflammation. *Curr. Transplant. Reports* **1**, 147–154 (2014).

346. Kezić, A., Stajic, N. & Thaiss, F. Innate Immune Response in Kidney Ischemia/Reperfusion Injury: Potential Target for Therapy. (2017) doi:10.1155/2017/6305439.

347. Newman, P. J. The biology of PECAM-1. *Journal of Clinical Investigation* vol. 99 3–8 (1997).

348. Relou, I. A. M., Gorter, G., Andrade Ferreira, I., Van Rijn, H. J. M. & Akkerman, J. W. N. Platelet endothelial cell adhesion molecule-1 (PECAM-1) inhibits low density lipoprotein-induced signaling in platelets. *J. Biol. Chem.* **278**, 32638–32644 (2003).

349. Yu, J. *et al.* Src kinase-mediates androgen receptor-dependent non-genomic activation of signaling cascade leading to endothelial nitric oxide synthase. *Biochem. Biophys. Res.*

Commun. **424**, 538–543 (2012).

350. Zheng, Y., Izumi, K., Yao, J. L. & Miyamoto, H. Dihydrotestosterone upregulates the expression of epidermal growth factor receptor and ERBB2 in androgen receptor-positive bladder cancer cells. *Endocr. Relat. Cancer* **18**, 451–464 (2011).

351. Ni, M. *et al.* Targeting Androgen Receptor in Estrogen Receptor-Negative Breast Cancer. *Cancer Cell* **20**, 119–131 (2011).

352. Fan, W. Q. *et al.* Insulin-like growth factor 1/insulin signaling activates androgen signaling through direct interactions of Foxo1 with androgen receptor. *J. Biol. Chem.* **282**, 7329–7338 (2007).

353. Yang, L., Li, Y. & Zhang, Y. Identification of prolidase as a high affinity ligand of the ErbB2 receptor and its regulation of ErbB2 signaling and cell growth. *Cell Death Dis.* **5**, e1211 (2014).

354. Contessa, J. N., Abell, A., Mikkelsen, R. B., Valerie, K. & Schmidt-Ullrich, R. K. Compensatory ErbB3/c-Src signaling enhances carcinoma cell survival to ionizing radiation. *Breast Cancer Res. Treat.* **95**, 17–27 (2006).

355. Min, H.-Y. *et al.* Targeting the insulin-like growth factor receptor and Src signaling network for the treatment of non-small cell lung cancer. *Mol. Cancer* **14**, 113 (2015).

356. Li, L. & Okusa, M. D. Macrophages, dendritic cells, and kidney ischemia-reperfusion injury. *Semin. Nephrol.* **30**, 268–277 (2010).

357. Gynther, P. *et al.* Mechanism of 1α,25-dihydroxyvitamin D3-dependent repression of interleukin-12B. *Biochim. Biophys. Acta - Mol. Cell Res.* **1813**, 810–818 (2011).

358. Daniel, C. *et al.* The TGFβ/Smad 3-signaling pathway is involved in butyrate-mediated vitamin D receptor (VDR)-expression. *J. Cell. Biochem.* **102**, 1420–1431 (2007).

359. Lai, J. J. *et al.* Monocyte/macrophage androgen receptor suppresses cutaneous wound healing in mice by enhancing local TNF-α expression. *J. Clin. Invest.* **119**, 3739–3751 (2009).

360. Malek, M. & Nematbakhsh, M. Renal ischemia/reperfusion injury; from pathophysiology to treatment. *J. Ren. Inj. Prev.* **4**, 20–207 (2015).

361. Xia, Y. *et al.* Piperine inhibits IL-1β-induced IL-6 expression by suppressing p38 MAPK and STAT3 activation in gastric cancer cells. *Mol. Cell. Biochem.* **398**, 147–156 (2015).

362. Gao, W. *et al.* Hypoxia and STAT3 signalling interactions regulate pro-inflammatory pathways in rheumatoid arthritis. *Ann. Rheum. Dis.* **74**, 1275–1283 (2015).

363. Masood, R. *et al.* Kaposi sarcoma is a therapeutic target for vitamin D3 receptor agonist. *Blood* **96**, 3188–3194 (2000).

364. Yang, N. *et al.* Blockage of JAK/STAT signalling attenuates renal ischaemia-reperfusion injury in rat. *Nephrol. Dial. Transplant.* **23**, 91–100 (2008).

365. Matsuda, T. *et al.* Cross-talk between signal transducer and activator of transcription 3 and androgen receptor signaling in prostate carcinoma cells. *Biochem. Biophys. Res. Commun.* **283**, 179–187 (2001).

366. Lo, H. W. *et al.* Nuclear interaction of EGFR and STAT3 in the activation of the iNOS/NO pathway. *Cancer Cell* **7**, 575–589 (2005).

367. Jiang, Y.-Q., Zhou, Z.-X. & Ji, Y.-L. Suppression of EGFR-STAT3 signaling inhibits tumorigenesis in a lung cancer cell line. *Int. J. Clin. Exp. Med.* **7**, 2096–9 (2014).

368. Concha-Benavente, F., Srivastava, R. M., Ferrone, S. & Ferris, R. L. EGFR-mediated tumor immunoescape The imbalance between phosphorylated STAT1 and phosphorylated STAT3. *Oncoimmunology* **2**, 1–3 (2013).

369. Park, K. *et al.* Single-center experience of 600 living donor renal transplants: univariate analysis of risk factors influencing allograft outcome. *Transplant. Proc.* **24**, 1447–9 (1992).

370. Lin, M. *et al.* The protective effect of baicalin against renal ischemia-reperfusion injury through inhibition of inflammation and apoptosis. *BMC Complement. Altern. Med.* **14**, 19 (2014).

371. Hoesel, B. & Schmid, J. A. The complexity of NF-κB signaling in inflammation and cancer. *Molecular Cancer* vol. 12 (2013).

372. Alberti, C. *et al.* Ligand-dependent EGFR activation induces the co-expression of IL-6 and PAI-1 via the NFkB pathway in advanced-stage epithelial ovarian cancer. *Oncogene* **31**, 4139–4149 (2012).

373. Fan, C. Y., Melhem, M. F., Sefic Hosal, A., Rubin Grandis, J. & Leon Barnes, E. Expression of androgen receptor, epidermal growth factor receptor, and transforming growth factor α in salivary duct carcinoma. *Arch. Otolaryngol. - Head Neck Surg.* **127**, 1075–1079 (2001).

374. Biscardi, J. S. *et al.* c-Src-mediated phosphorylation of the epidermal growth factor receptor on Tyr845 and Tyr1101 is associated with modulation of receptor function. *J. Biol. Chem.* **274**, 8335–43 (1999).

375. Wu, W., Graves, L. M., Gill, G. N., Parsons, S. J. & Samet, J. M. Src-dependent phosphorylation of the epidermal growth factor receptor on tyrosine 845 is required for zinc-induced Ras activation. *J. Biol. Chem.* **277**, 24252–24257 (2002).

376. Mcmurchy, A. N. *et al.* Point mutants of forkhead box P3 that cause immune dysregulation, polyendocrinopathy, enteropathy, X-linked have diverse abilities to reprogram T cells into regulatory T cells. *J. Allergy Clin. Immunol.* **126**, 1242–1251 (2010).

377. Gu, H., Ding, L., Xiong, S. dong, Gao, X. ming & Zheng, B. Inhibition of CDK2 promotes inducible regulatory T-cell differentiation through TGFβ-Smad3 signaling pathway. *Cell. Immunol.* **290**, 138–144 (2014).

378. Zhang, Q. *et al.* TNF-α impairs differentiation and function of TGF-β-induced Treg cells in autoimmune diseases through Akt and Smad3 signaling pathway. *J. Mol. Cell Biol.* **5**, 85–98 (2013).

379. Tone, Y. *et al.* Smad3 and NFAT cooperate to induce Foxp3 expression through its enhancer. *Nat. Immunol.* **9**, 194–202 (2008).

380. McGaffin, K. R. & Chrysogelos, S. A. Identification and characterization of a response element in the EGFR promoter that mediates transcriptional repression by 1,25-dihydroxyvitamin D3 in breast cancer cells. *J. Mol. Endocrinol.* **35**, 117–33 (2005).

381. Song, J. young *et al.* Epidermal growth factor competes with EGF receptor inhibitors to induce cell death in EGFR-overexpressing tumor cells. *Cancer Lett.* **283**, 135–142 (2009).

382. Huen, S. C. *et al.* GM-CSF promotes macrophage alternative activation after renal ischemia/reperfusion injury. *J. Am. Soc. Nephrol.* **26**, 1334–1345 (2015).

383. Ishibashi, K. *et al.* Nuclear ErbB4 signaling through H3K9me3 is antagonized by EGFR-activated c-Src. *J. Cell Sci.* **126**, 625–637 (2013).

384. Jones, F. E., Welte, T., Fu, X. Y. & Stern, D. F. ErbB4 signaling in the mammary gland is required for lobuloalveolar development and Stat5 activation during lactation. *J. Cell Biol.* **147**, 77–87 (1999).

385. Tvorogov, D. *et al.* Somatic mutations of ErbB4: Selective loss-of-function phenotype affecting signal transduction pathways in cancer. *J. Biol. Chem.* **284**, 5582–5591 (2009).

386. Han, W., Sfondouris, M. E. & Jones, F. E. Direct coupling of the HER4 intracellular

domain (4ICD) and STAT5A signaling is required to induce mammary epithelial cell differentiation. *Biochem. Biophys. Reports* **7**, 323–327 (2016).

387. Park, K. M., Kim, J. I., Ahn, Y., Bonventre, A. J. & Bonventre, J. V. Testosterone is responsible for enhanced susceptibility of males to ischemic renal injury. *J. Biol. Chem.* **279**, 52282–52292 (2004).

388. Vogetseder, A. *et al.* Proliferation capacity of the renal proximal tubule involves the bulk of differentiated epithelial cells. *Am. J. Physiol. - Cell Physiol.* **294**, (2008).

389. Witzgall, R., Brown, D., Schwarz, C. & Bonventre, J. V. Localization of proliferating cell nuclear antigen, vimentin, c-Fos, and clusterin in the postischemic kidney. Evidence for a heterogenous genetic response among nephron segments, and a large pool of mitotically active and dedifferentiated cells. *J. Clin. Invest.* **93**, 2175–2188 (1994).

390. Muglia, V. F. & Prando, A. Carcinoma de células renais: Classificação histológica e correlação com métodos de imagem. *Radiol. Bras.* **48**, 166–174 (2015).

391. Hansson, J. *et al.* Evidence for a morphologically distinct and functionally robust cell type in the proximal tubules of human kidney. *Hum. Pathol.* **45**, 382–393 (2014).

392. Fang, F. *et al.* Loss of ACE2 Exacerbates Murine Renal Ischemia-Reperfusion Injury. *PLoS One* **8**, (2013).

393. Chappell, M. C. Nonclassical Renin-Angiotensin System and Renal Function. in *Comprehensive Physiology* vol. 2 2733–52 (John Wiley & Sons, Inc., 2012).

394. Zheng, S. *et al.* Ang-(1-7) promotes the migration and invasion of human renal cell carcinoma cells via Mas-mediated AKT signaling pathway. *Biochem. Biophys. Res. Commun.* **460**, 333–340 (2015).

395. Wang, X. *et al.* Decrease of phosphorylated proto-oncogene CREB at ser 133 site inhibits growth and metastatic activity of renal cell cancer. *Expert Opin. Ther. Targets* **19**, 985–995 (2015).

396. Huynh, T. P. *et al.* Glucocorticoids Suppress Renal Cell Carcinoma Progression by Enhancing Na,K-ATPase Beta-1 Subunit Expression. *PLoS One* **10**, e0122442 (2015).

397. Bab-Dinitz, E. *et al.* A C-terminal lobe of the β subunit of Na,K-ATPase and H,K-ATPase resembles cell adhesion molecules. *Biochemistry* **48**, 8684–8691 (2009).

398. Tomita, Y., Bilim, V., Hara, N., Kasahara, T. & Takahashi, K. Role of IRF-1 and caspase-7 in IFN-γ enhancement of Fas-mediated apoptosis in achn renal cell carcinoma cells. *Int. J. Cancer* **104**, 400–408 (2003).

399. Collet, N. *et al.* PPARγ is functionally expressed in clear cell renal cell carcinoma. *Int. J. Oncol.* **38**, 851–857 (2011).

400. Reel, B. *et al.* The effects of PPAR-γ agonist pioglitazone on renal ischemia/reperfusion injury in rats. *J. Surg. Res.* **182**, 176–184 (2013).

401. Funk, J. A. & Schnellmann, R. G. Accelerated recovery of renal mitochondrial and tubule homeostasis with SIRT1/PGC-1α activation following ischemia-reperfusion injury. *Toxicol. Appl. Pharmacol.* **273**, 345–354 (2013).

402. Cavalcanti, E. *et al.* JAK3/STAT5/6 pathway alterations are associated with immune deviation in CD8 T cells in renal cell carcinoma patients. *J. Biomed. Biotechnol.* **2010**, 935764 (2010).

403. Salvadori, M., Rosso, G. & Bertoni, E. Update on ischemia-reperfusion injury in kidney transplantation: Pathogenesis and treatment. *World J. Transplant.* **5**, 52 (2015).

404. Yu, H., Xu, S.-S., Cheng, Q.-Q., He, L.-M. & Li, Z. [Expression and clinical significance of Toll-like receptors in human renal carcinoma cell 786-0 and normal renal cell HK-2]. *Zhonghua Yi Xue Za Zhi* **91**, 129–31 (2011).

405. Karami, S. *et al.* Vitamin D Pathway Genes, Diet, and Risk of Renal Cell Carcinoma. *Int. J. Endocrinol.* **2010**, 11 (2010).

406. Arnold, S. J. & Robertson, E. J. Making a commitment: Cell lineage allocation and axis patterning in the early mouse embryo. *Nature Reviews Molecular Cell Biology* vol. 10 91–103 (2009).

407. A Dongre, R. W. New insights into the mechanisms of epithelial–mesenchymal transition and implications for cancer. *Nat. Rev. Mol. Cell Biol.* **20**, 69–84 (2019).

408. E Ferretti, A. H. Mesoderm specification and diversification: from single cells to emergent tissues. *Curr. Opin. Cell Biol.* **61**, 110–116 (2019).

409. MA Nieto, R. H. R. J. J. T. EMT: 2016. *Cell* **166**, 21–45 (2016).

410. Batlle, E. The transcription factor snail is a repressor of E-cadherin gene expression in epithelial tumour cells. *Nat. Cell Biol.* **2**, 84–89 (2000).

411. Cano, A. The transcription factor snail controls epithelial–mesenchymal transitions by repressing E-cadherin expression. *Nat. Cell Biol.* **2**, 76–83 (2000).

412. S Brabletz, T. B. The ZEB/miR-200 feedback loop—a motor of cellular plasticity in development and cancer? *EMBO Rep.* **11**, 670–677 (2010).

413. B Craene, G. B. Regulatory networks defining EMT during cancer initiation and progression. *Nat. Rev. Cancer* **13**, 97–110 (2013).

414. CJ David, J. M. Contextual determinants of TGFβ action in development, immunity and cancer. *Nat. Rev. Mol. Cell Biol.* **19**, 419–435 (2018).

415. CH Heldin, M. V. A. M. Regulation of EMT by TGFβ in cancer. *FEBS Lett.* **586**, 1959–1970 (2012).

416. XM Meng, D. N.-P. H. L. TGF-β: the master regulator of fibrosis. *Nat. Rev. Nephrol.* **12**, 325–338 (2016).

417. David, C. TGF-β tumor suppression through a lethal EMT. *Cell* **164**, 1015–1030 (2016).

418. Horiguchi, K. Role of Ras signaling in the induction of Snail by transforming growth factor-β. *J. Biol. Chem.* **284**, 245–253 (2009).

419. Janda, E. Ras and TGFβ cooperatively regulate epithelial cell plasticity and metastasis: dissection of Ras signaling pathways. *J. Cell Biol.* **156**, 299–314 (2002).

420. Meno, C. Mouse Lefty2 and zebrafish antivin are feedback inhibitors of Nodal signaling during vertebrate gastrulation. *Mol. Cell* **4**, 287–298 (1999).

421. M Oft, R. A. A. B. Metastasis is driven by sequential elevation of H-ras and Smad2 levels. *Nat. Cell Biol.* **4**, 487–494 (2002).

422. X Sun, E. M. M. L. G. M. Targeted disruption of Fgf8 causes failure of cell migration in the gastrulating mouse embryo. *Genes Dev.* **13**, 1834–1846 (1999).

423. TP Yamaguchi, K. H. M. H. J. R. fgfr-1 is required for embryonic growth and mesodermal patterning during mouse gastrulation. *Genes Dev.* **8**, 3032–3044 (1994).

424. X Zhou, H. S. L. L. B. H. M. K. Nodal is a novel TGF-β-like gene expressed in the mouse node during gastrulation. *Nature* **361**, 543–547 (1993).

425. Su, J. *et al.* TGF-β orchestrates fibrogenic and developmental EMTs via the RAS effector RREB1. *Nature* **577**, 566–571 (2020).

426. Maric, C. Sex, diabetes and the kidney. *American Journal of Physiology - Renal Physiology* vol. 296 F680 (2009).

427. Reed, D. K. & Arany, I. Sex hormones differentially modulate STAT3-dependent antioxidant responses during oxidative stress in renal proximal tubule cells. *In Vivo*

(Brooklyn). **28**, 1097–1100 (2014).

428. Clotet, S. *et al.* Stable isotope labeling with amino acids (SILAC)-based proteomics of primary human kidney cells reveals a novel link between male sex hormones and impaired energy metabolism in diabetic kidney disease. *Mol. Cell. Proteomics* **16**, 368–385 (2017).

429. de Miguel, F., Lee, S. O., Onate, S. A. & Gao, A. C. Stat3 enhances transaction of steroid hormone receptors. *Nucl. Recept.* **1**, 1–8 (2003).

430. Levy, D. E. & Lee, C. What does Stat3 do? *J. Clin. Invest.* **109**, 1143–1148 (2002).

431. Dimri, S., Sukanya & De, A. Approaching non-canonical STAT3 signaling to redefine cancer therapeutic strategy. *Integr. Mol. Med.* **4**, (2017).

432. Sellier, H., Rébillard, A., Guette, C., Barré, B. & Coqueret, O. How should we define STAT3 as an oncogene and as a potential target for therapy? *JAK-STAT* **2**, e24716 (2013).

433. Cuadros, T. *et al.* HAVCR/KIM-1 activates the IL-6/STAT-3 Pathway in ccRCC and Determines Tumor Progression and Patient Outcome. *Cancer Res.* **74**, 1416–1428 (2014).

434. Lorente, D. *et al.* The role of STAT3 protein as a prognostic factor in the clear cell renal carcinoma. Systematic review. *Actas Urológicas Españolas (English Ed.* **43**, 118–123 (2019).

435. Lorente, D. *et al.* Analysis of the nuclear expression of pSer727-STAT3 as a prognostic factor in patients with clear cell renal carcinoma. *Actas Urol. Esp.* **44**, 245–250 (2020).

436. Liu, N. W. *et al.* Impact of ischemia and procurement conditions on gene expression in renal cell carcinoma. *Clin. Cancer Res.* **19**, 42–49 (2013).

437. Schweizer, L. *et al.* The androgen receptor can signal through Wnt/β-Catenin in prostate cancer cells as an adaptation mechanism to castration levels of androgens. *BMC Cell Biol.* **9**, (2008).

438. Lonergan, P. & Tindall, D. Androgen receptor signaling in prostate cancer development and progression. *J. Carcinog.* **10**, (2011).

439. Chen, S., Xu, Y., Yuan, X., Bubley, G. J. & Balk, S. P. Androgen receptor phosphorylation and stabilization in prostate cancer by cyclin-dependent kinase 1. *Proc. Natl. Acad. Sci. U. S. A.* **103**, 15969–15974 (2006).

440. Lin, H. K. *et al.* Suppression Versus Induction of Androgen Receptor Functions by the Phosphatidylinositol 3-Kinase/Akt Pathway in Prostate Cancer LNCaP Cells with Different Passage Numbers. *J. Biol. Chem.* **278**, 50902–50907 (2003).

441. Ueda, T., Bruchovsky, N. & Sadar, M. D. Activation of the androgen receptor N-terminal domain by interleukin-6 via MAPK and STAT3 signal transduction pathways. *J. Biol. Chem.* **277**, 7076–7085 (2002).

442. Aaronson, D. S. *et al.* An androgen-IL-6-Stat3 autocrine loop re-routes EGF signal in prostate cancer cells. *Mol. Cell. Endocrinol.* **270**, 50–56 (2007).

9.ANNEXES

9. ANNEXES

Table XXXVI. List of patients used in this study to conduct RT-qPCR experiments

Sample	Sex	Age (yrs)
93N	men	36
47N	men	40
100N	men	56
80N	men	66
77N	men	69
101N	men	70
97N	men	70
99N	men	76
84N	men	80
64N	men	-
94N	women	53
95N	women	53
79N	women	54
87N	women	63
103N	women	65
67N	women	67
96N	women	68
92N	women	68
86N	women	83

Table XXXVII. List of patients used in this study to conduct ELISA experiments

Sample	Sex	Age (yrs)
046	men	24
013	men	29
032	men	40
U4A	men	46
30	men	47
U53A	men	48
U39A	men	51
U5A	men	52
028	men	53
U15A	men	55
U17A	men	55
016	men	56
U24A	men	58
U56A	men	59
042	women	40
015	women	41
047	women	41
U42A	women	42
U16A	women	51
U12A	women	53
U50A	women	53
U21A	women	54
U58A	women	55
U11A	women	58

Table XXXVIII. Mechanistic relationship of the links of the MoA justifying the role roles of androgens in renal IRI/ regeneration

Link	Protein A	Protein B	Sign	References
1	PIAS2	AR	1	PMID: 25434787, PMID: 11117529
2	EGFR	CADH1	-1	PMID: 24211838
3	EGFR	PGH2	1	PMID: 26137580, PMID: 28352075
4	EGFR	STAT3	1	PMID: 15950906, PMID: 25232393, PMID: 24501692, PMID: 14966128
5	EGFR	renal IRI/regeneration	1	-
6	EGFR	renal IRI/regeneration	-1	-
7	EGFR	NFKB1	1	PMID: 23915189, PMID: 22158046
7	EGFR	CASP3	1	PMID: 19380191
8	FOS	EZRI	1	PMID: 19164283
9	IL2RA	renal IRI/regeneration	-1	-
10	IL6	renal IRI/regeneration	1	-
11	ITB1	renal IRI/regeneration	-1	-
12	AR	PIAS2	1	PMID: 27672034
13	AR	EGFR	1	PMID: 21613411
14	AR	CADH1	-1	PMID: 18794357
15	AR	SRC	1	PMID: 22771325
16	AR	PGH2	1	PMID: 23715826, PMID: 23415714
17	AR	STAT3	1	PMID: 11322786
18	AR	BTG2	-1	PMID: 22266859
19	AR	SMAD3	-1	PMID: 25315188, PMID: 11707452
20	AR	TNFA	1	PMID: 19907077
20	AR	CADH2	1	PMID: 23658830
20	AR	CCR2	1	PMID: 19907077
21	AR	ERBB2	1	PMID: 21741601, PMID: 21613411
21	AR	IGF1R	1	PMID: 17202144
21	AR	ERBB3	1	PMID: 21741601
22	VDR	EGFR	-1	PMID: 16087726
23	VDR	IL6	-1	PMID: 11050002
24	VDR	CADH1	1	PMID: 22213313
25	VDR	IL12B	-1	PMID: 21310195
26	CADH1	renal IRI/regeneration	-1	-
27	SRC	EGFR	1	PMID: 10075741, PMID: 11983694
28	SRC	PECA1	1	PMID: 12775720
29	SRC	STAT3	1	PMID: 19372587, PMID: 12244095

30	SRC	ERBB4	-1	PMID: 23230144, PMID: 21441918
31	SRC	RHG35	1	PMID: 19822667
32	EZRI	renal IRI/regeneration	-1	-
33	PECA1	renal IRI/regeneration	1	-
34	ATF3	renal IRI/regeneration	-1	-
35	TENA	ITB1	1	PMID: 23958855
36	IL12B	renal IRI/regeneration	1	-
37	PGH2	renal IRI/regeneration	1	-
38	STAT3	IL6	1	PMID: 25234193, PMID: 24525913
39	STAT3	CADH1	-1	PMID: 22205702, PMID: 18320073
40	STAT3	PGH2	1	PMID: 24127267
41	STAT3	renal IRI/regeneration	1	-
42	STAT3	TGFB1	1	PMID: 25740948, PMID: 24573038, PMID: 28154170
42	STAT3	IL8	1	PMID: 24525913
43	RHOA	renal IRI/regeneration	-1	-
44	BTG2	renal IRI/regeneration	-1	-
45	SMAD3	FOS	1	PMID: 11262418
46	SMAD3	VDR	1	PMID: 17471513
47	SMAD3	ATF3	1	PMID: 12718878
48	SMAD3	TENA	1	PMID: 15001984
49	SMAD3	FOXP3	1	PMID: 24978614 , PMID: 23243069, PMID: 18157133
50	ERBB4	STAT5A	1	PMID: 10508857,PMID: 19098003, PMID: 23230144, PMID: 28955922
50	ERBB4	STAT5B	1	PMID: 10508857, PMID: 19098003
51	FOXP3	IL2RA	1	PMID: 21036387
52	RHG35	RHOA	-1	PMID: 15102857, PMID: 9548756
53	Androgens	AR	1	-
54	TGFB1	renal IRI/regeneration	1	-
54	IL8	renal IRI/regeneration	1	-
55	TNFA	renal IRI/regeneration	1	-
55	CADH2	renal IRI/regeneration	1	-
55	CCR2	renal IRI/regeneration	1	-
56	ERBB2	SRC	1	PMID: 19372587, PMID: 24810047
56	IGF1R	SRC	1	PMID: 26041671
56	ERBB3	SRC	1	PMID: 16267617
57	NFKB1	renal IRI/regeneration	1	-
57	CASP3	renal IRI/regeneration	1	-
58	STAT5A	renal IRI/regeneration	-1	-
58	STAT5B	renal IRI/regeneration	-1	-
59	SMAD3	BRCA1	-1	PMID: 15735739

| 60	SRC	FAK1	1	PMID: 16966330
61	SRC	STAT1	1	PMID: 10358079, PMID: 9344858, PMID: 9344858/ PMID: 10358079, PMID: 9344858, PMID: 9344858
62	SRC	STAT1	1	PMID: 10358079, PMID: 9344858, PMID: 9344858/PMID: 10358079, PMID: 9344858, PMID: 9344858
63	SRC	STAT1	1	PMID: 10358079, PMID: 9344858, PMID: 9344858/ PMID: 10358079, PMID: 9344858, PMID: 9344858
64	SRC	STAT1	1	PMID: 10358079, PMID: 9344858, PMID: 9344858/PMID: 10358079, PMID: 9344858, PMID: 9344858
65	SRC	STAT1	1	PMID: 10358079, PMID: 9344858, PMID: 9344858/ PMID: 10358079, PMID: 9344858, PMID: 9344858
66	STAT3	STAT1	1	Uniprot: P40763
67	BRCA1	STAT1	1	PMID: 10792030, PMID: 17374731
68	FAK1	STAT1	1	PMID: 11278462, PMID: 20576130
69	STAT1	IL1B	1	PMID: 17032168
70	STAT1	CCL2	1	PMID: 17255531
71	STAT1	NOS2	1	PMID: 16140971, PMID: 17251186
72	STAT1	PGH2	1	PMID: 16685393, PMID: 21882257
73	STAT1	renal IRI/regeneration	1	-
74	IL1B	renal IRI/regeneration	1	-
75	CCL2	renal IRI/regeneration	1	-
76	NOS2	renal IRI/regeneration	1	-
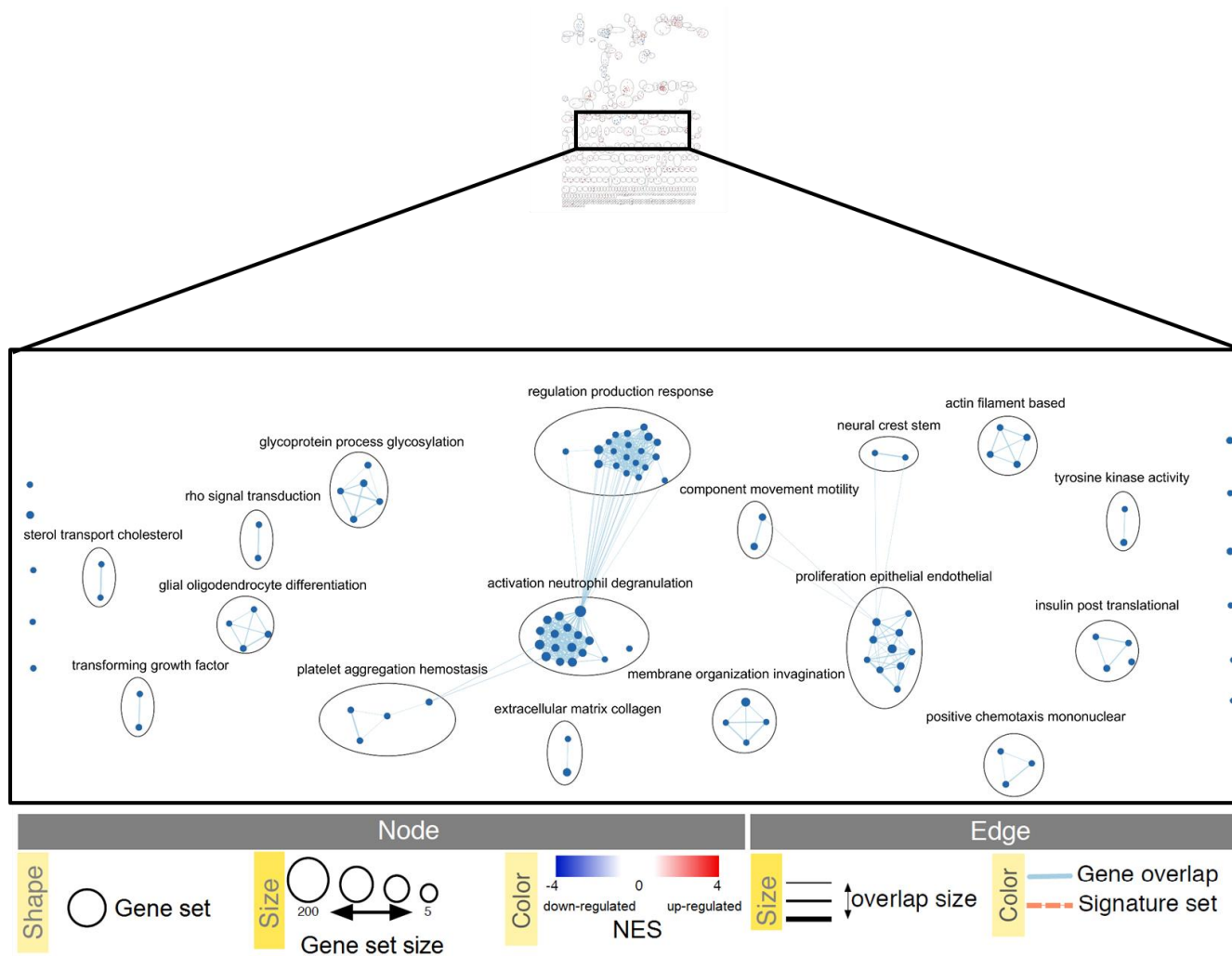
Figure 60. Enrichment map of over-represented genes in individual sex comparison F.PSvsF.PR following GSEA analyses. Representation of different clusters (nodes) regulated in the comparison.
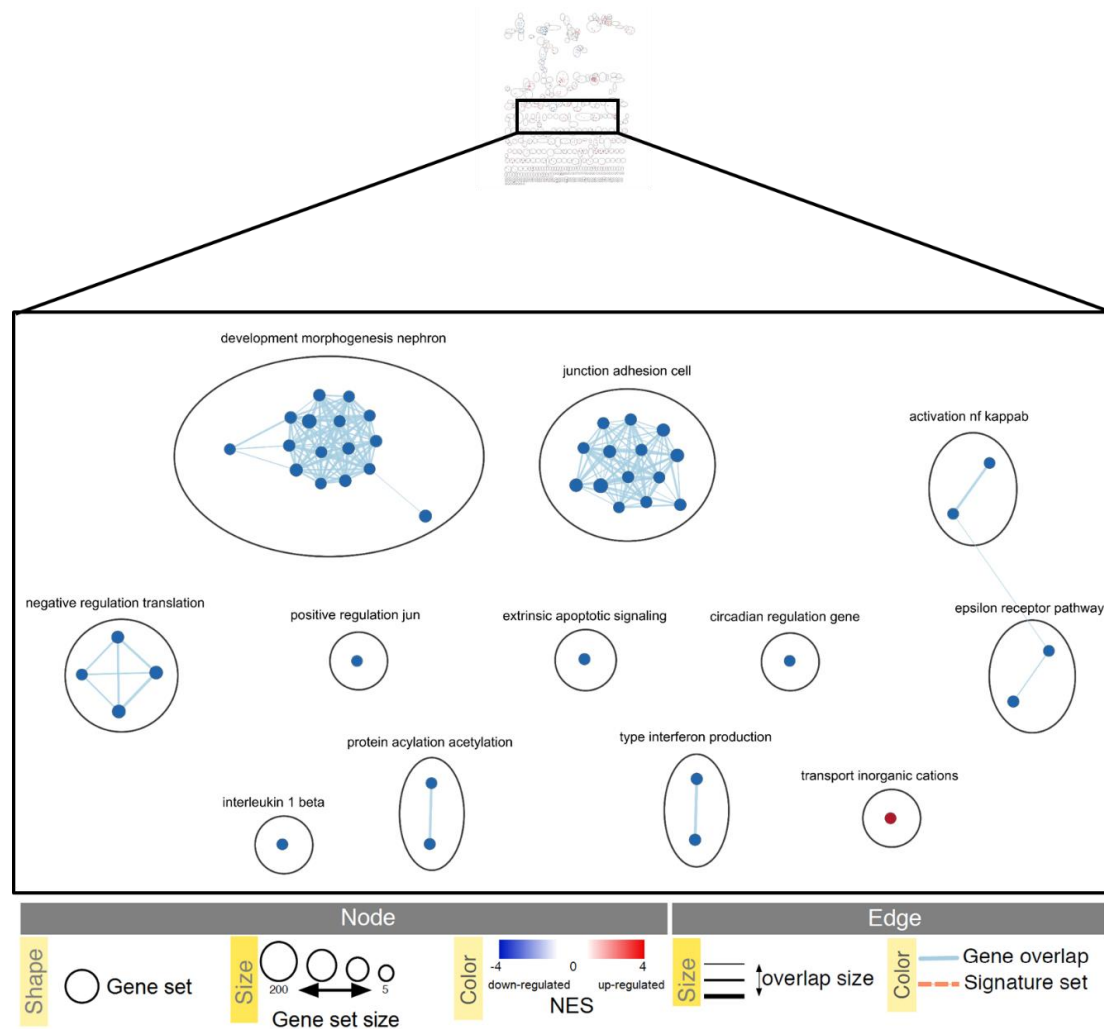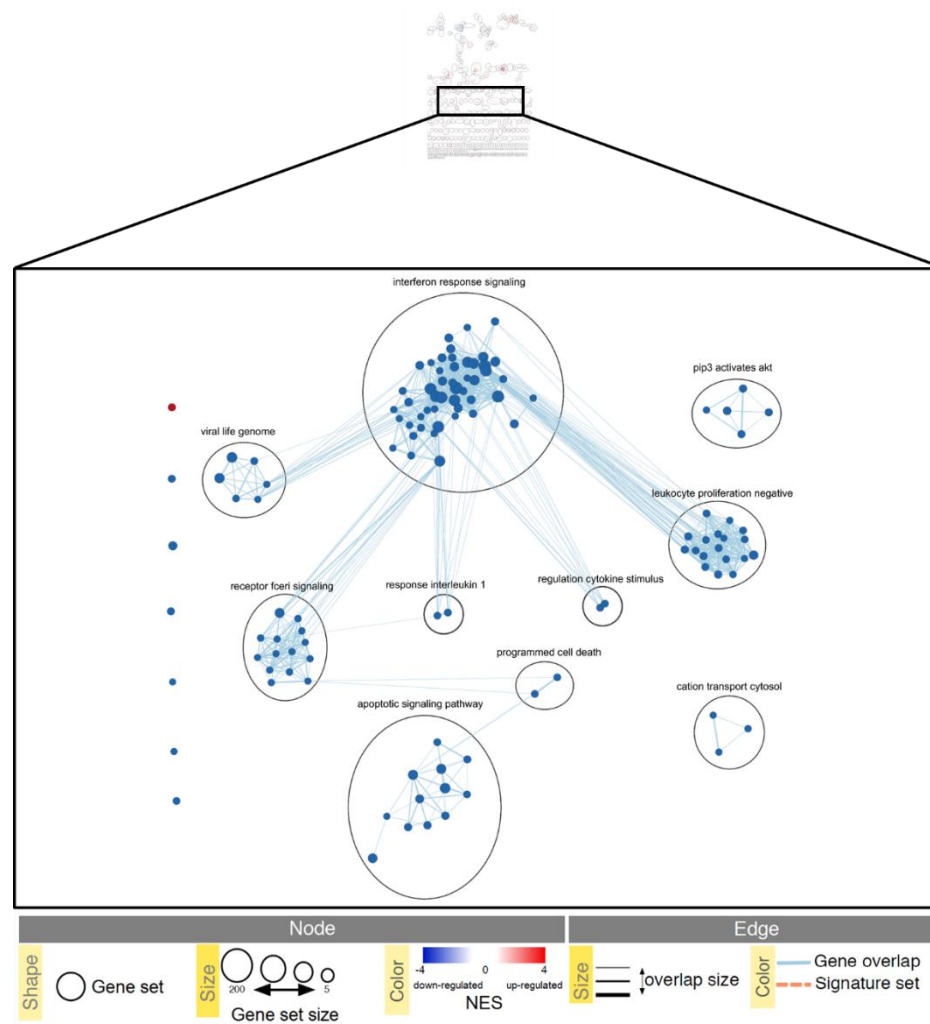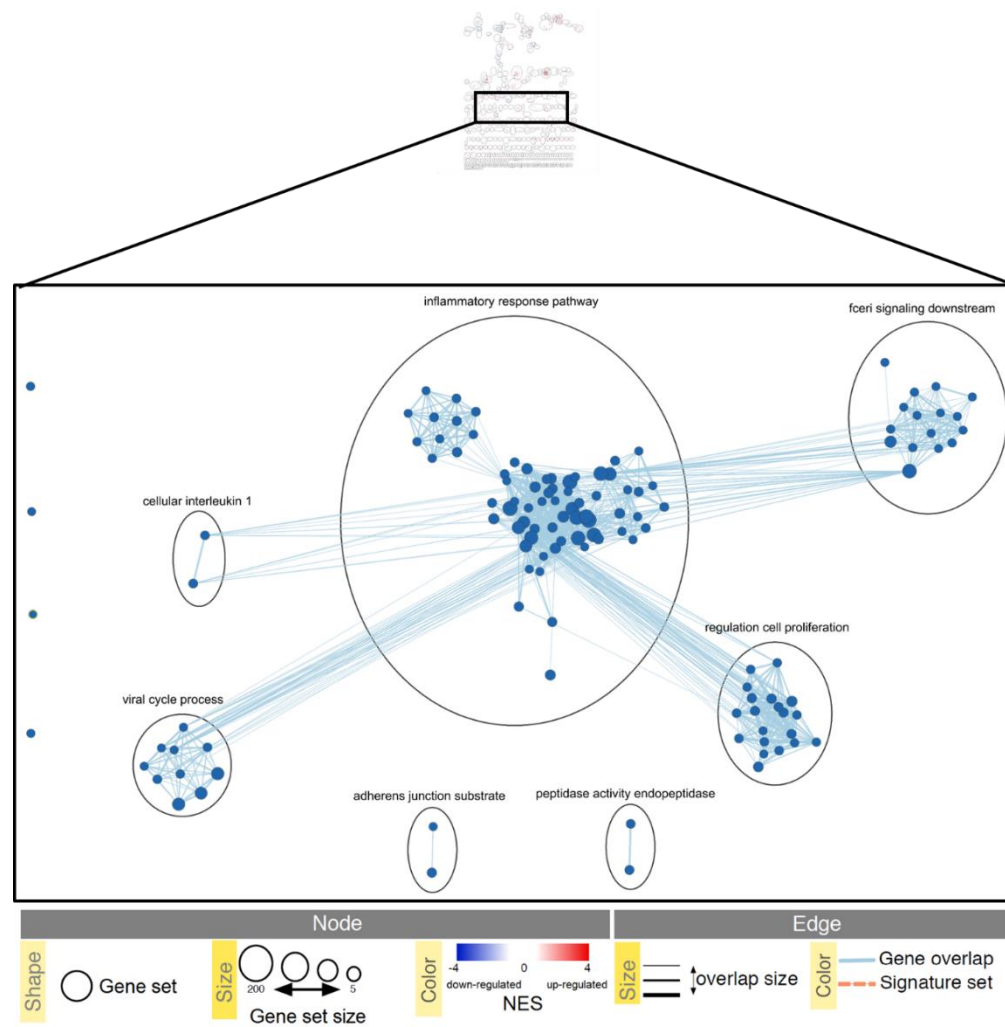
Figure 61. Enrichment map of over-represented genes in individual sex comparison F.WL vsF.PS following GSEA analyses. Representation of different clusters (nodes) regulated in the comparison.
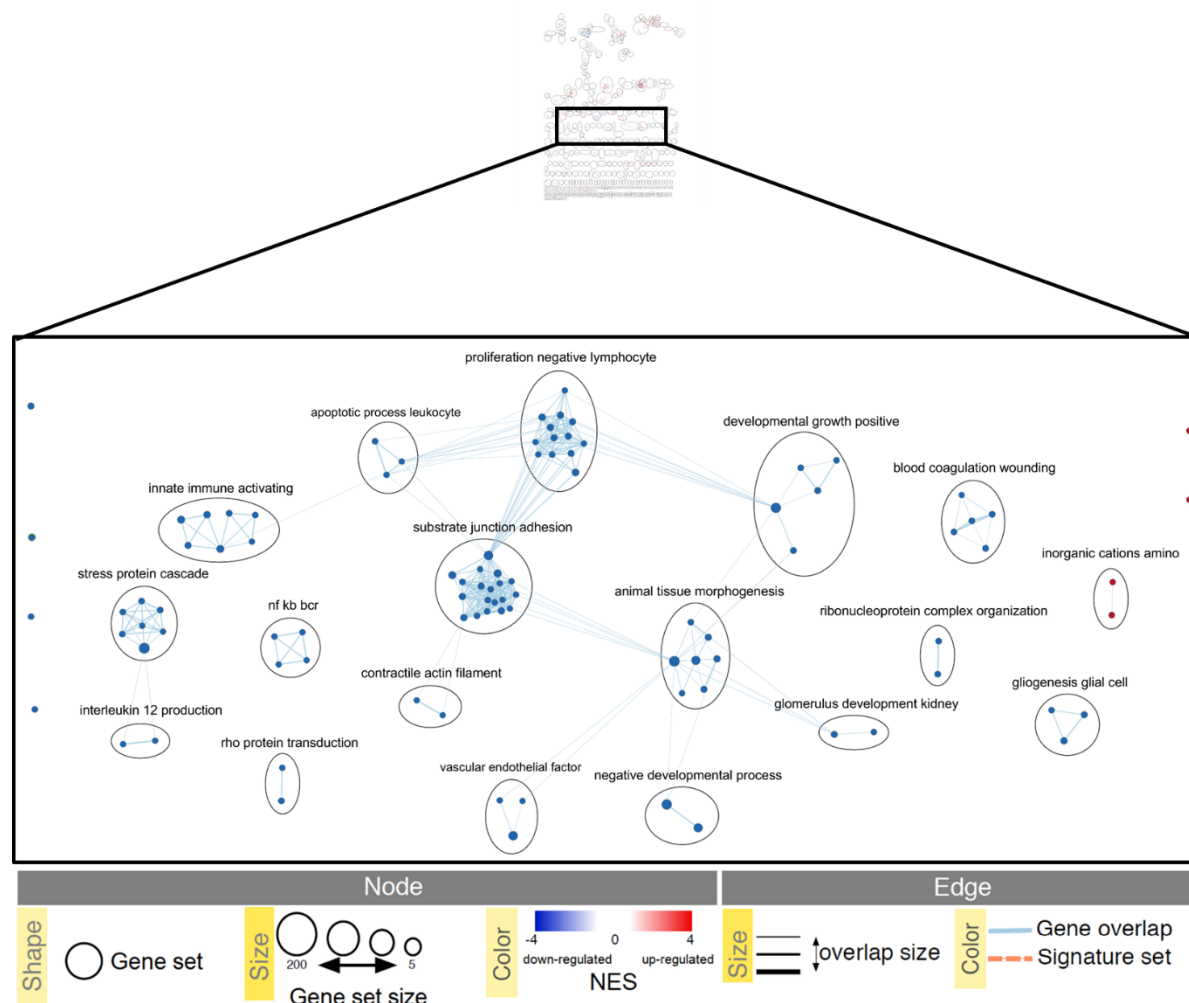
Figure 62. Enrichment map of over-represented genes in individual sex comparison F.WLvsF.PR following GSEA analyses. Representation of different clusters (nodes) regulated in the comparison.
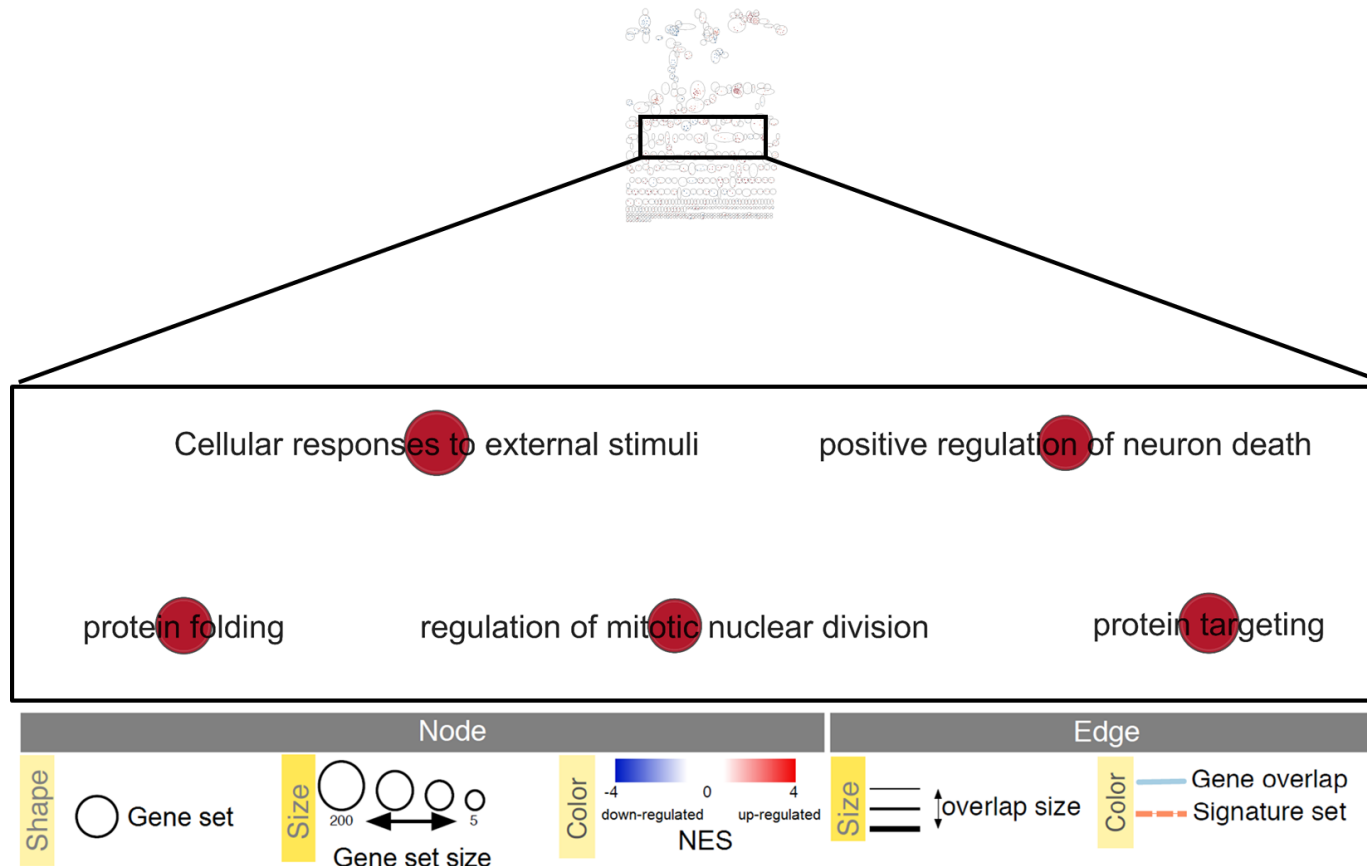
Figure 63. Enrichment map of over-represented genes in individual sex comparison MPSvsMPR following GSEA analyses. Representation of different clusters (nodes) regulated in the comparison.
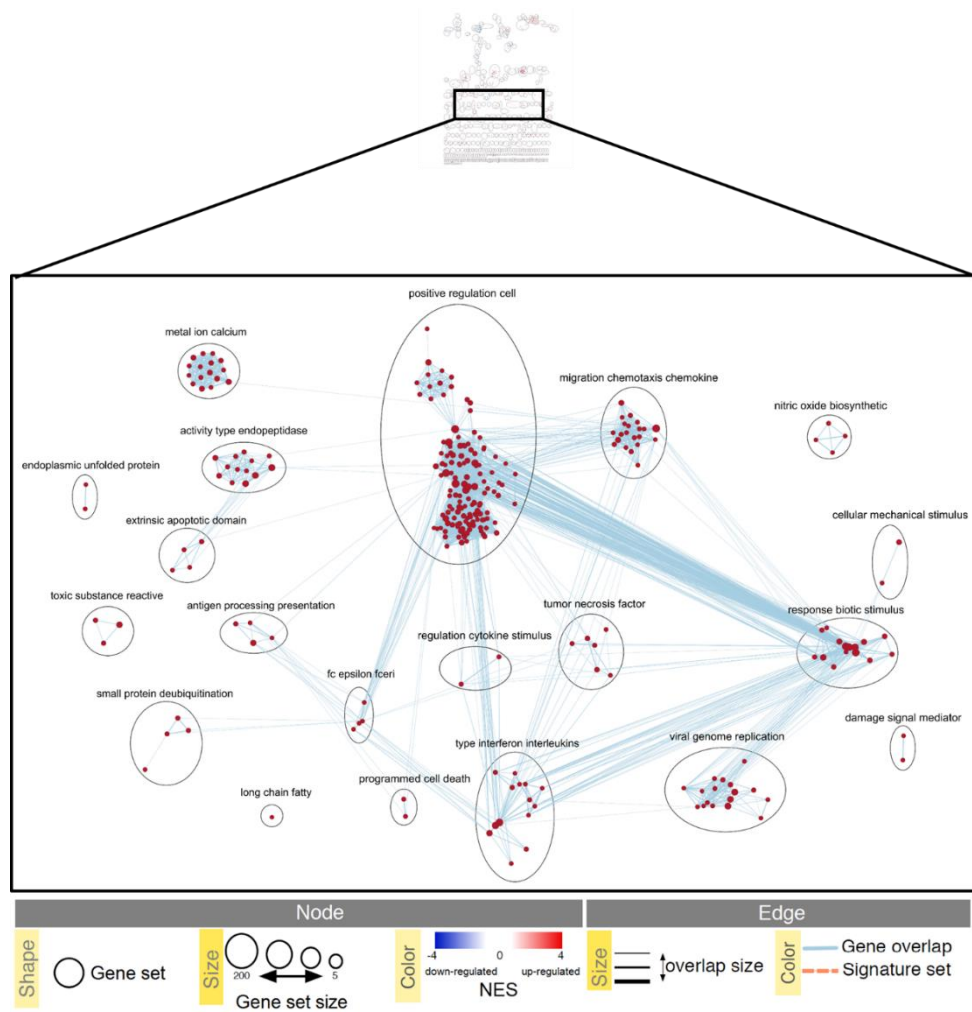
Figure 64. Enrichment map of over-represented genes in individual sex comparison MWLvsMPS following GSEA analyses. Representation of different clusters (nodes) regulated in the comparison.
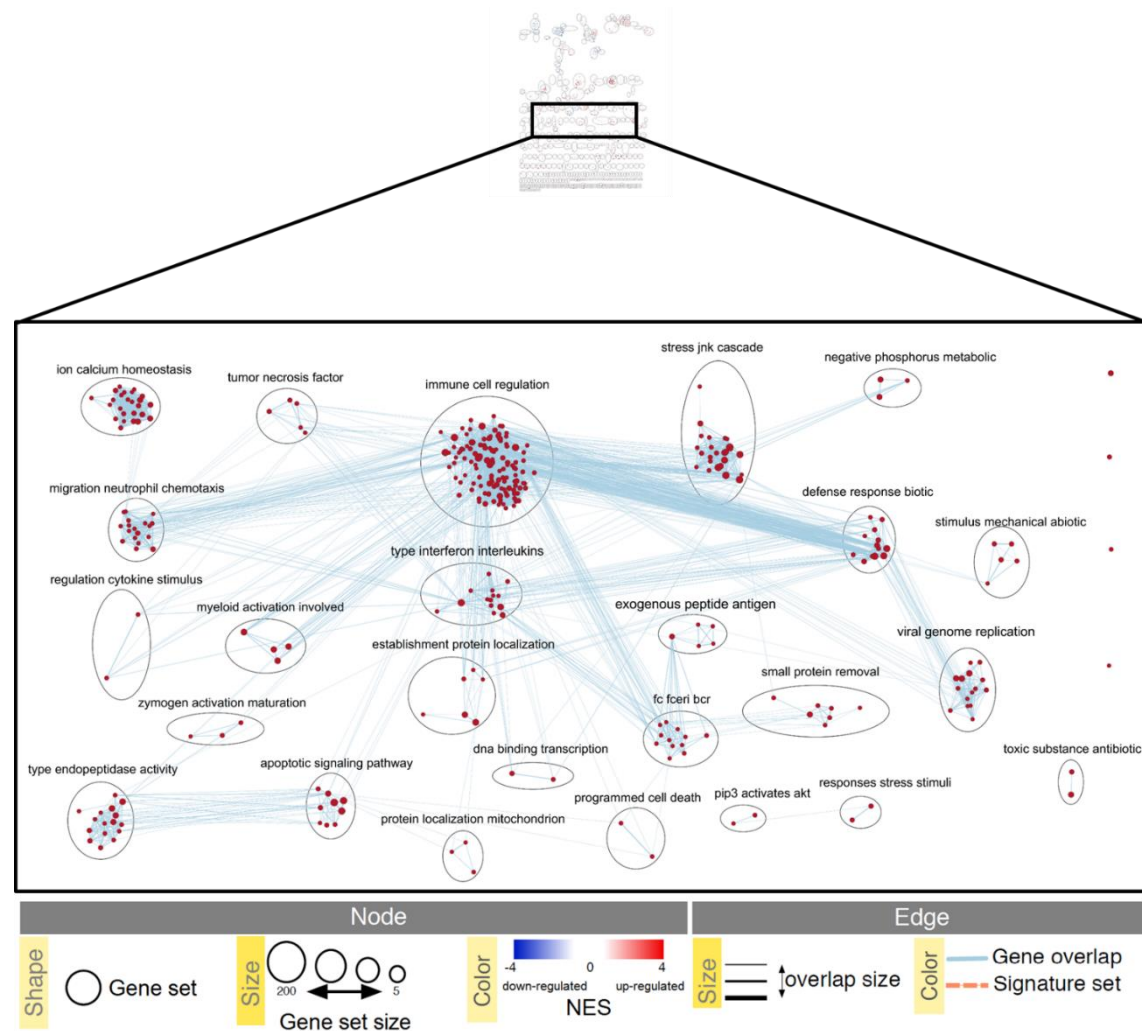
Figure 65. Enrichment map of over-represented genes in individual sex comparison MWLvsMPR following GSEA analyses. Representation of different clusters (nodes) regulated in the comparison.
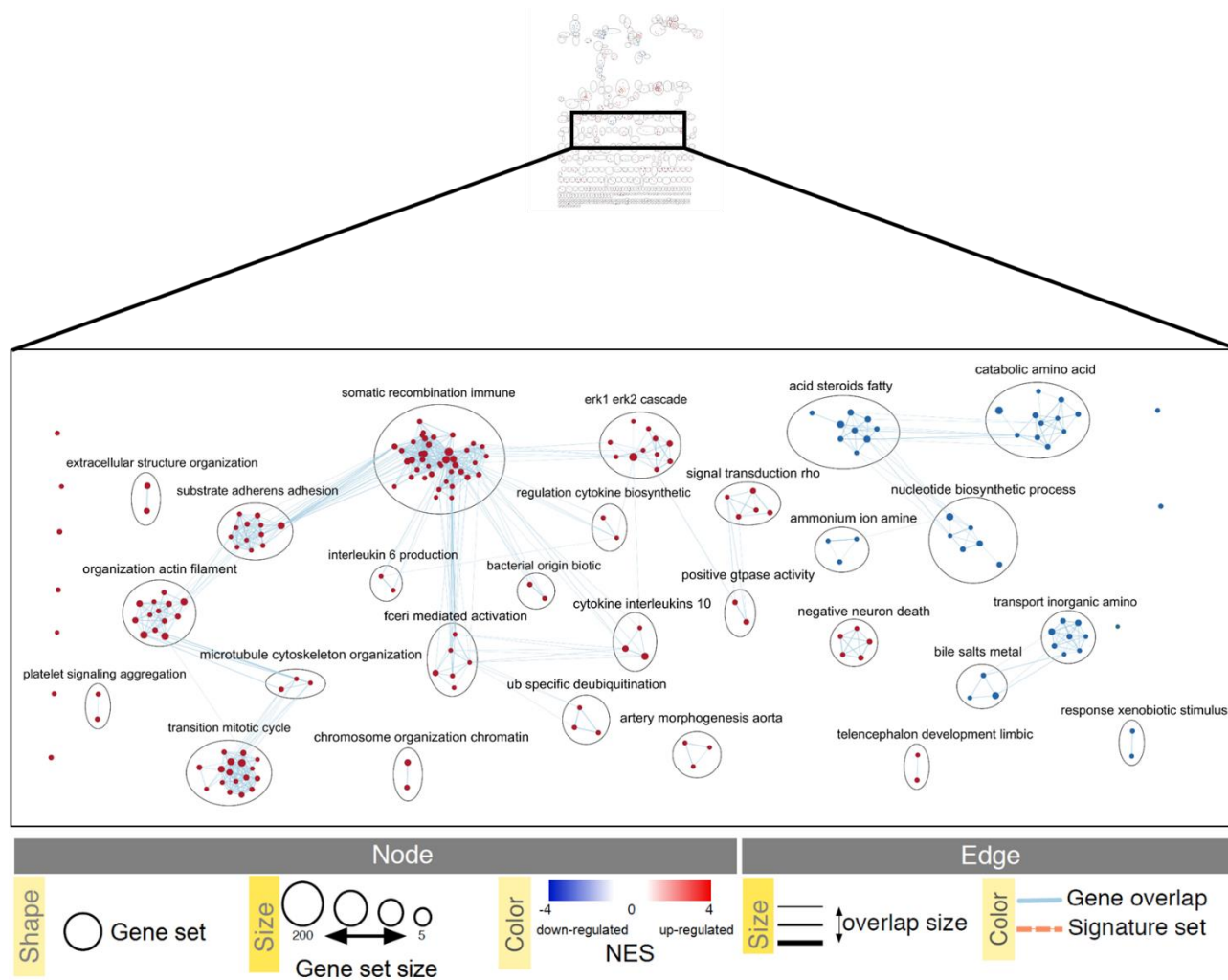
Figure 66. Enrichment map of over-represented genes in individual sex comparison   MPRvsFPR   following GSEA analyses. Representation of different clusters (nodes) regulated in the comparison.

Figure 67. Enrichment map of over-represented genes in individual sex comparison MPSvsFPS following GSEA analyses. Representation of different clusters (nodes) regulated in the comparison.

Figure 68. Enrichment map of over-represented genes in individual sex comparison   MWLvsFWL following GSEA analyses. Representation of different clusters (nodes) regulated in the comparison